

Sediment Sorting During Hopper Dredging and Pumpout Operations



This page intentionally left blank.

Sediment Sorting During Hopper Dredging and Pumpout Operations

March 2019

Authors:

S. Jarrell Smith
Anthony M. Priestas
Duncan B. Bryant
Katherine E. Brutsché
Kelsey A. Fall

Prepared under BOEM Award M16PG00023

by

Engineering Research and Development Center
Coastal and Hydraulics Laboratory
U.S. Army Corps of Engineers
3909 Halls Ferry Road
Vicksburg, MS 39180

US Department of the Interior
Bureau of Ocean Energy Management
Headquarters



This page intentionally left blank

DISCLAIMER

Study concept, oversight, and funding were provided by the US Department of the Interior, Bureau of Ocean Energy Management (BOEM), Environmental Studies Program, Washington, DC, under Contract Number M16PG00023 with the US Army Corps of Engineers (USACE) Jacksonville District. Additional funding was provided by the USACE National Regional Sediment Management (RSM) Program and USACE Jacksonville District. This report has been technically reviewed by BOEM, and it has been approved for publication. The views and conclusions contained in this document are those of the authors and should not be interpreted as representing the opinions or policies of the US Government, nor does mention of trade names or commercial products constitute endorsement or recommendation for use.

REPORT AVAILABILITY

To download a PDF file of this report, go to the US Department of the Interior, Bureau of Ocean Energy Management [Data and Information Systems webpage \(http://www.boem.gov/Environmental-Studies-EnvData/\)](http://www.boem.gov/Environmental-Studies-EnvData/), click on the link for the Environmental Studies Program Information System (ESPIS), and search on 20xx-xxx. The report is also available at the National Technical Reports Library at <https://ntrl.ntis.gov/NTRL/>.

CITATION

Smith SJ, Priestas AM, Bryant DB, Brutsché KE, Fall KA. 2019. Sediment sorting by hopper dredging and pumpout operations. Sterling (VA): U.S. Department of the Interior, Bureau of Ocean Energy Management. OCS Study BOEM 2019-010. 138 p.

ACKNOWLEDGMENTS

The research presented in this report would not have been possible without the many contributions from BOEM staff, the dredging industry, and supporting offices of the US Army Corps of Engineers (USACE). The authors would like to thank Douglas Piatkowski, Leighann Brandt, Dr. Michael Miner, and Paul Knorr (BOEM) and Dr. Clay McCoy (USACE Jacksonville District; Regional Sediment Management (RSM) Regional Center of Expertise) for the development of the study concept and their valuable input toward the study plan and methods.

This research would not have been possible without the contributions of the dredging industry. Industry members gave early feedback on suggested sampling streams on the dredge. Great Lakes Dredging and Dock hosted the project team for several reconnaissance visits aboard their hopper dredges, and ultimately hosted the research team in the execution of the field sample collection. The authors specifically thank Bill Hanson, Robert Ramsdell, and Jeremy Remme for their assistance in planning and logistical support of the field study. Captain James "Woody" Hoffman and his crew aboard the *Liberty Island* accommodated the field research team in every possible way to ensure safe access to samples aboard the dredge. Elizabeth Godsey and Nathan Lovelace (USACE-Mobile District) are thanked for their support of this work through logistical support and provision of background data and reports on the Ship Island Restoration Project.

Support for development and implementation of the Interagency Agreement was provided by Jackie Keiser, Jason Engle, and Dr. Kelly Legault of the RSM Regional Center of Expertise and USACE Jacksonville District in coordination with the BOEM team members listed above. The Technical Points of Contact for the project were Dr. Clay McCoy and Leighann Brandt. The USACE Administrative Point of Contact was Liz Fiocchi and the BOEM Contracting Officer and Contracting Officer Representative were Joanne Murphy and Doug Piatkowski, respectively. Funding for this research was provided by BOEM, the USACE National RSM Program, and USACE Jacksonville District. Ms. Linda Lillycrop (USACE-ERDC) was Program Manager for RSM, and Dr. Clay McCoy (USACE Jacksonville District) was Project Manager for funding contributed by BOEM and Jacksonville District.

SUMMARY

Beach nourishment projects using dredged material must often meet sediment compatibility requirements including: sediment size, sediment sorting, mineral content, sediment color, and fine-sediment ($< 63 \mu\text{m}$) content. In many instances, the application of these regulations does not account for changes in these sediment characteristics from borrow areas to beach placement sites. Hopper dredging operations for beach and nearshore placement typically include periods of overflow, which is recognized to produce some degree of separation between the size fractions of the dredged sediment. The degree of separation and the controlling factors are the subject of this research. This report reviews prior research of sediment separation by hopper dredges and describes a field sampling campaign in which collected samples are used to define the fines content at the varying stages of the dredging process from borrow site to hopper to beach. The field study, conducted onboard the dredge *Liberty Island* at the Ship Island Restoration Project near Biloxi, Mississippi, found the fines content reduced sequentially from the borrow area, hopper, and beach. Hopper overflow removed 61% of the fine-sediment mass contained in the borrow area, and beach outwash removed 67% of the fines contained in the hopper. These two losses combined accounted for a removal of 87% of the fines dredged from the borrow area. Of the fine-sediment mass removed, 70% was removed by the overflow process and 30% was removed by beach outwash. These findings are consistent with other research (Coor and Ousley 2019) of change in fine-sediment content from more than 100 beach nourishment projects on the Florida coast. The present study combined with the work of Coor and Ousley represent a significant body of data to support the quantitative accounting of

changes in sediment properties by hopper dredging operations when evaluating beach compatibility. This report recommends several approaches for implementing the research findings in hopper dredging and beach nourishment planning and operations.

Table of Contents

List of Figures.....	iii
List of Tables.....	iv
Abbreviations and Acronyms	v
Definitions.....	vi
Executive Summary	vii
1 Introduction.....	1
2 Background.....	3
2.1 Site Description	3
2.1.1 Study Site	3
2.1.2 TSHD <i>Liberty Island</i>	5
2.2 TSHD Processes	6
2.2.1 Modeling	7
3 Methods	8
3.1 Sampling	9
3.1.1 Fines Content of the Horn Island Pass Borrow Area 1	9
3.1.2 Fines Content of the Dredge	11
3.1.3 Fines Content of the Beach	21
3.2 Sample Processing and Laboratory Analysis	22
3.2.1 Scour Pool Samples	22
3.2.2 Dredge Inflow, Hopper Bed, and Beach Samples.....	22
3.2.3 Merging Sieve and Laser Diffraction Size Distributions	23
3.3 Quantifying Loss of Fines	24
4 Results	25
4.1.1 Borrow Area.....	25
4.2 Dredge Sediments	26
4.2.1 Settled and Suspended Fines	26
4.2.2 Inflow, Hopper Bed, and Beach Sediments.....	26
4.2.3 Variability of the Fines Fraction.....	27
4.3 Change in Fines Content	29
4.4 Mud Aggregates	30
5 Discussion and Future Considerations	34
5.1 Separation of Sand and Fines by Dredging and Placement Processes	34
5.2 Beach Color	36
5.3 Assessment of Sampling and Analysis Approach	37
5.4 Recommendations for Future Studies	38
5.5 Implications for Practice and Policy	40
5.5.1 Dredging Practice.....	40
5.5.2 Beach and Nearshore Placement Policy.....	41
6 Summary and Conclusions	42

7 References44
Appendix A Conceptual Model of Sediment Routing During Dredging and Pumpout46
Appendix B. Laboratory Testing of Sampling Methods68
Appendix C Boring Logs and Sample Analysis from Horn Island Pass Borrow Area 1 (HIP1).....104

List of Figures

Figure 1. Site map of the MSCIP-Ship Island Phase 1 restoration project.	4
Figure 2. Horn Island Pass Borrow Areas 1–3.	5
Figure 3. The TSHD <i>Liberty Island</i>	6
Figure 4. Process diagram with sediment sampling and loss points.	7
Figure 5. Cumulative overflow losses as a function of the dimensionless hopper load parameter.	8
Figure 6. Borrow Area HIP1.	11
Figure 7. Distributions of vessel dwell time and percent fines.	11
Figure 8. Schematic diagram of sampling locations on the <i>Liberty Island</i>	13
Figure 9. Sampling assembly used to collect hopper inflow samples.	14
Figure 10. Bottle sampling method used to collect hopper inflow sediments.	15
Figure 11. Idealized vertical distribution of sediment at the conclusion of hopper loading.	16
Figure 12. Gravity corer and collected sample.	18
Figure 13. Plate sampling procedure.	18
Figure 14. Distribution of hopper bed sampling methods applied to dredge loads.	19
Figure 15. The extrusion and subsampling procedure for hopper bed cores.	20
Figure 16. The scour pool at the conclusion of a dredge load.	21
Figure 17. Pan of moist sample with specimens removed for analysis.	23
Figure 18. Example merged size distribution.	24
Figure 19. Averaged sediment size distributions for the inflow, hopper bed, and beach.	27
Figure 20. Fines content at the borrow area, inflow, hopper bed, and beach.	29
Figure 21. Fines content by sampling location.	30
Figure 22. Mud aggregates observed on the hopper bed surface and beach.	31
Figure 23. Mud aggregates collected in samples of the hopper bed.	32
Figure 24. Sediment lightness associated with sample location.	33
Figure 25. Relationship between Munsell Value and the fraction of fines.	34
Figure 26. Comparison of fines loss rate to percent change.	36

List of Tables

Table 1. The TSHD <i>Liberty Island</i> dimensions and operating parameters.	6
Table 2. Geotechnical properties of samples recovered from HIP1.	9
Table 3. Dredge plant <i>Liberty Island</i> load sampling dates and times.	12
Table 4. Sampling and analysis methods for quantifying fines content of the hopper bed.	17
Table 5. Fines content estimated from borrow area samples and dredge tracks.	25
Table 6. Fine fraction in the hopper bed.	26
Table 7. General sediment characterizations averaged by sampling location.	27
Table 8. Correlation matrix for percent fines by sample location.	28
Table 9. Summary statistics of the fraction of fines between sample locations.	30
Table 10. Munsell color codes averaged by sample location.	33
Table 11. Summary of fitted model parameters and 95% confidence limits for data in Figure 20.	34
Table 12. Hypothesis testing of sample means from sampling locations in the dredging process.	35

Abbreviations and Acronyms

ASTM	American Society for Testing and Materials
BOEM	Bureau of Ocean Energy Management
CFD	Computational Fluid Dynamics
CHL	Coastal and Hydraulics Laboratory
CS	Coarse sand or construction sand
DOI	Department of the Interior
DQM	Dredging Quality Management
EFDC	Environmental Fluid Dynamics Code
ERDC	Engineering Research and Development Center
ESPIS	Environmental Studies Program Information System
FS	Fine sand
GLDD	Great Lakes Dredging and Dock
HIP1	Horn Island Pass Borrow Area 1
LD	Laser diffraction
LL	Liquid limit
MRE	Mean relative error
MSCIP	Mississippi Coastal Improvements Program
MV	Munsell Value
PI	Plasticity index
PL	Plastic limit
PLUMES	Plume Measurement System
PTM	Particle Tracking Model
RE	Relative errors
RSM	Regional Sediment Management
SAJ	South Atlantic Division Jacksonville District
SD	Standard Deviation
SEM	Standard error of the mean
TDS	Tons dry solid
TSHD	Trailing Suction Hopper Dredge
USACE	United States Army Corps of Engineers
USCS	Unified Soils Classification System
USDA	United States Department of Agriculture
VS	Vicksburg silt
YSI	Yellow Springs Instrument

Definitions

Borrow Area: Offshore area from which sediments used for beach nourishment are excavated.

Beachfill: Sand placed directly on the shoreface for the purposes of increasing the width or elevation of the beach.

Dragarm: Articulated pipeline and support members that connect a trailing suction hopper dredger draghead to the dredger. The dragarm lowers the draghead to the seabed during dredging.

Draghead: Implement on a trailing suction hopper dredger through which bed sediment is drawn into the suction pipe. The draghead guides the suction pipe along the sea bed.

Economic Loading: Practice of allowing a period of hopper overflow to achieve a greater load of sediment within the hopper.

Fine Sediment: Sediment passing the #230 sieve (nominal diameter <63 μm).

Florida Sand Rule: A colloquial reference to Florida's regulatory requirements concerning sediment compatibility for beach nourishment projects.

Hopper: Compartment between the fore and aft of a dredge vessel used for holding sediment and water suctioned from the seabed.

Outfall: Exit point of a pipeline where the discharge of water or sediment slurry first enters the surrounding environment.

Outwash: Zone over which a sediment load is distributed after issuing from an energetic transport environment into a much milder transport environment. In geology, outwash plains, fans, or zones develop near the terminus of glaciers or mountainous streams. Outwash zones are characterized by the sorting of the transported materials by size due to negative gradients in transport potential. In the case of dredging, the outwash zone refers to the zone over which dredged sediment slurry delivered by pipeline distributes over the receiving area of the flow. Coarse sediments will deposit close to the outfall and finer sediments will deposit farther into the outwash zone. Some very fine solids may remain in suspension and be carried with the flow into to the sea.

Overflow: Filling of the Trailing Suction Hopper Dredger's (TSHD) hopper beyond volumetric capacity by allowing supernatant water and suspended solids to pass over a weir and return to the water column.

Pumpout: Transfer of the hopper dredger sediment load from the hopper to the beach. The sediment load is slurred by jetting water into the load and transferring the sediment slurry through pipeline to the beach.

Transit: Any time interval during which the vessel is determined to be sailing either loaded or light, specifically not during identified dredging, turning, or disposal.

Executive Summary

Beach nourishment projects using dredged material must often meet sediment compatibility requirements including: sediment size, sediment sorting, mineral content, sediment color, and fine-sediment ($< 63 \mu\text{m}$) content. In many instances, the application of these regulations does not account for changes in these sediment characteristics from borrow areas to beach placement sites. Dredging operations via Trailing Suction Hopper Dredges (TSHDs) for beach and nearshore placement typically include periods of overflow, which is recognized to produce some degree of separation between the size fractions of the dredged sediment. The degree of separation and the controlling factors are the subject of this research. This report assembles prior research of sediment separation by hopper dredges and describes a field sampling campaign aboard a TSHD in which collected samples were used to define the fines content at the varying stages of the dredging process from borrow site to hopper to beach. The field study conducted at the Ship Island Restoration Project near Biloxi, Mississippi, produced the following findings:

- The fines content reduced sequentially from the borrow area, hopper, and beach. Hopper overflow removed 61% of the fine-sediment mass contained in the borrow area, and beach outwash removed 67% of the fines contained in the hopper. These two losses combined accounted for a removal of 87% of the fines dredged from the borrow area. Of the fine-sediment mass removed, 70% was removed by the overflow process, and 30% was removed by beach outwash.
- Mud aggregates were observed in most of the loads sampled. Aggregates were present in all sample locations: inflow, hopper, and beach. Mud aggregates were composed of 20% sand, 53% silt, and 28% clay. The mud aggregate material has a Unified Soil Classification System classification of CH, a fat clay with sand. Millimeter-scale and larger mud aggregates settle as fast as or faster than sand and are consequently prone to sedimentation in the hopper and on the beach. The packaging of fine sediment in aggregates represents a hindrance to the separation mechanisms of hopper overflow and beach outwash that would otherwise remove large fractions of the constituent particles of silt and clay. The fraction of fines content represented by the mud aggregates is unknown, but fraction of fines removed from the dredging operation would have been greater if the mud aggregates had been broken up by the dredging and placement operations.
- Associated with the loss of fine-sediment content was a lightening of the sand from the borrow area to the beach. The wet Munsell Value changed from 3.8 to 4.4 from the hopper inflow to the beach. Fine-sediment content and beach color are closely linked by the pronounced effect that a small fraction of typically dark fine sediment has on an otherwise light-colored quartz or carbonate sand. Berkowitz et al. (2019) have developed a laboratory testing method to express Munsell Value for beach sand with varying fine-sediment content. The approach agrees well with observed values of this study but requires additional evaluation and validation data prior to widespread application in practice.
- Knowledge of the relative loss of fine sediment associated with specific dredging process has strong potential for use in future project design. With this additional information, project engineers could design operations 1) to control the loss of fines near sensitive habitats or 2) to modify dredge operation to increase/decrease loss of fine sediment at a particular location.
- The data from the present study, combined with that of Coor and Ousley (2019) provide project managers with defensible fractions of fine-sediment loss from hopper dredging and placement operations for borrow areas ranging in fine-sediment content from 1% to 25%. With such an extensive data set available, conservative estimates of the change in fine-sediment content are possible.

- Predictive tools (in the form of those described by Spearman et al. [2011] and Boone and de Nijs [2018]) that model the separation of sand and fines should be considered to estimate the potential change in fine-sediment content of borrow area sediments caused by overflow. These predictive tools, with proper validation, could also be applied to investigate alternate dredging operation controls to increase or reduce fines loss at various stages of dredging and placement.
- The currently accepted protocols for ensuring sediment compatibility for beach fill sediments is commonly a qualitative process. The results of this study, combined with the work of others (Ousley et al. 2014, Coor and Ousley 2019, Berkowitz et al. 2019) indicate that a more quantitative approach is possible and should be developed to predict changes in sediment characteristics for shore protection, habitat, and aesthetic concerns. Such an approach, applied with the appropriate, scientifically backed precautions is the best way to ensure the appropriate use of sand resources in the coastal system.

1 Introduction

In shore protection, ecosystem restoration, and navigation projects, coastal project managers are required to ensure that sediment dredged from source areas (e.g., offshore borrow site, navigation channel, inlet complex) is compatible with the sediment characteristics at the placement site (e.g., the beach or nearshore). Compatibility factors to consider include sediment grain size, composition, sorting, and color (Dean 2003). Additionally, some state regulations across the nation (for example, Florida's "Sand Rule") specify allowable thresholds for fractional content of fine sediment (FDEP 2010; FL Admin. Code r. 62B-41.007(2)(j)). The definition of fine sediment may differ from state to state; however, it is generally recognized as either the sediment passing the #200 (75 μm) sieve, in accordance with the Unified Soil Classification System (USCS), or the material passing the #230 (63 μm) sieve in accordance with the Udden-Wentworth scale. The work herein uses the latter classification.

Nearly all direct beach placement work is performed with trailing suction hopper dredgers (TSHDs) or hydraulic cutterhead pipeline dredging. When determining compatibility between the source sediment and the native sediment, textural properties (e.g., sorting, mean grain size, and percent sand) are typically assumed to remain unchanged from the borrow area, through dredging and conveyance, to the placement site. However, it is generally recognized that hopper dredges implementing overflow (the intentional discharge of supernatant water) coarsen their load relative to the source material through preferential loss of fine sediment suspended in overflow. The gain in hopper load through this process is commonly called *economic loading*. Additional loss of fine sediment can occur during pumpout operations at the beach.

Presently, application of regulations such as Florida's "Sand Rule" do not consider any possible coarsening of the sediment load, change in color, or removal of fine-sediment content through the dredging process when assessing sediment compatibility. A revised practice which includes the effects of dredging processes on sand compatibility is likely to have an additional benefit of increasing sand resources available for beach nourishment.

The coarsening of dredged sediments by the practice of hopper overflow is well established. Taney (1965) described an "unexpected benefit" of a pumpout test of the TSHD *Comber* near the mouth of Chesapeake Bay. In this testing, the dredged material contained 20% fines (<75 μm), and the pumpout material, according to Taney, "contained practically no silt or clay." More specifically, the size distributions presented by Taney suggest that more than 99% of the sediment finer than 0.2 mm was removed. Hobson and James (1978) note that fine-sediment losses during dredging and pumpout are commonly observed in the turbid plumes present in the overflow and at the beach placement site. Hobson and James document two cases (New River, North Carolina, and Rockaway Beach, New York) where significant coarsening of the beach material was observed between the borrow area, the barge, and the beach. The authors conclude that the changes in mean size and sorting should be factored in the beachfill design and offer a method for predicting such changes based on their data from their two study sites. Much of the more recent work on the separation of sediment sizes by hopper overflow has focused on the concentration and characteristics of fine sediment in the overflow (Nichols et al. 1990, Miedema and Vlasblom 1996, Mikkelsen and Pejrup, 2000).

Two recent studies have returned focus to the load-coarsening effect of fine-sediment losses associated with the dredging process (Ousley et al. 2014, Coor and Ousley 2019). These two studies quantified the total loss of fine sediment by examining sediment size distributions of borrow area and beach sediment sources for 71 dredging and shore protection projects. Coor and Ousley conclude that the mean change in fine-sediment content for source material with 0.86%–25% fines was approximately 75%.

Whereas the prior work of Coor and Ousley (2019) quantified the percent change in fine sediment between the borrow area and beach placement site, the relative losses attributed to overflow versus beach outwash could not be determined. Thus, a field study was executed to determine the fine-sediment ($< 63 \mu\text{m}$) content at the borrow site, in the hopper dredge's settled bed, and on the beach. Thus, the primary objective of this work is to determine the size-dependent loss of sediment at each stage of the dredging process for beach nourishment projects through direct sampling aboard a TSHD and the beach immediately following placement.

The approach of this research entailed three phases. First, pertinent literature was reviewed to develop a conceptual model that includes the potential points in the dredging and placement process where size-dependent separation of sediment can occur. Based on the conceptual model, options for general sampling and analysis were developed. Sampling methods that were either critical or untested were laboratory tested to ensure low bias. A field sampling plan was then developed and executed based on the findings of the laboratory testing.

Herein, Section 2 provides background information regarding the study site, the TSHD utilized in the field campaign, and a basic overview of TSHD processes. Section 3 describes the sampling methods used in the field, laboratory and data analyses, and methods to quantify uncertainties. Section 4 presents the results of the field sampling campaign. Section 5 assesses the sampling and analysis approach with recommendations for future studies and considers the results in the context of dredging practice and beach placement policy. Section 6 concludes the report with a summary of conclusions drawn from this work. The conceptual model and laboratory testing phases of the work are summarized within the main body of this report; however, the full details are included in Appendices A and B.

2 Background

The USACE dredging schedule for beach nourishment and channel maintenance dredging was searched for project sites with hopper dredging and beach placement of sandy sediment with fines content of 5% or greater. Projects with borrow area fines content at the upper end of present practice were sought to better represent the sediment sorting processes of sediment with higher fines content, which presently are seldom approved for beach placement under existing regulation and practice. Ship Island Phase 1 of the Mississippi Coastal Improvements Program (MSCIP) Barrier Island Restoration Project was selected for field sampling. This project has multiple borrow areas with sampled fines contents greater than 4%. This section describes the study site, the TSHD sampled, and an overview of basic TSHD processes.

2.1 Site Description

2.1.1 Study Site

The field sampling campaign was conducted 20 June through 01 July 2018 on Ship Island and aboard the Great Lakes Dredging and Dock (GLDD) TSHD *Liberty Island*. For the duration of the sampling study, the *Liberty Island* dredged from a borrow area in Horn Island Pass and placed to the beach at the western end of East Ship Island (Figure 1). At the time of the field study, GLDD's TSHD *Ellis Island* was also active, dredging from borrow sites farther east, but discharging to the same locations on the beach at Ship Island. Additional details of the borrow area, dredge, and sampling are presented below.

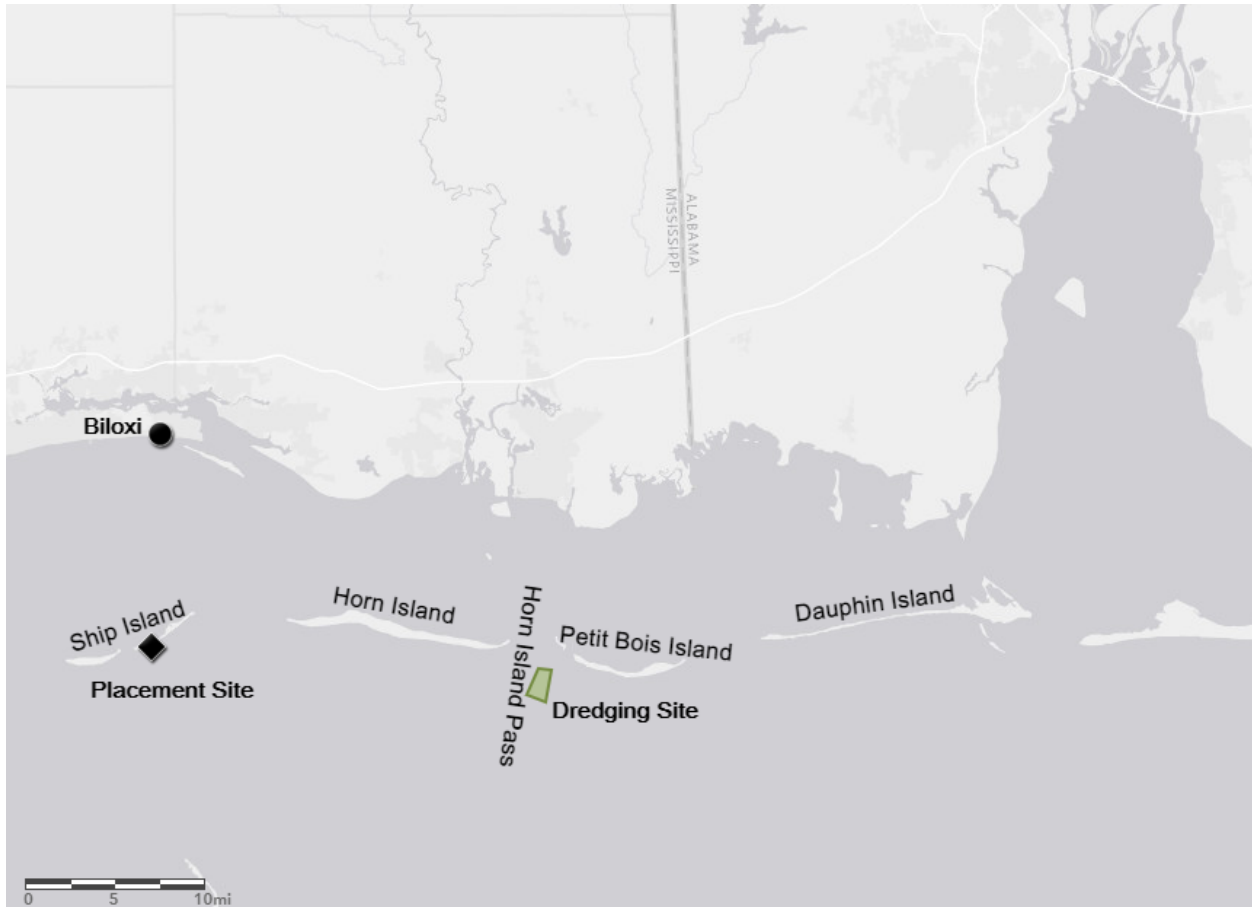


Figure 1. Site map of the MSCIP-Ship Island Phase 1 restoration project.

Horn Island Pass is located between Horn Island on the west and Petit Bois Island on the east (Figure 1). The Pascagoula Bar Channel provides navigation access through Horn Island Pass. The geotechnical investigation (FitzHarris and Godsey 2014) of the Mississippi Coastal Improvements Program Barrier (MSCIP) Island Restoration Project identified sand sources suitable for beach placement to the west of Horn Island Pass (Figure 2). FitzHarris and Godsey indicate that the sand sources at Horn Island Pass are located at the site where sediments dredged from the Pascagoula Bar Channel were formerly placed. (The dredged material placement sites are no longer in active use.) Three borrow areas are designated within the area as Horn Island Pass 1–3. Horn Island Pass Borrow Area 1 (HIP1) was the borrow site exclusively used by the *Liberty Island* over the course of the sampling study. HIP1 encompasses an area of approximately 680,000 m² (170 acres).

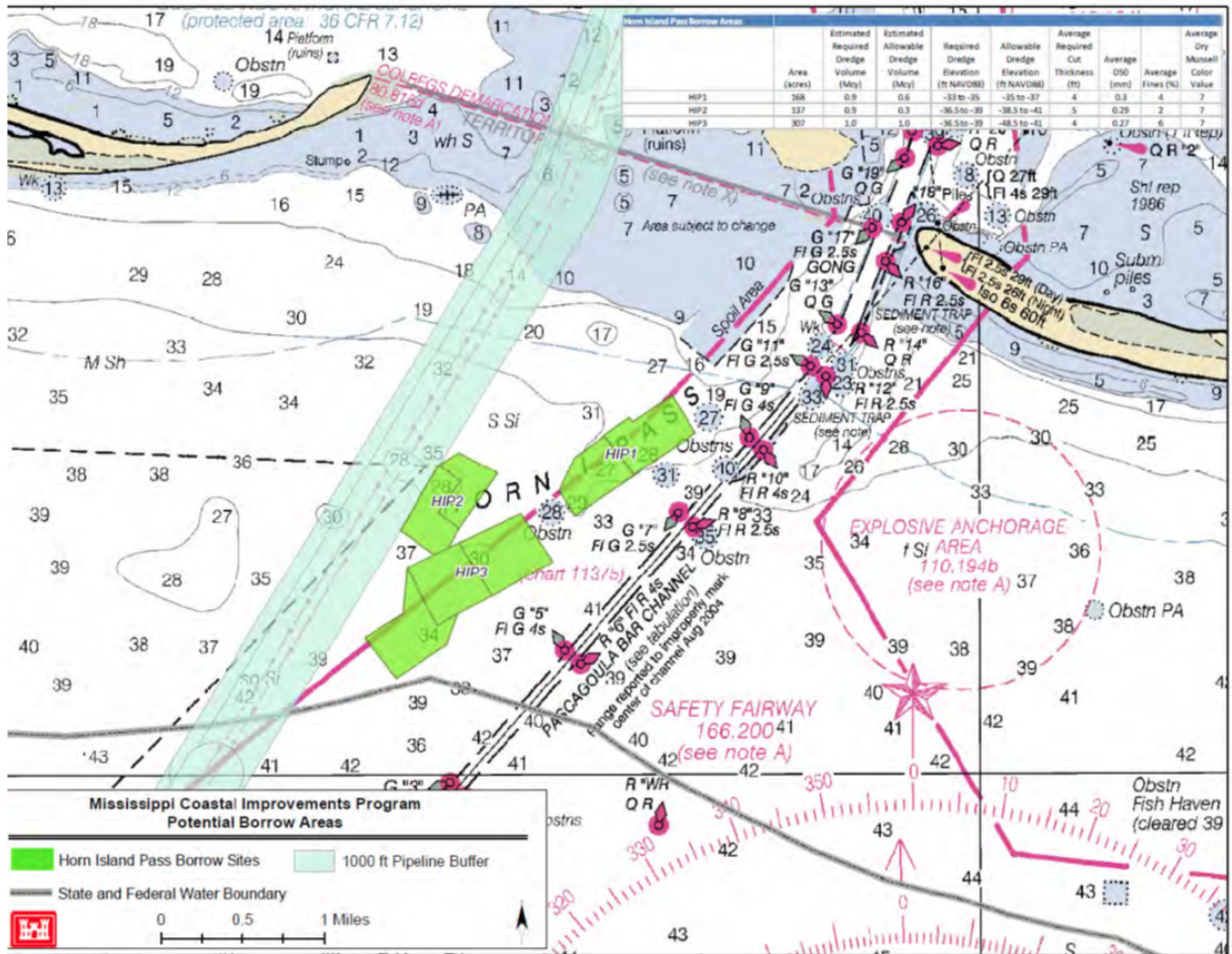


Figure 2. Horn Island Pass Borrow Areas 1–3.
 Source: FitzHarris and Godsey (2014). The borrow area of this study is HIP1.

2.1.2 TSHD Liberty Island

The trailing suction TSHD *Liberty Island* (Figure 3, Table 1) is operated by GLDD. During loading, the port and starboard dragheads remove sediment from the borrow area, and the sediment slurry is pumped through the dragarms and into a discharge box located centrally over the hopper. Flow from the discharge box issues both forward and aft toward the rectangular overflow weirs positioned near the fore and aft ends of the hopper. Settleable solids are retained in the hopper and suspended sediments are allowed to flow over the weir. Typical operation involves making long, continuous passes longitudinally through the borrow area. Frequently, more than one pass is required to fill the hopper. When turning is required, sediment loading is suspended during the turning maneuver. Upon achieving an economic load, the loaded dredge steams to the pumpout station and makes connection with the pipeline; then, the sediment load is slurried within the hopper and pumped to the beach through a pipeline. At the beach, dredged material exits the pipeline through a diffuser at the outfall and onto the receiving area of the beach. For the present beachfill operation, a barrier island cut is being filled. Because the fill is being placed without an existing beach slope, there is no need to construct berms to train the pipeline outwash to follow the shoreline. Within the outwash zone, settleable solids deposit on the beach and water, and a portion of the suspended fine sediment flows into the sea.



Figure 3. The TSHD *Liberty Island*.

Source: Great Lakes Dredge and Dock.

Table 1. The TSHD *Liberty Island* dimensions and operating parameters.

Basic Statistics	<i>Liberty Island</i>
Length	315 ft (96.0 m)
Breadth	59 ft (18.0 m)
Depth	28 ft (8.5 m)
Draft	28.3 ft (8.6 m)
Dredging Depth	108 ft (32.9 m)
Suction Diameter	31.5 in (800 mm)
Discharge Diameter	30 in (762 mm)
Hopper Capacity	6,540 yd ³ (5,003 m ³)
Total Installed Power	16,566 hp (11,612 kW)

2.2 TSHD Processes

The TSHD dredging process begins with sediment being drawn from the seabed by hydraulic forces into the draghead (Figure 4), through the dragarm, into the hopper. Once in the hopper, sediment with relatively fast settling velocities settles to the hopper bed. Finer sediment, with slower settling velocities, is unable to completely settle to the hopper bed and much of this finer sediment is transferred back to the water column via overflow. The sediment retained in the hopper is then transported by the TSHD to the pumpout station where the load is pumped via pipeline to the beach. During the dredging and placement processes, several sediment losses occur (Figure 4). These losses are the primary mechanisms by which

finer and coarser sediments are separated, resulting in changes in material composition between the borrow area and the beach. The relationships between the point of the TSHD dredging process and sampling points will be described in Section 3.

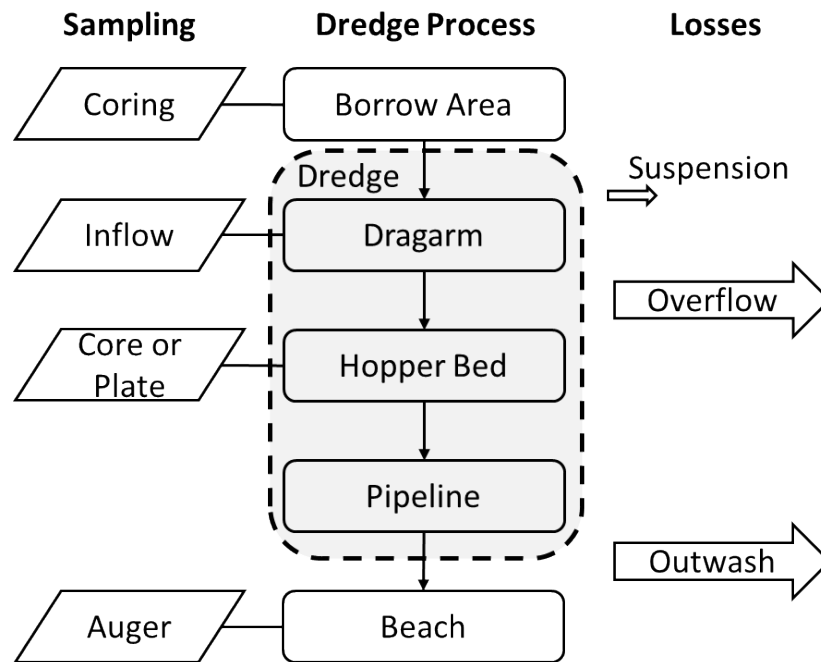


Figure 4. Process diagram with sediment sampling and loss points.

Sediment moved through the dragarm, hopper, and pipeline are considered part of the dredging process. Overflow and outwash are considered the primary loss mechanisms for fine sediment. Sampling points are selected to quantify the changes in fine-sediment content through the dredging process.

2.2.1 Modeling

Hoppers can be considered as large capacity settling tanks with an inflow and outflow. Much of the work on sedimentation within settling tanks was originally developed for the wastewater treatment industry. The ensuing theories were developed primarily for the purposes of removing suspended fines or ‘clarifying’ the water column through the settling process. Reference is made to Camp (1936, 1946) and Dobbins (1944), whose theory on sedimentation (rooted in the work of Hazen [1904]) within ideal settling tanks is often regarded as the basis for settling theory and overflow losses within TSHDs.

Vlasblom and Miedema (1995) and Miedema and Vlasblom (1996) further modified Camp’s model to incorporate grain size distribution, hindered settling effects, and a rising bed level. The model of Ooijens (1999) adds to the Miedema and Vlasblom (1996) model by introducing an unsteady state in flow volume and slurry concentration to estimate overflow losses considering the hopper as an ideal mixing tank. Van Rhee (2001, 2002) used both laboratory experiments and numerical modeling to investigate the hopper sedimentation process. The laboratory experiments delineated characteristic flow and sediment transport zones within a model hopper consisting of a settled sand bed, density flow over the bed, horizontal surface flow toward the outlet (overflow section) and sediment suspension. The one-dimensional model of hopper sedimentation was developed using the advection-diffusion equation for a poly-disperse mixture and includes the influence of the overflow rate. As opposed to the horizontal settling tank model of Camp, this model simulates hopper loading in the vertical dimension with sediments introduced from

the bottom fed by the density current, and the overflow located at the top. The model was compared with one-dimensional tests in a settling column which showed reasonably good agreement (Figure 5). Van Rhee (2002) later developed a 2D model based on the Reynolds-Averaged Navier Stokes equations with a $k\epsilon - \epsilon$ turbulence model. The modeled overflow losses compared similarly to the simplified Camp model of Miedema and Vlasblom (1996).

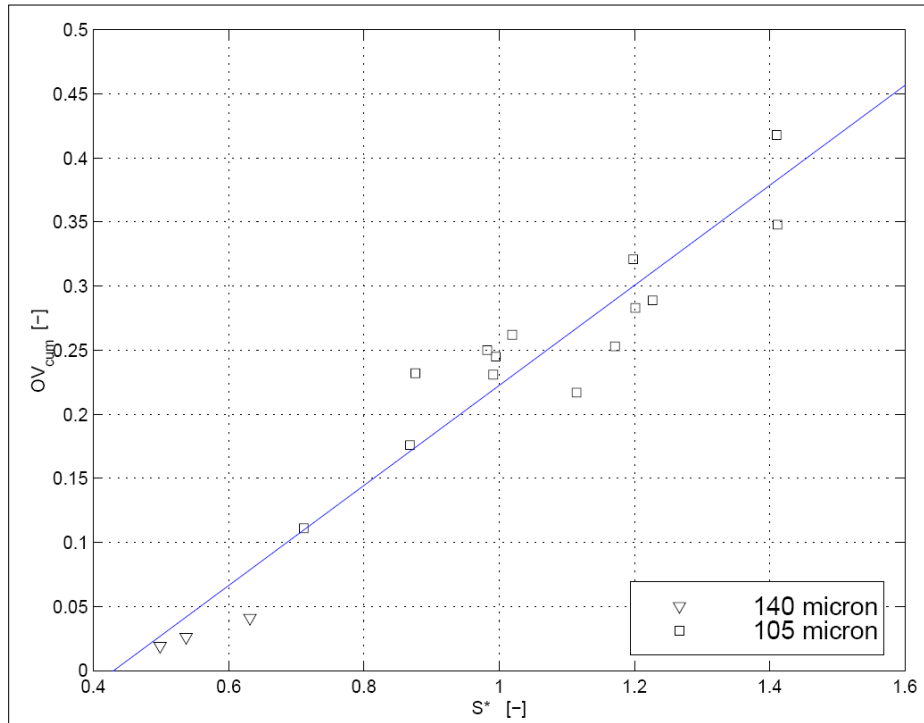


Figure 5. Cumulative overflow losses as a function of the dimensionless hopper load parameter. Based on sand fluxes. Adapted from van Rhee (2001).

The one-dimensional vertical and horizontal models of Spearman et al. (2011) and Boone and de Nijs (2018) account for sediment exchange between the bed and water column and are used to predict overflow concentrations with little computational effort.

The above models are used to quantify overflow losses in terms of the effect on production (i.e., the total mass of sediment lost per hopper load) or predict the sediment concentrations of the overflow plumes released into the ocean. However, the fraction of fines lost cannot be determined without knowledge of the particle size distributions (PSDs) at various points in the dredging process, which requires direct sampling.

3 Methods

Sampling was configured to quantify the fines content at the various stages of the dredging process. The greatest losses are associated with hopper overflow and beach outwash (Figure 4). The sampling scheme was developed to quantify the fines content at the beginning (borrow area or dragarm inflow), the intermediate stage (hopper bed), and the final position (beach). Section 2 and Appendix A provide

detailed descriptions of the dredging process and the physical and mechanical processes associated with each loss term. Details of the specific sampling and analysis methods applied in this research study are provided below.

3.1 Sampling

Prior to executing the field campaign, sampling and analysis methods were evaluated through controlled laboratory and numerical experiments to determine suitable field sampling procedures on a TSHD. Details of the testing of sampling methods are provided in Appendix B. The findings the sample-method testing included the following: 1) compositing of samples is appropriate for beach, hopper, and inflow sampling; 2) hydraulic sample splitting of samples containing sand is not recommended; and 3) two hopper bed sampling methods were recommended for the field campaign. The resulting sampling and analysis methods used in the field campaign are described below.

3.1.1 Fines Content of the Horn Island Pass Borrow Area 1

Twenty-foot-long vibracore samples were collected within HIP1 in 2010–2013 to define sediment characteristics for the MSCIP project (FitzHarris and Godsey 2014). The core barrels were split longitudinally and field-classified by an onboard geologist or geotechnical engineer. Samples were extracted from the cores in the upper horizons and in layers with distinctly different sand texture and/or color. If a two-foot or deeper layer of fine sediment was encountered, the sediment below that horizon was generally not considered for beachfill and consequently was not sampled for analysis. The physical properties of samples recovered from HIP1 are presented in Table 2. The analyses of these data for size compatibility, color compatibility, and fines content informed the designation of the site boundaries shown in Figure 2 and the cut elevations of -10 m for the northern half of the site and -10.7 m for the southern half of the site. The average cut depth for HIP1 is 1.2 m. The average fines content of all HIP borrow areas is 4.4%.

Table 2. Geotechnical properties of samples recovered from HIP1.

Sample ID	Year Collected	Latitude	Longitude	Elevation (m) NAVD88	Thickness (m)	Field USCS	Lab USCS	Wet Munsell Color Code	Wet Munsell Value	D50 (mm)	Fines Content (%)
BI-HP-9-10A	2010	30.19274	-88.54668	-11.0	0.4	SM	SM	2.5Y 3/2	3	0.23	12.7
BI-HP-10-10A	2010	30.19288	-88.54127	-9.7	0.9	SP	SP	2.5Y 4/2	4	0.29	3.2
BI-HP-10-10B	2010	30.19288	-88.54127	-10.5	0.9	SP	SP	2.5Y 4/1	4	0.26	3.5
BI-HP-15-10	2010	30.18942	-88.53846	-11.0	5.5	SC	-	-	-	-	-
BI-HP-18-10	2010	30.19567	-88.54340	-10.7	4.6	SC	-	-	-	-	-
BI-HP-25-10A	2010	30.18788	-88.54330	-10.6	0.8	SP	SP-SM	2.5Y 5/2	5	0.25	5.4
BI-HP-26-10A	2010	30.19048	-88.54306	-10.1	1.2	SP	SP	5Y 5/2	5	0.25	2.1
BI-HP-27-12A	2012	30.19757	-88.53702	-8.8	1.1	SP	SP	2.5Y 7/1	7	0.33	1.6
BI-HP-27-12B	2012	30.19757	-88.53702	-10.0	0.7	SP-SM	SP-SM	2.5Y 5.5/2	6	0.30	7.4
BI-HP-28-12A	2012	30.19687	-88.53180	-9.2	1.7	SP	SP	2.5Y 8/1	8	0.34	1.2
BI-HP-28-12B	2012	30.19687	-88.53180	-10.9	0.2	SP	SP	2.5Y 6/1.5	6	0.21	4.7
BI-HP-29-12A	2012	30.19422	-88.53372	-9.8	0.3	SP	SP-SM	2.5Y 6/2	6	0.32	6.7

Sample ID	Year Collected	Latitude	Longitude	Elevation (m) NAVD88	Thickness (m)	Field USCS	Lab USCS	Wet Munsell Color Code	Wet Munsell Value	D50 (mm)	Fines Content (%)
BI-HP-29-12B	2012	30.19422	-88.53372	-10.1	0.8	SP	SP	5Y 6/2	6	0.28	1.3
BI-HP-29-12C	2012	30.19422	-88.53372	-10.9	0.5	SP	SP	2.5Y 7/1.5	7	0.29	1.9
BI-HP-30-12A	2012	30.19495	-88.53765	-8.9	0.7	SP	SP	2.5Y 7/2	7	0.31	4.5
BI-HP-30-12B	2012	30.19495	-88.53765	-9.6	0.9	SP-SM	SP	2.5Y 6/2	6	0.27	3.4
BI-HP-30-12C	2012	30.19495	-88.53765	-10.5	0.8	SP	SP	2.5Y 5.5/2	6	0.32	1.7
BI-HP-38-12A	2012	30.19947	-88.53510	-9.1	1.1	SP	SP-SM	5Y 5/2	5	0.30	5.3
BI-HP-41-12A	2013	30.1987	-88.53372	-8.6	0.5	SP	SP	2.5Y 7/1	7	0.32	1.9
BI-HP-41-12B	2013	30.1987	-88.53372	-9.1	0.8	SP	SP-SM	2.5Y 5/2	5	0.29	6.4
BI-HP-41-12C	2013	30.1987	-88.53372	-9.9	0.9	SP	SP	2.5Y 6/2	6	0.28	4.1

Source: FitzHarris and Godsey (2014)

The fines content of each dredge load was estimated by spatial analysis of pre-project samples (FitzHarris and Godsey 2014) and the ship track of the dredge for each load. Twelve 6-m-long vibracore samples were extracted from the HIP1 borrow area during the period 2010–2012. Core spacing ranged from 150–600 m within the borrow area (Figure 6). For each core location, the fines content was averaged over the total thickness of the dredge cut by linear weighting of the fines content and subsample thickness. The area surrounding each core location was divided by Thiessen polygons to prescribe a representative area for each sample (Figure 6). Ship tracks while the *Liberty Island* was actively dredging were provided by the USACE National Dredging Quality Management Program (DQM). These ship tracks consist of a series of vessel positions at a 6-sec interval. Each position was associated with a Thiessen polygon, and the fractional distribution of positions within each polygon defines the linear weighting of fines content in each associated geotechnical sample. The fines content of each load was estimated by:

$$f_{L,BA} = \frac{\sum f_i N_i}{\sum N_i} \quad (1)$$

where f_i is fines fraction of each sample, and N_i is the number of positions within the i -th polygon. For the example provided in Figure 6, the distribution of positions by representative core and the depth-averaged fines content are provided in Figure 7. The resulting load-averaged fines content for this example is 3.4%. Assumptions applied in the above approach include the following: 1) the fines content surrounding each coring location is spatially uniform, 2) the fines content has not appreciably changed since time of sampling, 3) the sediment loading rate while dredging is constant, and 4) losses at the draghead are negligible.

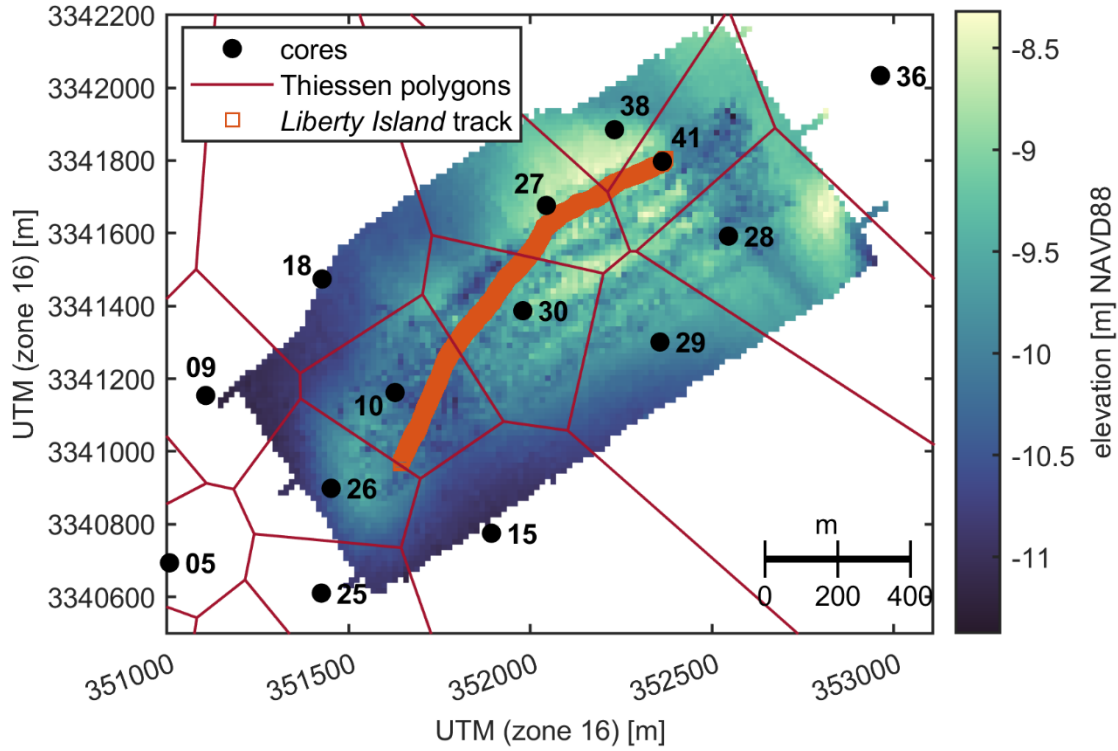


Figure 6. Borrow Area HIP1.

Shaded color indicates the 20 Jun 2018 condition survey. Vibracore positions and core IDs are given in black.

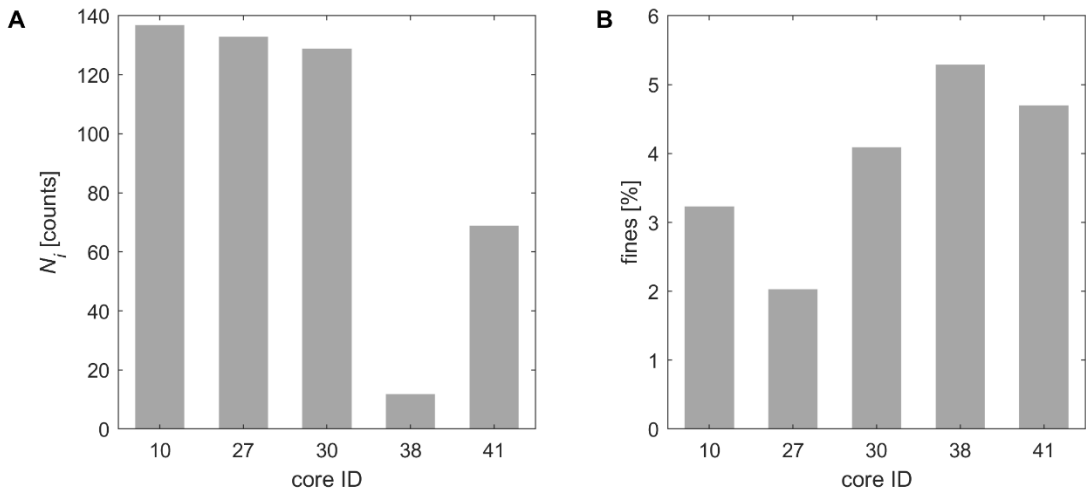


Figure 7. Distributions of vessel dwell time and percent fines.

Distribution of A) position counts and B) fines content by core ID from the example provided in Figure 6. The resulting load-averaged fines content is 3.4%.

3.1.2 Fines Content of the Dredge

Sediments were collected from the dredge to characterize the change in fines content at various points in the dredging process. A brief overview of the sampling locations on the dredge plant is provided here to

familiarize the reader with the spatial relationships between the sampling locations and dredge layout. Detailed discussions of the sampling procedures for corresponding sampling points follows.

Sampling points within the dredge plant consisted of the hopper inflow, the hopper bed, and the remaining ponded water overlying the hopper bed after dredging ceased (referred to herein as the scour pool). The purpose of the inflow sampling was to quantify the fines content entering the hopper from the borrow area. Sampling the sediment retained in the hopper allows for quantifying the change in fines content due to overflow losses and for comparing the change in fines content between the dredge plant and the beach placement site. Finally, sampling of the scour pool allows for adjustments to be made (if necessary) to the fines content of the hopper not captured during bed sampling. These sampling points were deemed sufficient to quantify the fines content through the dredging process, thus the overflow weir was not sampled. All sampling occurred from the catwalk of the main deck. A schematic diagram of the sampling locations is provided in Figure 8.

A total of 11 dredge loads were sampled, one per day, from 20 June–01 July, 2018. Specific times and durations are provided in Table 3; no sampling occurred for 27 June due to refueling. Recording the start and end times of the loading cycle was necessary to cross-reference with the dredge’s DQM data for borrow area characterization. Dredging fill times (load durations) were approximately one hour, except for loads 5–7 where the dredge plant was operating with only one dragarm requiring multiple passes through the borrow area.

Table 3. Dredge plant *Liberty Island* load sampling dates and times.

Date (2018)	20 June	21 June	22 June	23 June	24 June	25 June	26 June	28 June	29 June	30 June	1 July
Load no. ID	1	2	3	4	5	6	7	8	9	10	11
AM or PM	AM	PM	AM	AM	AM	PM	AM	AM	AM	PM	PM
Load start	10:50	12:25	9:45	10:40	9:32	13:05	10:28	10:15	10:07	13:11	13:05
Load end	11:40	13:35	10:45	11:45	11:35	15:35	12:55	11:10	10:57	14:15	14:12
Load duration	0:50	1:10	1:00	1:05	2:03	2:30	2:27	0:55	0:50	1:04	1:07

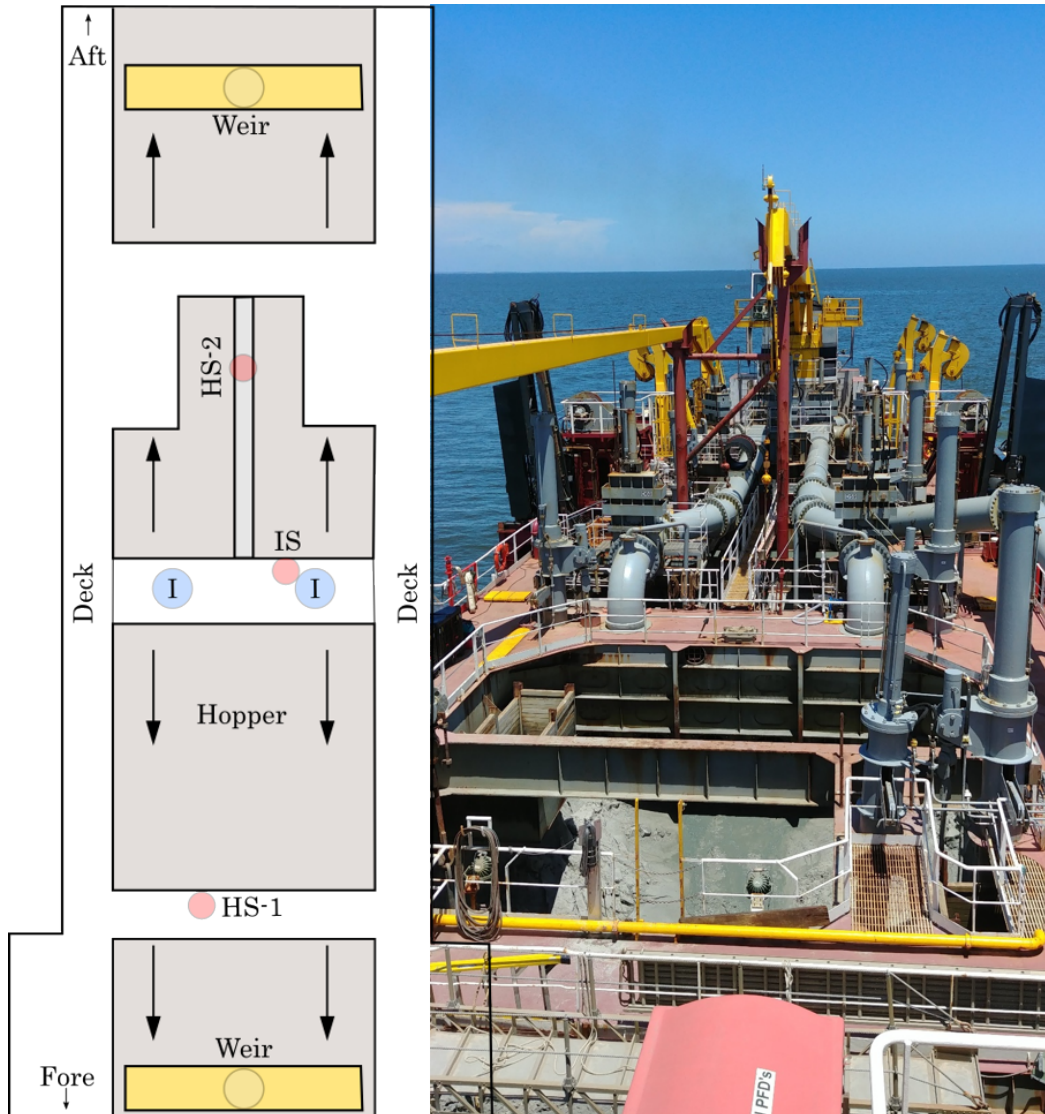


Figure 8. Schematic diagram of sampling locations on the *Liberty Island*.

Red dots indicate sampling locations (HS=hopper station; IS=inflow station; I=inflow pipes). Arrows represent general flow paths toward the two overflow weirs.

3.1.2.1 Inflow

The dredge inflow pipes terminate into screened discharge boxes to prevent large debris from passing into the hopper and to enable protected species observers to identify and quantify dredging “takes” of entrained organisms. The inflow sediments were pulled from one location at the bottom of the port-side discharge box via pump sampling (Figure 9).

The equipment used to sample the inflow consists of an intake assembly, a sampling assembly, and trash pump to supply suction. The intake assembly is a 3-m-long section of 5-cm (2-inch) galvanized pipe, fitted at the bottom with a 15-cm (3-inch) diameter screened intake nozzle. The sampling assembly consists of a vertical section of 15-cm plastic pipe with a primary discharge port at the top, and a 1.9-cm ($\frac{3}{4}$ -inch) sampling port located just below the primary discharge. Connected to the sampling port was a length of hose designed to reduce the discharge volume while maintaining an equivalent flow velocity to

facilitate sample collection. The trash pump used was a Honda-powered, 5-cm (2-inch) centrifugal trash pump capable of passing solids up to 2 cm in diameter. The pump was flushed clear of sediments prior to sampling and operated continuously throughout the loading cycle.

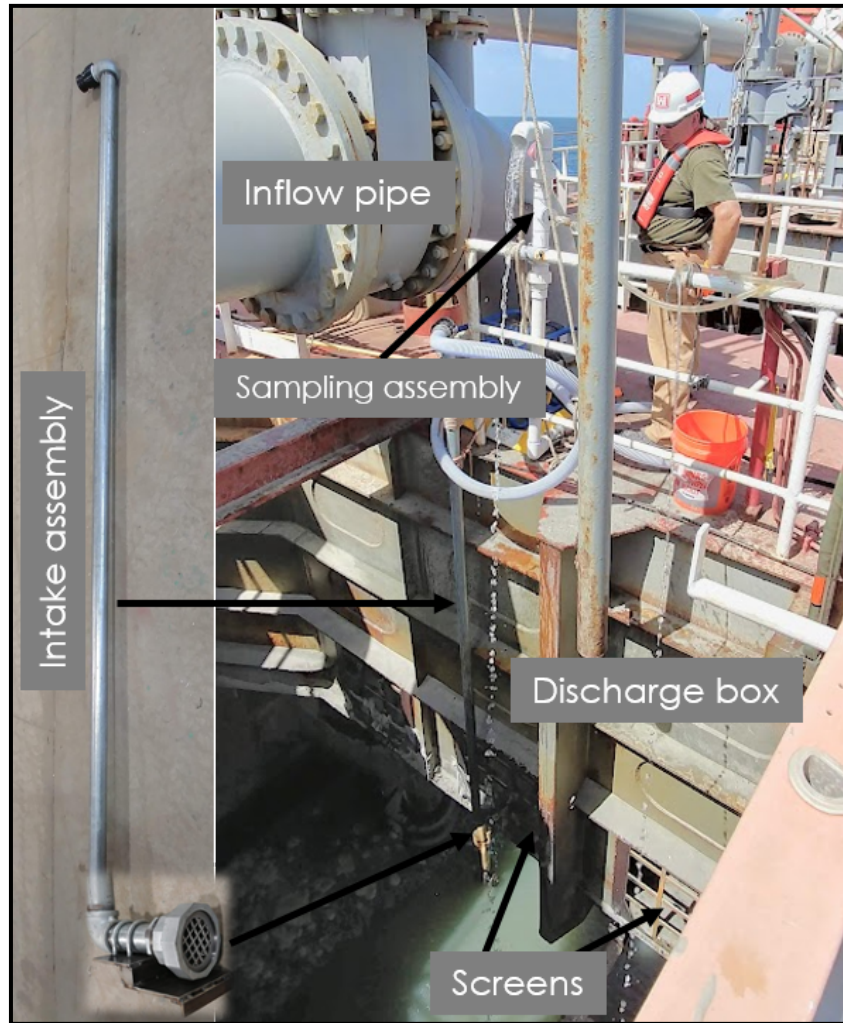


Figure 9. Sampling assembly used to collect hopper inflow samples.

Sample collection from the 1.9-cm hose was abandoned in favor of sampling directly from the discharge port after it was quickly realized that the pump could not maintain prime due to air entrainment (even when the discharge box was submerged). The resulting reduction in flow caused the sampling port hose to be clogged with sediment very soon after dredging commenced. To maintain prime, it was necessary to operate the pump at idle speed. Using the time to fill a 19-L (5-gallon) bucket, the measured flow rate was estimated at 3.8 L/s (60 gpm). At this discharge, the velocity through the 5-cm pipe is sufficient to keep sediments in suspension for the encountered sediment sizes.

Samples were collected by passing a 1-L Nalgene bottle directly through the flow using one controlled motion (Figure 10). Laboratory testing (Appendix B) showed that sediment concentrations derived from bottle sampling were statistically indistinguishable from those derived from more controlled sampling devices.



Figure 10. Bottle sampling method used to collect hopper inflow sediments.

Sampling began approximately 1 minute after the water from the discharge port went visibly dark and thereafter at the rate of one sample per minute. In the event the bottle was overfilled that sample was discarded. Retained volumes ranged from approximately 0.5-0.75 L/sample. Samples were composited into 19-L buckets throughout the loading cycle. Sample volumes collected per load ranged from 23–30 L. Inflow sediment concentrations by volume are usually on the order of 0.15–0.30, yielding several kilograms of sediment per load for analysis.

3.1.2.2 Hopper bed

Sediment mass may be contained in as many as three distinct zones within the hopper: 1) the settled sandy bed, 2) a fine, high-concentration suspension just above the sandy bed, and 3) in suspension as depicted in Figure 11. The approach for quantifying the sediment fractions in the hopper is to treat the setting as a column of sediment and water in a three-phase system as illustrated in Figure 11. Layer 1 is the settled, sandy bed, Layer 2 is the thin layer of fines settled from suspension, and Layer 3 is the sediment suspension above the bed. The mass of fines and sand per unit area can then be determined as follows:

$$m_f = f_{f,1}C_1L_1 + \frac{f_{f,2}M_2}{A_2} + f_{f,3}C_3L_3 \quad (2)$$

$$m_s = f_{s,1}C_1L_1 + \frac{f_{s,2}M_2}{A_2} + f_{s,3}C_3L_3 \quad (3)$$

where,

- m = sediment mass per unit area
- C = sediment mass concentration, mass per unit volume
- f = mass fraction of a given constituent
- M = total sediment mass
- A = sample cross-sectional area

- L = layer height
 $f_{,s}$ = subscripts indicating fine or sand, respectively
 $1,2,3$ = subscripts indicating the sediment layer to which the variable is associated

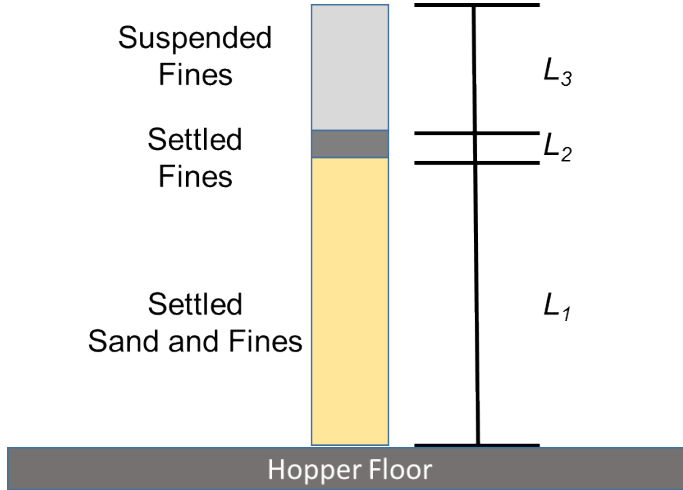


Figure 11. Idealized vertical distribution of sediment at the conclusion of hopper loading.

In the subject study, the settled fines layer (zone 2) was absent and the suspended fines layer (zone 3) was not uniformly distributed over the hopper surface. In this instance, zone 2 is negligible and the thickness of zone 3 was represented as $L_3 = V_{pond} / A_{hopper}$, where V_{pond} is the estimated volume of the scour pool and A_{hopper} is the surface area of the hopper. These approximations result in the following set of equations for fraction of fines in the hopper bed:

$$m_f = f_{f,1} C_1 L_1 + f_{f,3} C_3 \frac{V_{pond}}{A_{hopper}} \quad (4)$$

$$m_s = f_{s,1} C_1 L_1 \quad (5)$$

$$f_{f, hopper} = \frac{m_f}{m_s + m_f} \quad (6)$$

The variables of Equations (4) through (6) were defined during the sampling campaign by the samples and measurements provided in Table 4.

The retained material in the hopper is generally understood to vary in composition related to position relative to the inflow and outflow, hopper hydrodynamics, the bed level of the hopper, changes in sediment properties along the dredging path, and the sediment settling velocity. Longitudinal and vertical variations in sediment composition are expected to be the greater than lateral variation. Therefore, the hopper was sampled both vertically and longitudinally at two locations (HS1 and HS2), chosen to maximize sample representativeness within the limitations emplaced by accessibility and structures within the hopper. The locations were chosen approximately equidistant between the discharge box and the overflow weirs on alternate sides of the hopper, but closer to the vessel's centerline (see Figure 8).

This was done to avoid potential biasing from changing flow conditions in the proximity of the bulkheads and overflow weirs.

The settled bed was sampled using a combination of a shallow gravity corer and a custom plate sampler. The gravity corer was constructed from a push corer (manufactured by Wildco®), which was modified to increase weight and stability by adding a weighted sleeve and stabilizing fins to the main body (Figure 12). The gravity corer was fitted with a 5-cm diameter, 50-cm long, clear plastic core liner fitted with a plastic core catcher. Upon successful capture of a sample, the core liner with retained sample was stored upright for subsequent subsampling (described later), and a clean liner was inserted into the gravity corer.

The plate sampler (Figure 13) consists of a 25-cm diameter outer ring and 10-cm diameter inner disk (the sampling platform), which are connected with an impermeable, flexible rubber membrane. The sampling device is hoisted by a chain bridle connected to three lifting points on the outer ring. To collect a sample, the plate sampler is cast into the hopper and allowed to settle to the hopper bed. The flexible membrane allows the sampler to rest flat on the sediment bed. While resting on the sediment bed, material loading into the hopper buries the plate sufficiently to recover a sample. After waiting a prescribed amount of time (20–40 seconds for this study), the sampler is recovered. The inner disk sampling platform is raised approximately 5–10 cm, and a 5-cm diameter, 2-cm high subsampling ring is pressed through the sandy sample to refusal against the sampling platform (Figure 13B). Sediment surrounding the subsampling ring is cleared from the sampling plate and the sediment surface is screeded flush with the surface of the subsampling ring (Figure 13C). Finally, the sampling ring and subsample are slid onto to a tray (Figure 13D) for transfer to the sample bag. Additional details and laboratory testing of the plate sampler are provided in Appendix B.

Table 4. Sampling and analysis methods for quantifying fines content of the hopper bed.

Variable	Sampling Method	Analysis Method
C₁	Bed core or plate sample, composited	Total dry mass per composite sample volume
C₃	Pump sample	Suspended Sediment Concentration by filtration
f	Bed core/plate, pump	Wash to separate sand/fines dry sieve laser diffraction
V_{pond}	Tape and lead line	Average depth * average area
A_{hopper}	Source: GLDD	-
L₁	Lead line	-

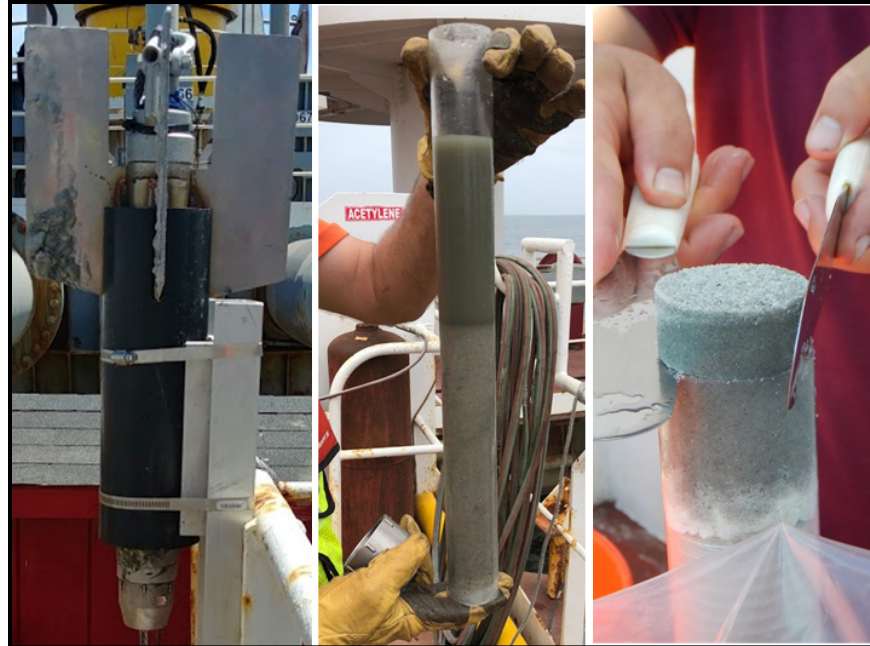


Figure 12. Gravity corer and collected sample.

(Left) gravity corer body, nose piece, and fins while resting in a sleeve fabricated for core processing, (center) core sleeve with retained sample, and (right) subsample collection.



Figure 13. Plate sampling procedure.

(Left) sediment sample recovered from the hopper bed with the plate sampler, (both center) subsampling ring inserted to the sampling platform and clearing of sediment from the sampling platform, (right) recovered subsample (see left hand of the researcher).

The gravity corer was selected as the primary device to sample the bed, while the plate sampler was used as an alternate in the event that sample retrieval was unsuccessful using the corer. Gravity coring devices are not typically used to sample sand-sized sediment due to the high friction of sand against the corer

walls; however, the hopper bed was expected to be fluidized enough to allow for sufficient penetration. The gravity corer was used exclusively for the first five loads, and both devices were used for the remaining loads. The plate sampler was deployed more often through loads 6–11 due to difficulties with sample loss and insufficient penetration depth—it was noted that cores with less than 10 cm of sediment were likely to be washed out upon retrieval. When both samplers were used, the general procedure was to cast the plate sampler in the event that the corer was unsuccessful. Figure 14 shows the distribution of the number of samples collected from each device and implicitly demonstrates the variability in the bed conditions during sampling.

Sampling began approximately 5–8 minutes after the start of dredging to allow enough sediment to accumulate in the hopper to avoid striking hopper infrastructure with the sampling devices. Sampling typically ceased when the hopper bed elevation was such that overflow velocities made sampling unsuccessful. Therefore, sampling durations were typically limited to approximately 30–40 minutes instead of one hour. For normal dredging durations of 1 hour, samples were taken once per 3 minutes; for longer durations (June 24–26), this was increased to one sample per 6 minutes.

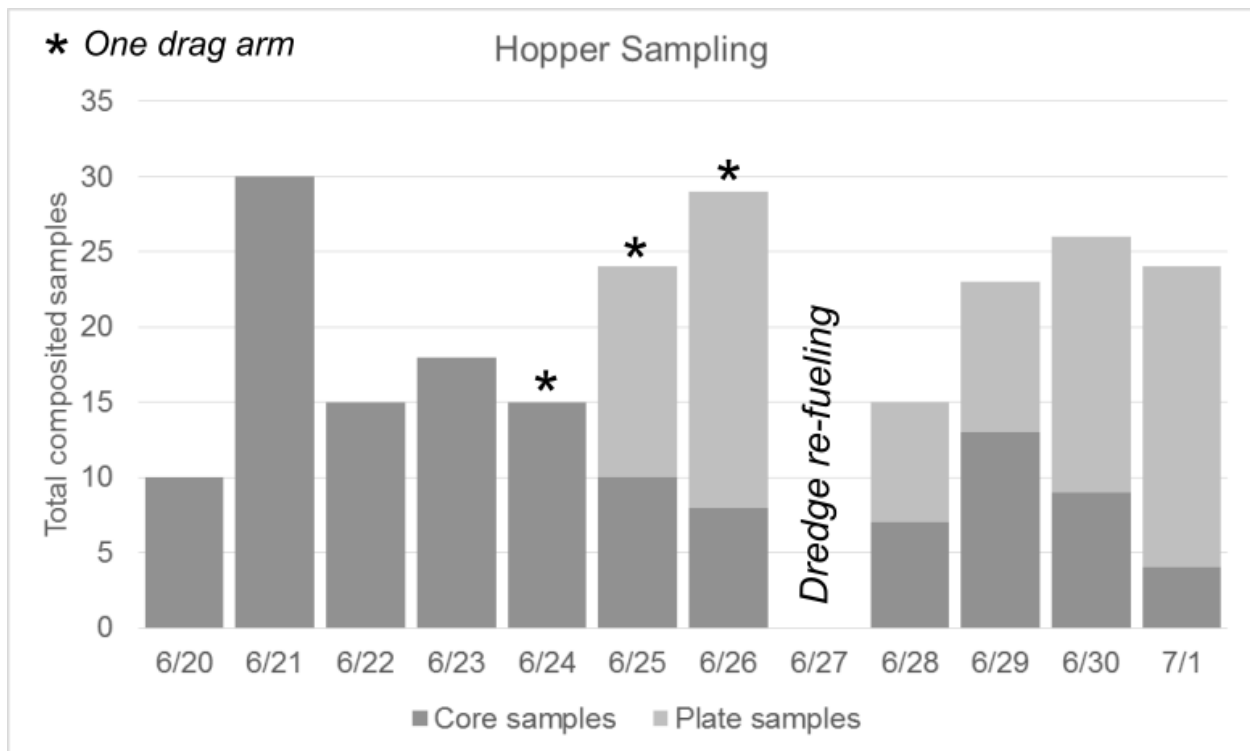


Figure 14. Distribution of hopper bed sampling methods applied to dredge loads.

Retrieved samples were reduced and composited on site by subsampling to a uniform volume. Cores were subsampled using an extrusion device (Figure 15). The upper surface typically had a layer of settled fines from the overlying water retained in the core liner, and therefore the upper 2 cm (at minimum) was always discarded. If the core length was 10 cm or less, the next 2 cm extruded from the core was retained for compositing. If the core was greater than 10 cm, a subsample was collected at a random location within the core. As previously described, a plastic ring, equivalent in volume to that of core subsamples, was used to collect samples from the plate sampler. Composited samples were stored in separate bags for each load and for each device.

An average of 20 samples were collected from each load, but the samples per load ranged from 10 to 30. Based on bed measurements before and after sampling, the average depth of sampling within the hopper was 7 m, giving an average vertical sampling interval of 0.3 m. The sampling range corresponds to a hopper volume of approximately 3,600 m³ (or 72% of its maximum capacity of 5,000 m³). Therefore, the sampling scheme was reasonable for capturing the intended vertical extent and resolution.



Figure 15. The extrusion and subsampling procedure for hopper bed cores

The core is placed in a core extrusion device which allows controlled core extrusions of a set length. The top 2 cm of the core is trimmed and discarded to exclude the settled fines cap. An additional 2 cm of core is extruded from a random position in the remaining core and sampled. These samples are composited in a single bag per dredge load.

3.1.2.3 Scour pool

Sediment discharge from inflow into the hopper resulted in a consistent scour pool that was visible once dredging ceased and the overlying water had drained. The scour pool's contribution to the fraction of fines retained in the hopper was determined by sediment concentration and scour pool volume measurements. At the completion of each load, a 0.5–0.75 L sample was collected into a bottle using the trash pump. The pool volume was estimated by taking multiple area and depth measurements across its two main axes (Figure 16). The pool area calculation was approximated as a rectangle because the port and starboard sides were bounded by bulkhead walls and the depth varied only slightly across transects.



Figure 16. The scour pool at the conclusion of a dredge load.

Image of a scour pool located near the general vicinity of the discharge boxes. HS-1 is the forward location of the hopper sampling station.

3.1.3 Fines Content of the Beach

Samples were collected from the placement area on the beach immediately following dredge pumpout operations, prior to grading the beach to project elevation, to avoid potential mixing of material from the *Liberty Island* with that previously placed by the *Ellis Island* (from a different borrow area). A soil sampling auger with a 7.5-cm diameter, 25-cm long sand bucket was used to collect samples. GLDD personnel surveyed for approximate elevation just prior to and immediately following pumpout to determine approximate thickness of the nourishment at that particular location for sampling purposes. Because the nourishment was not graded prior to sampling, the thickness of the pumpout sediment was greatest closest to the pipe and thinned toward the seaward edge of the nourishment, thus requiring more samples taken closer to the pipe and fewer farther seaward. The number of samples collected vertically through the deposit was based on the deposit thickness to ensure that samples were obtained from the appropriate hopper dredge load (i.e., samples were not taken into the underlying sediment from a previous load). For example, if the deposit thickness of the placement was 100 cm, approximately four samples would be taken vertically in the same location to obtain a representative sample through the entire deposit at that location. Several locations (typically four to five) along a single transect extending from the pipe to the seaward extent of the nourishment were sampled following the same methods. At each seaward location, fewer vertical samples were taken due to the reduced thickness of the nourishment at that location. All samples for a particular load were combined into one or two 19-L buckets that represented a composite sample for the load delivered to the beach.

3.2 Sample Processing and Laboratory Analysis

3.2.1 Scour Pool Samples

Samples collected from the scour pool were processed to determine the mass concentration of fines. First, the total volume of each sample was determined by shaking then transferring the entire sample bottle contents to a 1-L graduated cylinder. The sand content was excluded from the concentration measurement by pouring the contents of the graduated cylinder through a #230 mesh (63 μm opening size) followed by rinsing. The sample and rinse water were then vacuum filtered through pre-weighed, 90-mm diameter, 0.4- μm glass-fiber filters. The mass concentration of fines is taken as the mass retained on the glass-fiber filters divided by the total volume of the sample.

3.2.2 Dredge Inflow, Hopper Bed, and Beach Samples

Hopper inflow, hopper bed, and beach samples were processed by the following procedure:

1. **Initial processing**
 - a. **(Hopper Inflow and Beach) Decant overlying water.** Overlying water (if present) was removed by settlement and decanting. The decanting procedure was to allow any suspended fines to settle for at least 12 hours. The salinity of the overlying water was measured with a handheld Yellow Springs Instrument (YSI) Model 30 salinity meter. The overlying water was then transferred by peristaltic pump and pipette and passed through pre-weighed, 142-mm diameter, 0.4- μm glass-fiber filters. The mass of sediment retained on the filters was recorded for future analysis.
 - b. **(Hopper Bed) Determine total sediment mass.** The contents of each sample bag were mixed in a moist state to break up any large mud aggregates. The sample bags were placed open in a warm oven and dried. The dry samples were weighed to determine total sediment mass.
2. **Consolidate and mix samples.** When samples were contained in more than one container, these samples were combined. The moist samples were thoroughly hand mixed in a 50x70 cm rectangular mixing pan.
3. **Subsample.** After mixing, the sediment was spread into a layer of uniform thickness within the pan (Figure 17). A 1-cm wide spatula was used to remove a swath of sediment across the pan, generating three specimens for size analysis and one specimen for color analysis. This procedure follows the *moist procedure* according to ASTM D6913.
4. **Color analysis.** Sand color analysis was conducted with a Minolta CR-400 Colorimeter. Each specimen was placed in the moist state in a shallow layer in a petri dish. Color was measured at three separate locations on the sediment surface. Additionally, photographs were taken of each sample immediately following the color measurement.
5. **Wash fines.** Each specimen retained for size analysis was washed over a #200 (75 μm) sieve according to ASTM D1140 to separate fine and coarse sediments.
6. **Sieve coarse fraction.** The coarse fraction retained on the sieve was dried in a 50C oven. Once dry, the sand was sieved according to ASTM D6913 through a -4 to +4 ϕ sieve stack with 1/2 ϕ intervals.
7. **Splitting of fines.** The wash water from step 5 was set aside and the fines were allowed to settle from suspension. Much of the overlying water was decanted, as in step 1. The remaining concentrated suspension was passed through a cone splitter (Capel and Larson 1996), resulting in a 1:10 splitting of the specimen volume and sediment mass.
8. **Mass of fines.** One of the ten split specimens was vacuum filtered through a pre-weighed, 90-mm diameter glass-fiber filter to determine the mass of fines passing the #200 mesh. The recorded mass was multiplied by 10 to account for the 1:10 split from step 7.

9. **Size distribution of fines.** Two of the remaining split specimens were treated overnight in a solution of sodium metaphosphate (40 g/L) to disperse the fine particles. Size analysis was performed by the light scattering or laser diffraction method with a Malvern Mastersizer 2000 laser particle-sizer. The instrument measures particle size over the range 0.02 to 2,000 μm in 100 logarithmically spaced size bins. Specimens were placed into the instrument's liquid handling unit and sonicated for 60 seconds prior to analysis.



Figure 17. Pan of moist sample with specimens removed for analysis.

3.2.3 Merging Sieve and Laser Diffraction Size Distributions

Sand and fine sediment require separate size measurement procedures. Coarse and fine fractions of sediment were separated by washing through a #200 (75 μm) sieve. The coarse fraction was dried, weighed, and sieved. The fine fraction was concentrated and split into ten portions. One fine-sediment portion was filtered to determine fine-sediment mass; a portion of the remaining fines was dispersed and passed through a laser diffraction particle size analyzer. The two resulting size distributions were then merged according to the following procedure:

1. The sieve size of the washing screen (75 μm) was assigned as the mesh point between the two size distributions.
2. Any sediment mass from the pan of the dry sieving operation was added to the mass of fines for the specimen.
3. Any laser diffraction volume included in size bins above the coarse/fine split was neglected. The fractional volumes in each remaining laser diffraction bin was renormalized to sum to one.
4. The normalized bin fractions for both the sieve and laser diffraction size distributions were multiplied by their corresponding fraction of total sediment mass.
5. The resulting laser diffraction and sieve distributions were then merged.

Figure 18 shows raw sieve and laser diffraction size distributions and the resulting merged distribution produced by the procedure above.

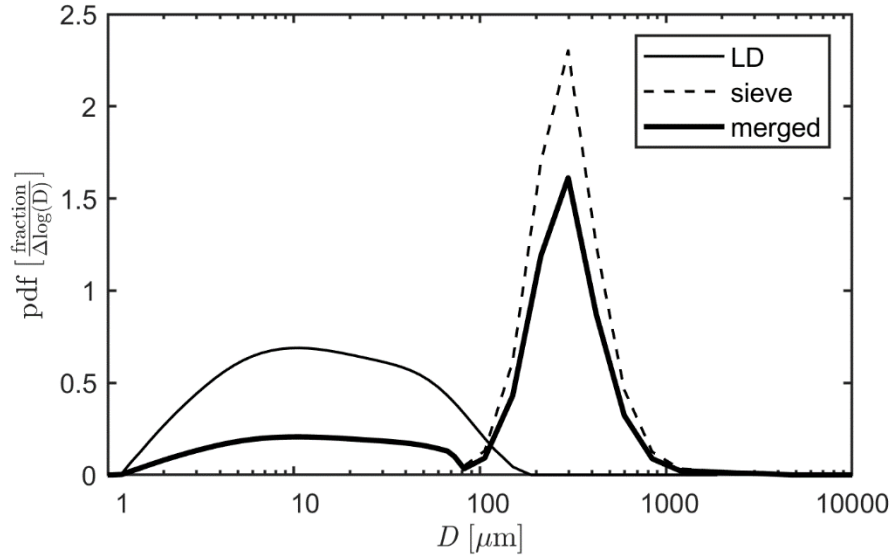


Figure 18. Example merged size distribution.

Size distributions from a sediment specimen that was separated by wet sieving are merged into a single distribution. The washed coarse ($>75\mu\text{m}$) fraction was sieved and the fine fraction ($<75\mu\text{m}$) was analyzed by laser diffraction (LD). The two analyses were merged by the method presented above. The fines content of this specimen is 30%.

3.3 Quantifying Loss of Fines

The difference in fines content of two samples is a fundamental quantity for this study. One metric of interest is the fraction of fines lost between two endpoints in the dredging process. One approach is to describe the changes with the relative percent change of the fines content between the endpoints as done by Coor and Ousley (2019). For this study, the fraction of fines lost between two samples is quantified using a mass-balance approach as follows. First the fraction of fines is defined as the ratio of the fines mass to the total mass.

$$f = \frac{M_f}{M_s + M_f} \quad (7)$$

The subscripts s and f refer to the sand fraction and fine-sediment fraction, respectively. The first sample is treated as having a mass of unity.

$$\begin{aligned} M_{f1} + M_{s1} &= 1 = f + (1 - f) \\ M_{s1} &= (1 - f_1) \end{aligned} \quad (8)$$

The second sample (acquired after some process) has lost some fraction (α) of sand and another fraction (β) of fine sediment.

$$\begin{aligned}
 M_{s2} &= (1-\alpha)M_{s1} = (1-\alpha)(1-f_1) \\
 M_{f2} &= (1-\beta)M_{f1} = (1-\beta)f_1
 \end{aligned}
 \tag{9}$$

Combining Equations 7 and 9 gives

$$f_2 = \frac{(1-\beta)f_1}{(1-\alpha)(1-f_1) + (1-\beta)f_1}
 \tag{10}$$

And solving for β ,

$$\beta = 1 - \frac{f_2(1-\alpha)(1-f_1)}{f_1(1-f_2)}
 \tag{11}$$

The expressions above are valid for the conditions: $[f_1 > 0]$, $[0 < f_2 \leq f_1]$, $[0 \leq \alpha \leq 1]$, and $[0 < \beta \leq 1]$.

4 Results

4.1.1 Borrow Area

Borrow area sediments were characterized using data retrieved from pre-project geotechnical reports. The fines content of each sampled load was estimated from analysis of the dredge track and the reported percentage fines retrieved from pre-project cores. These data are used as the baseline for comparing changes to sediment characteristics through the dredging and placement process.

In general, sediments within the cut depth of the borrow area are classified as a poorly graded (well-sorted) quartz sand with median and (graphic) mean grain diameters of 0.25 mm and 0.27 mm, respectively. The uniformity coefficient averages 2.1 and ranges from 1.5 to 3.5. Sediment color is generally in the gray family with low Munsell chroma and an average moist Munsell Value of 5 (although a Munsell Value of 6 was the most frequently occurring). The results of the fines analysis from the borrow area are presented in Table 5. The fines content of samples ranged from 3.1% to 4.4%. The mean value is 3.8% with a standard deviation of 0.4%.

Table 5. Fines content estimated from borrow area samples and dredge tracks.

Load Start Time (UTC-5)	Fines Content (percent)
6/20/2018 10:50	3.40
6/21/2018 12:25	4.23
6/22/2018 09:45	3.59
6/23/2018 10:40	3.34
6/24/2018 09:32	4.39
6/25/2018 13:05	3.80
6/26/2018 10:28	3.95
6/28/2018 10:15	3.92
6/29/2018 10:07	3.12
6/30/2018 13:11	3.60
7/1/2018 13:05	4.28

4.2 Dredge Sediments

4.2.1 Settled and Suspended Fines

As noted previously, the settled fines layer (L_2) was not present in the hopper (Figure 15). As the sediment bed approaches the elevation of the overflow weir, water velocities increase sufficiently to prohibit the settling of fines, as well-observed and modeled by other researchers (Vlasblom and Miedema 1995). On the other hand, a suspended fines layer (L_1) manifested only as a persistent scour pool once dredging ceased. Scour pool depths were typically 0.60 m and covered 10% to 20% of the hopper area.

The average scour pool volume was 50 m³ and varied from 34–71 m³ between loads. Pool volumes were therefore 1% or less of the total hopper volume (5,003 m³), and approximately 1.4% of the sampled hopper volume (~3,000 m³). Estimated sediment concentrations averaged 2.7±2.3 g/L (±1 SD) and are positively correlative (but not significantly so) to the percentage of fines by mass captured through filtering ($r = 0.59, p = 0.07$).

The mass of fines in the scour pool determined from concentrations was highly variable by load, ranging from 21 kg to 307 kg, with an average of 132 kg. Much of the variability in scour pool fines concentration can be attributed to sloshing, sample timing (which allows sediments to settle before being sampled), and the fines content of the inflow.

Using Equations 4–6, the mass of fines per area contained within the pool was quantified to determine its fractional contribution to the mass of fines estimated in the hopper. These results are summarized in Table 6. The fractional contribution of the suspended fines (L_3) layer to the total mass of fines contained within the hopper averaged 0.2% and was at most 0.5%.

Table 6. Fine fraction in the hopper bed.

Load No. ID	Date	L_1 (m)	V_{pond} (m ³)	A_{hopper} (m ²)	f_1	f_3	$\frac{C_1}{\left(\frac{kg}{m^3}\right)}$	$\frac{C_3}{\left(\frac{kg}{m^3}\right)}$	$\frac{m_f}{\left(\frac{kg}{m^2}\right)}$	$\frac{m_s}{\left(\frac{kg}{m^2}\right)}$	$\frac{m_{f3}}{m_f}$ (%)
1	20-Jun-18	7.11	47.4	520	0.012	0.001	1,755.7	5.5	149.1	12,340.8	0.34
2	21-Jun-18	6.85	43.9	520	0.011	0.001	1,869.7	3.4	136.9	12,663.8	0.21
3	22-Jun-18	7.50	66.5	520	0.026	0.001	1,584.8	1.4	309.0	11,573.8	0.06
4	23-Jun-18	6.82	56.0	520	0.007	0.001	1,680.8	0.5	80.6	11,382.5	0.07
5	24-Jun-18	6.93	34.1	520	0.024	0.001	1,657.9	0.9	277.8	11,218.2	0.02
6	25-Jun-18	7.12	36.3	520	0.010	0.001	1,795.5	7.7	132.1	12,660.0	0.41
7	26-Jun-18	7.11	71.4	520	0.010	0.001	1,648.2	4.3	118.3	11,599.6	0.49
8	28-Jun-18	6.61	45.2	520	0.016	0.001	1,634.3	0.9	169.2	10,640.3	0.05
9	29-Jun-18	6.75	66.0	520	0.013	0.001	1,598.8	1.6	138.7	10,655.3	0.14
10	30-Jun-18	6.68	45.4	520	0.010	0.001	1,686.4	3.0	114.4	11,155.4	0.22
11	1-Jul-18	6.62	41.5	520	0.007	0.001	1,666.0	0.5	73.1	10,958.6	0.06

Measured and calculated parameters produced to estimate the fraction of fines in the hopper. Variables are defined in Equations 4–6 and in Table 4.

4.2.2 Inflow, Hopper Bed, and Beach Sediments

A summary of sediment characteristics for the remaining sample locations is provided in Table 7. Inflow sediments consisted of 96% to 98% sand ($D_{50} = 0.29$ mm) and 0.6% shell gravel. The fraction of fines ranged from 1.2% to 3.8% and averaged 2.2%. Repeat analysis from triplicate subsamples per dredge load indicated an average standard deviation of 0.3% in the fines fraction.

The distribution of the coarse sediment fraction did not significantly change between the sample locations (Figure 19). Slight increases in sand content correspond to decreases in the silt and clay fractions which shifted the percentile diameters to slightly larger values (Table 7).

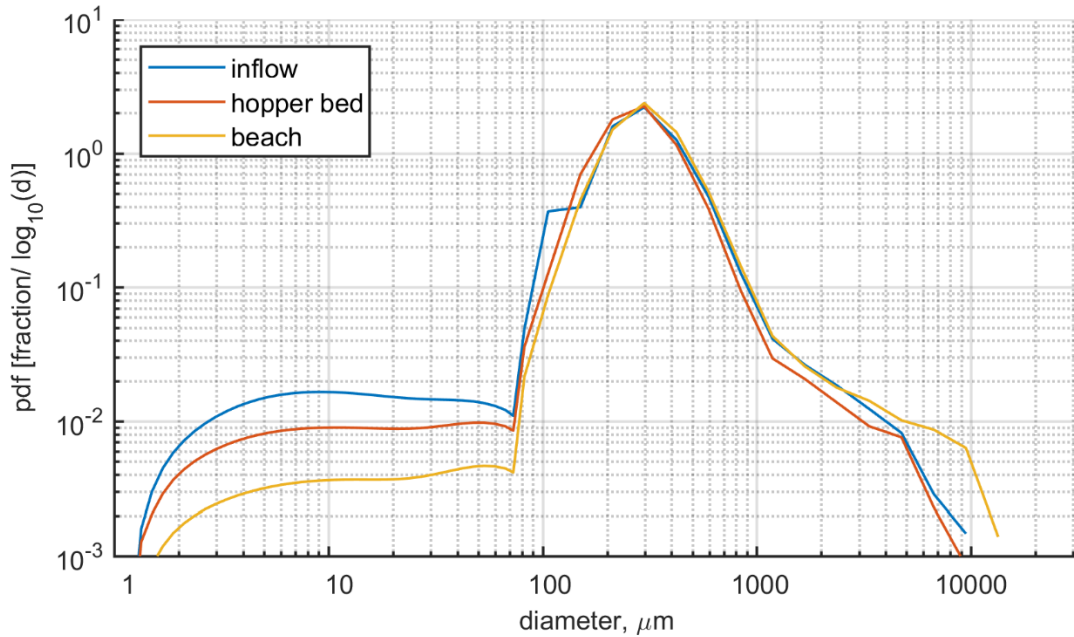


Figure 19. Averaged sediment size distributions for the inflow, hopper bed, and beach. Vertical scale indicates the relative abundance of sediment mass by size. N=11 for each location.

Table 7. General sediment characterizations averaged by sampling location.

Sample location	Shell Gravel (%)									Wet Munsell color		
		Sand (%)	Silt (%)	Clay (%)	% < 63 μm	D ₁₀ (mm)	D ₅₀ (mm)	D ₉₀ (mm)	C _u	H	V	C
Inflow	0.6	97.2	1.8	0.4	2.2	0.138	0.287	0.519	2.3	7.2 Y	3.8	1.1
Hopper	0.6	98.1	1.1	0.2	1.5	0.160	0.279	0.494	2.0	3.7 Y	4.0	1.5
Beach	0.9	98.6	0.5	0.1	0.5	0.182	0.303	0.544	1.8	5.9 Y	4.4	1.0

4.2.3 Variability of the Fines Fraction

Figure 20 presents the variation in percent fines by load and sample location. Here, the mean fines content for each sample location is plotted as a horizontal line, and results from repeat laboratory subsampling and analysis from each load are also plotted to show the variation in fines derived from laboratory testing. On average, the variation of the fines content from the borrow area is small, with a mean standard deviation of 0.4%. In contrast, the percent fines of inflow and hopper samples are more variable (0.8 and 0.6% mean standard deviations, respectively), while beach samples are less variable (0.2%). Figure 20

also shows that the trend of the fines content sampled at the inflow qualitatively mirrors that of the borrow area, although somewhat obscured by the greater variability of inflow results. Table 8 displays a correlation matrix for the percent fines between sample locations. The strongest correlation occurs between the inflow and beach samples, though it is not significant at the 95% confidence level ($p=0.13$).

Table 8. Correlation matrix for percent fines by sample location.

Sample location	Borrow area	Inflow	Hopper	Beach
Borrow area	1.00	-	-	-
Inflow	0.16	1.00	-	-
Hopper	0.12	-0.07	1.00	-
Beach	-0.36	0.49	-0.07	1.00
p-values	1	-	-	-
	0.63	1	-	-
	0.73	0.83	1	-
	0.28	0.13	0.83	1

P-values are given in the lower panel. N=11.

However, the variation of fines from repeat sample analyses is small, thus the inter-load variability is more a reflection of the change in fines content encountered at the borrow area, and the variability from sampling resolution and methods, than due to laboratory procedures.

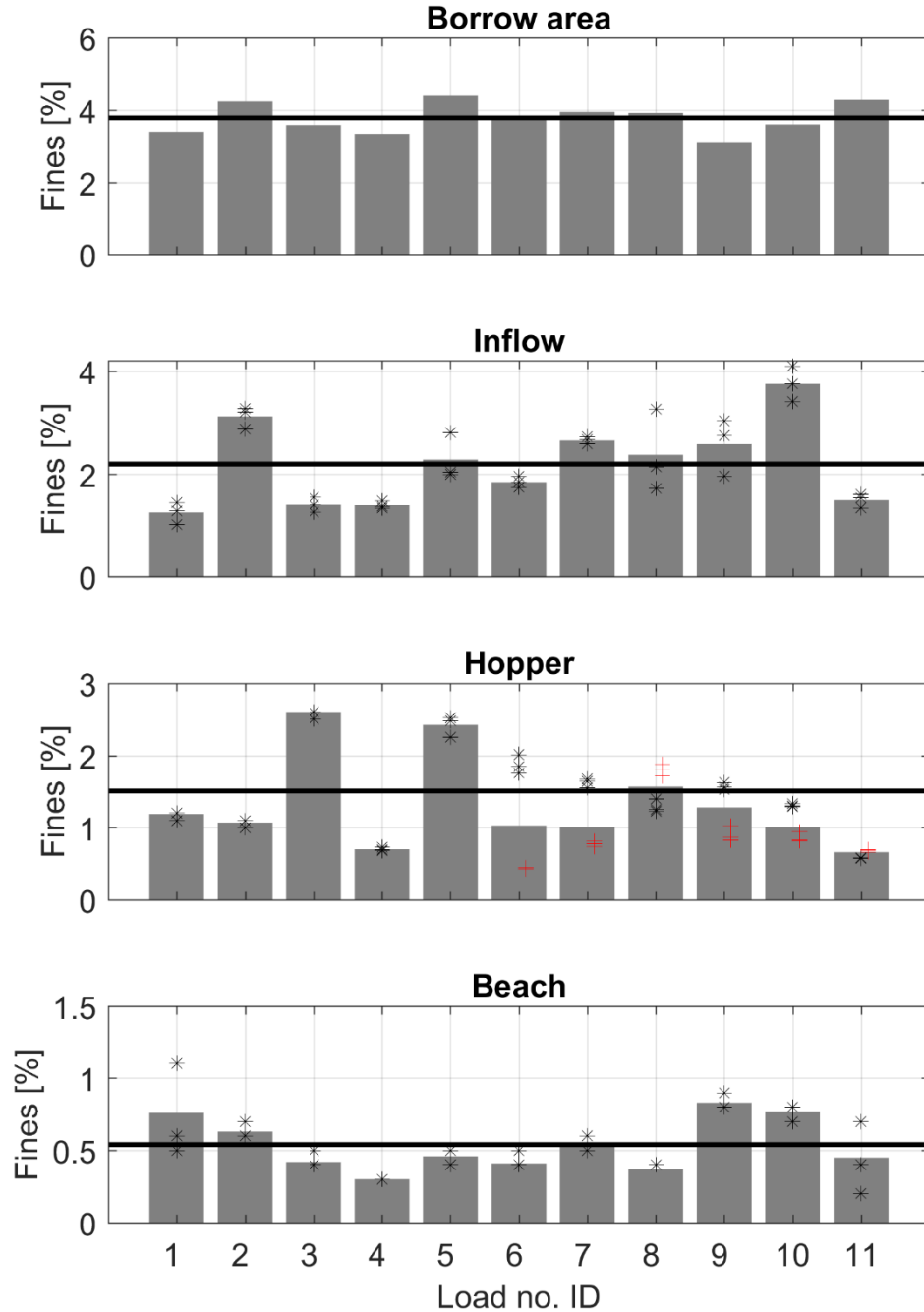


Figure 20. Fines content at the borrow area, inflow, hopper bed, and beach.

Average percentage of fines by mass for each composited load. Mean values are indicated by the horizontal line. Individual subsamples are plotted with black * symbols; in the hopper series, black * symbols denote samples collected using the gravity corer while red + symbols indicate samples collected using the plate sampler.

4.3 Change in Fines Content

The total reduction of the fines fraction between the borrow area and the beach placement site is presented in Figure 21 and Table 9. The fraction of fines reduced, on average, from 3.8% to 0.5%

between the borrow area and the beach. The percentage fines is generally reduced by one half between each stage of the dredging and placement process. Loss of fines between the inflow and hopper are predominately through the overflow weirs, while between the hopper and the beach it is predominately through outwash during pumpout on the placed beach. However, the apparent reduction of fines between the borrow area and the inflow were not expected to be significant. This points to potential sample biasing from the inflow, which is discussed further in the discussion section.

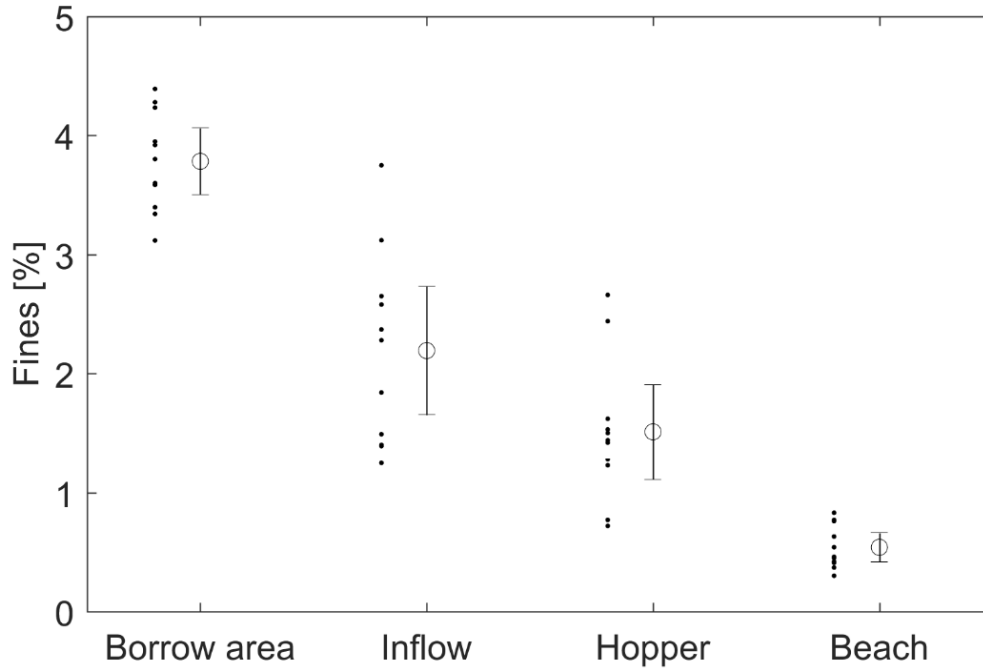


Figure 21. Fines content by sampling location.

Sequential reduction of the percentage fines with sampling location. Compositied values from each hopper load (Figure 16) are plotted as dots. Error bars represent the 95% confidence intervals.

Table 9. Summary statistics of the fraction of fines between sample locations.

Sample location	% fines (<math>< 63 \mu m</math>)			
	(mean)	(var)	(stdev)	(95% CL)
Borrow area	3.8	0.2	0.4	3.5 4.1
Inflow	2.2	0.6	0.8	1.7 2.7
Hopper	1.5	0.4	0.6	1.1 1.9
Beach	0.5	0.03	0.2	0.4 0.7

Note: stdev=standard deviation, var=variance, and 95% confidence limits. N=11 for all cases.

4.4 Mud Aggregates

Mud aggregates were observed in most of the loads sampled at the hopper inflow, at the hopper bed, and on the placed beach (Figure 22). The occurrence of mud aggregates within samples at all locations was

intermittent in time, likely associated with the patchy spatial distribution of muddy layers at the borrow area. Sampling at the beach and hopper indicate that the aggregates were distributed with depth at both locations. There are no known physical processes that would preferentially concentrate these aggregates at the surface of the bed. All observations suggest that these mud aggregates simply transport as individual particles with a relatively fast settling velocity.

At the conclusion of hopper loading, there were instances of a clean sandy bed (Figure 22A) or a sandy bed with abundant mud aggregates (Figure 22B–D). The same observations were true near the vicinity of the pipeline outfall on the beach (Figure 22E–F).

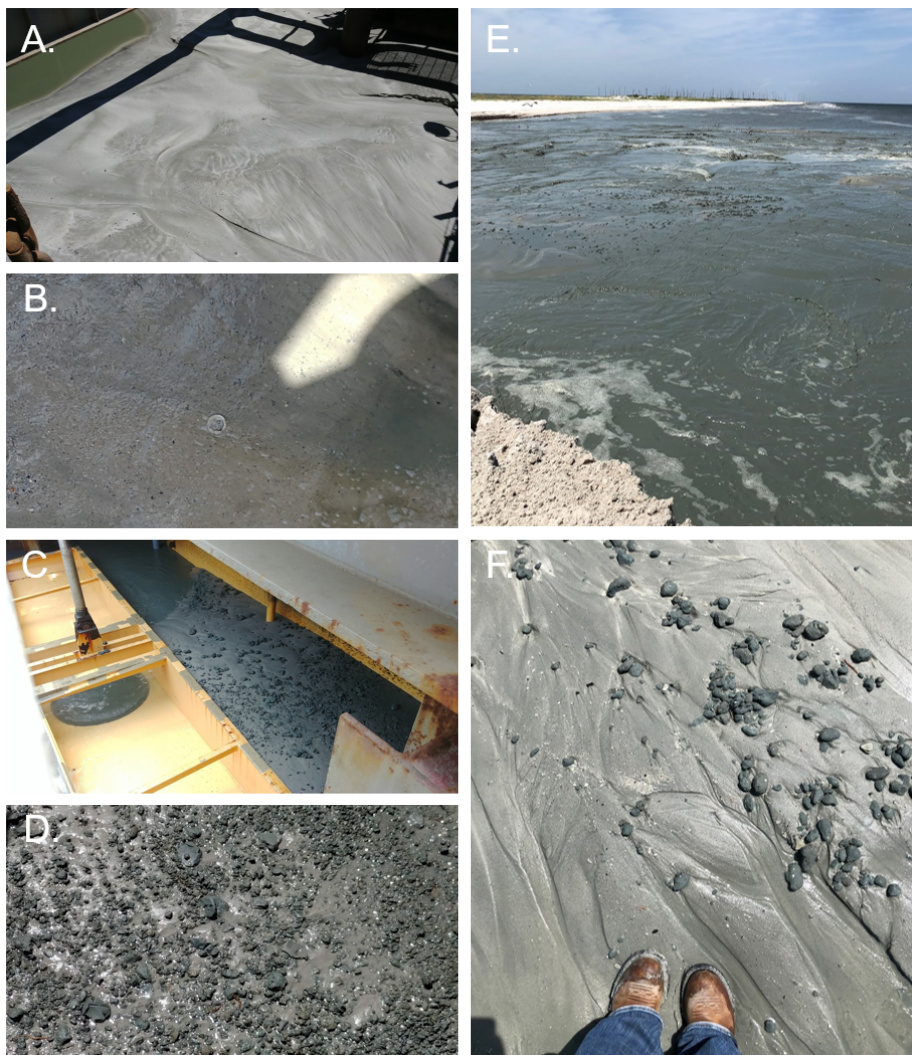


Figure 22. Mud aggregates observed on the hopper bed surface and beach.

Bed condition of the hopper (A–D) and beach (E–F). (A) shows a hopper bed free of settled fines or mud aggregates, (B–D) the hopper bed with slight to heavy mud aggregate deposits, and (E–F) mud aggregates deposited on the beach.

Most of the aggregates visible in Figure 22 are several to 10-cm in size and were characterized by a relatively flat, plate-like shape. Smaller aggregates were evident in samples collected from the hopper bed (Figure 23) and also from the beach. These smaller aggregates ranged in size from sub-mm to 10 mm in size and were variable in abundance as illustrated in Figure 23.

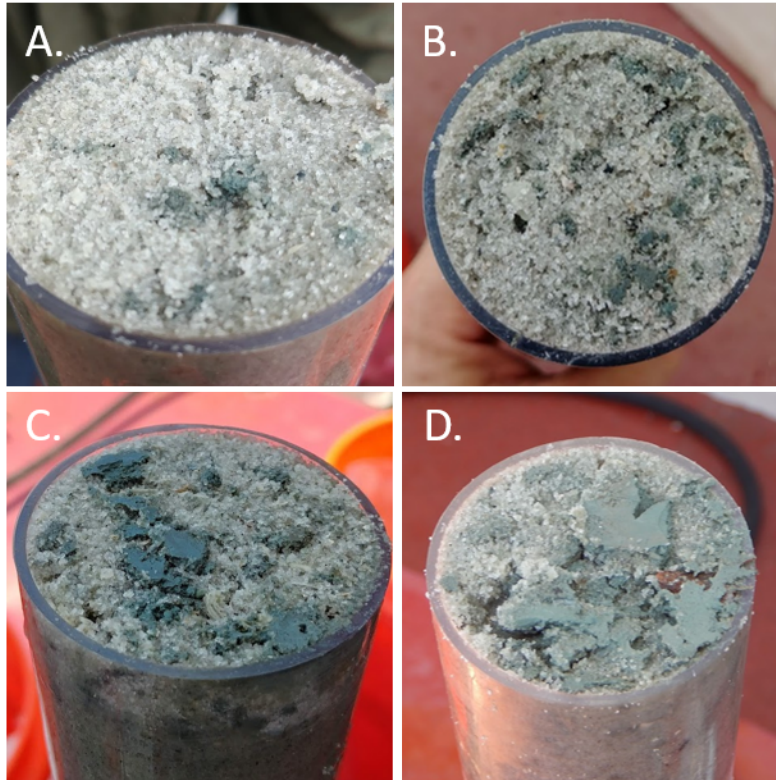


Figure 23. Mud aggregates collected in samples of the hopper bed.

Mud aggregate concentration varies in these examples from light (A) to heavy (D).

Large mud aggregates were recovered from the beach and sample analysis was performed on a composited sample by the sample preparation and analysis methods presented earlier. The mud aggregate material was found to be 20% sand, 53% silt, and 28% clay, giving a silt:clay ratio of 1.90. Atterberg limits testing was performed on the mud aggregate material, following ASTM D4318. The sediments composing the mud aggregates had a liquid limit (LL) of 71.1%, plastic limit (PL) of 20.5%, and plasticity index (PI) of 50.5%. According to the USCS (ASTM D2487), this material would be classified as CH, fat clay with sand. The in-situ water content of the mud aggregates was 65%, less than the LL.

Color analysis

Color measurements for the borrow area were supplied from the pre-project geotechnical report (see Table 1). For the remaining sampling locations, color measurements were obtained in the laboratory from composited samples prior to removal of fines through wet sieving. The results are compiled in Table 8.

The only notable changes in sediment color are related to Munsell Value (MV); the reader is reminded that MV is related to sediment lightness—higher values imply lighter sediment. The reported MV of the borrow area was particularly high (5–6). In contrast, the average MV of the inflow samples was 3.8 but progressively increased to 4.4 between the inflow and beach samples (0.6 unit change). Therefore, the sediment became slightly lighter as fines were removed through the dredging and placement process (Figure 24, Table 10). This change is because silts and clays that comprise fine sediment tend to be dark, and their incorporation into quartzose sands exerts significant control on overall sediment lightness. The color obtained from composited mud aggregates collected on site were classified as dark gray and had a measured MV of 3.8.

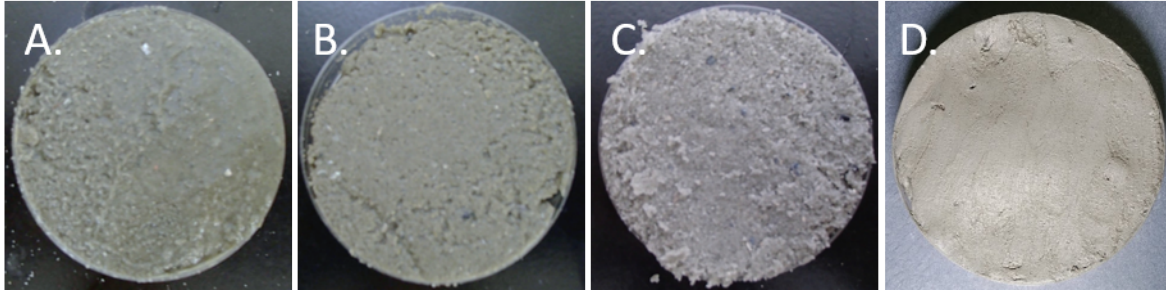


Figure 24. Sediment lightness associated with sample location.

Images showing changes in sediment lightness, which is sensitive to the fines content of the samples, between samples obtained from the inflow (A), dredge hopper (B), and beach (C). Composited mud aggregates is shown in panel (D), though the image was taken in slightly different lighting condition.

A puzzling result is that the average MV of the mud aggregates (100% fines) and the inflow sediments (2.2% fines) are equivalent. Similarly, it is also noted that the MV of the inflow and borrow area sediments are dramatically different. This could be due to differences in the way Munsell color codes were obtained (color chips versus colorimeter) and is discussed further in the discussion section.

Table 10. Munsell color codes averaged by sample location.

Sample Location	Average			Standard Deviation		
	H	V	C	H	V	C
Borrow area	2.5 Y	5.7*	2.0	-	-	-
Inflow	7.2 Y	3.8	1.1	1.2 Y	0.1	0.1
Hopper	3.7 Y	4.0	1.5	0.2 Y	0.2	0.1
Beach	5.9 Y	4.4	1.0	0.8 Y	0.2	0.1
Mud aggregates	2.0 GY	3.8	0.9	0.2 GY	0	0

Borrow area colors were estimated from Table 1; *codes derived from Munsell color chart. Color of Inflow, Hopper, and Beach samples were measured using a digital colorimeter. Color measurements prior to fines removal.

To examine the total shift in MV related to fines content, color measurements were also taken on samples after the fines were removed through washing. In this case, the MV of hopper and beach samples was 4.7 and 5.0, respectively. No measurements were obtained for inflow samples though the MV is expected to be close to 5.0 because the mineralogy of the sediment is similar. Thus, a MV=5.0 is the approximate maximum expected lightness that borrow area sediments can achieve at the placement site without further alteration (e.g., solar bleaching) in the event of 100% fines loss.

Considering the expectation that the sediments with more fines should be darker, the relationship between the fines content and MV was explored further. Previous laboratory work (Berkowitz et al. 2019) suggests that MV can be modeled as an exponential decay function between two sediment end points, one with 0% fines and one with 100% fines. This equation reads,

$$\hat{V}(f) = \begin{cases} C + Ae^{-kf}, & 0 < f < 1 \\ V_1, & f = 1 \\ V_0, & f = 0 \end{cases} \quad (12)$$

where \hat{V} is the predicted MV, f is the fraction of fines by mass, V_1 is the MV for $f=1.0$, V_0 is the MV for $f=0$, $A = (V_0 - V_1)$, and $C = V_1$. The parameters for the model fit (Table 11) were determined using the method of nonlinear least squares. The data with fitted curve and 95% prediction bands are presented in Figure 25. The modeled MV evolves from 4.9 ($f=0$) to 3.7 ($f=1.0$), which very closely approximates measured values given above. Therefore, using samples collected from borrow site geotechnical investigations, it is possible to develop a curve to predict MV shifts for nourished beaches if fine-sediment losses can also be predicted (see Berkowitz et al. [2019] for additional details).

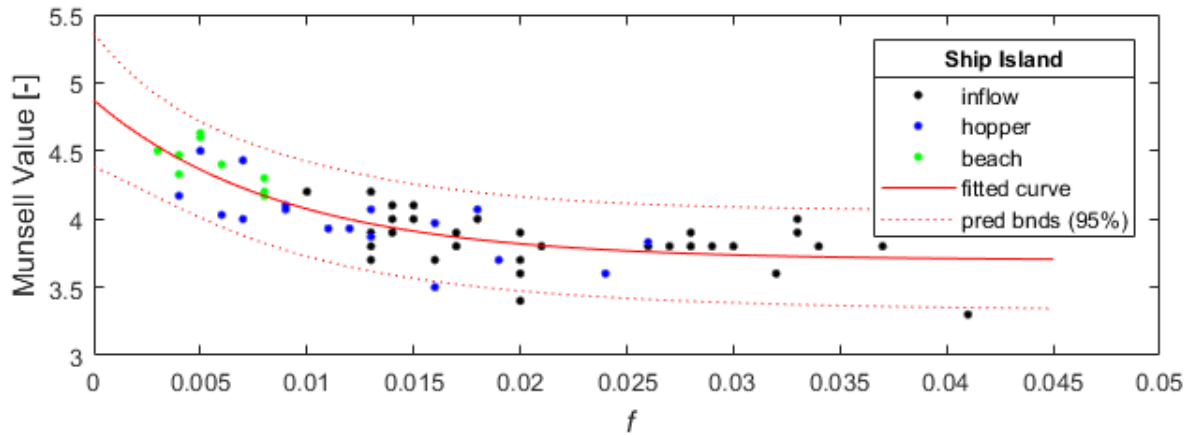


Figure 25. Relationship between Munsell Value and the fraction of fines.

Samples are taken from the dredge *Liberty Island* and corresponding beach placement site. Larger MV indicates lighter sediment.

Table 11. Summary of fitted model parameters and 95% confidence limits for data in Figure 20.

k	A	C	k_L (95%)	k_U (95%)	A_L (0.95)	A_U (0.95)	C_L (95%)	C_U (95%)
113.8	1.17	3.70	54.91	172.8	0.88	1.47	3.57	3.83

5 Discussion and Future Considerations

5.1 Separation of Sand and Fines by Dredging and Placement Processes

The objectives of the field sampling campaign are to 1) determine the change in fine-sediment content at various stages of the dredging process from borrow area to beach and 2) determine the variability in the separation of fine sediment and sand and the associated contributing factors (such as sediment composition and dredging operations). Field samples collected during 11 hopper loads provide a convincing trend of decreasing fine-sediment content with progression through the dredging process (Figure 21). The means between the borrow area/beach, borrow area/hopper, and inflow/beach are significantly different ($p < 0.01$, $N=11$) (Table 12). These observations definitively demonstrate the sequential reduction in fines content from the borrow area, hopper, and beach.

The borrow area and inflow samples should be equivalent samples. The comparison of sample means for borrow area and inflow (Table 12) clearly indicate that it is very unlikely that the population means are equal. Although there is a fine-sediment loss mechanism (suspension by the draghead), it is unlikely that

this loss mechanism is large enough to explain the differences in the sample means between the borrow area and the hopper inflow. The borrow area sample averages represent a numerical composite of the pre-project borrow area sampling. Although these samples could poorly represent individual loads or portions of loads due to unaccounted borrow site spatial variability, the samples should closely represent the mean fines content of the dredged sediments. As for the inflow samples, there is concern that inevitable biases arise from sampling at a single point at the discharge box. The sand content could be substantially enriched near the lower portion of the grate due to sand settling compared to the upper fluid levels in the discharge box. (If sand settling enriches the lower layer with sand, then the upper layer would be enriched in fines compared to the average sediment composition). Pipeline flow of sand slurries is commonly stratified (Matoušek 1997, Wilson et al. 2006) with sand concentrations greatest near the bottom of the pipes and lower above. Given that the cross-sectional area of the discharge box is substantially larger than that of the inflow pipes, it stands to reason that vertical concentration gradients in the discharge box are greater than that in the inflow pipe. This study does not have data to discount the hopper inflow samples, but the validity of these samples is suspect.

Table 12. Hypothesis testing of sample means from sampling locations in the dredging process.

Location 1	Location 2	% fines (< 63 μm)		
		$\bar{F}_1 - \bar{F}_2$	σ_{f1-f2}	p
Borrow Area	Hopper	2.3	0.22	<<0.001
Inflow	Hopper	0.7	0.30	0.021
Hopper	Beach	1.0	0.19	<<0.001
Borrow Area	Beach	3.3	0.13	<<0.001
Borrow Area	Inflow	1.6	0.27	<<0.001

$H_0: \bar{F}_1 - \bar{F}_2=0$, $H_1: \bar{F}_1 > \bar{F}_2$, evaluated with one-tailed, Student's t test. N=11.

The fraction of fines lost from borrow area to beach is of interest in understanding the effectiveness of the two primary modes of fine separation: hopper overflow and beach outflow. Applying Equation 11 to the sample means at the borrow area, hopper, and beach (assuming no overflow or outwash of sand) indicates a loss fraction for fines (β) of 0.61 associated with hopper overflow, 0.67 for beach outwash, and 0.87 for combined overflow and outwash. In terms of relative contribution, 70% of the total fine-sediment mass reduction was achieved during loading (by overflow) compared to 30% during pumpout (via outwash).

Ousley et al. (2014) presents fine-sediment content for borrow site and post-placement beach samples for 11 project sites on the Atlantic and Gulf of Mexico coasts of Florida. Coor and Ousley (2019) expanded the dataset to N=103. More than 80% of the projects with at least 3% fines at the borrow area have fines loss rates greater than 75%. Coor and Ousley (2019) calculate the fine-sediment loss rate differently than the mass-based approach derived in this report (Equation 11). The metric used by Coor and Ousley is the relative percent change in fines content. The differences between percent change in fines content (Coor and Ousley 2019) and percent loss (this report) is presented in Figure 26. For cases with either low initial fines content or high loss rate, the differences between percent change in fines and the loss rate of fines are small. For cases with initial fines content higher than 5% and fines loss rates less than 80%, the numerical differences between the two metrics could be significant. Nonetheless, Coor and Ousley find a median percent change of 70% (similar to the findings of this study) and that more than 70% of the projects in their dataset had greater than 50% change in fine-sediment content.

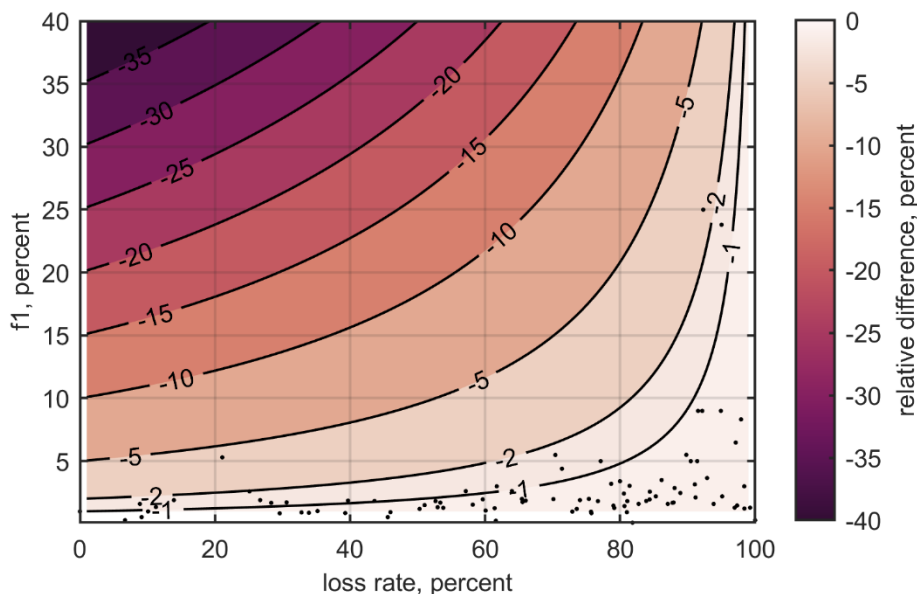


Figure 26. Comparison of fines loss rate to percent change.

Contours indicate the relative difference between percent change in fines (as given by Coor and Ousley 2019) and percent loss of fines (as given in this report). Negative values indicate that percent change is less than percent loss. Loss rate indicates the percent loss (this report) and f1 indicates the initial fines content. The data points (.) are from Coor and Ousley (2019).

From a different perspective, one could assert that if the loss fraction (β) was known for a given set of operating conditions (sediment, dredging plant, beach configuration, etc.), then the fines content delivered to the beach could be projected by the expression in Equation 10. For example, if a conservative measure was in place to deliver no more than 4% fines from the borrow area to the hopper, then the upper limit of fines content in the borrow area would be 10% (with $\beta = 0.61$ for overflow alone). If instead the limiting fines content to deliver to the beach is 4%, then the upper limit of fines content in the borrow area would be closer to 25% (with $\beta = 0.87$ for combined overflow and outwash). Fines content is not the sole compatibility condition, so obviously other factors such as color, size compatibility, and shell would have to be considered. Additionally, the propensity for the generation of mud aggregates (which reduces β) is likely to be associated with higher fines content at the borrow site, so reasonable upper limits would need to be established for this practice. Other datasets would need to be collected or evaluated from this perspective to increase confidence in this approach to estimating fines content delivered to the beach.

5.2 Beach Color

MV determined from the borrow area during pre-project sampling (FitzHarris and Godsey 2014) was determined by color chart comparison; MV determined in the present study from the inflow, hopper, and beach were determined with a digital colorimeter. MV determined for the borrow area by color chart (MV=5.7) was nearly two units of MV lighter than that determined from the hopper inflow by colorimeter (MV=3.8). This observation highlights a key difference in the methods for determining color. Use of the Munsell color chart is subjective and relies on the experience and skill of laboratory technicians (USDA 2017) to match the sediment sample with the corresponding color chip. MV variation between standards is expected to vary by no more than approximately 0.3 units (Rabenhorst et al. 2015), and a comparison between a digital colorimeter and a group of individuals experienced in reading color chips indicated a mean difference of approximately 0.5 units (Rabenhorst et al. 2015). These differences are significantly

smaller than the ones observed in the present study between the MV reported in FitzHarris and Godsey (2014) and that measured from the inflow samples by digital colorimeter. For the purposes of assessing color change from the borrow site to the beach, MV measured by colorimeter on samples from the inflow, hopper bed, and beach will apply.

Fines content and beach color are closely related, as the often dark fine-sediment content has the capacity to appreciably darken an otherwise light quartz sand (Berkowitz et al. 2019). Table 10 and Figure 25 illustrate the effect of fine-sediment content from the study site on MV. The inflow sediment is relatively dark, with a MV of 3.8 and increases in lightness to MV of 4.0 and 4.4 in the hopper bed and beach, respectively. Berkowitz et al. (2019) present a new method for estimating MV change associated with fine-sediment content. This method agrees favorably with the data presented in Figure 25. Given that fines content and beach color are both sand compatibility requirements, the method developed by Berkowitz et al. should be valuable in assessing the color change potential of offshore sand resources and the fines content requirement of the placed sand on the beach to meet color compatibility requirements. Additional datasets with coupled fines content and wet MV are required to further evaluate and validate this new approach to estimating color change between borrow areas and beach nourishment projects.

5.3 Assessment of Sampling and Analysis Approach

Variability of the fines content between composited samples is assessed to determine the cause of the variability, which can be due to natural variability of the source area, sampling methods and techniques, and sample analysis procedures.

Variability due to sample analysis procedures can be evaluated by quantifying the dispersion of results between triplicate subsamples extracted from composited samples. The averaged standard deviations for inflow, hopper, and beach subsamples were very small (0.3%, 0.1%, and 0.1%, respectively) and therefore contribute little to the overall variability observed between loads. Accordingly, high confidence is placed on the laboratory procedures to provide repeatable results despite the relative complexity of the procedure sequence and the small masses of fines analyzed.

Natural variability in sediment composition from the dredging source is also considered. The fines content of the borrow area had relatively little variability between loads ($SD = 0.4\%$). The HIP1 borrow area is a former dredge material disposal site, thus heterogeneities in sediment composition could be expected. However, due to the relatively coarse sampling resolution its spatial variability is uncertain.

Inflow samples were intended to verify the composition of the borrow area, but due to sampling issues described above, they may not truly reflect the sediment composition of the dredged areas. However, the general trend in the fines content between loads was similar (corresponding increases and decreases in fines) even if the magnitude of the change was not. The leading assumption to explain the discrepancy is the setup of concentration gradients within the discharge box causing samples to be light in fines relative to the borrow area. Some variability of the inflow may also be associated with using a bottle to capture samples since it is difficult to capture the cross-section of the discharge stream in its entirety. Yet, previous laboratory results showed this method produces comparable results to more sophisticated sampling methods when deployed with careful technique (Appendix B).

Composited hopper samples were observed to have the greatest variation in fines content between loads. In contrast to inflow samples, the average fines content of the hopper per load does not follow borrow area trends. Since samples were composited, it is not possible to evaluate the vertical distribution of fines retained in the hopper, which may be caused by time variations of inflow and the settling characteristics of the sediment. However, the sampling techniques and sampling resolution in time and space can be considered.

Ideally, vertical sampling should be spaced uniformly and with enough resolution to capture potential changes to borrow site sediments. While the average number of samples collected from the hopper appeared to be adequate for vertical resolution (1 sampler per 30 cm of bed rise), they are not uniformly spaced. Difficulties using the gravity corer resulted in fewer successful casts and thus fewer total samples, which were not well distributed vertically. For example, fewer than 20 samples for 4 out of the first 5 loads were collected when the corer was used exclusively. Successful casts tended to occur in groups at various time intervals during loading, which may be related to the degree of bed fluidization and or avalanching of the sediment bed. In either case, these processes appear to be variable in space and time as the dredge operator alternates primary flow between the fore and aft overflow weirs. In contrast, the rate of successful casts increased using the plate sampler and made up 60% of the total number of samples for the loads in which it was used (loads 6–11). The high success rate of casting the plate sampler compensates for the increased time it takes to collect a sample and recast, but allows for a more uniform vertical sampling distribution.

Two horizontal sampling positions are probably sufficient to adequately characterize hopper sediments, though this cannot be confirmed because samples from the fore and aft positions were not analyzed separately. Sample representativeness is also hampered by the decreased time span in which to take samples. Because no samples were taken in the first 8 minutes to avoid striking infrastructure in the hopper, the bottom 10% to 13% of the hopper is not represented in the composited samples. Noteworthy, however, is that multiple observations of vertical bed scarps that formed during pumpout appeared homogeneous and did not reveal stratigraphic evidence of settled fines layers, except for some minor layers in the upper 10–15 cm observed for one or two loads.

In addition to sampling resolution, a sufficient amount of material is required to properly represent the bulk sediment characteristics at each sampling location. Greater heterogeneities in a population require larger sample volumes to adequately capture population characteristics. Individual sample volumes collected from the hopper were 36 cm³, with total composited volumes averaging 0.5 L. This is contrasted with sample volumes collected on the beach, which averaged 20 L per load. It is tempting to state that the increased sample volumes may be partly responsible for the decreased variability of the beach fines, which was the lowest of all sampling locations ($s = 0.2\%$), but its relative magnitude compared to the mean (the coefficient of variation, cv) is equivalent to that of the inflow samples ($cv = 0.4$). Hopper samples, on the other hand, have a coefficient of variation equal to 1.2. This high variability is likely due to the presence of mud aggregates within select hopper samples. In the presence of mud aggregates, larger sampling volumes are beneficial to this extent. For example, composited plate samples were nearly always lighter in fines (mean = 0.9%) compared to core samples (mean = 1.5%) (see Figure 18), though the significance that the means are equal ($p = 0.06$) is inconclusive.

Mud aggregates (here composed of 80% fines) of various sizes were encountered randomly during sectioning of the hopper cores (see Figure 23). Large aggregates included in the sample then represent a disproportionate mass of fines relative to the composited sample. No attempt was made to avoid mud aggregates during core sectioning, thus their contribution to the total fines content is entirely random and is the most likely explanation for the high variability and lack of trend with the inflow and borrow data. Mud aggregates may also explain the relatively high coefficient of variability observed in the beach data because mud aggregates were scattered across the beach face. Aggregates have settling velocities greater than their constituent particles and are therefore more prone to being retained in the hopper and on the beach.

5.4 Recommendations for Future Studies

Based on the experiences of this study, a number of recommendations are provided regarding sampling procedures and the extension of the approach to other borrow sites.

- 1) Sampling of the hopper inflow provides challenges in obtaining representative samples. As described previously, vertical concentration gradients typically exist in the pipeline flow between the dragheads and the hopper inflow. Upon entering the discharge box or manifold, flow is slowed and distributed, likely resulting in increased vertical concentration gradients of coarse material and additionally longitudinal gradients in concentration associated with the transfer of material from the discharge box or manifold to the hopper. Sampling the inflow is not a critical component to quantify loss rates if adequate resolution of sediment characteristics within the borrow area is available.

Careful consideration of vertical concentration gradients is recommended for sampling of any sand suspension in the dredging process. If inflow sampling is required, the sampling assembly should be modified or redesigned to account for concentration gradients in the hopper discharge box and air entrainment in the slurry. The intake assembly of the current design should consist of a 2–3 port vertical manifold to better capture samples across these potential gradients. Alternatively, a sampling loop could be installed in the inflow pipes. Such a sampling loop back-passes a portion of flow from downstream to upstream and is introduced in such a manner that creates a vertical mixing of the pipeline contents.

The bottle method (described in Appendix B) of sample collection worked well provided the flow from the sampling assembly was reduced so as to not cause excessive splash-out or overflow. The sampling rate and volume of sample that was determined in Appendix B was manageable with one person.

- 2) Hopper sampling using the modified gravity corer proved difficult. The gravity coring method is labor intensive and had a poor sample recovery rate, which reduced vertical resolution of the hopper bed sampling in the first several loads. However, when the gravity corer was successful it yielded larger sample volumes for improved sample sizes. The alternative method for hopper sample collection was the plate sampler. The plate sampler is lighter, easier to cast, and had a better sample recovery rate.

Given the heterogeneous distribution of mud aggregates in the loads sampled, greater composite sample volumes from the hopper are desired. A 10- to 100-fold increase in composite sample volume would still have been manageable in the laboratory and would have benefited the results by likely reducing sample variability. For gravity cores, increasing the length of subsamples from the gravity corer yields larger sample volumes. For the plate sampler, the subsampling ring height and/or diameter can be increased to yield larger sample volumes.

- 3) In an ideal study, cores would be collected over the full depth of the placed beach template after the placement of many loads by the dredge. By this approach, placed sediments would be sampled across all depths of placement. Due to the operation of two hopper dredges from two different placement sites, the present study adopted a procedure of sampling after each load over the placed depth of that particular load. In this case, access was limited to the subaerial portion of the placed sediments, and there was undoubtedly some subaqueous material from some loads that was inaccessible to sampling. The hand auger used on the beach worked well for the present study, but future studies should consider using a smaller diameter auger to allow a greater number of coring positions for the same composite sample volume.
- 4) The present study, the work of Ousley et al. (2014), and Coor and Ousley (2019) provide a relatively large dataset on the loss of fines from borrow areas with less than 5% fine-sediment content. Data at higher fines content are relatively sparse. Future studies should focus on borrow areas or navigation projects with fines content in excess of 10%.

- 5) Studies similar to the present one should be conducted to determine the loss of fine sediments for beach and open-water placement by cutter-suction pipeline dredging and bottom dumping from a TSHD in nearshore placement. Each of these studies could increase the confidence in the fine-sediment loss rates developed in the present study.
- 6) Research is needed to better understand when mud aggregates (mud balls) are likely to form during the dredging process. Assessments of the presence of such materials would factor into reducing the expected fine-sediment loss rates for some borrow areas.
- 7) The present study documented fine-sediment losses at a relatively unconfined situation at the pipeline outwash zone. Lengthy confined outwash zones would result in milder slopes for outwash and would likely favor increased retention of finer sediments. Additional research is needed to refine estimates of outwash losses to include the influence of the outwash zone fluid velocities, slope, and length on fine-sediment losses.

5.5 Implications for Practice and Policy

This study, combined with the observations of Ousley et al. (2014) and Coor and Ousley (2019) prompts discussion of the relevance and potential application of this new information related to dredging practice and policy.

5.5.1 Dredging Practice

In the present study, changes in fines content between borrow area, hopper, and beach were estimated for a TSHD. The hopper dredging operation with overflow and pumpout removed a combined 87% of the fine-grained sediment present in the borrow area samples. Most of the fine-sediment removal (70%) occurred near the borrow area associated with overflow, and the remaining 30% was removed as washout on the beach face. Knowledge of the relative loss of fines by location or dredging process could be incorporated into future project design applications in order to 1) control the loss of fines near sensitive habitats or 2) modify dredge operation to increase/decrease loss of fines at a particular location.

The data of this study, combined with the data from the literature, suggest that a predictive capability for loss of fines from sandy borrow areas is possible. At the very least, the conservative recommendations of Coor and Ousley (2019) in assuming, at most, a 50% loss of fines associated with dredging and placement operations would be appropriate for sandy sites within the limits of the dataset (with as much as 25% fine-grained content). At a higher-level of fidelity, a one-dimensional vertical (1DV) or one-dimensional horizontal (1DH) numerical modeling approach of the overflow and settlement of solids in the hopper. Spearman et al. (2011) and Boone and de Nijs (2018) have recently demonstrated the application and accuracy of such models for the primary purpose of estimating the concentration of the overflow plume. These models also could be applied to estimate the fines content of the hopper load. This class of models could be applied in numerical experimentation to develop or refine simpler expressions for estimating the loss of fines. Additionally, these models could be applied outright as a tool for estimating the change in fine-sediment content associated with hopper overflow and evaluating the modification of dredge operation to enhance fines loss.

Mud aggregates observed to deposit in the hopper and on the beach highlight an important consideration related to fine-sediment content at the borrow site. Because the aggregated mud particles settle faster than their constituent sediment, they are not as effectively separated from sand. The propensity to remain aggregated is likely related to the clay content and water content of the fine sediment. Additional attention

to characterizing even thin lenses of clay in borrow areas is warranted if the appearance of mud aggregates on the beach is a concern.

Although this study was conducted with a TSHD, the results are relevant to other similar dredging methods. Other hydraulic dredging operations, such as cutter-suction-pipeline, have a similar fine-sediment loss processes (beach outwash) as the hopper-pumpout operation. These types of operations could be expected to have similar removal of fines as the hopper pumpout observed in this study. Increased confidence in the loss rates associated with varying sediment characteristics, dredge characteristics, and dredging operations will be gained with the addition of additional observations from the field and reanalysis of existing data.

5.5.2 Beach and Nearshore Placement Policy

The “Sand Rule” (F.A.C. 62B41-007(2)(j)) enacted by Florida’s Environmental Protection Agency and other similar regulations establish sediment compatibility requirements for coastal construction projects. These requirements are in place to ensure compatibility of construction materials with the existing beach. In the case of beachfill sand, compatibility factors include grain size, sorting, mineral composition, fines content, and color. From an aesthetics perspective, the established threshold of fines content under the Florida Sand Rule (5%) likely results from a heuristic approach, relying on decades of coastal construction experience. Accordingly, the threshold value of 5% is applied to the borrow area, and not the resulting beach fill, perhaps with the experiential knowledge that the placed material is observed to be aesthetically acceptable.

The coarsening effect of dredged sediment through overflow processes has been recognized since the early stages of dredging and pumpout operations that included overflow (Taney 1965). Much of the subsequent research in the following decade focused on textural changes (shifts in grain size distributions) between source and placed sediments as it affects the stability of beach fill for nourishment projects. Moreover, it is recognized that the practice of hopper overflow preferentially removes sediment components with small settling velocity, which usually associates with fine grain sizes (silt and clay). The removal of fine sediment also impacts sediment color. In the interest of ensuring compatibility of sediment removed from offshore borrow areas with the native beach material, the effects of dredging and placement must be considered in the compatibility assessment.

The currently accepted protocols for determining sediment compatibility for beach fill sediments is commonly a qualitative process. According to the Florida Department of Environmental Protection,

There is no quantitative protocol for determining similarity because the data and science does not exist for a quantitative determination of similarity needed to maintain the general character and environmental function of the material occurring on the beach and in the adjacent dune and coastal system. Therefore, in the absence of additional scientific research, this will remain a qualitative process of reviewing quantitative data. (FDEP 2010)

The results of this study, combined with the work of others (Ousley et al. 2014, Coor and Ousley 2019, Berkowitz et al. 2019) indicate that a more quantitative and scientifically defensible approach is possible and should be developed to predict changes in sediment characteristics for shore protection, habitat, and aesthetic concerns. Such an approach, applied with the appropriate, scientifically backed precautions, is the best way to ensure the appropriate use of sand resources in the coastal system.

6 Summary and Conclusions

A field study of the separation of sand and fine sediment by dredging and placement operations was conducted 20 June through 01 July 2018 on the Ship Island Restoration Project off the coast of Mississippi. At the borrow site, fine-sediment content was estimated from pre-project geotechnical samples and the ship track of the dredge. On the TSHD, *Liberty Island*, samples were collected from the inflow to the hopper and the hopper bed. At the beach, samples were collected from the beach immediately following pumpout. Eleven hopper loads were sampled in this way, and samples were processed in the lab to determine fine-sediment content, grain size distribution, sediment color, and other physical sediment characteristics. These results of the field research study combined with the observations of others lead to the following conclusions:

- The sampling approach and methods, vetted through laboratory testing, were to a large degree successful in obtaining the necessary samples from the field. The most notable issue in the collected samples is an apparent coarse bias in the samples collected from the hopper inflow. Samples collected at the inflow appear poor in fines (or rich in sand) compared to the borrow area analysis. A likely explanation of this discrepancy is the sampling from near the bottom of the discharge box, which likely resulted in sampling from near the bottom of a vertical gradient in sand concentration. The inflow samples were redundant with the borrow area characterization, so they were excluded from further analyses. Recommendations of further improvements to the field sampling plan are provided above in the discussion.
- Variability due to sample analysis procedures can be evaluated by quantifying the dispersion of results between triplicate subsamples extracted from composited samples. The averaged standard deviations for inflow, hopper, and beach subsamples was very small (0.3%, 0.1%, and 0.1%, respectively) and therefore contribute little to the overall variability observed between loads. Accordingly, high confidence is placed on the laboratory procedures to provide repeatable results despite the relative complexity of the procedure sequence and the small masses of fines analyzed.
- The fines content reduced sequentially from the borrow area, hopper, and beach. Hopper overflow removed 61% of the fine-sediment mass contained in the borrow area, and beach outwash removed 67% of the fines contained in the hopper. These two losses combined accounted for a removal of 87% of the fines dredged from the borrow area. Of the fine-sediment mass removed, 70% was removed by the overflow process and 30% was removed by beach outwash.
- Mud aggregates were observed in most of the loads sampled. Aggregates were present in all sample locations: inflow, hopper, and beach. Mud aggregates were composed of 20% sand, 53% silt, and 28% clay. The mud aggregate material has a USCS classification of CH (fat clay with sand). Millimeter-scale and larger mud aggregates settle as fast as or faster than sand and are consequently prone to sedimentation in the hopper and on the beach. The packaging of fine sediment in aggregates represents a hindrance to the separation mechanisms of hopper overflow and beach outwash that would otherwise remove the constituent particles of silt and clay. The fraction of fines content represented by the mud aggregates is unknown, but fraction of fines removed from the dredging operation would have been greater had the mud aggregates been broken up by the dredging and placement operations.
- Associated with the loss of fine-sediment content was a lightening of the sand from the borrow area to the beach. The wet MV changed from 3.8 to 4.4 from the hopper inflow to the beach. Fine-sediment content and beach color are closely linked by the pronounced effect that a small fraction of typically dark fine sediment has on an otherwise light quartz or carbonate sand. Berkowitz et al. (2019) have developed a laboratory testing method to express MV for beach sand

with varying fine-sediment content. The approach agrees well with observed values of this study, but requires additional evaluation and validation data prior to widespread application in practice.

- Knowledge of the relative loss of fines associated with specific dredging process has strong potential for use in project design. With this additional information, project engineers could design operations to 1) control the loss of fines near sensitive habitats or 2) modify dredge operation to increase/decrease loss of fines at a particular location.
- The data from the present study, combined with that of Coor and Ousley (2019), provide project managers with defensible fractions of fine-sediment loss from hopper dredging and placement operations for borrow areas ranging in fine-sediment content from 1% to 25%. With such an extensive data set available, estimates of the fine-sediment content after beach placement can be made by applying a simple mass-balance-based equation (Equation 10) of this report.
- Predictive tools (in the form of those described by Spearman et al. [2011] and Boone and Nijs [2018]) that model the separation of sand and fines should be considered to estimate the potential change in fine-sediment content of borrow area sediments caused by overflow. These predictive tools, with proper validation, could also be applied to investigate alternate dredging operation controls to increase or reduce fines loss at various stages of dredging and placement.
- The currently accepted protocols for ensuring sediment compatibility for beach fill sediments is commonly a qualitative process. The results of this study, combined with the work of others (Ousley et al. 2014, Coor and Ousley 2019, Berkowitz et al. 2019) indicate that a more quantitative and scientifically defensible approach is possible and should be developed to predict changes in sediment characteristics for shore protection, habitat, and aesthetic concerns. Such an approach, applied with the appropriate, scientifically backed precautions, is the best way to ensure the appropriate use of sand resources in the coastal system.

7 References

- Berkowitz JF, VanZomeren CM, Priestas AM, Price JJ. Forthcoming 2019. Incorporating color change propensity into dredged material management to increase beneficial use opportunities. ERDC Technical Report (publication pending). Vicksburg(MS): US Army Engineer Research and Development Center.
- Boone J, de Nijs MAJ. 2018. 1DH model predicts transport and sedimentation inside a hopper. *Terra et Aqua*. 150:33-43.
- Camp TR. 1936. A study of the rational design of settling tanks. *Sewage Works Journal*. 8:742-758.
- Camp TR. 1946. Sedimentation and the design of settling tanks. *Transactions of the American Society of Civil Engineers*, 2285:895-936.
- Capel PD, Larson SJ. 1996. Evaluation of selected information on splitting devices for water samples. USGS Water-Resources Investigations Report 95-4141. 103 p.
- Coor JL, Ousley JD. Forthcoming 2019. Historical analysis of fines lost during beach nourishment. ERDC-CHL CHETN. Vicksburg (MS): U.S. Army Engineer Research and Development Center.
- Dean RG. 2003. *Beach nourishment: theory and practice*. Singapore: World Scientific. 420 p.
- Dobbins WE. 1944. Effect of turbulence on sedimentation. *Transactions of the American Society of Civil Engineers*. 2218:629.
- [FDEP] Florida Department of Environmental Protection. 2010. Design, siting, and other requirements. Florida Administrative Code 62B-41.007
- FitzHarris M, Godsey E. 2014. Mississippi Coastal Improvements Program Barrier Island Restoration Project, offshore sand borrow investigation, 2010-2014, geotechnical engineering report, appendix A. Mobile (AL): U.S. Army Corps of Engineers.
- Hazen A. 1904. On sedimentation. *Transactions of the American Society of Civil Engineers*. Paper No. 980: 45-88.
- Hobson RD, James WR. 1978. Importance of handling losses to beach fill design. *Proceedings of the International Conference on Coastal Engineering*. Hamburg, Germany
- Matousek V. 1997. Flow mechanism of sand-water mixtures in pipelines [dissertation]. Delft (Netherlands): Delft University.
- Miedema SA, Vlasblom WJ. 1996. Theory of hopper sedimentation. New Orleans (LA): 29th Annual Texas A&M Dredging Seminar.
- Mikkelsen OA, Pejrup M. 2000. In situ particle size spectra and density of particle aggregates in a dredging plume. *Marine Geology*. 170:443-459.
- Nichols M, Diaz RJ, Schaffner LC. 1990. Effects of hopper dredging and sediment dispersion, Chesapeake Bay. *Environmental Geology and Water Sciences*. 15(1), pp.31-43.
- Ooijens SC. 1999. Adding dynamics to the Camp model for the calculation of overflow losses. *Terra et Aqua*. 76:12-21.

- Ousley JD, Kromhout E, Schrader MH, Lillycrop LS. 2014. Southeast Florida sediment assessment and needs determination (SAND) study, Final Report. ERDC-CHL TR-14-10. Vicksburg (MS): U.S. Army Engineer Research and Development Center.
- Rabenhorst MC, Schmeehling A, Thompson JA, Hirmas DR, Graham RC, Rossi AM. 2015. Reliability of soil color standards. *Soil Science Society of America Journal*. 79(1).
- Spearman J, DeHeer A, Aarninkhof S, Van Koningsveld M. 2011. Validation of the TASS system for predicting the environmental effects of trailing suction hopper dredgers. *Terra et Aqua*. 125:14-22.
- Taney, NE. 1965. A vanishing resource found anew. *Shore and Beach*. 23(1): 23-26.
- [USDA] U.S. Department of Agriculture, Soil Science Division Staff. 2017. Soil survey manual. USDA handbook 18. Ditzler C, Scheffe K, Monger HC, editors. Washington (DC): U.S. Department of Agriculture. 639 p.
- van Rhee C. 2001. Numerical simulation of the sedimentation process in a trailing suction hopper dredge. Kuala Lumpur (Malaysia): Proceedings of the 16th World Dredging Conference.
- van Rhee C. 2002. Modeling the sedimentation process in a trailing suction hopper dredger. *Terra et Aqua*. 86:18-27.
- Vlasblom WJ, Miedema SA. 1995. A theory for determining sedimentation and overflow losses in hoppers. Amsterdam: Proceedings of 14th World Dredging Congress. p. 183-202.
- Wilson KC, Addie GR, Sellgren A, Clift R. c2006. Slurry transport using centrifugal pumps. 3rd Ed. Springer Science & Business Media.

Appendix A Conceptual Model of Sediment Routing During Dredging and Pumpout

This appendix presents a conceptual model of the hopper dredging and pumpout process. The model begins with an overview of the dredging process from source to placement area, then identifies points of sediment sorting and loss of fine sediment during that process. Generally, fine-sediment losses occur in the hopper during overflow and at the placement site during outwash. Once placed on the beach or the nearshore, sediments can be further winnowed by natural coastal processes (i.e., waves and currents). This appendix also includes a discussion on the transport processes of the fine sediment in the overflow plume. The appendix concludes with discussions of uncertainty in quantifying losses, the proposed laboratory testing plan, and field sampling plan.

1 Conceptual Model

The primary aim of this work is to determine the size-dependent loss of sediment at each stage of the dredging process from a TSHD. Other dredge types, such as mechanical dredgers, are not considered here.

This section briefly summarizes the loading cycle and sedimentation processes within TSHDs and identifies the points of separation where sediments may be fractionated or removed. Additionally, the mass balance of material flow is defined for each stage in the process and used as the basis to quantify those losses.

In TSHDs the dredging cycle can be categorized into three primary stages: 1) removal of the bed material, 2) loading of the hopper, and 3) discharging the hopper load through pumpout, rainbowing, or bottom dump. Referring to Figure A-1, first, sediments are hydraulically excavated from the borrow area (B) through a drag head and impeller pump system while the dredger is in forward motion. The sediment-water mixture, which is about 10–20% solids by volume (Bray et al. 1997), is then discharged into the hopper (H) at point (I) at a given flow rate (Q_{in}) and mixture density (C_{in}). As the hopper fills, particles segregate as coarser particles settle to the bottom while finer particles remain in suspension depending on size distribution, slurry density, and hydrodynamic conditions within the hopper. Once the slurry level (η) reaches the level of overflow (η_{ov}), excess water and suspended sediments are expelled through an overflow weir (W) that discharges into the water column either near the water surface or through the base of the ship's hull. Pumping is stopped when the bed level reaches the overflow weir, which is adjustable in the constant tonnage system (CTS) or fixed in the constant volume system (CVS). Finally, discharging of the hopper load is accomplished by either direct dumping through bottom doors or use of a split hull, rainbowing (pressurized aerial discharge from the bow), or direct pumpout (P) onto a shoreline (BCH) or confinement area, as depicted in Figure A-1B.

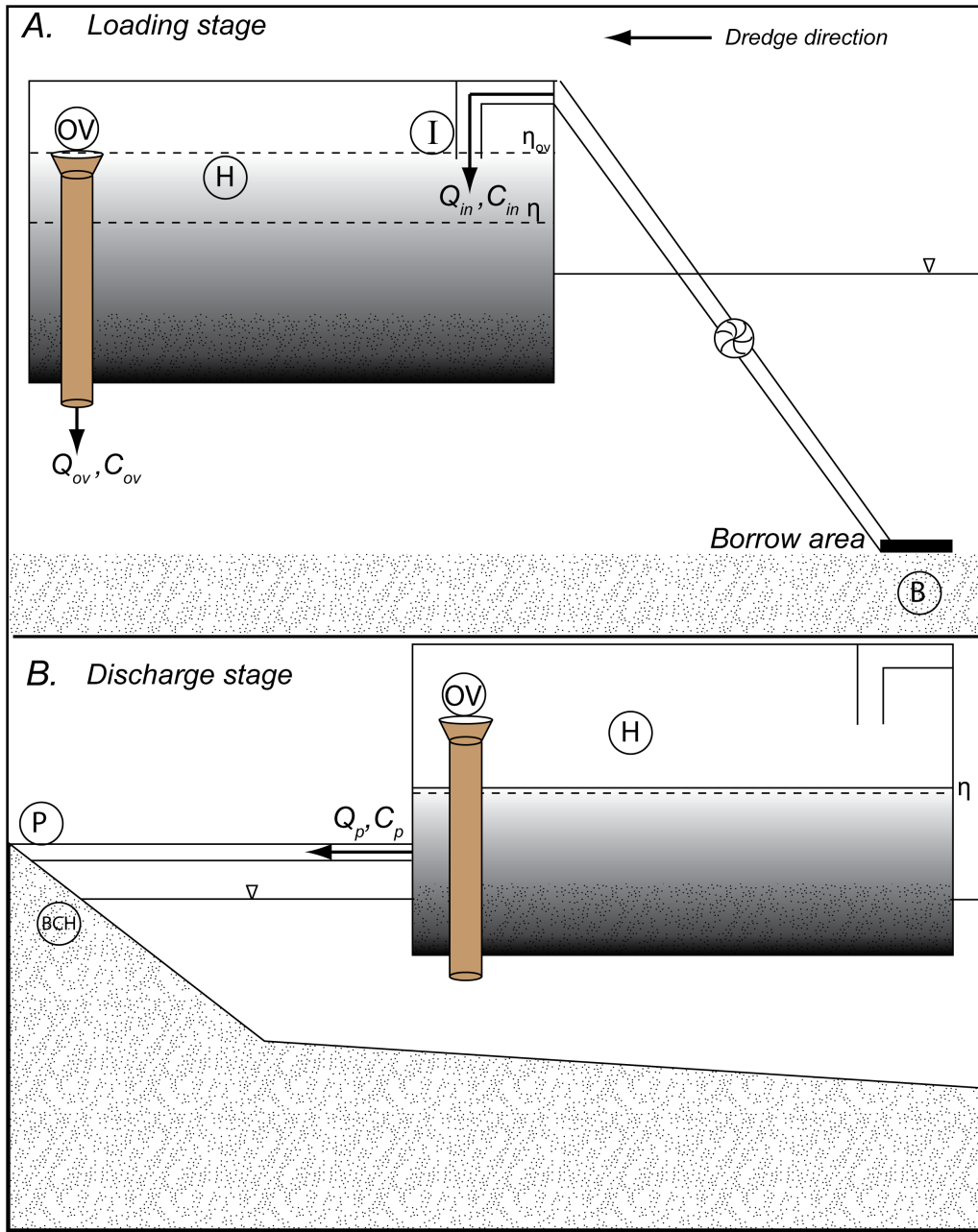


Figure A-1. Schematization of the loading and discharge cycles of TSHD operations.

Loading stage (A) and discharge stage (B) of a TSHD with through-hull overflow weir system (OV). A mass-balance approach is used to determine the loss of fine material between the borrow area (B) and placement area along a beach (BCH). The mass-balance approach tracks flow (Q) and sediment concentration (C) at the inflow (I), overflow (OV), and pumpout (P).

The removal of sediments during overflow is expected to be the primary conduit for the loss of fines. The separation of fines may also occur during pumpout onto the shoreface of a beach; turbulence may resuspend sediment, and return flow from the outfall may entrain and transport fine sediments, which are then carried offshore and alongshore in addition to winnowing by subsequent waves and tides. The goal

of the present research is to quantify these losses at each point in this process using a mass-balance approach (). For this approach, the following assumptions are made:

1. Negligible loss of fines at the drag head
2. Negligible effect or likelihood that overflow sediments are reintroduced at the drag head
3. Negligible loss of fines associated with pipeline transport
4. All sediments are fully retained within the hopper during the loading stage (except during overflow) and fully removed during the discharge stage

At the site of the drag head, some sediment resuspension may occur as the drag head is often equipped with jets or teeth to loosen the sediment prior to being suctioned in order to improve production efficiency, or equipped with turtle deflectors which are designed to push a sand wave ahead of the dragarm. These modifications may serve to increase fine-sediment resuspension at the bed. Additionally, resuspension may occur if the forward speed of the dredger is too fast (i.e., not optimized relative to suction capacity). In general, however, these are not thought to contribute significantly to the loss of fines because the pressure difference over the drag head causes flow potentials some width away from the drag head (Vlasblom 2007), which is speculated to minimize resuspension. Instead, based on previous experience, there exists the possibility that some finer material from the overflow plume (discharged from the hopper) may settle and be re-entrained into the drag head, enriching the inflow with fine sediment, though this would be dependent of site specific conditions. Additional losses may occur through leakage of the hopper doors or hull and through pipeline connections; however, these losses are considered negligible from a mass-balance perspective. It is expected that not all sediment will be completely removed from the hopper during discharge, which will add to the uncertainty estimates using this approach.

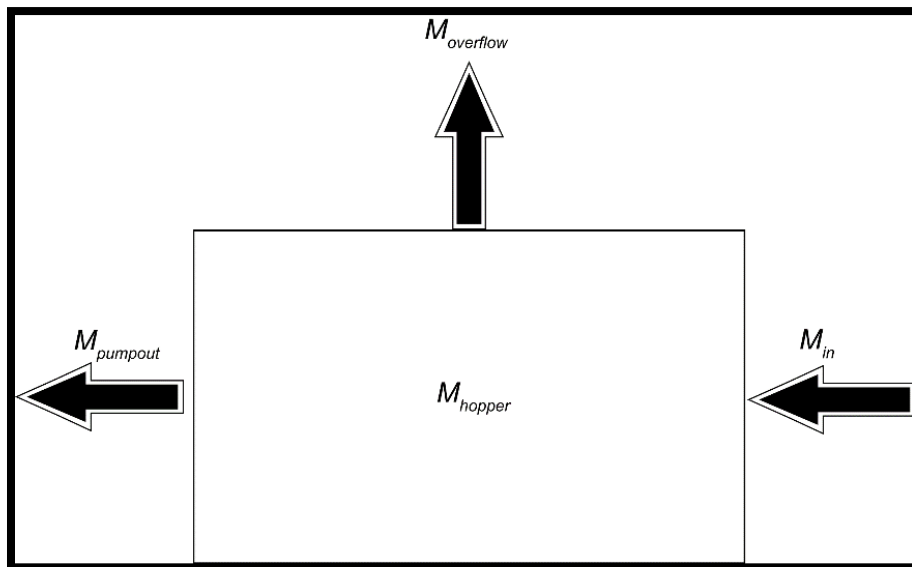


Figure A-2. Mass balance of sediments during a dredging cycle.

The total mass of sediments entering the hopper ($M_{in} = Q_{in}C_{in}$) (Figure A-2) is balanced by the sum of masses exiting thus,

$$M_{in} - (M_{overflow} + M_{pumpout}) = 0 \quad (A-1)$$

$$M_{in} = M_{overflow} + M_{pumpout} \quad (A-2)$$

During the loading stage, the mass retained in the hopper is

$$M_{hopper} = M_{in} - M_{overflow} = M_{pumpout} \quad (A-3)$$

During the discharge stage, the mass transferred to the placement area during pumpout is equal to the mass retained in the hopper (Equation A-3) assuming no leakage from the hopper and 100% of the sediment was removed.

The mass flow of sediments into the hopper can be expressed as,

$$\frac{dm_{in}}{dt} = Q_{in}\rho_m = Q_{in}(\rho_w(1 - C_v) + \rho_s C_v) \quad (A-4)$$

where,

$$Q_{in} = \text{flow rate [m}^3/\text{s]}$$

$$\rho_m = \text{slurry density [kg/m}^3], \rho_w = \text{water density [kg/m}^3]$$

$$\rho_s = \text{sediment density [kg/m}^3], C_v = \text{volume fraction occupied by sediment [-]} \equiv \frac{\rho_m - \rho_w}{\rho_s - \rho_w}$$

However, the percentage of fines lost in the dredging process does not require explicit knowledge of the slurry density and can be quantified by measuring the flow in and out of the hopper and the sediment concentration by mass. The total mass of sediments into the hopper is,

$$m_{in} = \sum Q_{in} C_{in} \Delta t_{in} \quad (A-5)$$

where C_{in} is the incoming slurry sediment concentration.

If the particle size distribution is known, the percentage of fines (f) is also known, so that the mass of fines into the hopper is,

$$m_{in} = \sum Q_{in} C_{in} f_{in} \Delta t_{in} \quad (A-6)$$

During loading, sediment mass is assumed to be fully retained inside the hopper while the slurry level (η) in the hopper is below the level of the overflow weir (η_{ov}). Once $\eta = \eta_{ov}$ the flow volume into the hopper is equal to the flow discharged at the weir ($Q_{in} = Q_{ov}$). Likewise, the sediment mass discharged through the overflow weir can be estimated as,

$$m_{ov} = \sum Q_{in} C_{ov} \Delta t_{ov} \quad (A-7)$$

where Δt_{ov} is the dredging time past overflow. The total mass of sediment retained in the hopper is calculated as,

$$m_H = m_{in} - m_{ov} = \sum Q_{in}(C_{in}t_{in} - C_{ov}t_{ov}) \quad (\text{A-8})$$

The average fraction of sediments lost through overflow is estimated as the ratio of overflow to inflow sediment mass,

$$ov = \frac{m_{ov}}{m_{in}} \quad (\text{A-9})$$

Similarly, the fraction of fines lost during overflow is,

$$f_{ov} = \frac{m_{fov}}{m_{fin}} \quad (\text{A-10})$$

The fines content during pumpout, which theoretically should equal that of the hopper, could be used as a check against the calculation for the fines content retained in the hopper (Equation A-5).

2 Separation of Sediment by Hopper Dredging

This section reviews the processes related to size fractionation of sediment and their subsequent removal through the dredging cycle.

2.1 Tank Sedimentation

Sedimentation in general is categorized into Types 1–4 as described in the ensuing text. In Type 1 settling, discrete particles settle freely and independently according to Stokes' Law and independent of concentration. Particle sizes do not change, and therefore settling times are constant. In Type 2 settling, particles may flocculate and grow, which accelerates their fall velocity, also in accordance to Stokes' Law; settling times are therefore nonlinear. Type 3 is characterized by hindered settling, whereby settling velocities are reduced due to modification of the flow field induced by very high particle concentrations. Finally, Type 4 refers to compression settling, which describes the process of sediment compaction and resulting upward displacement of water.

The decrease in settling velocity is often described by the power law formulation from Richardson and Zaki (1954):

$$\frac{w(c)}{w_o} = (1 - c)^n \quad (\text{A-11})$$

where w is the hindered settling velocity, w_o is the settling velocity of a single grain in still water, and c is the average volumetric sediment concentration; the exponent n depends on the Reynolds number and is typically between 2.5 and 5.5. Van Rijn (1984) suggested a value of $n = 4$ for very fine to medium sand.

For sand grains, the transition to hindered settling occurs when particle concentrations are on the order of 10–20% by volume depending on particle type (Tomkins et al. 2005). Formulations by Soulsby (1997), Toorman and Berlamont (1991), Winterwerp (1999), and others have also been proposed to account for cohesive floc settling at high concentrations.

All four settling types are likely physically represented at different stages in the loading process. As sediments enter the hopper (assumed to be fully retained prior to overflow), they immediately segregate according to settling type, the nature of which depends on particle size, shape, concentration, and degree of cohesiveness. During segregation, a sediment-water interface develops and some fraction of the finer sediments will remain suspended in the overlying water column, assisted by a net upward velocity of water from the hindered settling effect, while coarser sediments will settle or partially settle prior to overflow. The depth of the water layer will outpace the bed layer thickness until overflow is reached. Prior to overflow, water velocities are relatively low, allowing grains to settle. During overflow, flow velocity increases and sediments in suspension are discharged as the bed continues to rise. The rising bed level further increases the flow velocity above the bed, which can contribute to scouring and acceleration of overflow losses depending on grain size; therefore, the dredging of finer sediments increases total overflow losses (Miedema and Vlasblom, 1996). A rule of thumb given by Vlasblom (2007) states that sediment with $d_{50} < 75 \mu\text{m}$ are entrained in overflow, though this does not consider fine sediments in the form of clay balls, aggregates, and flocs which have greater settling velocities.

2.1.1 Models of Tank Sedimentation and Separation

Hoppers can be considered as large capacity settling tanks with an inflow and outflow. Much of the work on sedimentation within settling tanks was originally developed for the wastewater treatment industry. The ensuing theories were primarily developed for the purposes of removing suspended fines or ‘clarifying’ the water column through the settling process. Reference is made to Camp (1936, 1946) and Dobbins (1944), whose theory on sedimentation (rooted in the work of Hazen [1904]) within ideal settling tanks is often regarded as the basis for settling theory and overflow losses within hopper dredges.

The Camp model (Figure A-3) considers the trapping efficiency of sediments subjected to steady, uniform flow. The ideal basin is separated into an inflow zone, a settling zone, and an outflow zone. Sediments enter the basin in the direction of uniform, horizontal flow with uniform concentration in the vertical plane. Each particle then settles at a constant rate according to Stokes’ Law. As such, the particle trajectories move along downward trending parallel paths across the length of the basin, equal to the vector sum of horizontal flow v_H and vertical settling velocities v_s . All particles are removed from the flow (i.e., the flow is “clarified”) if they settle at a distance less than the length of the basin (by corollary, removal from flow implies retention in the basin). In Camp’s model, this vector is the critical settling velocity sometimes called the overflow rate or surface loading rate; as applied to hoppers this is often referred to as the *hopper load parameter* defined as $v_0 = v_H \left(\frac{D}{L} \right) = \frac{Q}{A}$, where Q is the volumetric inflow rate, D and L are basin depth and length, respectively, and A is the basin area. In the Camp model, sediments entering from the top of the basin, which settle at a rate equal to or greater than the critical flow velocity, will be retained. Slower settling particles will be retained only if they entered the zone starting from a lower depth in the basin. Ultimately, sediment retention is independent of basin depth in this model. For this reason, and considering Type 1 settling behavior only, the settling efficiency depends only on the overflow rate (hopper load parameter); smaller overflow rates increase settling efficiency (retention) for a non-rising bed level. Thus, Camp’s model can estimate the flow-weighted concentration in the overflow by depth averaging over the outlet zone. Camp (1946) and Miedema and Vlasblom (1996) later added turbulence effects and resuspension by scouring to investigate the resulting changes in settling efficiency.

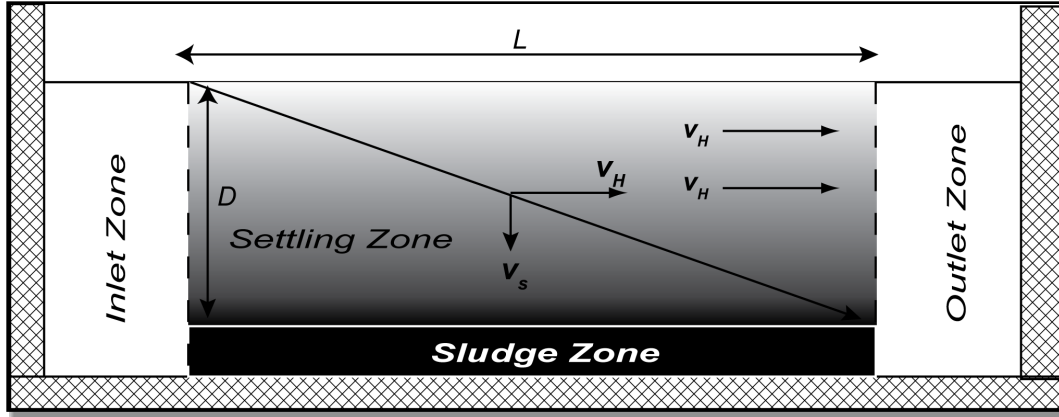


Figure A-3. Conceptual model of an ideal settling tank.

In this model, D is the basin depth, and L is the basin length. Sediment enters the basin from the inlet zone with a uniform vertical concentration and horizontal velocity V_H . Particles then settle with velocity V_s according to Stokes' Law. A particle is considered lost to overflow only if the vector sum of V_H and V_s is greater than the basin length (i.e., the settling time is less than the time to travel the distance L). Adapted from Camp (1936).

Vlasblom and Miedema (1995) and Miedema and Vlasblom (1996) further modified Camp's model to incorporate grain size distribution, hindered settling effects, and a rising bed level; the constant horizontal flow field was retained with no vertical velocities except those derived from turbulence. The outflow concentration is calculated instantaneously based on the incoming flow concentration and settling efficiency. The model generates loading curves (i.e., production rate in tons dry solid [TDS]) based on measures of influent mixture flow and density. The settling efficiency is determined by accounting for turbulence and velocity changes due to a rising bed level for either a CTS or CVS hopper. The model produces an evolution of the grain size distribution and then calculates the mass of solids lost during overflow.

The model of Ooijens (1999) adds to the Miedema and Vlasblom (1996) model by introducing an unsteady state in flow volume and slurry concentration to estimate overflow losses considering the hopper as an ideal mixing tank. Virtual concentrations were used as input to the model and compared to measured overflow losses, which were estimated using shipboard measurements of incoming flow (Q_{in}) and volumetric sediment concentration (C_{vin}) along with the change in measured TDS (Rullens 1993) for a given time interval (Δt) and particle density ($\rho_s = 2650 \text{ kg/m}^3$),

$$ov = \frac{C_{vin}Q_{in}\Delta t\rho_s - TDS(t) - TDS(t - \Delta t)}{C_{vin}Q_{in}\Delta t\rho_s} \quad (\text{A-12})$$

The model captured the estimated overflow loss reasonably well for two of three dredging test cases with a reported correlation of 0.75 to 0.85.

Van Rhee (2001, 2002) used both laboratory experiments and numerical modeling to investigate the hopper sedimentation process. Five different flow field regions of a model hopper were identified based on visual observations from laboratory experiments that used a rectangular glass-sided settling tank. Referring to Figure A-4 these are: the inflow section (1), settled sand bed (2), density flow over the bed (3), horizontal surface flow toward the outlet (overflow section) (4), and sediment suspension (5). The incoming flow creates an erosion crater and density current from which sediments are deposited resulting

in a rising bed level. Part of the sediment that does not settle moves upward into suspension, and the incoming flow induces a strong horizontal flow toward the overflow section.

The amount of fine material lost in the overflow was quantified over 19 experiments. The experiments showed that cumulative overflow losses could be expressed as a linear function of the dimensionless hopper load parameter $H^* = v_o/w_o(1 - c)^n$, which is the overflow rate divided by the sedimentation velocity of the suspension (i.e., hindered settling given by Equation A-11); therefore, overflow losses increase with the hopper load parameter. This linear relationship was found to improve if the load parameter was instead based on sand fluxes (ratio between the inflow fluxes and settling fluxes) given as,

$$S^* = \left(\frac{c_{in}}{c_{bed}} \right)^{1 - n_o - c_{bed}} H^* \quad (A-13)$$

where c_{in} and c_{bed} are the inflow and bed concentrations, respectively, and n_o is the porosity. Since c_{bed} is not known, it is assumed equal to c_{in} as a first approximation. The cumulative overflow loss was regressed against S^* to obtain,

$$Ov_{cum} = 0.39(S^* - 0.43) \quad (A-14)$$

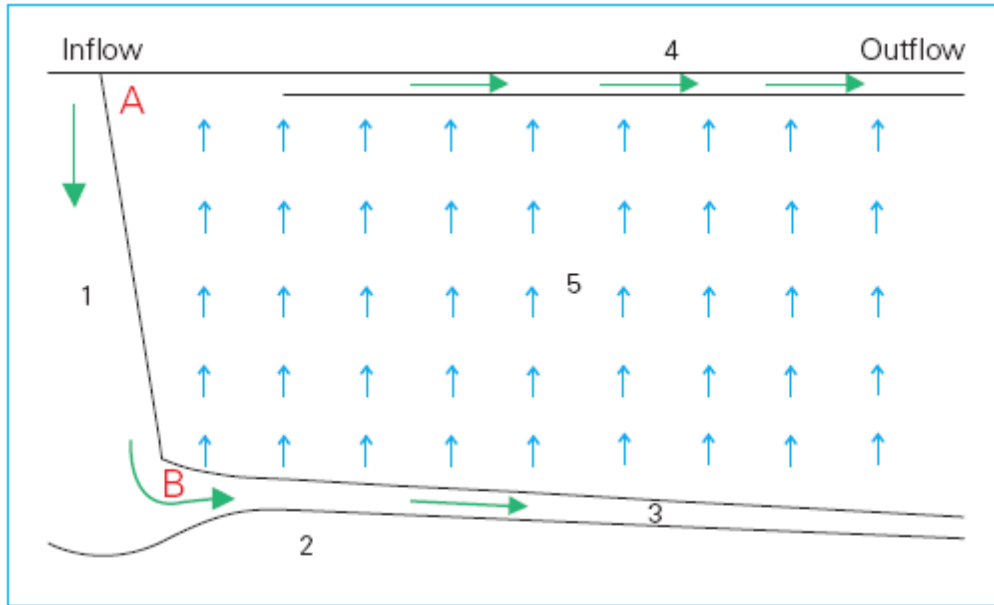


Figure A-4. Schematization of flow for a single inlet settling tank.

Numbers refer to the following: inflow section (1), settled sand bed (2), density flow over the bed (3), horizontal surface flow toward the outlet (overflow section) (4), and sediment suspension (5). The incoming flow creates an erosion crater and density current from which sediments are deposited resulting in a rising bed level. Part of the sediment that does not settle moves upward into suspension, and the incoming flow induces a strong horizontal flow toward the overflow section. Figure adapted from van Rhee (2002).

The author noted that it is uncertain if the relationship holds for different scales, and it only accounts for spherical grains of uniform diameter. Likewise, the concentration at the bottom is not known and must be approximated by the incoming concentration.

One of the conclusions based on the laboratory study was that turbulence plays a lesser role in sedimentation processes within hoppers, though that may not hold at prototype scale. Given the oft-observed viscous flow behavior during hopper loading stages, that conclusion may be applicable in many cases.

For the modeling component, a one-dimensional model of hopper sedimentation was developed using the advection-diffusion equation for a poly-disperse mixture and includes the influence of the overflow rate (hopper load parameter). As opposed to the horizontal settling tank model of Camp, this model simulates hopper loading in the vertical dimension with sediments introduced from the bottom fed by the density current, and the overflow located at the top. The model was compared with one-dimensional tests in a settling column, which showed reasonably good agreement (Figure A-5). Van Rhee (2002) later developed a 2D model based on the Reynolds-Averaged Navier Stokes equations with a $k\epsilon - \epsilon$ turbulence model. The modeled overflow losses compared similarly to the simplified Camp model of Miedema and Vlasblom (1996).

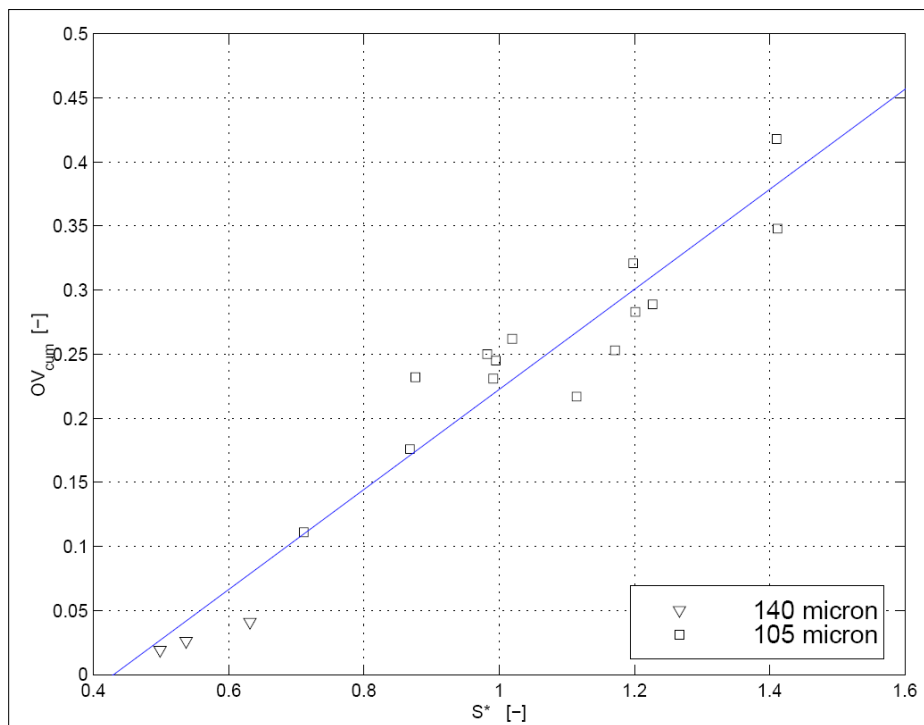


Figure A-5. Cumulative overflow losses as a function of the dimensionless hopper load parameter based on sand fluxes.

Adapted from van Rhee (2001).

Miedema (2009b) investigated the influence of the bed rise velocity on the hopper load parameter as the decrease in the hopper depth influences the settling time and increases the overflow rate. This gives rise to a modified hopper load parameter and settling efficiency. A secondary research topic, which examined potential scaling laws from small to large capacity hoppers, determined to keep the hopper load parameter constant, to derive other scale laws for the flow, and not to scale the sand (Miedema 2009a).

In all of the above models, the monitoring system aboard the dredge is used to quantify flow and sediment concentration into the hopper. Overflow losses are typically quantified in terms of the effect on

production, i.e., total mass of sediment lost per hopper load. However, the fraction of fines lost cannot be determined without knowledge of the PSDs at various points in the dredging process. Because PSDs are not part of the monitoring system, direct samples must be taken for particle size analysis and quantification of the fraction of fines lost.

2.2 Separation of Sediment by Pipeline Outfall and Beach Processes

Previous research regarding sediment dispersion at a pipeline outfall is dominated by open-water placement of material (i.e., nearshore placement). Models have been created to illustrate the mixing zone of dredged material, as well as the near-to-far field models of mixing. Models have also been created to simulate the underflow at discharge points caused by the formation of fluid mud layers at the bed that flow away from the discharge point and are dependent on bottom slope, ambient currents, and their initial discharge trajectory (Teeter 2002). These models are summarized in this section; however, they only apply to open-water placement of material. In many cases, the studies do not summarize separation of the sediment based on grain size, rather than the dispersion of the dredged material as a whole. Much of the literature regarding separation of fines at this point in the process (i.e., pipe outfall on the beach) was attributed to beach processes that occur naturally before, during, and after placement of material on the beach.

2.2.1 Pipeline Outfall

Pipeline outfalls associated with open-water disposal of dredged material have been studied since the 1970s to determine potential environmental impacts of dredging due to suspension of sediments in the water column (e.g., Gordon 1974, Brandsma and Divoky 1976, Henry et al. 1978, Nichols and Thompson 1978). These studies were mainly focused on resuspension and the behavior of the material to predict the extent and duration of the fluid mud and ultimately determine potential environmental impacts due to dredging. In subsequent studies, focus was turned to the dispersion and underflow of the material once it was placed in the open water. Teeter (1994) describes three dispersion phases of pipeline disposal of dredged material: discharge plume descent, underflow spreading and entrainment of the underflow material into the overlying ambient flow, and passive dispersion. The Plume Measurement System (PLUMES) was used at a field site in the James River Estuary in Virginia to detect relative concentrations, measure current fields, and chart vessel position during a dredging event. Suspended sediment samples were also collected for ground truthing. The field data indicated that the discharged sediment descended and reached the bed directly below the discharge point. An underflow formed and spread to a distance approximately 100 m from the source, and the spreading was controlled by the bathymetry of the site. It was also concluded that most entrainment would occur during higher current speeds

Although no literature was found on studies regarding pipeline outfall on the beach, the sedimentation processes due to outwash on the beach are similar to those in the hopper. Sorting of sediments during beach outwash is governed by the balance of particle settling and the physical processes of the flow. Sediment in the pumped slurry within the pipeline are kept in suspension by maintaining sufficiently high flow velocities (and turbulent mixing) in the pipe. The flow exiting the pipe plunges into a mixing cell and then spreads out under gravitational effects as dictated by the geometry of the beach and exit velocity of the flow. The beach geometry may be altered by temporary construction works such as berms or dikes to direct the outflow and/or enhance sedimentation. As the flow becomes less confined and spreads under gravitational forcing, velocities typically decrease, leading to decreased turbulent mixing and deposition of the suspended sediments. The degree of sedimentation is governed by factors such as the horizontal velocities, the beach slope, water depth in the outfall flow, length of the outwash path, and sediment settling velocity. Fine-sediment losses during outwash may be reduced when berms or dikes are used for mitigating surf zone turbidity.

2.2.2 Modeling of Discharge from Pipeline Outfalls

Several models illustrate discharge at pipeline outfalls. CORMIX is a U.S. Environmental Protection Agency near-field mixing analysis model that simulates the initial mixing of the dredged material immediately upon submerged discharge from the dredge pipe (Doneker and Jirka 2007, MG Associates 2012, Purnama et al. 2016). The Pipeline Discharge FATE (PDFATE) model is used to evaluate underflow spreading and to predict the deposition of sediments on the bottom as well as entrainment of sediments in the water column (Teeter 2000, 2001; MG Associates 2012). The model formulation includes deposition of sediment particles according to concentration dependent settling rates and shear stress thresholds related to sediment characteristics, entrainment of overlying water into the underflow, appropriate flow properties of the underflow suspension, lateral spreading of the underflow, and variable bottom slope (Teeter 2001, MG Associates 2012). To determine long term fate of material once it deposits on the bottom, the Environmental Fluid Dynamics Code (EFDC) coupled with the SEDiment dynamics algorithms as developed by Ziegler, Lick, and Kerssemaker (SEDZLJ) model is often used (Ziegler and Lick 1986, 1988; Jones and Lick 1999, 2001). EFDC is a model for simulating three-dimensional flow, transport, and biogeochemical processes in surface water systems (Hamrick 1996). EFDC was modified by the Sandia National Laboratories to include sediment dynamics such as erosion and bed load transport, bed sorting, and armoring (James et al. 2010, Thanh et al. 2008, MG Associates 2012). The USACE later incorporated EFDC-SEDZLJ in the Long Term Fate (LTFATE) modeling analysis for material placed in open water (e.g., Hayter et al. 2012). These models are generally not applicable for subaerial pipeline outfalls on the beach; however, they are applicable for nearshore placement.

2.2.3 Separation of Sediment due to Nearshore and Beach Processes

Once material is placed on the beach, sediment separation due to natural beach and nearshore processes such as waves and currents can occur. The concept that fine material winnows out of beach sands through hydrodynamic or aeolian forcing is well established (e.g., Stapor and Tanner 1975, McCave 1978, Kana and Mohan 1998); however, recent studies have begun to focus on detailed monitoring of sediment characteristics following beach nourishments to determine if current state regulations regarding placing certain amounts of fines on beaches are necessary (e.g., Warrick 2013, Goodrich and Warrick 2015, Maglio et al. 2015). Generally, because fine material has a slower settling velocity than coarse material, once material is suspended in the water column, fine sediment is entrained in the orbital motions of the wave for a longer time, and consequently, the fine fraction of the sediment is transported further offshore than the coarse fraction (e.g., Dean 1973, Dean 1977, Hallermeier 1981).

Warrick (2013) studied a nourishment at Imperial Beach, California, which contained 40% fines by weight. The study showed that the mean residence time of fine material suspended in the surf zone through wave action was approximately 1 hour. Decreases in fine sediment within the surf zone along the beach were due to offshore transport due to rip currents. In the swash zone, because the material was placed directly on the beach, elevated levels of suspended fines lasted several days after nourishment as fine material was being winnowed from the beach. Deposition of the fine material was greatest on the seafloor directly offshore of the nourishment area; however, a mass balance of the sediment suggested that the majority of fine sediment was deposited over 2 km away from the nourishment site, or to water depths greater than 10 m. The study concluded that the fate of fine material was strongly influenced by wave conditions, surf zone and rip current transport, and the vertical density and flow conditions of coastal waters. Goodrich and Warrick (2015) summarized this study as well as a study conducted at Santa Cruz Harbor. The two demonstration projects were used as tools to communicate with coastal managers regarding the use of material with relatively large amounts of fines in beach and nearshore nourishments.

Maglio et al. (2015) studied several beach nourishment projects in Florida to determine fines loss through the dredging process. Specifically, at Egmont Key, Florida, fine material initially found on the surface of

beach and in the nearshore immediately post-placement was no longer seen in successive surface sediment samples along the profile five months post-placement, indicating that fine sediment found on the surface was likely winnowed through wave-current processes and transported away from the beach.

2.3 Transport Processes in TSHD Overflow Plumes

During overflow of TSHDs the suspended sediments passing over the overflow weir are introduced outside of the dredge and into the water column. In most cases, the overflow stream is denser than the surrounding water and a negatively buoyant cloud or jet is formed. This dense, *dynamic plume* is transported toward the sediment bed primarily by buoyancy effects. During the descent of the dynamic plume, ambient water is entrained into the plume and the plume becomes less dense. The descent of the dynamic plume may be arrested by neutral buoyancy or interaction with the bed. During descent and interaction with the TSHD hull or propellers, turbulence may eject and mix smaller clouds of suspended sediment with cloud densities that are nearly equal to the surrounding water body. In this case, the settlement of the clouds can become dominated by particle settling. These *passive plumes* settle at rates governed by the size and density of individual particles suspended in the cloud.

2.3.1 Dynamic Plume

The TSHD dynamic plume is challenging to observe and sample in the field environment as it is typically positioned beneath the hull of the moving dredge. Due to the difficulties of directly measuring the dynamic plume in the field, most research of the governing processes has been performed with physical and numerical modeling. Chu and Lee (1996) provide a review of theoretical physical processes of plumes and jets in crossflow. Winterwerp (2002) conducted experimental laboratory studies relating the relative importance of dynamic plume spreading by mixing and gravity effects. Recently, de Wit et al. (2014) expanded upon this work by examining the interaction of the dynamic overflow plume with the near-field effects of the TSHD hull and propellers under varying operational parameters with a combination of physical and Computational Fluid Dynamics (CFD) models.

2.3.2 Passive Plume

Relatively speaking, the TSHD passive plume has received much more attention in recent research. The passive plume is of interest, primarily because of the slower settling rates of suspended sediment in the passive plume and consequently the greater capacity for these suspended sediments to be transported relatively large distances from the dredging site. To appropriately model the passive plume, numerous dredge and sediment properties must be defined. At the TSHD, the density and overflow rate of dredged material must be determined, as well as the sediment size distributions. The mass exchange rate (or exchange fraction) between the dynamic plume and the passive plumes must be quantified, along with the initial vertical distribution of passive plumes. Furthermore, the settling rates of suspended sediment must be determined. Advances in optical and acoustic instrumentation in the 1990s permitted measurement of suspended sediment concentrations and sizes in dredge plumes (Kraus and Thevenot 1992, Land and Bray 2000, Mikkelsen and Pejrup, 2000). Spearman et al. (2007, 2011) summarize field research performed in the early 2000s in Europe to determine the exchange rate between the dynamic and passive plumes. Mikkelsen and Pejrup (2000) documented increasing suspended particle size with distance from the dredging operation, suggesting that flocculation was an important process influencing settling rates in passive plumes. Smith and Friedrichs (2011) deployed their Particle Imaging Camera System (PICS) in a TSHD overflow plume in San Francisco Bay to measure suspended particle size, settling velocity, and density. Smith and Friedrichs found that flocculation occurred in the overflow plume and a population of dense *bed aggregates* was present, which further increased the settling velocity of the suspended aggregates relative to their constituent particles.

2.3.3 Modeling of the Overflow Plume

The buoyancy-driven dynamic plume and the particle-settling-dominated passive plume are governed by different physical processes operating over distinctly different time- and space-scales. Consequently, numerical modeling of these two phases of the overflow plume is typically handled with separate frameworks and modules for the distinct phases. The required process representations for modeling the overflow plume begin with the overflow process of the TSHD itself. The mass rate of overflow is expected to vary in space and time. A model representing the variances in the mass rate of overflow and the composition of overflow provides the initial conditions for the dynamic plume. The dynamic plume model would then represent the descent of the plume from the overflow discharge to the bed or a position of neutral buoyancy in the water column. Included in this process would be any mixing of sediment into the water column as passive plumes. Finally, a passive plume model will transport suspended sediment contained in passive clouds until conditions permit deposition.

The modular description of the modeling workflow described above is common among dredged material plume and outfall modeling (Koh and Chang 1973, Johnson 1990, Spearman 2011). The models derived from these efforts (CDFATE and TASS) operate on a Lagrangian cloud-based framework. Lackey and Smith (2008) applied the initial passive plume estimates of the bottom dump model, STFATE, as initial conditions to the Lagrangian Particle Tracking Model (PTM) for a navigation dredging study. The advantage of this approach is that the local-scale Lagrangian cloud models can approximate overflow and the dynamic plume, while a high-fidelity 3D Lagrangian model (such as PTM) can represent particle mixing and deposition in the far field. Point-based Lagrangian models such as PTM offer significant advantages over the cloud-based Lagrangian approach, primarily through higher fidelity of transport processes over long distances. The coupling of appropriate hopper and dynamic plume models to a 3D, point-based Lagrangian sediment transport model (in the style of Lackey and Smith [2008]) will be further explored over the course of this research.

In addition to the numerical modeling framework, specific issues of fine-sediment separation in the hopper and fine-sediment settling velocities in the passive plumes must be addressed. Separation of sand and fines by hopper overflow is largely dependent upon the settling velocity of sediment particles. Sand-sized and coarser sediment particles have relatively large settling velocities (typically 6 mm/s or more), which allow them to settle in the hopper, and disaggregated fine sediments have small settling velocities (typically less than 2 mm/s), which allow them to be maintained in suspension to the overflow weir. However, fine sediments may be cohesive, forming aggregates that are greater in size but less dense than the constituent particles. The largest of these aggregates, known as clay balls in the dredging community, are recognized to deposit in hopper dredges during overflow (Palermo and Randall 1990, Burt and Hayes 2005). However, these fine-sediment aggregates are likely to form in a wide range of sizes. Smith and Friedrichs (2011) documented 40–250 μm fine-sediment aggregates settling at rates as fast as 5 mm/s in a TSHD overflow plume. Smith and Friedrichs further postulated that larger, faster settling aggregates were likely trapped in the hopper. In fact, dense *bed aggregates* 300 μm or larger would have settling velocities equal to or greater than fine sand. Of course, fine-sediment aggregates produced during the dredging process must survive the large mechanical and hydrodynamic stresses of the dredging process. The strength of mud aggregates (Krone 1963, Kranenburg 1994) is related primarily to the density of particle packing (or bulk density) and the cohesion of the minerals (related to clay mineralogy). Considering these issues, bed density, fines content, and some measure associated with the cohesiveness of the fine-grained material may be key predictors of the target sediment's propensity to produce fine-sediment aggregates, which influences the separation rate of fine sediments from the desired sand.

Flocs are low-density aggregations of fine-sediment particles that are formed in the water column through inter-particle collisions and aggregation. The bonds formed through aggregation are initially weak, and consequently flocs are relatively delicate. When exposed to turbulent shear or collisions with the bed or other suspended particles, flocs may be broken into smaller, constituent particles or disaggregated

completely. Therefore, *flocculation* is a balance between aggregation and disaggregation. Factors favoring aggregation are particle concentration, turbulent shear, and particle cohesiveness. Factors favoring disaggregation are high turbulent shear. Flocculation is relevant to the transport of the passive overflow plume in that as particle sizes increase, so do settling velocities. Therefore, flocculation can lead to decreased transport distances and increased sedimentation rates surrounding the dredging site compared to the case of completely disaggregated fine sediment. Mikklesen and Pejrup (2001) and Smith and Friedrichs (2011) have observed particle sizes of fine sediment increasing with time in passive overflow plumes, suggesting that flocculation can occur in these situations. Smith and Friedrichs further observed that the increase in particle size with flocculation led to a doubling of settling velocity over a period of 80 minutes. Size and settling velocity of suspended particles in the passive plume will be quantified in the subject research in such a way as to inform the numerical modeling of these processes.

3 Sampling Methods

The primary aim of sediment sampling is to determine sediment size distributions and mass concentrations at all stages in the dredging, transport, and placement process. Ample guidance is available on the sampling of bed materials and suspended loads within riverine and coastal environments. However, guidance for sampling from hopper dredgers is generally lacking, and the majority of what is known from the literature originates from a few studies. This section reviews the proposed methods for sediment sampling and processing in order to characterize bed materials at the borrow and placement sites, and track the size and quantity of sediments entering and exiting the TSHD. These methods include direct physical sampling and indirect surrogate monitoring using instrumentation.

3.1 Bed Material Sampling

To determine the proportion of fine sediments lost in the process of dredging and placement, it is necessary to collect samples at both borrow and placement sites. Accurately quantifying the loss of fines through dredging requires an accurate characterization of bed materials at the dredge site. Bed materials at depth are often collected through the use of grab, drag, or core-type samplers; the suitability of each depends on the in situ grain size, consolidation, water depth, required sample volume, and the necessity to recover an undisturbed versus disturbed sample.

3.1.1 Grab Samplers

Grab samplers (e.g., Shipek and Van Veen samplers) are clamshell-style gravity samplers that have opposing jaws to scoop and retain surficial sediments. The jaws are closed upon impact with the bottom by weights, springs, or cords. These samplers work best for fine sediments as coarser sediments, such as coarse sand, may prevent the jaws from closing properly or completely. The penetration depth of most grab samplers is about 10–15 cm, while sample volumes are typically 3–15 L depending on sampler dimensions.

3.1.2 Drag Samplers

For coarser sediments, a drag sampler is sometimes more appropriate. A drag sampler used by field workers at the Coastal and Hydraulics Laboratory uses a steel pipe about 1 m long, closed on one end, 10 cm in diameter flaring to 20 cm on the open end. The sampler is allowed to drag behind a moving vessel using a length of rope two to three times the water depth to keep the sampler horizontal. An advantage of the drag sampler is that the retrieved sample may better represent the average bed composition at the surface because the sample is taken across a larger spatial extent. For this project, however, the

penetration depth should exceed the expected dredging depth to obtain a representative composite sample. Disadvantages of this sampler are that it remains open, potentially losing some fine material during retrieval.

3.1.3 Core Samplers

Coring devices are used to take relatively undisturbed bed samples. Penetration into the surface is accomplished using gravity as they are heavily weighted. Box corers typically penetrate between 0.4–0.75 m and yield sample volumes from 10 to 200 L. Once at the penetration depth, a cable releases a closing shovel underneath the box before retrieval. Similarly, free-fall corers use a weighted stainless steel tube fitted with a cutting head to penetrate the sediment and steering fins to keep the corer vertical. Sediment is captured within a plastic casing, and sample loss is prevented by means of a core catching device at the opening and flaps that seal off the core surface.

Sediment sampling at the nourishment area following pumpout can be achieved through the use of vibracoring. Cores should be taken in the moist state to prevent collapse and at a sufficient depth to capture the horizon between native and placed sediments. The entire portion of the core above the horizon should be retained to maintain sample representativeness so that an appropriate subsample can be prepared for grain size analysis.

3.2 Overflow Weir Sampling

Reliable measurements of the solids concentration passing an overflow weir may only be achieved through direct sampling, as turbulence, bubbles, and vertical gradient of sediment concentration prohibit the use of surrogate monitoring via sensors (HR Wallingford 2003). Sampling of the overflow weir may be accomplished using bottle, flow-through, or pump samplers.

3.2.1 Bottle Sampling

Bottle samplers, in their most basic form, uses a collection bottle attached to a dipping pole or rope to extract a sample. Kerssemakers (2004) used a modified version to sample the overflow weir of the TSHD *Cornelia*. Here, a 1.0 L bottle was placed within a steel container and, using a rope, lowered to a depth of about 30 cm at the center of the overflow pipe. A second rope was used to open the lid of the steel container once in position; approximate fill times varied between 2 and 6 seconds. Sample contents were transferred to a separate container, then the bottle was flushed with a known water volume to remove residual sediments; this volume is later subtracted for concentration calculations. Given the simplicity of this method, a high sampling frequency can be achieved. A considerable disadvantage is that it cannot be known precisely when the bottle is filled; overfilling the bottle likely results in sample bias (Kessermakers 2004).

3.2.2 Flow-through Sampling

The flow-through sampler allows a sediment-water mixture to pass from the front to the rear of the sampler, ideally without accelerating (isokinetic). This type of sampler was also used by Kessermakers (2004) to compare mass concentrations of samples taken using the bottle sampler. The flow-through sampler consisted of an aluminum body with dimensions 40 x 20 x 5 cm, giving a sample volume of 4 L. This custom sampler used rubber-sealed doors held open at the ends using elastic bands that close using a release cord. When closing, the timing of the doors was slightly offset to increase volume capture because the sampler is not completely submerged. The flow-through samplers were deployed using guide ropes attached to the outer flange of the weir pipe parallel to the direction of flow (Figure A-6). Kerssemakers (2004) reported that each sample took about 3–4 minutes to obtain; at least 10 samples are needed to

characterize the overflow period (HR Wallingford 2003). Using a rotation of three crews and three samplers, a sampling rate of one per minute was achieved, a total yield of 30–50 samples per 40 minute overflow period.



Figure A-6. Photo of the custom flow-through sampler used by Kerssemakers (2004).

Image on the right shows the sampler deployed on the bell mouth of an overflow weir. Figure adapted from HR Wallingford (2003).

There was a concern that turbulence generated around the sampler's opening meant that the flow into the sampler was not likely isokinetic, which may bias the sample. Additionally, this method appeared to be somewhat cumbersome in that it required a crew of 10 to collect samples at the aforementioned rate (HR Wallingford 2003).

3.2.3 Pump Sampling

Pump sampling draws a sample into a collection bottle by applying a vacuum to a sampling tube. The sampling tube should be completely submerged and placed in a zone where the slurry is well mixed. Guidance on pump sampling of open channel flows suggests that the orientation of the intake be pointed downstream relative to flow direction to maximize sample representativeness (Gray and Landers 2014). This implies that the intake be pointed vertically downward within the throat of the overflow pipe and lowered to a sufficient depth to minimize air entrainment. The diameter of the sampling tube should be chosen such that velocities within it are high enough to prevent sedimentation. Bosman et al. (1987) suggested that the intake velocity was three times greater than the ambient fluid velocity (they were measuring sediment concentrations under waves). However, pump sampling is not recommended according to some guidelines, stating that significant errors may arise due to momentum effects (HR Wallingford 2003). Additionally, the limited diameter of the intake tube would not be able to capture a vertically integrated sample because the flow depth over the weir may be up to 30 cm (HR Wallingford 2003). To overcome this, an open-ended housing could be fabricated that attaches to the intake of the tube from which a representative sample is drawn. Such modified pump-sampling devices are under consideration for the laboratory sampling evaluation.

3.3 Uncertainty in Quantifying Losses

With any experimental endeavor comes measurement error and uncertainty. It is incumbent upon the researcher to communicate estimates of the uncertainties in the measurements of the research. The researchers on this team will quantify the measurement uncertainties following the principles of error analysis (Taylor 1997). This exercise will be completed during the experimental planning phase of the research and will be documented in the field experiment plan. The field uncertainty estimates will

incorporate findings of the laboratory evaluation of sampling methods and, later, results of the field measurements themselves.

4 Conclusions

Models exist for representing the settling rate of sandy sediments in TSHD hoppers. Although these models have shown some skill in representing specific dredging operations, they are limited in their capacity to predict the quantity of fines lost during the dredging process because PSDs are currently undetermined without direct sampling. Having particle size distribution information would prove valuable not only in predicting the loss of fines, but also in developing a comprehensive source term for modeling the fate of overflow plumes.

Additionally, research is required to quantify the propensity of fine sediments, particularly those with appreciable clay content, to form robust aggregates that settle at rates comparable to that of sand. These aggregates could significantly increase the retention of fine-grained sediments in the hopper in some instances. Research is needed to characterize the flocculation propensity of fines separated from sandy materials during hopper overflow. Previous research (Mikkelsen and Pejrup 2000, Smith and Friedrichs 2011) has identified flocculation as a first-order process in passive overflow plumes. Smith and Friedrichs further determined that settling velocities in suspension doubled in a period of just over an hour due to flocculation of the suspended sediment.

A modeling framework was discussed for representing transfer of sediment from the hopper overflow to the water column in suspension. The framework involves modular near-field models of the hopper retention and overflow process, followed by cloud-based Lagrangian representation of the dynamic plume. The dynamic plume model then will generate initial conditions of the passive plume clouds of suspended sediment. The passively transported sediment can be represented with 3D point-based Lagrangian methods, such as the PTM. This approach has been demonstrated previously by Lackey and Smith (2008) with a bottom dumping operation with STFATE generating the initial cloud conditions for PTM.

Previous research regarding sediment dispersion at a pipeline outfall is primarily related to open-water disposal of sediment and the fluid mud flows that occur at the bed as a result. Models exist to demonstrate this mixing and dispersion; however, they do not show the separation of fine material specifically. On the beach, there have been studies that aim to quantify fines loss through natural beach processes. However, there have not been studies that combine fines loss through the pipeline outfall with placement on the beach. In other words, more investigation into the fines loss during the outfall and return water resulting from the slurry needs to be completed.

5 References

- Bosman JJ, Elsbeth, van der Velden ETJM, Hulsbergen CH. 1987. Sediment concentration measurement by transverse suction. *Coastal Engineering*. 11:353-370.
- Brandsma MG, Divoky DJ. 1976. Development of models for prediction of short-term fate of dredged material discharged in the estuarine environment. Contract Report D-76-5. Vicksburg (MS): U.S. Army Engineer Waterways Experiment Station. 297 p.
- Bray RN, Bates AD, Land JM. 1997. *Dredging: A handbook for engineers*. London: Arnold.

- Burt NT, Hayes DF. 2005. Framework for research leading to improved assessment of dredge generated plumes. *Terra et Aqua*. 98:20-31.
- Camp TR. 1936. A study of the rational design of settling tanks. *Sewage Works Journal*. 8:742-758.
- Camp TR. 1946. Sedimentation and the design of settling tanks. *Transactions of the American Society of Civil Engineers*. 2285:895-936.
- Chu VH, Lee JHW. 1996. General integral formulation of turbulent buoyant jets in cross-flow. *Journal of Hydraulic Engineering*. 122(1): 27-34.
- de Wit L, van Rhee C, Talmon A. 2014. Influence of important near field processes on the source term of suspended sediments from a dredging plume caused by a trailing suction hopper dredger: the effect of dredging speed, propeller, overflow location and pulsing. *Environmental Fluid Mechanics*. 15(1)41-66.
- Dean RG. 1973. Heuristic models of sand transport in the surf zone. In: *First Australian Conference on Coastal Engineering, 1973: Engineering Dynamics of the Coastal Zone*. Sydney (Australia): Institute of Engineers. p. 215-221.
- Dean RG. 1977. Equilibrium beach profiles: U.S. Atlantic and Gulf Coasts. Newark (DE): University of Delaware Department of Engineering. Ocean Engineering Technical Report, No. 12. 45 p.
- Dobbins WE. 1944. Effect of turbulence on sedimentation. *Transactions of the American Society of Civil Engineers*. 2218:629.
- Doneker R, Jirka GH. 2007. CORMIX user manual – a hydrodynamic mixing zone model and decision support system for pollutant discharges into surface waters. Report EPA-823-K-07-001.
- Goodrich KA, Warrick JA. 2015. Fines: rethinking our relationship. In: Wang P, Rosati JD, Cheng J, editors. *Coastal Sediments 2015*; 2015 May 11-15; San Diego, CA. Singapore: World Scientific Publishing Co.
- Gordon RB. 1974. Dispersion of dredge spoil dumped in near-shore waters. *Estuarine and Coastal Marine Science*. 2:349-358.
- Gray JR, Landers MN. 2014. Measuring suspended sediment. In: Ahuja S, editor. *Comprehensive water quality and purification*. 1:157-204.
- Hallermeier RJ. 1981. Terminal settling velocity of commonly occurring sand grains. *Journal of Sedimentology*. 28(6), 859-865.
- Hamrick JM. 1996. User's manual for the environmental fluid dynamics computer code. Gloucester Point (VA): Virginia Institute of Marine Sciences.
- Hayter E, Smith SJ, Demirbilek ZD, Lin L. 2012. Dredged material placement site capacity analysis for navigation improvement project at Grays Harbor, WA. Vicksburg (MI): U.S. Army Engineer Research and Development Center. ERDC/CHL TR-12-18.
- Hazen A. 1904. On sedimentation. *Transactions of the American Society of Civil Engineers*. Paper No. 980: 45-88.
- Henry G, Neal RW, Greene SH. 1978. Laboratory investigation of the dynamics of mud flows generated by open-water pipeline disposal operations. Vicksburg (MS): U.S. Army Engineer Waterways Experiment Station. Technical Report D-78-46.

- HR Wallingford. 2003. Protocol for the field measurement of sediment release from dredgers. HR Wallingford Ltd. & Dredging Research Ltd. Issue 1.
- James S, Jones C, Grace M, Roberts J. 2010. Advances in sediment transport modelling. *Journal of Hydraulic Research*. 48(6)754-763.
- Johnson BH. 1990. User's guide for models of dredged material disposed in open water. Vicksburg (MS): U.S. Army Engineer Waterways Experiment Station. Technical Report D-90-5.
- Jones CA, Lick W. 1999. Effects of bed coarsening on sediment transport. In: Spaulding ML, Butler HL, editors. *Estuarine and coastal modeling. Proceedings of the 6th International Conference on Estuarine and Coastal Modeling*; 1999 Nov 2-4; New Orleans, LA. p. 915-930.
- Jones CA, Lick W. 2001. Sediment erosion rates: their measurement and use in modeling. In: *Texas A&M Dredging Seminar*. College Station (TX): American Society of Civil Engineers. p. 1-15.
- Kana TW, Mohan RK. 1998. Analysis of nourished profile stability following the fifth Hunting Island (SC) beach nourishment project. *Coastal Engineering* 33. 117-136.
- Kerssemakers KA. 2004. Overflow sampling of trailing suction hopper dredgers: a case study on the TSHD Cornelia [thesis]. Delft (Netherlands): Delft University of Technology.
- Koh RCY, Chang YC. 1973. *Mathematical Model for barged ocean disposal of waste*. Washington (DC): U.S. Environmental Protection Agency. EPA 660/2-73-029.
- Kranenburg C. 1994. The fractal structure of cohesive sediment aggregates. *Estuarine and Coastal Shelf Science*. 39: 451-460.
- Kraus NC, Thevenot MM. 1992. The Plume Measurement System (PLUMES): first announcement. Vicksburg (MS): U.S. Army Engineer Waterways Experiment Station. Technical Note DRP-1-06.
- Krone RB. 1963. A study of rheological properties of estuarial sediments. Vicksburg (MS): U.S. Army Engineer Waterways Experiment Station. Technical Bulletin No. 7.
- Lackey TC, Smith SJ. 2008. Application of the particle tracking model to predict the farfield fate of dredged suspended sediment at the Willamette River. In: Randall R, editor. *Proceedings of the Western Dredging Conference*; 2008 Jun 8-11; St. Louis, MO. Western Dredging Association. p. 39-60.
- Land JM, Bray RN. 2000. Acoustic measurement of suspended solids for monitoring of dredging and dredged material disposal. *Journal of Dredging Engineering*. 2(3)1-17.
- Maglio CK, Ousley JD, Coor JL. 2015. Sediment Engineering Thru Dredging and With Nature (SETDWN) – fate of fines in the dredging and placement process. In: Wang P, Rosati JD, Cheng J, editors. *Coastal Sediments 2015*; 2015 May 11-15; San Diego, CA. Singapore: World Scientific Publishing Co.
- McCave IN. 1978. Grain-size trends and transport along beaches: Example from eastern England. *Marine Geology* 28.
- MG Associates. 2012. Dredge discharge and bottom deposition analysis for open water placement of dredged material at the mouth of Calibogue Sound, South Carolina. Report prepared for GEL Engineering.
- Miedema SA. 2009a. A sensitivity analysis of the scaling of trailing suction hopper dredges. In: *Proceedings of the 40th Texas A&M Dredging Seminar*. Newton (PA): Western Dredging Association.

- Miedema SA. 2009b. The effect of bed rise velocity on the sedimentation process in hopper dredges. *Journal of Dredging Engineering*. 10(1)10-31.
- Miedema SA, Vlasblom WJ. 1996. Theory of hopper sedimentation. In: *Proceedings of the 29th Annual Texas A&M Dredging Seminar*; 1996 Jun, New Orleans, LA.
- Mikkelsen OA, Pejrup M. 2000. In situ particle size spectra and density of particle aggregates in a dredging plume. *Marine Geology*. 170:443-459.
- Nichols MM, Thompson GS. 1978. A field study of fluid mud dredged material: its physical nature and dispersal. Vicksburg (MS): U.S. Army Engineer Waterways Experiment Station. Technical Report D-78-40.
- Ooijens SC. 1999. Adding dynamics to the Camp model for the calculation of overflow losses. *Terra et Aqua*. 76:12-21.
- Palermo MR, Randall RE. 1990. Practices and problems associated with economic loading and overflow of dredge hoppers and scows. Vicksburg (MS): U.S. Army Engineer Waterways Experiment Station. Technical Report DRP-90-1.
- Purnama A, Baawain MS, Dongdong S. 2016. Simulation of sediment discharges during an outfall dredging operation. *International Journal of Oceanography*. 2016, Article ID 8097861. doi:10.1155/2016/8097861.
- Richardson JF, Zaki WN. 1954. Sedimentation and fluidization, part I. *Transactions of the Institution of Chemical Engineers*. 32:35-53.
- Rullens R. 1993. Production measurement methods for trailing suction hopper dredgers [Thesis]. Delft (Netherlands): TU Delft.
- Smith SJ, Friedrichs CT. 2011. Size and settling velocities of cohesive flocs and suspended sediment aggregates in a trailing suction hopper dredge plume. *Continental Shelf Research*. 31: S50-S63.
- Soulsby R. 1997. *Dynamics of marine sands, a manual for practical applications*. London (UK): Thomas Telford.
- Spearman J, Bray RN, Land J, Burt TN, Mead CT, Scott, D. 2007. Plume dispersion modeling using dynamic representation of trailer dredger source terms. In: Maa JPY, Sanford LP, Schoellhamer DH, editors. *Estuarine and coastal fine sediment dynamics*. Amsterdam (Netherlands): Elsevier. p. 417-448.
- Spearman J, DeHeer A, Aarninkhof S, Van Koningsveld M. 2011. Validation of the TASS system for predicting the environmental effects of trailing suction hopper dredgers. *Terra et Aqua*. 125:14-22.
- Stapor FW, Tanner WF. 1975. Hydrodynamic implications of beach, beach ridge and dune grain size studies. *Journal of Sedimentary Research*. 45(4).
- Taylor JR. 1997. *An introduction to error analysis*. 2nd Edition. Sausalito (CA): University Science Books.
- Teeter AM. 1994. Dredged material dispersion from the vicinity of pipeline discharge. In: McNair EC, editor. *Dredging '94: Proceedings of the Second International Conference on Dredging and Dredged Material Placement*; 1994 Nov 13-16; Lake Buena Vista, FL. Tyler's Beach (VA): American Society of Civil Engineers. p. 918-927.
- Teeter AM. 2000. Underflow spreading from an open-pipeline disposal. Vicksburg (MS): U.S. Army Engineer Research and Development Center. ERDC TN-DOER-N7.

- Teeter AM. 2001. Simulating underflow spreading from a shallow-water pipeline disposal. Vicksburg (MS): U.S. Army Engineer Research and Development Center. ERDC TN-DOER-N11.
- Teeter AM. 2002. Sediment dispersion near dredge pipeline discharge in Laguna Madre, Texas. Vicksburg (MS): U.S. Army Engineer Research and Development Center. ERDC TN-DOER-N16.
- Thanh PXH, Grace MD, James SC. 2008. Sandia National Laboratories environmental fluid dynamics code: sediment transport user's manual. SAND2008-5621.
- Tomkins MR, Baldock TE, Nielsen P. 2005. Hindered settling of sand grains. *Sedimentology*. 52:1425-1432. doi:10.1111/j.1365-3091.2005.00750.x
- Toorman E, Berlamont J. 1991. A hindered settling model for the prediction of settling and consolidation of cohesive sediment. *Geo-Marine Letters*. 11:179-183.
- van Rhee C. 2001. Numerical simulation of the sedimentation process in a trailing suction hopper dredge. In: *Proceedings of the 16th World Dredging Congress; 2001 Apr 2-5; Kuala Lumpur, Malaysia*.
- van Rhee C. 2002. Modeling the sedimentation process in a trailing suction hopper dredger. *Terra et Aqua*. 86:18-27.
- van Rijn LC 1984. Sediment transport: part 2. Suspended load transport. *Journal of Hydraulic Engineering, ASCE*. 111:1613-1641.
- Vlasblom WJ. 2007. *Trailing Suction Hopper Dredger [Lecture Notes]*. [accessed 2017 Jan 9]. <http://www.dredgingengineering.com>.
- Vlasblom WJ, Miedema SA. 1995. A theory for determining sedimentation and overflow losses in hoppers. In: *Proceedings of 4th World Dredging Congress; 1985 Nov; Amsterdam*. p. 183-202.
- Warrick JA. 2013. Dispersal of fine sediment in nearshore coastal waters. *Journal of Coastal Research*. 29(3):579-596.
- Winterwerp J. 1999. *On the dynamics of high-concentrated mud suspensions [Ph.D. thesis]*. The Netherlands: Delft University of Technology.
- Winterwerp JC. 2002. Near-field behavior of dredging spill in shallow water. *Journal of Waterway, Port, Coastal, and Ocean Engineering*. 128:96-98.
- Ziegler CK, Lick W. 1986. A numerical model of the resuspension, deposition and transport of fine-grained sediments in shallow water. Santa Barbara (CA): University of California. Technical Report ME-86-3.
- Ziegler CK, Lick W. 1988. The transport of fine-grained sediments in shallow waters. *Journal of Environmental Geology*. 11(1): 123-132.

Appendix B. Laboratory Testing of Sampling Methods

This appendix describes laboratory experiments conducted to determine suitable field sampling procedures on a trailing suction hopper dredger (TSHD) to include: sampling locations, sampling methods, composite sampling techniques, and sampling intervals. At the time that testing was performed, sampling was considered at the hopper inflow, hopper bed, and overflow weir. Ultimately, some of these sampling locations and techniques were abandoned for the field sampling campaign, but the results of these tests are included here for the consideration of future studies.

Section 2.1 describes testing materials and methods including a sample splitter experiment and a numerical experiment using USACE National Dredging Quality Management (DQM) data to determine the sampling frequency required to obtain acceptable sampling error from the dredging process. Section 2.2 consists of the results from the overflow weir, hopper sampling, sample splitting, and numerical experiment for determining sample frequency. A discussion and conclusions of the results are provided in Section 3.3.

1 Materials and Methods

This appendix details the materials, design, and procedures used to test physical sampling and sample analysis methods. The first section provides details on the sediments used in this study followed by a section describing the laboratory hopper overflow and subsequent sampling methods. The final sections detail the hydraulic sample splitter tested for sample analysis and a numerical experiment to determine the error introduced by the sampling frequency.

1.1 Sediment

Three sources of sediment were used for the laboratory testing, a locally sourced loess referred to as Vicksburg silt (VS), a fine sand (FS), and a coarse sand (CS) commonly used in mortar mix. Respective median grain sizes were determined to be 0.23, 1.86, and 4.08 mm. The grain size distributions for each are provided in Figure B-1, which shows the VS as well-graded and FS and CS as poorly graded.

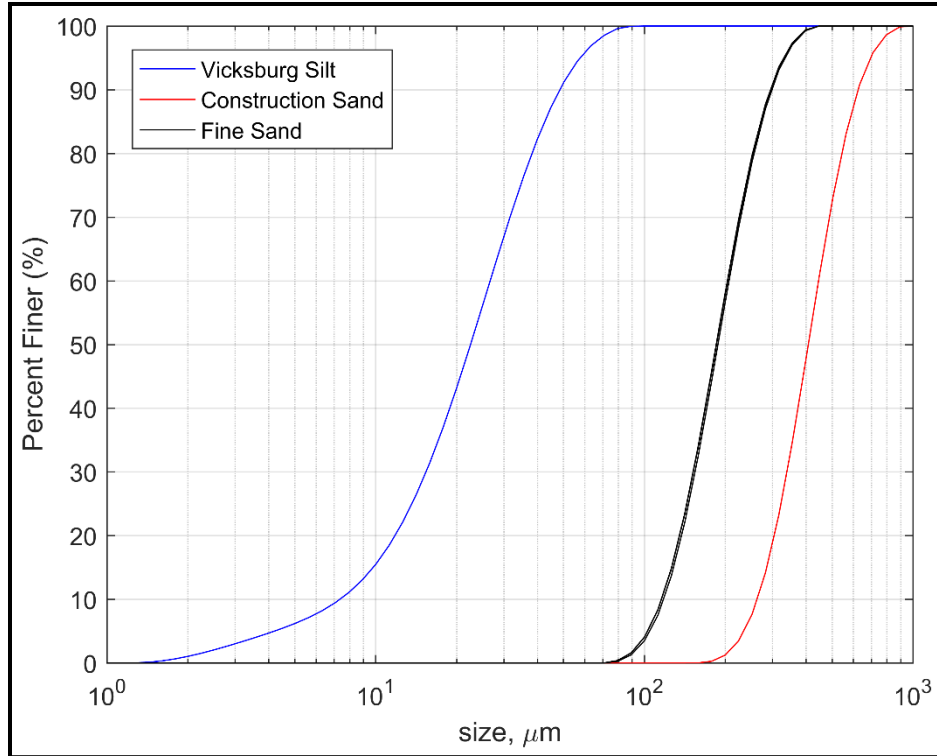


Figure B-1 Size gradations of tested sediment.

Size gradations of the Vicksburg silt (VS), fine sand (FS) and coarse construction sand (CS) used in the overflow experiments.

1.2 Overflow Experiments

This section describes the laboratory setup and procedures for sampling hopper overflow. The overflow experiments were designed to test different sampling methods, specifically the appropriate time interval for collecting samples from hopper overflow. These tests were not designed to mimic the flow and sediment dynamics within a prototype hopper. Instead, the only necessary design criteria included scaling the flow rate over the weir and matching the vertical loading rate of the sediment bed, considered in the hopper load parameter, H^* , as defined by van Rhee (2001) in (B-1). The numerator, v_0 , is the vertical loading rate calculated by dividing the hopper flow rate by the hopper area. The denominator, w_s is the hindered settling velocity based on the sediment concentration as defined by Richardson and Zaki (1954) in (B-2); here, w_0 is the single grain settling velocity, C is the concentration and n is an empirical coefficient dependent on grain size.

$$H^* = \frac{v_0}{w_s} \quad (\text{B-1})$$

$$w_s = w_0(1 - C)^n \quad (\text{B-2})$$

The experiments conducted in the laboratory were meant to represent a typical dredging event; therefore a sediment concentration of 15% (by volume) was chosen, which corresponds to 400 g/L by mass. This

concentration is a reasonable value for inflow concentration, which can vary from 10%–30%, however is low enough to pump as a slurry without special equipment.

1.2.1 Weir Overflow

To test the sampling and compositing hypothesis a model hopper was designed to simulate basic hopper sedimentation and overflow conditions (Figure B-2). The primary components consist of a supply tank, a weir tank, and a receiving tank. The supply tank holds the sediment mixture and represents the hopper inflow. The weir tank represents the prototype hopper and includes an overflow weir at its downstream end. The receiving tank contains all the contents collected from the overflow and is representative of the outflow from the hopper. The components are described in further detail below.

The stainless steel supply tank has a maximum volume of 1,540 L. The bottom of the cylindrical supply tank is beveled and feeds into a 10 cm (4 inch) nominal pipe connected to a Honda WT40 gas-powered trash pump capable of handling solids up to 2.54 cm in diameter (Figure B-3) and has a maximum flowrate of 28.4 L/s (450 gpm). To maintain sediments in suspension, the tank also has two mixing paddles located at the tank bottom and mid-depth driven by an electric motor at 120 rpm. A set of ball valves were used to recirculate the mixture from the pump to the supply tank and for transferring to the weir tank. The flow rate of the transferred material was monitored using an in-line Endress+Hauser Proline Promag 50 electromagnetic flowmeter.

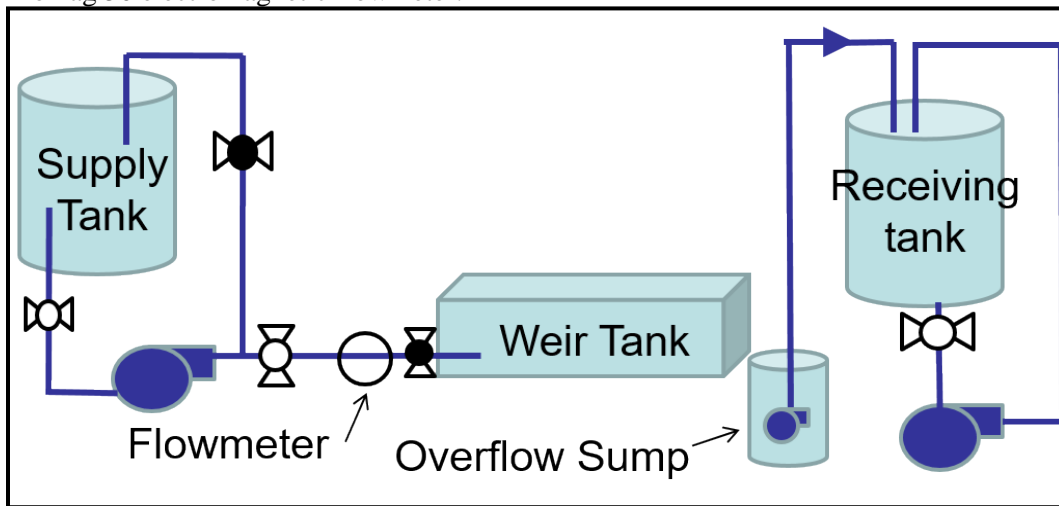


Figure B-2. Weir overflow schematic.



Figure B-3. Sediment mixing tank.

Figure B-4 provides a schematic of the designed depth of settled sand, maximum water depth, and freeboard distance. The basin is 88.4 cm deep with an area of 62.8 cm x 152.4 cm. The overflow weir is 53.9 cm from the basin floor with an opening width of 10.16 cm. A target inflow rate of 4.7 L/s was determined to achieve the desired sediment loading rate of 5 mm/s, which was controlled using a gate valve immediately upstream of the weir tank. The design volume of sand collected in the tank is 384 L, which equates to bed height of 41.2 cm assuming a uniform distribution with a bulk density of 1,600 kg/m³. The expected bed height was used to determine the maximum water depth over the weir. The flow rate and exit velocity of the overflow was calculated using the sharp crested weir equation (with a $C_d = 0.6$), which was designed to be similar to that encountered in dredge plants.

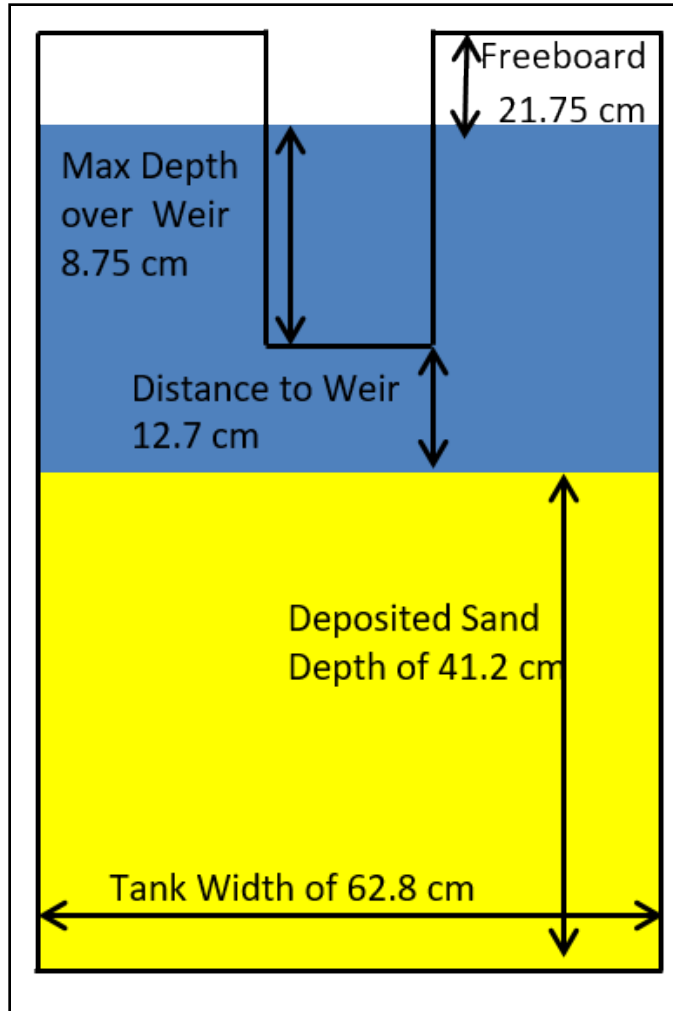


Figure B-4. Schematic of weir tank.

Tank dimensions shown with design depths of sand, water, and design freeboard. Not to scale.

The overflow discharged from the weir was captured in a separate aluminum basin. At the end of the loading cycle, the material was then transferred to the receiving tank using a nominal 5 cm (2-inch) sump pump. Special attention was taken during testing to move all the overflow material to the receiving tank. The receiving tank was identical to the supply tank except a nominal 2-inch (5 cm) gas-powered semi-trash pump was used to recirculate the contents of the tank. The maximum flowrate of the receiving tank pump was approximately 15.8 L/s (250 gpm). A photograph of the laboratory setup with the process moving from left to right following the blue line is shown in Figure B-5.

The sediments used for the experiment consisted of three constant volume mixtures created with increasing fines content of 10%, 20%, and 30%. Each mixture was created in triplicate for repeatability and statistical significance. To achieve the 10% fines mixture, 526 kg of CS and 59 kg of VS was combined with 1,241 L of water. Respectively for the 20% and 30% fines mixtures, the masses were 468 kg CS + 117 kg VS + 1,241 L water, and 409 kg CS + 175 kg VS + 1,241 L water. All sediment masses used in the mixture calculations were corrected for moisture content prior to mixing. The testing procedure is provided in Table B-1.

Table B-1. Overflow sampling test procedure.

1	Check plumbing
2	Identify pre-measured sediment bags for test
3	Prepare sampling bottles and sampling method/equipment
4	Check that flowmeter/scale are logging
5	Fill tank 1 with desired amount of water
6	Turn on recirculation pump and paddles for supply tank
7	Add construction sand to supply tank
8	Add Vicksburg silt to supply tank
9	Let supply tank mix for 5 minutes
10	Take samples from supply tank
11	Start logging flowmeter and scale data
12	Begin flow into weir tank and monitor flowmeter
13	Sample overflow from weir tank every 20 seconds
14	Begin pumping overflow in the receiving tank
15	Turn pump and paddles for the receiving tank
16	Once empty turn pump and paddles off for the supply tank
17	Ensure all overflow is included in receiving tank after overflow stops
18	Let receiving tank run for 5 minutes
19	Take samples from receiving tank

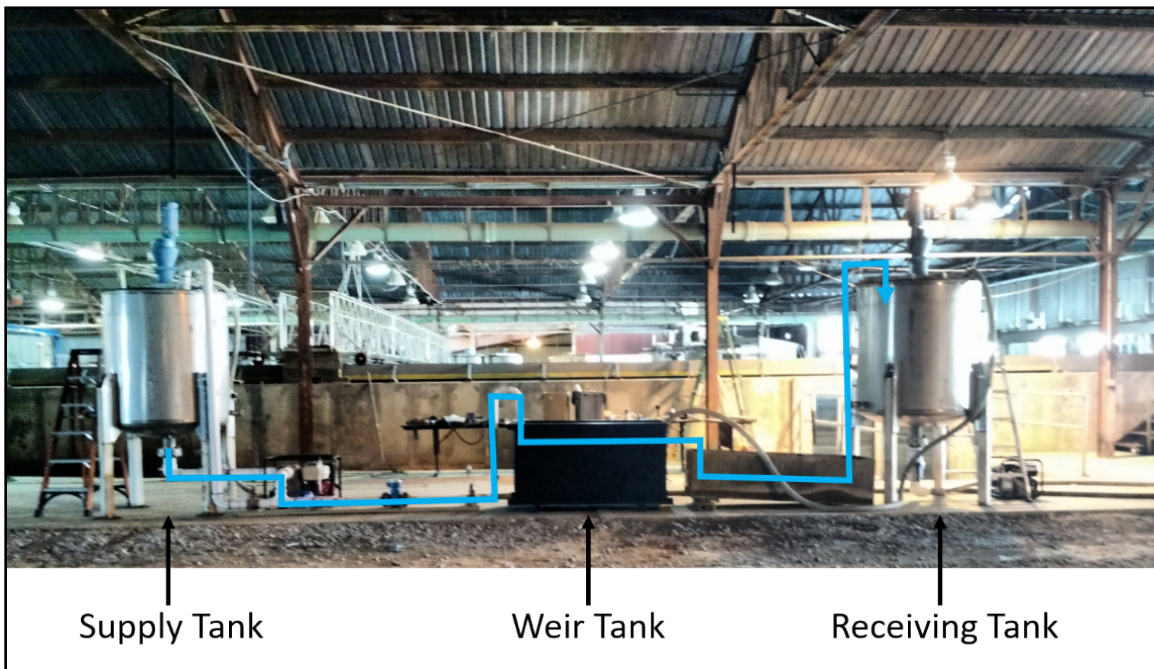


Figure B-5. Photograph of weir overflow laboratory setup.

Laboratory setup indicates supply tank, weir tank, and receiving tank. The blue line indicates the path of flow from the supply tank to the receiving tank.

1.3 Sampling Methods

1.3.1 Overflow Weir

The overflow weir (Figure B-6) was sampled directly using three different sampling devices to identify any potential biases in sediment concentrations and grain size distributions between sampler types. A total of nine tests (B-J) were conducted, grouped by the percentage fines ($< 63 \mu\text{m}$) in the sediment mixtures (

Table B-2). For each test, a sample was collected approximately every 20 seconds which yielded roughly 14 samples per test for a 5-minute overflow period. Half of these samples were used to determine sediment concentration by mass, while the other half were used for grain size analysis and determination of the fraction of fines. Two samples ($\sim 0.5 \text{ L}$ each) were also collected at the receiving tank for comparison against the overflow samples.



Figure B-6. Model weir tank in overflow.

Table B-2. Test matrix for weir overflow sampling.

% Fines	Test ID	Sampler Type
0.1	H	Bottle
0.1	I	Box
0.1	J	Tube, Hopper
0.2	B	Bottle
0.2	C	Box
0.2	D	Tube
0.2	K	Hopper

0.3	E	Bottle
0.3	F	Box
0.3	G	Tube

The sampling devices consisted of a “bottle” sampler, a “box” sampler, and a “tube” sampler (Figure B-7). The bottle sampler (Figure B-7A) is simply a 1-L Nalgene bottle that was dipped by hand into the overflow. Care was taken not to overflow the bottle, which could bias the sample; any overfilled bottles were discarded then resampled.

The box sampler (Figure B-7B) was designed to take an integrated sample through a column of the overflow. The narrow design and thin side walls are meant to minimize turbulence and allow for isokinetic (undisturbed flow) sampling for the design flow velocity. A bottle was used to collect samples from the outflow port as flow is continuously passed through the sampler for the duration of overflow. The tube sampler (Figure B-7C) consists of a vertical array of metal ports that are tapered and thinning in the direction of incoming flow. The ports direct flow into a vertical tube with an outflow port at the bottom for sample collection. Like the box sampler, the tube sampler rests on the lip of the weir allowing flow to pass through continuously while samples are taken at the outflow port.

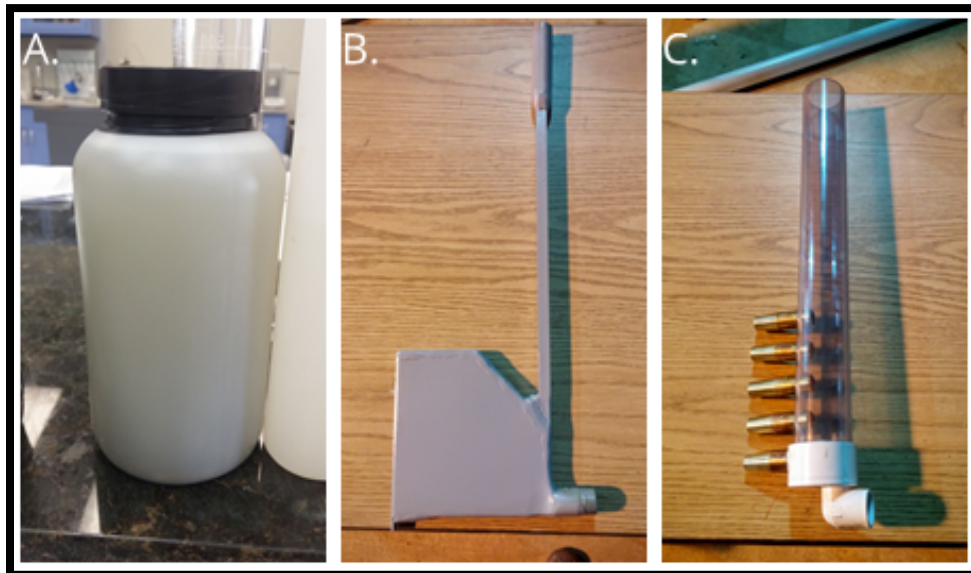


Figure B-7. Photos of the three weir overflow sampling devices.

A) bottle, B) box, and C) tube

1.3.2 Dredge Hopper

A significant challenge of the project is to capture representative sediment samples from the hopper. While sampling the hopper bed during the loading cycle, special attention must be made to minimize bias introduced from any sampling technique used.

Three general techniques were proposed to capture representative hopper samples: 1) collect samples via vibracoring once dredging has ceased, 2) collect samples from the collapsing side wall of sediment during pumpout operations, and 3) collect samples from the rising bed surface during the loading cycle. The vibracoring option was eliminated based on safety concerns of conducting such an operation on the dredge deck as well as concerns about achievable penetration depth. Option 2 is considered viable, but the

question of the number of samples needed, and the distribution of sample locations to achieve sample representativeness, remains. Thus, option 3 was decided to be the safest and most representative means to obtain hopper samples. For these laboratory experiments two custom devices were tested, a pipe sampler and a plate sampler. Laboratory tests were designed and conducted to evaluate the effectiveness of the samplers described in detail below.

1.3.2.1 Pipe sampler

The pipe sampler is a nominal 7.6-cm (3-inch) diameter PVC pipe, 15.3-cm long and closed at one end with a total volume of roughly 1.5 L. The pipe sampler was attached to a pole and lowered to the sediment surface for 15 seconds (Figure B-8), which was meant to fill the sampler based on a typical vertical bed rise velocity of 5 mm/s within a prototype hopper. After each collection, the contents of the sampler were emptied into a bucket and composited to obtain a bulk size distribution and percentage of fines that should represent the average composition in the tank. Two trials were conducted using the pipe sampler (

Table B-2, tests J & K). For each trial, three to four samples were collected and composited for grain size analysis.

For comparison, the weir tank was also cored using a 10-cm diameter polycarbonate tube. The composition of this core was treated as being closer to the “true” representation of the sediment. Surface fines retained in the core were discarded in order to make a proper comparison.

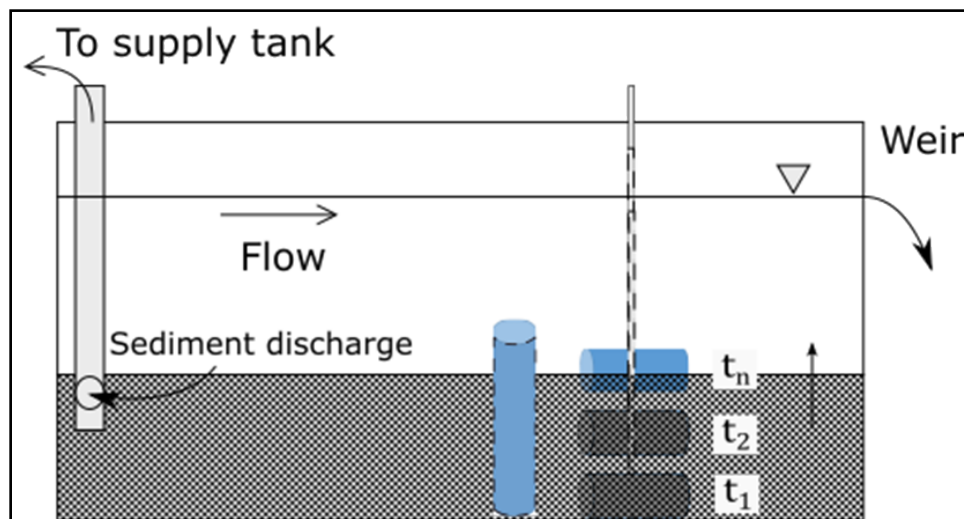


Figure B-8. Schematic cross-sectional view of the weir tank with bed samplers.

Samples are taken during the overflow period as the bed develops and rises which fills the sampler. A core is taken adjacently once the surface water is drained.

1.3.2.2 Plate sampler

The plate sampler consists of an inner, 10-cm diameter aluminum disk and an outer 25-cm diameter ring. Each disk and ring is fabricated in two parts that sandwich a strong, flexible, vinyl membrane (Figure B-9).

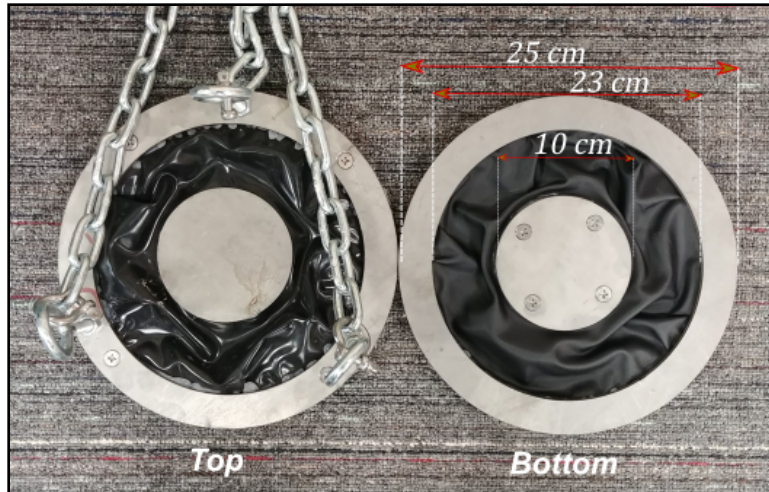


Figure B-9. Plan view of the plate sampling device.

The fully constructed version with chain bridling is shown on the left.

The operational aspects of the sampler are illustrated in Figure B-10 (A–D). The low-profile design is intended to eliminate sheltering effects by resting flat on the sediment bed until retrieval (A). Under load the membrane flexes and creates a shallow bowl to retain the sediment sample (B). The contents are exposed for sampling by pushing the plate onto a riser (C). Finally, a subsample is taken by pushing a short core with known volume to refusal above the center plate (D).

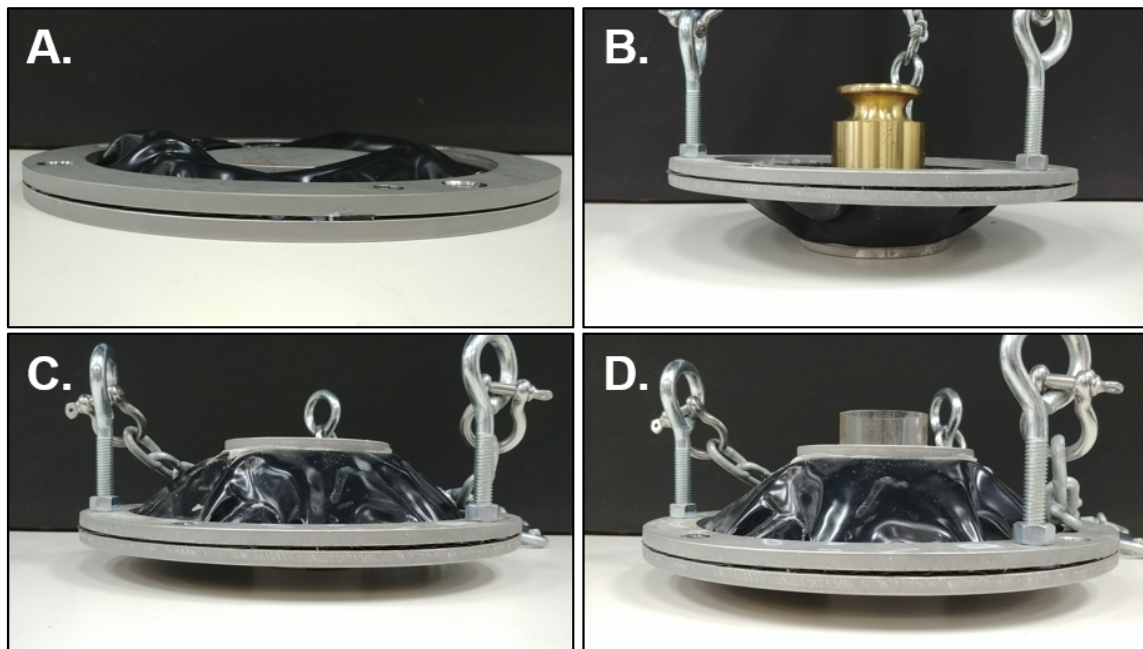


Figure B-10. Generalized operational aspects of the plate sampler.

Rest position (A), under load upon retrieval (B), and sample recovery position (C & D).

Chain bridling is attached to the sampler to facilitate deployment. The sampling technique consists of lowering the sampler to the hopper bed, waiting a specified period for burial, and retrieving. Upon retrieval, the membrane flexes and creates a shallow bowl when full to protect the sample from washing

out during retrieval (Figure B-11). Any remaining surface fines that would otherwise cause a positive bias are discarded during the subsampling procedure using the short core, which is illustrated in detail in Figure B-12.



Figure B-11. Laboratory testing of the plate sampler.

Deployment (left) and retrieval (right) of the plate sampler in the model hopper tank.

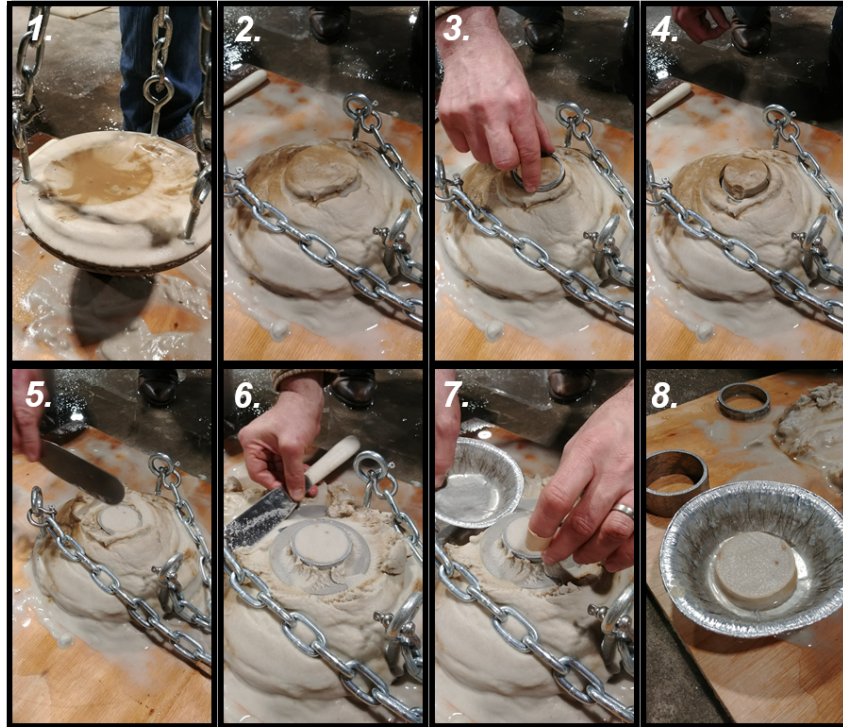


Figure B-12. Image sequence showing the subsample recovery procedure.

Sample retrieval (1), resting on riser (2), short core pushed to refusal (3, 4), surface sediment removed (5), sediment cleared from inner plate (6), subsample transferred to container (7, 8).

The plate sampler experiments were conducted independently of the previous tests and therefore used a slightly different experiment setup, which is described below.

Two test mixtures were created using silt/sand ratios of 0.10 and 0.30 using the VS and FS sediments. Each mixture was batched to approximately 635 kg total weight divided into thirty-two 5-gal buckets.

A schematic diagram of the experiment setup is shown in Figure B-13. The system was designed for continuous flow while maintaining head in the sediment supply tank. Water was supplied to the sediment tank using a small gas-powered 2-inch intake semi-trash pump, which was then transferred to the weir tank using a similar pump. Flow to the weir tank was monitored using an electromagnetic flow meter. Flow rate to the weir tank and head within sediment tank was maintained by adjustment of a series of gate valves.

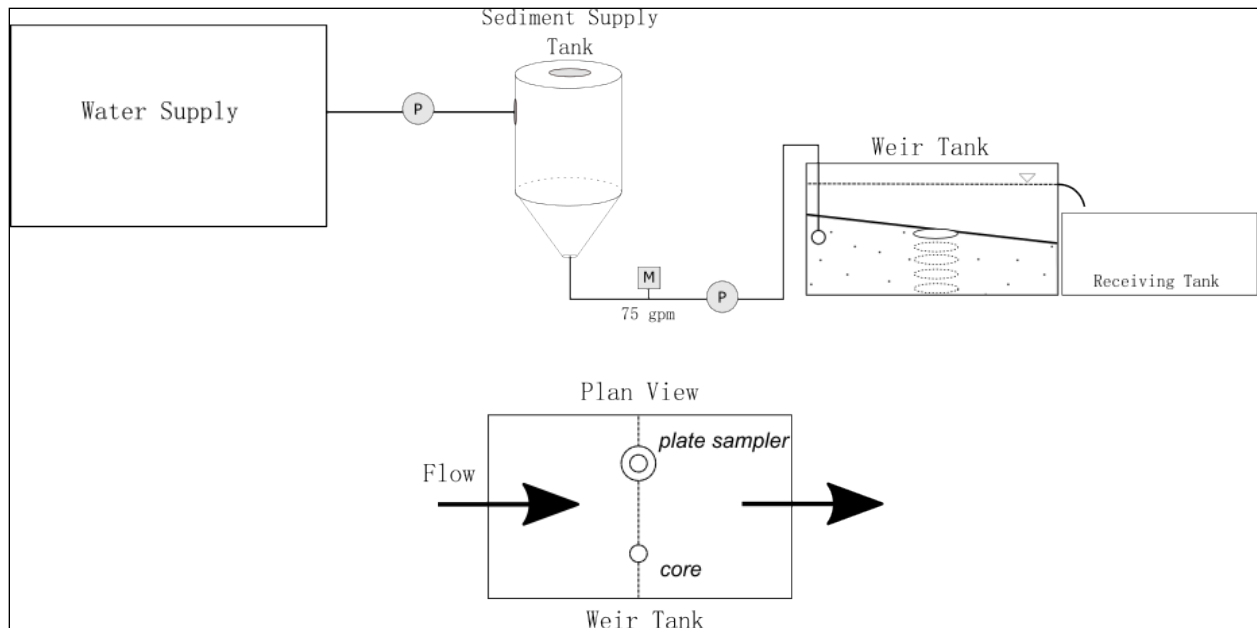


Figure B-13. Schematic diagram of the plate sampler experiment design.

Once the target flow rate (75 gpm) and desired head was achieved, sediment was introduced to the supply tank at a rate of one bucket per minute. The plate sampler was then lowered to the bed and a sample recovered for every four buckets of material introduced (enough to be assured the sampler was buried). Thus, a total of eight samples were recovered for each test. Samples were recovered at the same position midway of the tank (Figure B-13, plan view). Once all the sediment was introduced, flow was stopped, and a 2-inch diameter core was taken at the opposite side of the plate sampler (Figure B-13, plan view). The contents of the core were emptied into a bucket except for the upper 5 cm at the sediment-water interface to avoid biasing the sample with fines from the overlying water column (Figure B-14). Core recovery for test 1 (10% fines) was roughly 90%, while for test 2 it was roughly 60%.



Figure B-14. Image of recovered core example used to compare against composited bed samples.

1.3.2.3 Sample analysis

The sediment from the composited bed samples and core were dried overnight in a 50° C oven for 24 hours then prepared for mechanical sieving. Observations of the dried sediment noted the presence of aggregated silt. As a consequence, it was necessary to mechanically agitate the samples using a rubber-tipped pestle to break apart the aggregates until no longer observed. The sediment was then split using a riffle splitter to a target mass of about 50 g (per ASTM standards to prevent sieve overloading) and mechanically sieved at the sand/fine boundary using a no. 230 (63 μ m) sieve. The percentage by weight passing the no. 230 sieve was taken as the percentage of fines in the sample. The fines fraction of the core was treated as the true but unknown value from which to compare the composited bed samples and determine the associated error.

1.4 Hydraulic Splitting of Sediment-Water Mixtures

This section considers the use of a large recirculating tank for the purpose of splitting sediment-water mixtures. Inflow and/or weir sampling could involve the capture of 30–60 L of slurry per load that must then be reduced (via sample splitting or subsampling) to a manageable volume or mass for laboratory analysis. Existing hydraulic means (such as cone or churn splitters) for splitting of suspended sediment samples containing sand are prone to bias associated with the rapid settling of sand. Further, they are not practical for splitting large volumes at high sediment concentration. These tests explore whether or not subsamples extracted from the tank are reliably characteristic of the population contained within.

1.4.1 Recirculating Tank System

The recirculating system consists of a 377 L (100 gal) semi-conical tank outfitted with a flexible nominal 5 cm (2 inch) suction line attached to a trash pump with a flow capacity of 9.5 L/s (150 gpm) (Figure B-15). The suction line runs from the bottom of the tank to the return line, which is a vertical section of 2-inch PVC that is routed back into the tank via through-wall connector. Attached to the terminating end

of the return line is a metal diffuser to disperse the sediment mixture. Two ports were installed from which to draw samples, one off the middle of the tank and one off the return line. The intake side of the mid-tank port runs to the center of the tank and has an open-ended tee attachment to restrict the sampling zone and minimize sample bias. The return line port is located in the vertical section of the return line. The placements of the sampling ports are based on locations of high turbulence to allow for increased mixing efficiency. The flow rate was monitored using an in-line electromagnetic flow meter.

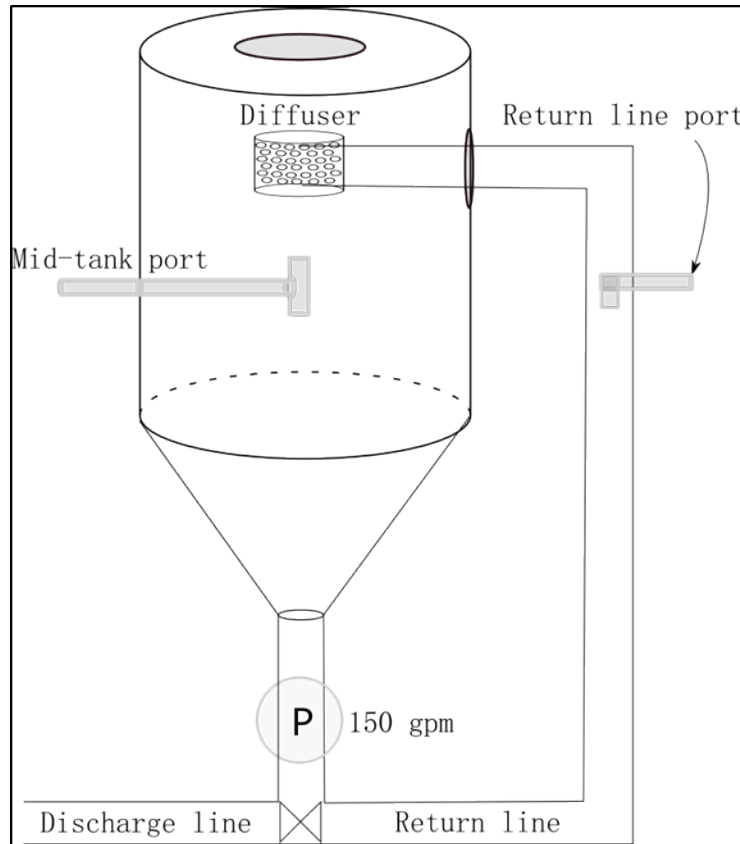


Figure B-15. Recirculating tank schematic for hydraulic sample splitting.

1.4.2 Sediment Mixtures and Test Schedule

Sediments used in the tests consisted of CS, FS, and VS sediments (Table B-3). Grain size characteristics for these three sediments were provided in Section 2.1. A total of six tests were conducted. The sediment mixtures for tests 1–3 were the construction sand (CS) and silt (as previously described) with silt content of 0.10, 0.20, and 0.30, respectively. The mixtures for tests 4–6 were comprised of the same sand/silt ratios but used FS in place of CS (); five replicate samples were collected for each test. The target dry sediment mass introduced to the system was 19 kg to obtain an average sediment concentration by mass in the tank of 50 g/L. Care was taken to ensure that the sediment concentration in the tank was accurately quantified. As such, sediment masses were weighed out to the nearest gram, and for each sediment type the average moisture content was obtained by evaporation to account for the additional water volume. Water volumes pumped into the tank system were measured to the nearest gallon (with accuracy +/-1%) using the flow meter.

Table B-3. Sample splitting test matrix.

Test No.	Test ID	Sand Type	% Sand / %Silt	Sample Method
1	A1	CS	90/10	Mid-tank spigot
	A2	CS	90/10	Tank return line
2	B1	CS	80/20	Mid-tank spigot
	B2	CS	80/20	Tank return line
3	C1	CS	70/30	Mid-tank spigot
	C2	CS	70/30	Tank return line
4	D1	FS	90/10	Mid-tank spigot
	D2	FS	90/10	Tank return line
5	E1	FS	80/10	Mid-tank spigot
	E2	FS	80/20	Tank return line
6	F1	FS	70/30	Mid-tank spigot
	F2	FS	70/30	Tank return line

Notes: "CS" refers to construction sand, while FS refers to fine sand (see text for median size information).

1.4.3 Splitting Procedure

First, the recirculating tank was filled with a known water volume, 370 L. While at maximum flow (150 gpm, 9.5 L/s), the target sediment mass at the assigned sand/silt proportion was then slowly added; silt was introduced first and mixed for 3 minutes before slowly introducing the sand. Once the sand was added, the slurry was allowed to mix for an additional 5 minutes to optimize mixture homogeneity; this allowed for roughly 7–8 full volume mixing cycles based on the tank evacuation time of 0.66 min. Next, samples were withdrawn from the mid-tank port followed by the return line port, each being received into a 1-L bottle. For each test, five independent samples were collected at each port for repeatability and error analysis. A minimum volume of 0.5 L was collected for analysis, and care was taken not to overfill bottles to prevent sample biasing (any overfilled samples were noted as such, mostly for a few samples at the return line due to its high discharge velocity). Finally, the remaining slurry was pumped out of the system and the tank cleaned and prepared for the next test.

1.4.4 Analysis Methods

Samples were analyzed for sediment concentration and grain size distribution. Sediment concentrations were determined by evaporation according to ASTM standards (ASTM D3977-77). Once the concentrations were determined, samples were re-slurried to a minimum volume of 250 mL and split using a fluorocarbon cone splitter with 10 discharge ports (Capel and Larson 1995, Wilde et al. 2014). Aliquots from 3 of the 10 ports were retained for grain size analysis using a Malvern laser scattering instrument.

1.5 Composite Sampling of Hopper Inflow

A numerical experiment was conducted to determine the appropriate discrete sampling interval of hopper inflow in order to achieve a representative mean.

1.5.1 Data Source

The data for this analysis is taken from the DQM system for a TSHD plant operating along the Florida coast in 2014. The records for 147 loads are used for this analysis starting with load 1 on 11/19/2014 and ending for load 147 on 12/28/2014. DQM data were recorded on average every 7.8 s. Although over 30 data metrics are reported, this analysis used the date, time, starboard inflow specific gravity and starboard inflow velocity. The inflow specific gravity was used to calculate the mass concentration (g/L). Figure B-16 provides the inflow velocity and mass concentration for load 93. The dredge made two passes on this load with a pause in dredging identifiable by the inflow velocity falling to nearly zero and specific gravity equal to unity between 20:45 and 21:20. No information is provided in DQM system for sediment gradation, thus this analysis only considers the concentration into the hopper.

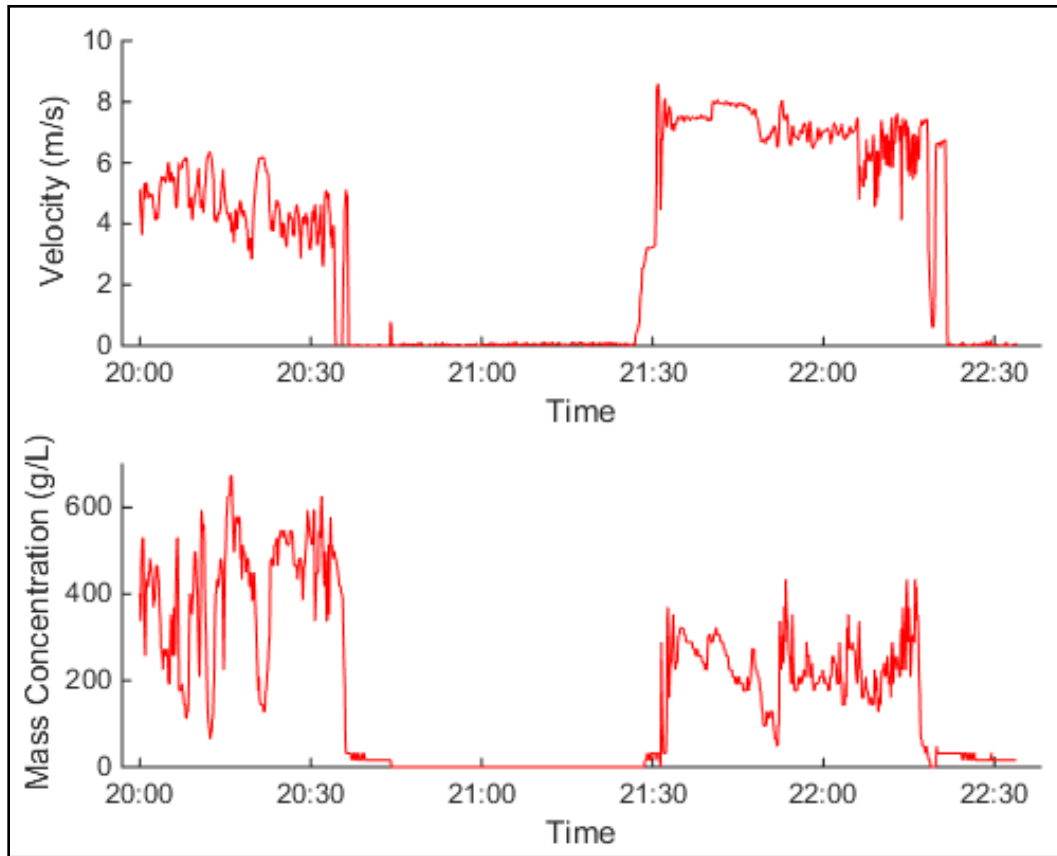


Figure B-16. Recorded starboard velocity and specific gravity for hopper load 93.

1.5.2 Analysis Method

For each load the total sediment input, M , into the hopper through the starboard inflow was found by numerically integrating the mass flux. The sediment mass flux was calculated as the product of the instantaneous volume flux, Q , and mass concentration, C , (estimated from slurry density). This numerical integration used the trapezoidal rule as shown in (B-3) and assumed the volume flux, Q , was equal to the DQM reported port inflow velocity.

$$M = \sum_1^n \frac{(Q_{n-1} \times C_{n-1}) + (Q_n \times C_n)}{2} \Delta t \quad (\text{B-3})$$

Any DQM data point where the inflow velocity was less than 30.5 cm/s was not included as this indicated the dredge was not actively dredging. Finally the average sediment mass concentration for the entire load, \bar{C} , was found by dividing the integrated sediment mass M by the integrated volume, V . The integrated volume was found using (B-4).

$$V = \sum_1^n \frac{(Q_{n-1}) + (Q_n)}{2} \Delta t \quad (\text{B-4})$$

The first method assumed samples are taken at specific intervals. For example, starting with the first sample and choosing every 20th sample results in a time interval of 156 seconds. These selected samples are then averaged to compute an average concentration without consideration of the flowrate. However, an additional comparative dataset can be found by starting at the second sample and choosing every 20th sample. Figure B-17 shows this sampling strategy being applied to load 93 with the sampled points for no phase shift (Subset 1) and a phase shift of 10 (Subset 2) with a sampling interval of 156 seconds or every 20th sample. Thus, this method finds the average mass concentration for a load for every possible interval up to 600 s considering every possible time shift and is referred to as “fixed interval sampling.”

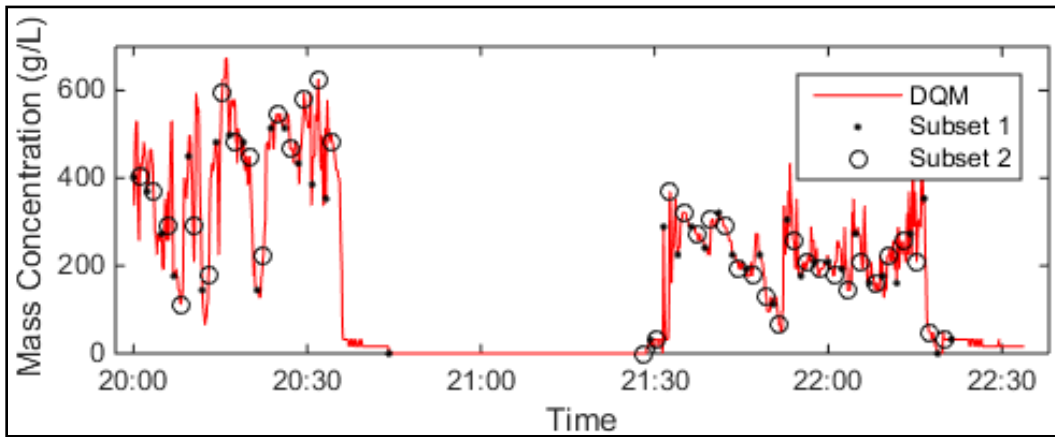


Figure B-17. Example of subset sampling Load 93.

A fixed sampling interval with no phase shift (Subset 1) and a phase shift of ten (Subset 2).

The second method assumed random sampling intervals. For example, a sample size of 20 may have been chosen for a load that takes 20 min to dredge. These samples are pulled randomly but not uniformly in time. The average sampling interval is the length of dredging record divided by the number of samples, or in this example, 60 s. These randomly sampled concentration measurements can be averaged and compared to the correct average concentration. As with the previous sampling method, no consideration for the associated flowrate for each sample is given. However, one random sampling does not provide a strong comparative point, but it is possible to randomly sample the set creating many realizations. Figure B-18 provides an example of two subsets for load 93 using this method. This method finds the average concentration for a load for 100 random perturbed realizations for every average sampling interval up to 600 s and is referred to as “random interval” sampling.

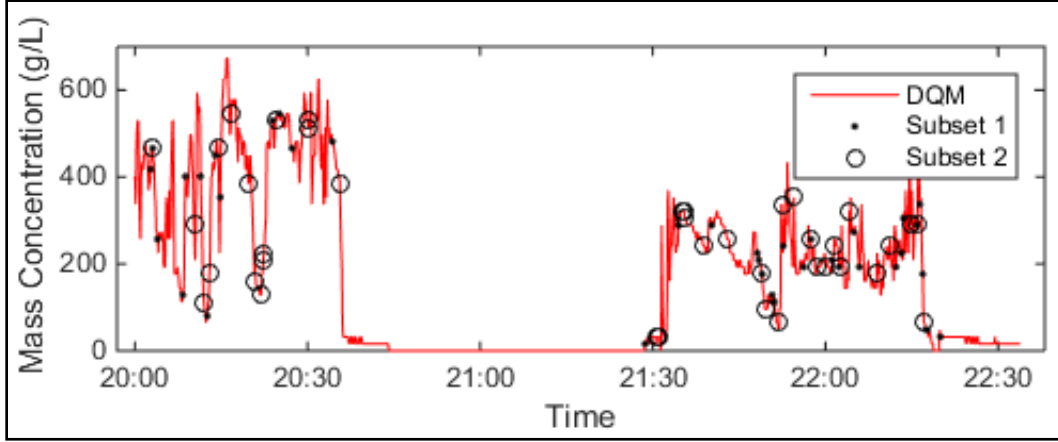


Figure B-18. Example of two subset samplings of Load 93.

Two random sampling realizations with average sampling interval of 156 s. Note that the samples are pulled randomly, not at a fixed sampling interval.

The averages of the sampled concentrations are compared to the correct average mass concentration given by using (B-3) and (B-4), and the absolute relative error, E , is calculated using (B-5).

$$E = 100 \times \frac{|\bar{c}_{sampled} - \bar{c}_{correct}|}{\bar{c}_{correct}} \quad (B-5)$$

This procedure is repeated for many realizations of each sampling strategy for data from 147 hopper loads, resulting in a probabilistic estimate of the expected errors associated with each sampling and compositing strategy. The mean absolute relative error, \bar{E} for all 147 loads for a given time interval was determined by:

$$\bar{E}(t) = \frac{1}{n} \sum_{n=1}^{147} E_n(t) \quad (B-6)$$

The bias was calculated by the same method as above for the relative error instead of the percent error. Additionally, for a given sampling interval all the errors were used to populate a lognormal distribution that is used to calculate the 95% standard error for a given load. A lognormal distribution is chosen because the percent error could never be negative whereas a normal distribution would allow for some percentage of the results to have a negative percent error. Two parameters are needed to quantify a lognormal distribution, the mean, μ , and standard deviation, σ , of the variable's natural logarithm. The variance, or square of the standard deviation, can also be used. These values were combined from each load to define a lognormal distribution that represented the absolute error for each sampling interval. This was achieved by taking an average of the lognormal distribution means, μ , and combining the variances, σ^2 .

2 Results

This section presents the results of laboratory and numerical testing and analysis aimed at addressing the sampling and analysis plan for conducting field sampling to address sediment sorting and separation during hopper dredging and placement operations.

2.1 Physical Sampling

2.1.1 Weir Overflow

The sediment passing the overflow weir consisted mostly of fines, which comprised $95.5\% \pm 1.3\%$ (mean \pm SD) of the total sample averaged across all tests. The fines content for each test was analyzed to discern differences between sampling devices, as well as differences between the numerically averaged overflow samples and composited receiving tank samples.

Figure B-19 shows there was little difference between the average percent fines from individual weir samples and the composited value obtained from receiving tank samples ($95.9\% \pm 0.2\%$), which also showed little variability irrespective of initial fines content of the starting mixture (10%, 20%, 30%). Likewise, there was little variability in the fines percentage between sampling devices (Figure B-19).

Results from the analysis of sediment concentrations for all experiments are summarized in Table B-4. Sediment concentrations showed little variability between sampling devices (Figure B-20). The largest uncertainty in concentration (mean \pm SE) between sampling devices occurred for the tests using 30% fines, which increased slightly from 124 ± 4 , 128 ± 3 , and 133 ± 2 g/L for bottle, box, and tube methods, respectively. Since the percentage of fines over the weir was nearly uniform at 95%, the measured concentrations tend to increase proportionally to the percent fines of the starting mixture from the supply tank, also with little variability between the overflow and receiving tank (Figure B-21).

Except for the box sampler, no systematic trend in concentration was detected between sampling methods with increasing fines content of the mixtures (Figure B-22). The standard deviation in concentration of the box sampler increased with increasing fines content, from 1.6 to 5.2 to 8.4 g/L for mixtures with 10%, 20%, and 30% fines, respectively.

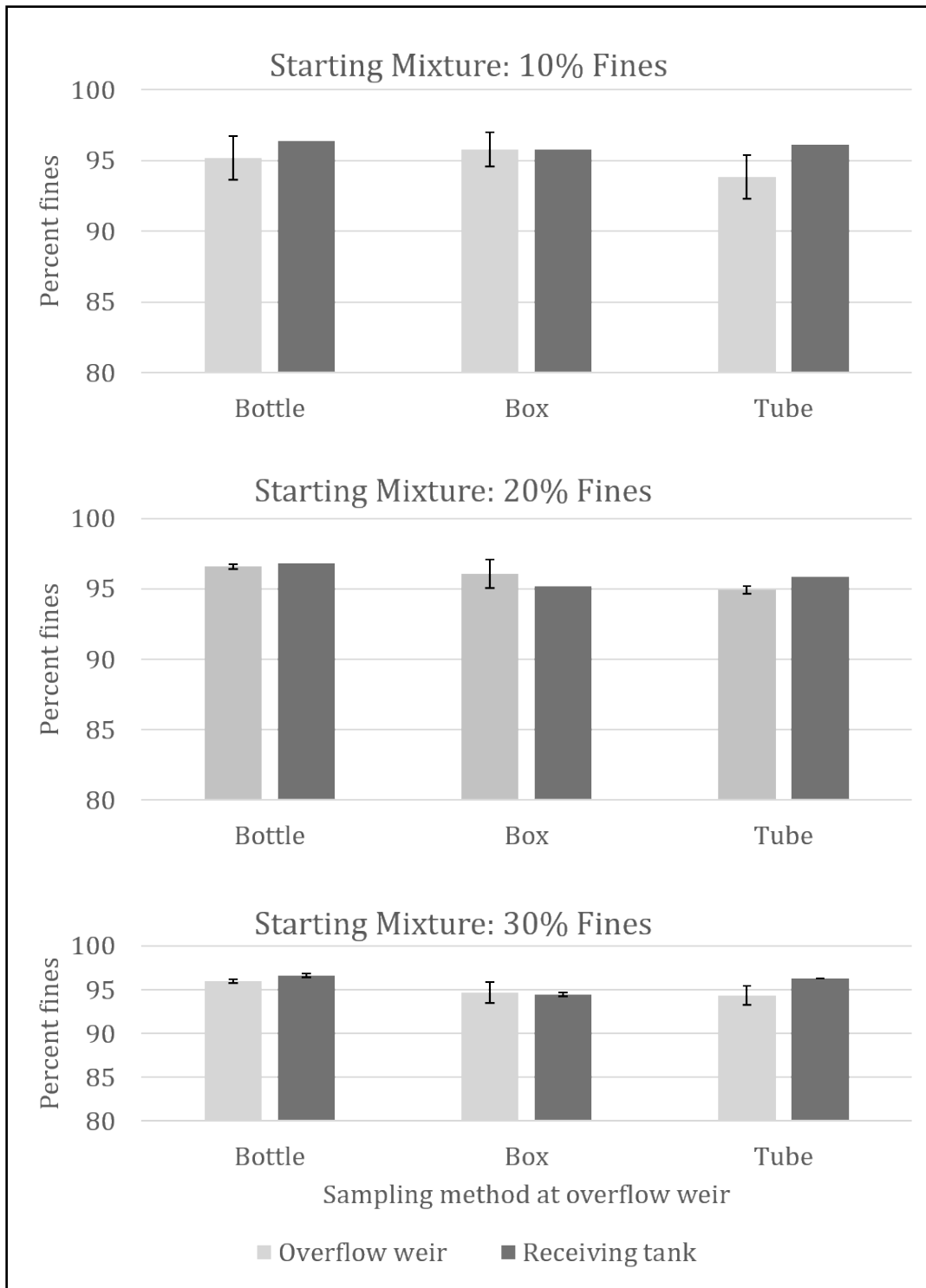


Figure B-19. Results of weir sampling tests.

Average percent fines between weir overflow samples and receiving tank samples. Sampling method only refers to the overflow weir.

Table B-4. Summary table of sediment concentrations for each experiment.

Experiment IDs annotated with “R” refer to receiving tank samples, while those with “W” refer to weir tank samples. SD refers to standard deviation, and SE refers to the standard error of the mean.

% fines	Experiment ID	N	Sampling method	Mean C (g/L)	SD	SE
10%	HR	2	Bottle	42.46	0.71	0.50
10%	HW	7	Bottle	38.83	10.12	3.83
10%	IR	2	Box	40.79	0.64	0.45
10%	IW	6	Box	42.02	1.62	0.66
10%	JR	2	Tube	43.67	0.91	0.65
10%	JW	6	Tube	44.32	2.78	1.13
20%	BR	2	Bottle	85.24	1.28	0.90
20%	BW	6	Bottle	82.39	4.86	1.99
20%	CR	2	Box	88.64	1.16	0.82
20%	CW	7	Box	85.86	5.23	1.98
20%	DR	2	Tube	87.96	0.11	0.07
20%	DW	6	Tube	82.49	18.03	7.36
30%	ER	2	Bottle	125.54	0.35	0.25
30%	EW	7	Bottle	123.99	9.66	3.65
30%	FR	2	Box	131.36	0.65	0.46
30%	FW	6	Box	127.52	8.37	3.42
30%	GR	2	Tube	130.77	0.77	0.55
30%	GW	6	Tube	132.52	5.93	2.42

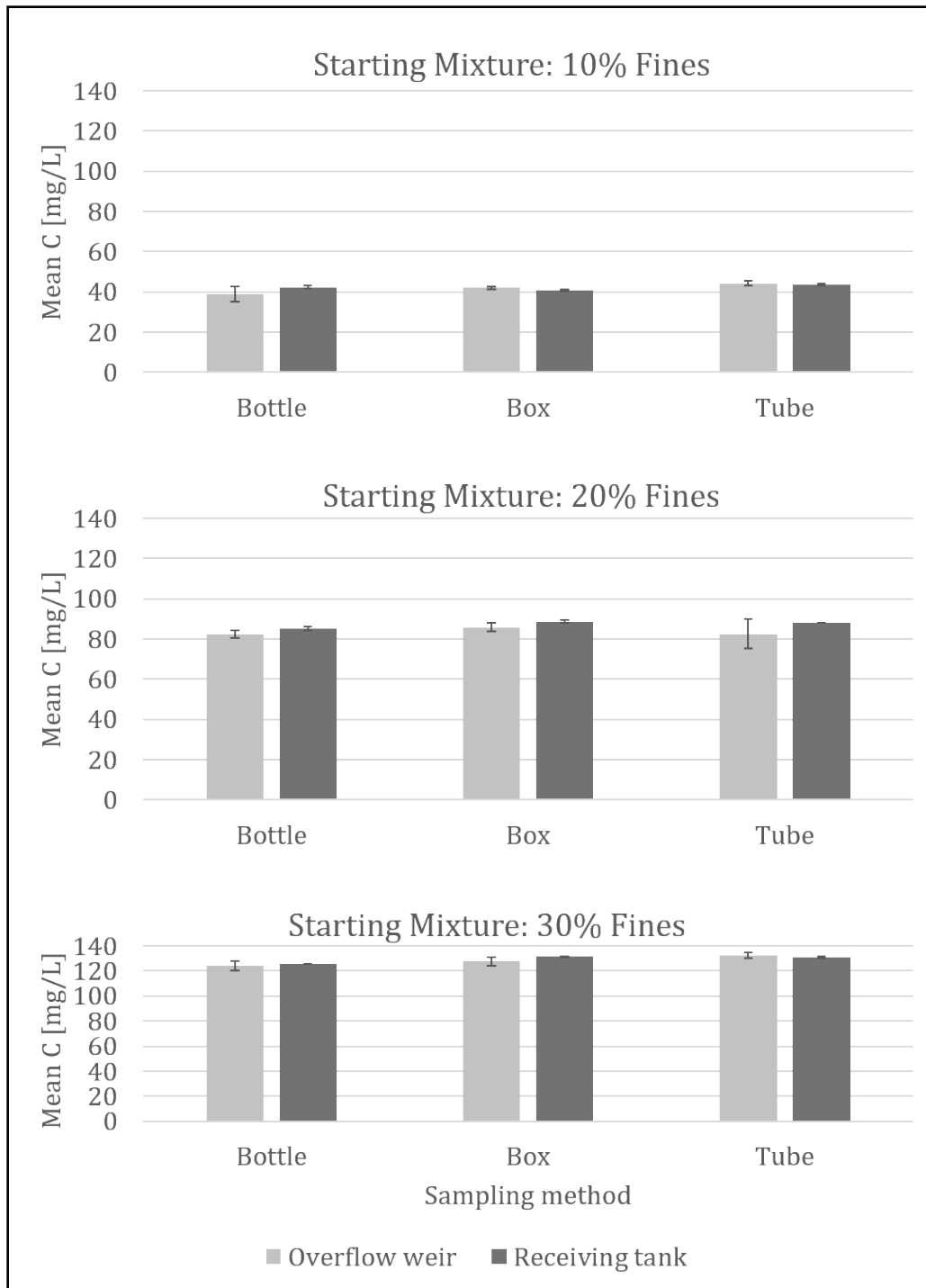


Figure B-20. Average concentration for the different methods of weir overflow sampling and receiving tank.

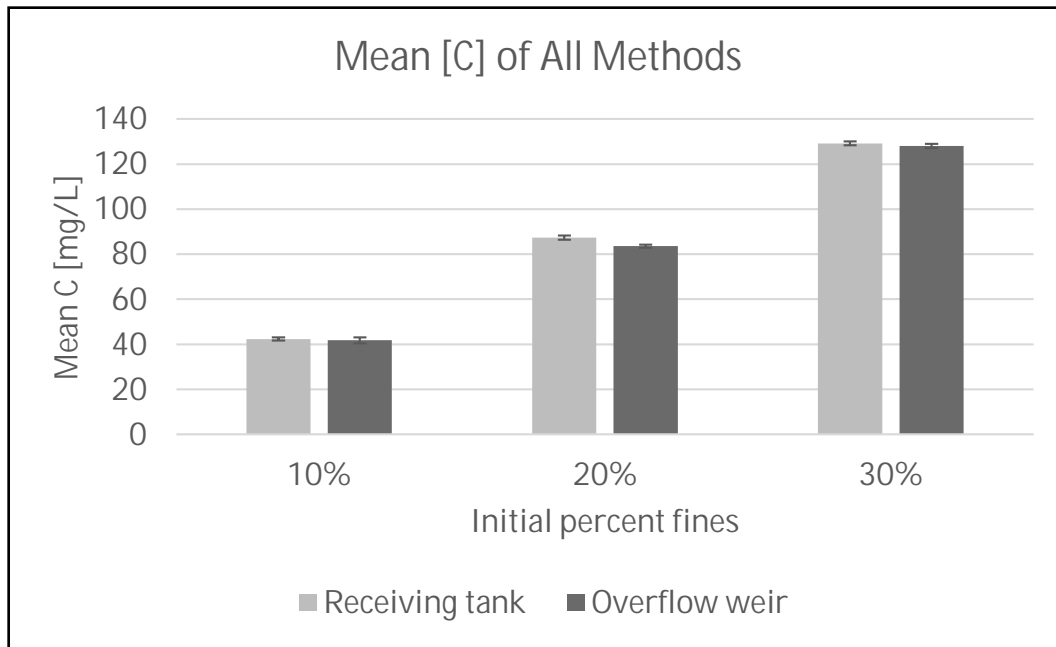


Figure B-21. Mean concentration for all sampling methods for weir overflow and receiving tank samples.

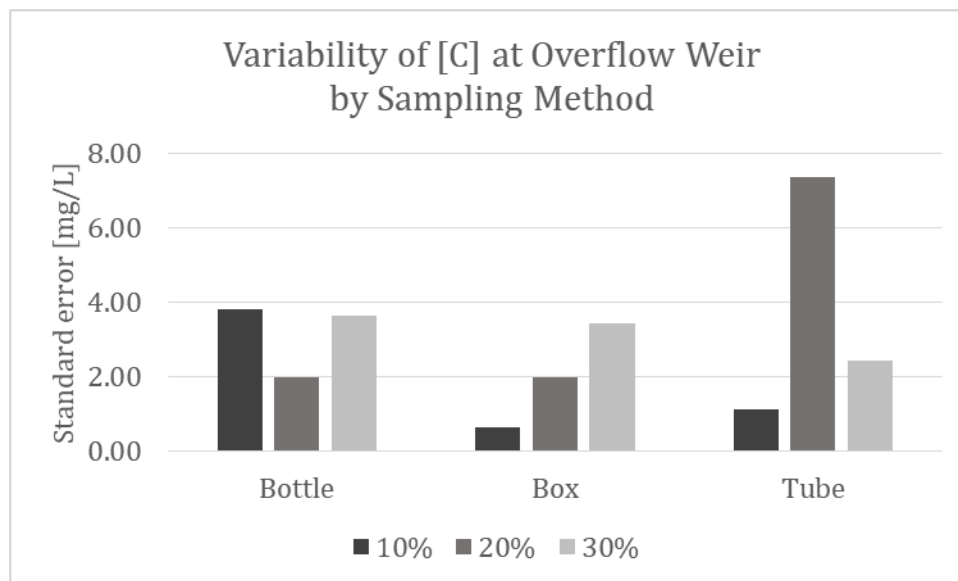


Figure B-22. Variability of concentration for each weir overflow sampling method.

Relative errors (RE) between sample mean concentrations and receiving tank concentrations are provided in Table B-5. The tank mean is considered the “true” or expected value. The relative error of any sampler was within 10%. On average the concentrations from the weir samples were lower than expected (six out of nine cases). Computing the mean relative error (MRE) for each sampler (Table B-5) shows that the bottle sampler had the greatest deviation from the expected value (-4.4%) compared to the box and tube samplers which had MRE of -1.0% and -1.1%, respectively.

Table B-5. Results of weir sample testing.

Summary table of comparing the relative errors (RE) in concentrations between the weir samples and the mean value in the receiving tank for all sediment mixtures and sampling devices. The MRE of each sampling method across all tests is also provided.

Test % fines	Method	Tank mean [g/L]	N	Weir mean [g/L]	N	RE [%]
10	Bottle	42.46	2	38.83	6	-8.6
10	Box	40.79	2	42.02	6	3.0
10	Tube	43.67	2	44.32	7	1.5
20	Bottle	85.24	2	82.39	6	-3.3
20	Box	88.64	2	85.86	7	-3.1
20	Tube	87.96	2	82.49	6	-6.2
30	Bottle	125.54	2	123.99	7	-1.2
30	Box	131.36	2	127.52	6	-2.9
30	Tube	130.77	2	132.52	6	1.3
Method		MRE [%]				
Bottle		-4.4				
Box		-1.0				
Tube		-1.1				

2.1.2 Hopper Sampling via Pipe Sampler

The percentage fines of sediment retained in the hopper was compared between the pipe sampler and corer for two starting mixtures (10% and 20%). For each case, the composited sediment collected by the pipe sampler overestimated the fines content by 111% and 57%, respectively (Figure B-23). The sediments collected by the corer are considered the “true” composition; however, note that the percent fines from tests J and K did not double despite a doubling of fines of the starting mixture from 10% to 20%. Similarly, the percent fines captured by the pipe sampler were similar between tests (3.5% and 3.2%) despite a doubling of fines of the starting mixture.

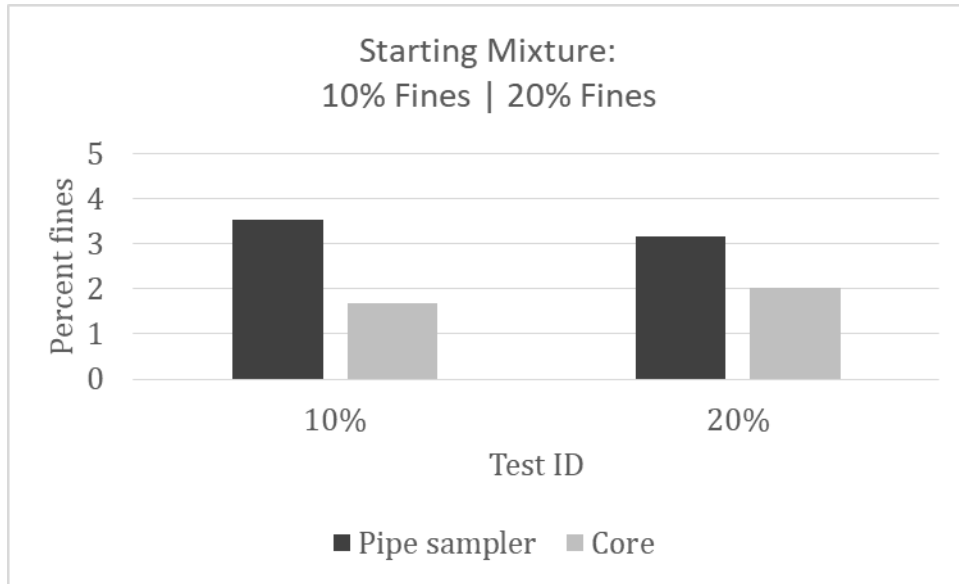


Figure B-23. Comparison of the percentage fines retained in the hopper tank collected by the pipe sampler and a core for two test cases.

2.1.3 Hopper Sampling via Plate Sampler

The percentage fines captured by the plate sampler was 5.4% for the 10% silt mixture and 6.2% for the 30% silt mixture. This is compared to 4.3% and 7.7% fines captured by the cores for the same mixtures, respectively. Therefore, the plate sampler slightly overestimated the fines content for the 10% silt mixture, while it slightly underestimated the fines for the 30% silt mixture. This represents an absolute error of 20–25%. However, statistical significance cannot be established due to the limited number of experiment runs.

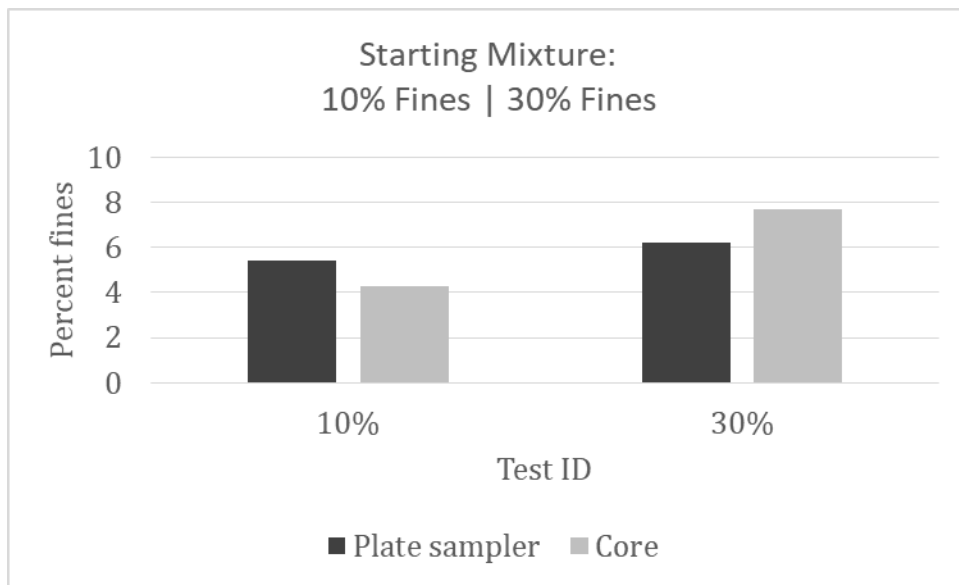


Figure B-24. Results comparing the percentage fines captured using the plate sampler and a 2-inch diameter core.

2.2 Hydraulic Sample Splitting

2.2.1 Sediment Composition

Table B-6 provides a summary of the sediment size characteristics, percent sand, and percent fines.

Table B-6. Results of hydraulic sample splitting.

ID	Sand Type	D_{10} (μm)	D_{50} (μm)	D_{90} (μm)	Sand %	Fines %	Initial Mud/sand	Final Mud/sand
T10C	CS	25	339	619	81.1	18.9	0.11	0.23
R10C	CS	199	387	665	90.1	9.9	0.11	0.11
T20C	CS	18	293	574	70.0	30.0	0.25	0.43
R20C	CS	33	341	603	82.7	17.3	0.25	0.21
T30C	CS	11	127	493	48.1	51.9	0.43	1.08
R30C	CS	20	357	625	76.5	23.5	0.43	0.31
T10F	FS	110	194	322	96.4	3.6	0.11	0.04
R10F	FS	122	210	351	98.0	2.0	0.11	0.02
T20F	FS	92	182	313	93.1	6.9	0.25	0.07
R20F	FS	104	186	312	95.4	4.6	0.25	0.05
T30F	FS	27	162	307	83.1	16.9	0.43	0.20
R30F	FS	43	178	328	88.2	11.8	0.43	0.13

Averaged sediment characteristics of samples collected from the mid-tank port (T) and the return line port (R). Initial mud/sand ratios represent the starting sediment mixture for a given test followed by ratios after sampling. IDs appended with C refer to construction sand tests and F refer to fine sand tests. Percentile grain diameters in red highlight significant deviation from the average.

Sediment concentrations between the mid-tank port and return line port were markedly different. Figure B-25 shows the average concentrations for each mixture and sampling port. The dashed line designates the known system concentration of 50 g/L. For each test, concentrations showed little variability (N=5) at either sampling port, though the standard error of the mean (SEM) was slightly higher for samples collected at the return line; values ranged from 0.4-0.8 g/L at the mid-tank port and from 1.1-3.1 g/L at the return line port.

These data are further reduced in Figure B-26 and provides a good summary of the results. Overall, sediment concentrations collected at the mid-tank port averaged 40 ± 2 g/L for the coarse sand tests and 45 ± 1 g/L (mean \pm SEM) for the fine sand tests, and were therefore closest to the known concentration of 50 g/L. Still, these values represent respective errors of 19% and 11%. In contrast, sediment was much more concentrated in the return line port, which averaged 117 ± 5 g/L and 75 ± 4 g/L (mean \pm SEM) for the coarse and fine sand tests and represent errors of 134% and 50%, respectively.

From examining the ratios of the sand to mud content before and after sample collection, the fines contents are often similar or overrepresented in the CS tests and underrepresented in the FS tests.

2.2.2 Sediment Concentration

Sediment concentrations between the mid-tank port and return line port were markedly different. Figure B-25 shows the average concentrations for each mixture and sampling port. The dashed line designates the known system concentration of 50 g/L. For each test, concentrations showed little variability (N=5) at either sampling port, though the SEM was slightly higher for samples collected at the return line; values ranged from 0.4-0.8 g/L at the mid-tank port and from 1.1–3.1 g/L at the return line port.

These data are further reduced in Figure B-26 and provides a good summary of the results. Overall, sediment concentrations collected at the mid-tank port averaged 40 ± 2 g/L for the coarse sand tests and 45 ± 1 g/L (mean \pm SEM) for the fine sand tests, and were therefore closest to the known concentration of 50 g/L. Still, these values represent respective errors of 19% and 11%. In contrast, sediment was much more concentrated in the return line port, which averaged 117 ± 5 g/L and 75 ± 4 g/L (mean \pm SEM) for the coarse and fine sand tests and represent errors of 134% and 50%, respectively.

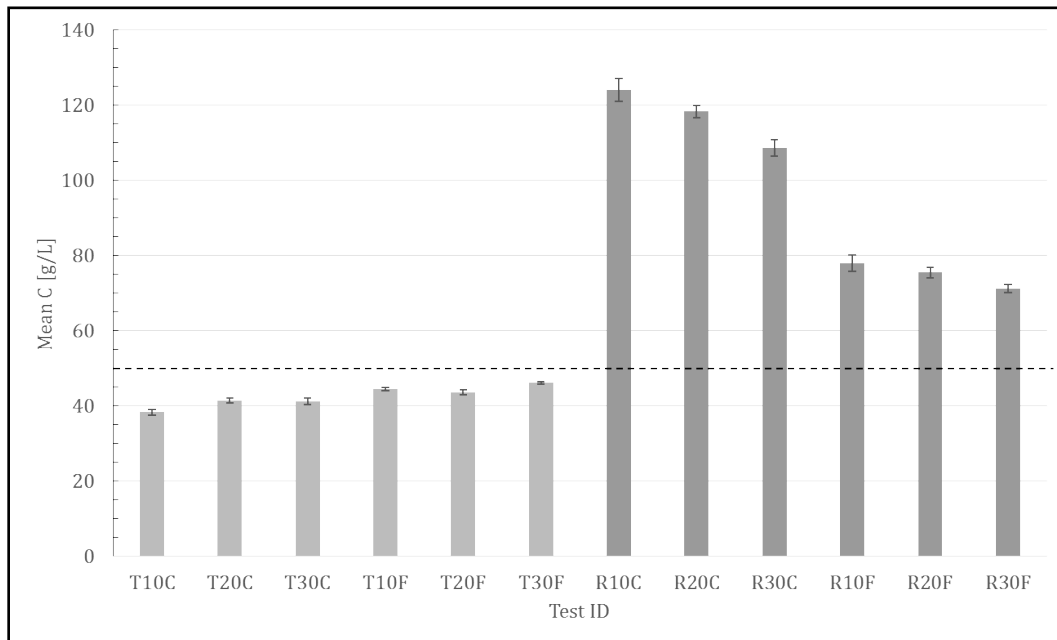


Figure B-25. Hydraulic splitting concentrations by test and port.

Error bars represent the standard error of the mean. T = tank port, R = return line port, F = fine sand, and C = construction sand. Dashed line shows the known system concentration.

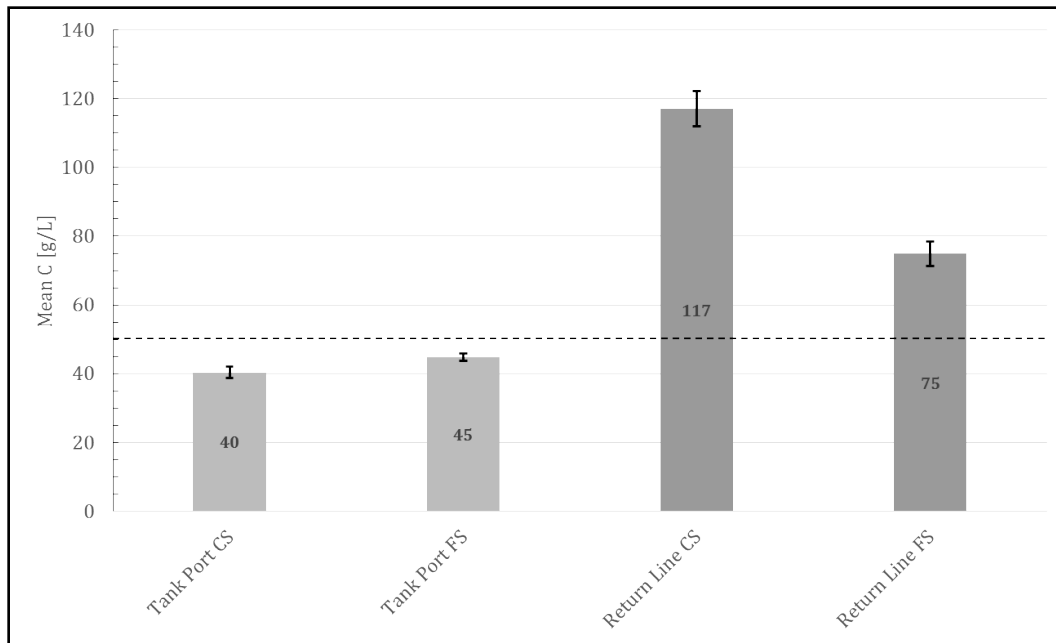


Figure B-26. Hydraulic splitting results by port and sediment type.

Sediment concentrations averaged by sampling port and sediment type. Error bars represent the averaged standard error of the mean. Dashed line shows the known system concentration.

Sand and mud concentrations were determined by multiplying the mean concentration of a given test by its fraction of sand or mud (Figure B-27). The sampled concentrations from each test can then be compared to the expected concentrations of sand and mud, (Figure B-27—E10, E20, and E30). Due to sand's settling velocity, the concentration of sand is expected to be slightly higher in the rising flow of the return line and slightly lower in the descending flow of the tank. The relative magnitude of these concentration variances increases with settling velocity and decreases with flow speed in the return line. For the testing configuration, the sand concentration biases were expected to be on the order of a few percent. Due to the slow settling velocity of fine sediment, the concentration of fine sediment is expected to be very close to equal in the return line and tank. The results presented in Figure B-27 show much more variation in both total concentration and fractional concentration than expected. The total concentration in the return line is much higher than expected, and the mid-tank total concentrations are similarly lower than expected. These observations suggest that there could be inadequate mixing by the tank diffuser and perhaps gravity flow down the tank walls that bypasses the mid-tank sampling position. This flow down the tank walls would also concentrate sediment at the bottom of the conical tank and increase sediment concentration in the return line. The variations from expected values in mud concentration are likewise unexpected. The measured mud concentrations vary by more than a factor of two, both higher and lower, from the expected values.

The underlying principles of the large-volume hydraulic splitter are sound. The testing results presented here highlight the difficulty in splitting suspended sediment samples, particularly those with fast-settling particles. The authors recommend further testing of the concept in the future with particular attention given to redesign of the flow diffuser in the upper portion of the tank and sample analysis methods for the sand/fine split. Alternatively, samples with fast-settling particles can be dewatered and split in a moist state.

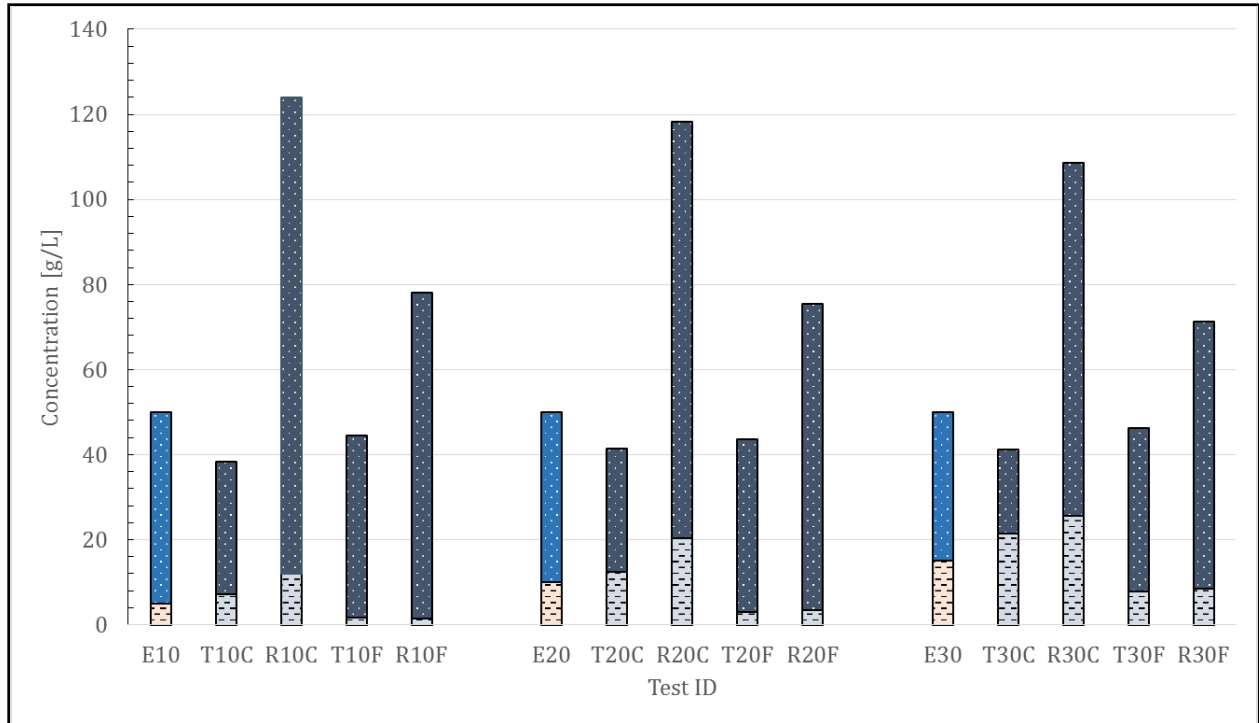


Figure B-27. Hydraulic splitting test results by constituent concentration.

Averaged concentrations of mud (dashed pattern) and sand (dotted pattern) for each test grouped by initial mud content (10%, 20%, 30%). T = tank port, R = return line port, C = construction sand, and F = fine sand. For comparison, the expected concentrations of sand and mud are also plotted (E10, E20, E30).

2.3 Numerical Experiments

To determine appropriate sampling methods and intervals for the dredge inflow, a numerical experiment was undertaken. Figure B-28 provides the mean and 95% confidence intervals of the absolute relative error in mass concentration for both fixed and random interval sampling. The mean absolute relative error of the mass concentration is approximately 3% smaller for the fixed interval sampling versus the random interval sampling. The 95% interval error is approximately 15% larger for the random interval sampling versus the fixed sampling for any average sampling interval over 200 s. At a sampling interval of 60 s, a 4% error is introduced with the fixed interval sampling compared to 7% for the random interval sampling. Both sampling methods show a mean absolute error of less than 10% with a sampling interval less than 200 s. Even at sampling intervals less than 30 s, error is present on the order of 4%. This error is the result of the difference between the first moment of mass flux (the true measure given by (B-3)) and the arithmetic mean (an approximation of the true measure). Additionally, the fixed interval and random interval method produced a relative bias of -1.36% and -1.23%, respectively, for the calculated average concentration.

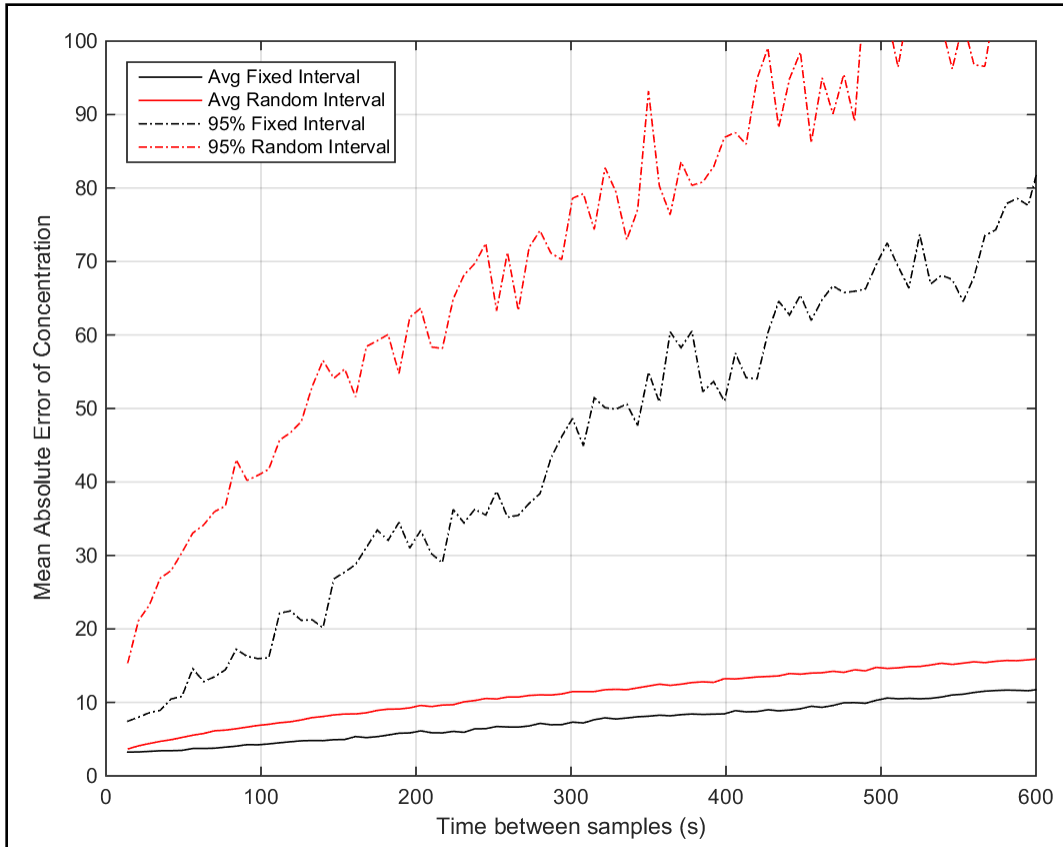


Figure B-28. Results of numerical experiment of inflow sampling interval.

The mean absolute error and the 95% interval percent error for both the fixed and random interval sampling.

3 Discussion

The goal of this appendix is to evaluate specific sediment sampling and measurement techniques to be applied on TSHDs to determine the fraction of fine sediments present at various stages of the dredging process. Several specific sampling-related topics were explored, including:

- to determine whether samples from the TSHD can be composited (or combined) to form physically averaged samples
- to test a hydraulic means of subsampling large-volume, composited samples
- to determine suitable sampling methods for collecting samples within the dredge from the inflow slurry, the hopper sediment bed, and the hopper overflow
- to determine the appropriate sampling interval for the hopper inflow

These research topics were evaluated through a set of laboratory and numerical experiments described in previous sections. A discussion of the results of the laboratory and numerical experiments is provided in this section. Particular emphasis in the discussion is given to recommendations for the field data collection campaign to quantify the separation of sediments during the dredging and beach placement processes.

3.1 Sample Compositing

Sample compositing (or physical averaging) is a method by which samples are collected in time, space, or both and physically mixed to form an “averaged” sample. An inherent assumption in arithmetic averaging is the uniform weighting of samples (all samples are equally valued). For the proposed field study, sample compositing is considered for hopper inflow sampling, hopper bed sampling, and beach coring.

A primary concern with compositing hopper inflow samples is that the covariance of hopper inflow flowrate and slurry concentration can contribute to sample bias. Bias is introduced by arithmetic averaging (physical or numerical) of inflow concentration instead of from the first moment of the inflow sediment mass flux. A numerical experiment was conducted to determine the error introduced by compositing samples, including the effects of sampling interval and regularity. The numerical experiment resampled data of hopper inflow rate and slurry density with two sampling schemes and a range of sampling intervals to determine the difference between the arithmetic mean of slurry concentration and the true value of mean slurry concentration (as estimated by the first moment of sediment mass flux). The results of the numerical experiment indicate a small mean error (or bias) on the order of -1%. (In this case, negative bias means that the arithmetic mean of the composited sample is less than the true value estimated from the first moment of sediment flux.) The small bias indicated by the analysis suggests that compositing of the physical inflow samples for concentration and size analysis is appropriate.

3.2 Sample Splitting

Sample compositing often results in sample volumes or masses that are too large for the intended laboratory sample analysis methods. In these instances, the sample must be split in a representative manner without introducing bias. There are well-documented procedures for splitting of dry and moist soil and sediment samples; however, suspended sediment samples present particular challenges in that the settling velocity of coarse sediments such as sand and gravel is sufficiently large to interfere with complete and unbiased hydraulic mixing of the sample. Inadequately mixed suspensions generally result in bias, as the sample will be withdrawn either from a sediment-rich or sediment-poor portion of the suspension and not be representative of the population.

This study attempted to configure a hydraulic sample splitter for the purposes of splitting composited hopper bed, hopper overflow, and/or hopper inflow samples. The hydraulic splitter was tested with mixtures of sand and silt. The results of the hydraulic sample splitter indicate that coarser sediments are inadequately mixed by the present design. The biases in the return line sample are suspected to be associated with inadequate mixing of the sample by the flow diffuser in the upper tank and consequent gravitational settling and concentration of the coarser sediments in the bottom section of the conical tank. Concentration of the sample in this location resulted in increased concentration in the return line and relatively sparse concentration of coarse sediment near the mid-tank withdrawal point. The conclusion of this work is that the present design of this system is inadequate for the requirements of the present study and alternate approaches will be more appropriate.

The preferred approach for the field study is to settle and decant water from any suspended sediment samples from the composited samples and quantify sediment mass in the decanted water. Suspended solids will be quantified by filtering decanted water through large glass-fiber filters. The settled sediments can then be subsampled in a moist or dry state, which is much less prone to particle-settling-related biases.

3.3 Sampling Methods

Sampling methods were tested for acquiring samples from the hopper inflow, the hopper sediment bed, and the hopper outflow.

3.3.1 Overflow Weir

Three sampling devices (bottle, box, tube) were tested to determine applicability for sampling at hopper overflow weirs. Each device was tested in a controlled laboratory experiment aimed at quantifying the suspended sediment concentration and size fractionation of a sediment suspension passing with similar depth and flow velocity as a prototype hopper overflow weir. These tests served to identify advantages/disadvantages of one design over another and anticipate potential issues that might arise when deployed on a dredge.

All three sampling devices provided very similar estimates of average concentration and mud content when compared to samples from the recovery tank. These favorable evaluations suggest that when the flow depth and flow velocity of the weir are comparable to the testing conditions that any of the sampling methods would be appropriate. For deeper depths of flow, the bottle sampler may be prone to overflowing and therefore bias. The box and tube samplers are readily scalable to provide sampling over the full depth of overflow. Although the preference for one sampler over another may only depend on the unique operating logistics of a dredging vessel, there is reason to think that pump sampling (via the box or tube sampler) may offer significant advantages. For example, Kerssemakers (2004) used custom bottle and flow-through samplers to collect samples from a standpipe-style overflow weir aboard the TSHD *Cornelia*. This work clearly demonstrated the challenges of collecting overflow samples; it was uncertain whether or not their devices were capturing representative samples due to either overflowing (in the case of the bottle sampler) or sampler positioning within the weir. With the box and tube samplers, there is no concern of overflowing and both are more likely to capture a depth integrated sample of the overflow (especially the box sampler). Additionally, a sample could be drawn continuously by attaching a suction line to the discharge outlet from which to draw samples. This allows for greater flexibility in setting sampling intervals, which is an important consideration for compositing purposes.

3.3.2 Hopper Bed Sampling

The preliminary design for a hopper sampler consisted of pipe with one capped end resting on its side (pipe sampler), as described in Section 3.3. During testing, it was noted that sampler orientation had a

marked effect on sediment capture. Sediment was captured sufficiently only when the sampler was oriented parallel to the primary direction of flow (Figure B-8). Results from two independent tests indicated a sampling bias by preferential collection of fine sediments relative to that collected by an adjacent core from the bed. The suspected cause of the bias is attributed to 1) a sheltering effect by the pipe that allowed suspended fine sediments to settle within the sampler and/or 2) sub-maximum filling of the sampler that allowed suspended fines to be collected in the overlying water within the sampler during retrieval. The limited testing of the pipe sampler indicated that its characteristics were unsuitable for sampling the hopper bed.

Given the unsatisfactory performance of the pipe sampler, a plate sampler was designed and constructed to address sample bias from sheltering effects. The operational concept was proven in the laboratory experiments and suggests that bed samples from a dredge hopper can be reliably obtained in a consistent manner.

The apparent bias in the fraction of fines obtained using the plate sampler was both positive and negative compared to cored samples; these differences cannot be explained with any statistical significance given the constraints on the number of trials conducted. However, the results showed much better agreement compared to those derived using the pipe sampler. Although more trials would be necessary to fully evaluate the plate sampler, it remains a viable option for collecting representative hopper samples from the dredge. Other devices considered (though not tested here) to collect samples from the hopper bed were surface grab devices, and gravity corers.

The PONAR sampler is a clamshell-style gravity sampler that has opposing jaws to take surficial sediment samples to a depth of about 10 cm. They are often equipped with top-facing rubber flaps to allow water to pass through upon descent. They are easy to operate but the major disadvantages envisioned are the 1) potential for premature closing in high turbulence environments, 2) loss of sample due to incomplete closing (usually with sandy, coarse sediments), and 3) high propensity of biasing during retrieval (not completely shielded). Grab samplers are particularly susceptible to washout of fine-grained sediment (FieldsCapri and Schumacher 2004). Based on these factors, it was eliminated as a viable sampling option.

Gravity core samplers are weight-assisted coring devices used to take vertical profiles of the sediment. The sediment is contained within a polycarbonate tube equipped with a core catcher to aid in sample recovery. They are most often used for soft, loosely consolidated fine-grained sediments. However, the sandy sediment within the upper layers of dredge hopper bed may be fluidized enough to allow for sufficient penetration, and therefore this option remains a viable sampling option.

3.3.3 Inflow Sampling

Collecting samples from the hopper inflow will be achieved using a pump-sampling device. The intake of the sampling hose will be positioned directly within the inflow discharge. Slurry will be withdrawn from the dredge inflow with an engine-driven trash pump. Samples will be collected from the trash pump discharge on a periodic basis from the trash pump effluent. Proper testing of a sampler for this purpose was not feasible in the laboratory due to the large discharge volumes expected at the dredge inflow.

Primary concerns of inflow sampling are the potential biasing of inflow samples by compositing of samples and excessive error introduced by inadequate sampling of the inflow. The sample compositing concern was addressed through a numerical analysis (discussed above). The numerical experiment also examines appropriate sampling interval of the inflow. Sampling theory indicates that sample approximation of the population improves with increased sample size. The numerical experiment indicated an improved estimate of the true mean slurry concentration with reduced sample interval (equivalent to increased numbers of samples). Regular sampling in time was clearly better than random

sampling in time, reducing the mean absolute error by approximately 5% and the upper limit of absolute error by 10% to 20%. The gains of regular sampling are presumably due to the inherent time variability in the inflow rate and slurry concentration. Regular sampling over the entire loading cycle would also be important for capturing variations in sediment composition during the loading cycle. A mean absolute error less than 10% can be obtained with composited samples collected at regular intervals of 120 seconds or less. If the sampling interval is further reduced to 90 s, the mean absolute error reduces to less than 5%. These sampling intervals are physically feasible with the proposed pump sampling. Additionally, the results of the numerical experiment can be applied as an estimate of the expected error for the actual sampling intervals performed in the field.

3.4 Conclusions

The findings of the laboratory and numerical evaluations described in this appendix lead to the following conclusions related to field studies:

- 1) The three devices (box, bottle, and tube) used to measure the sediment properties of the hopper overflow generated estimates of suspended sediment concentration and size distribution that were on average within 4% or less relative to samples obtained from the recovery tank. The choice of sampling device to apply in a field setting is most likely dependent on access to the hopper overflow location and characteristics of the overflow, such as depth of overflow, velocity of overflow, or weir geometry.
- 2) Numerical evaluation of inflow data for 147 hopper loads indicates that compositing of the hopper inflow samples will result in low bias and acceptable accuracy. Sample compositing is also acceptable for increased sampling of the hopper bed, hopper suspended load, and beach coring activities.
- 3) A hydraulic sample splitter to reduce the volume of composited hopper inflow samples was evaluated and found to be unacceptable in its capacity to mix sand-sized sediment. All sample splitting for the field study will be accomplished by moist or dry sample splitting according to established standards and procedures. Suspended sediment samples will be settled and decanted prior to sample splitting to avoid hydraulic separation and bias.
- 4) The numerical experiments of the inflow data provided guidance for the necessary sampling interval to accurately describe the concentrations. A fixed interval between samples had less error than a random interval, demonstrating the need for regular sampling over the entire filling operation. Sampling intervals of 90- to 120-seconds contribute sampling errors less than +/- 5% and 10%, respectively.
- 5) Sampling the deposited sediment of the hopper requires that the method not create a shelter from the flow and turbulence. Sheltering increases the percent fines of the sample, biasing the results. Other important concerns are likelihood of sample recovery, ease of use, and safety. Based on these concerns, vibracores, pipe samplers, and surface grabs were eliminated as sampling options. Therefore, the two options considered here that provide the best chance of collecting representative hopper samples are the gravity corer and the plate sampler.

4 References

- Capel PD, Larson SJ. 1996. Evaluation of selected information on splitting devices for water samples. Sacramento (CA): U.S. Geological Survey. USGS Water-Resources Investigations Report 95-4141. 103 p.
- FieldsCapri J, Schumacher BA. 2004. Literature review and report: surface sediment sampler database. U.S. Washington (DC): U.S. Environmental Protection Agency. EPA/600/R-03/115 (NTIS PB2004-101011).
- Kerssemakers KA. 2004. Overflow sampling of trailing suction hopper dredgers: a case study on the TSHD Cornelia [thesis]. Delft (Netherlands): Delft University of Technology.
- Richardson JF, Zaki WN. 1954. Sedimentation and fluidization, part I. Transactions of the Institution of Chemical Engineers. 32:35-53.
- van Rhee C. 2001. Numerical simulation of the sedimentation process in a trailing suction hopper dredge. In: Proceedings of the 16th World Dredging Congress; 2001 Apr 2-5; Kuala Lumpur, Malaysai.
- Wilde FD, Sandstrom MW, Skrobialowski SC. 2014. Selection of equipment for water sampling (Ver. 3.1, Book 9, Chapter A2). In: Techniques of Water-Resources Investigations. Reston (VA): U.S. Geological Survey.

Appendix C Boring Logs and Sample Analysis from Horn Island Pass Borrow Area 1 (HIP1)

This appendix contains sediment coring information from borrow site HIP1 near Pascagoula, Mississippi. Included are a site map, boring logs, and sample analysis results. All included information is from the Mississippi Coastal Improvements Program Barrier Island Restoration Project, Offshore Sand Borrow Investigation, 2010–2014, Geotechnical Engineering Report (prepared by Michael FitzHarris and Elizabeth Godsey of the US Army Corps of Engineers, Mobile District).

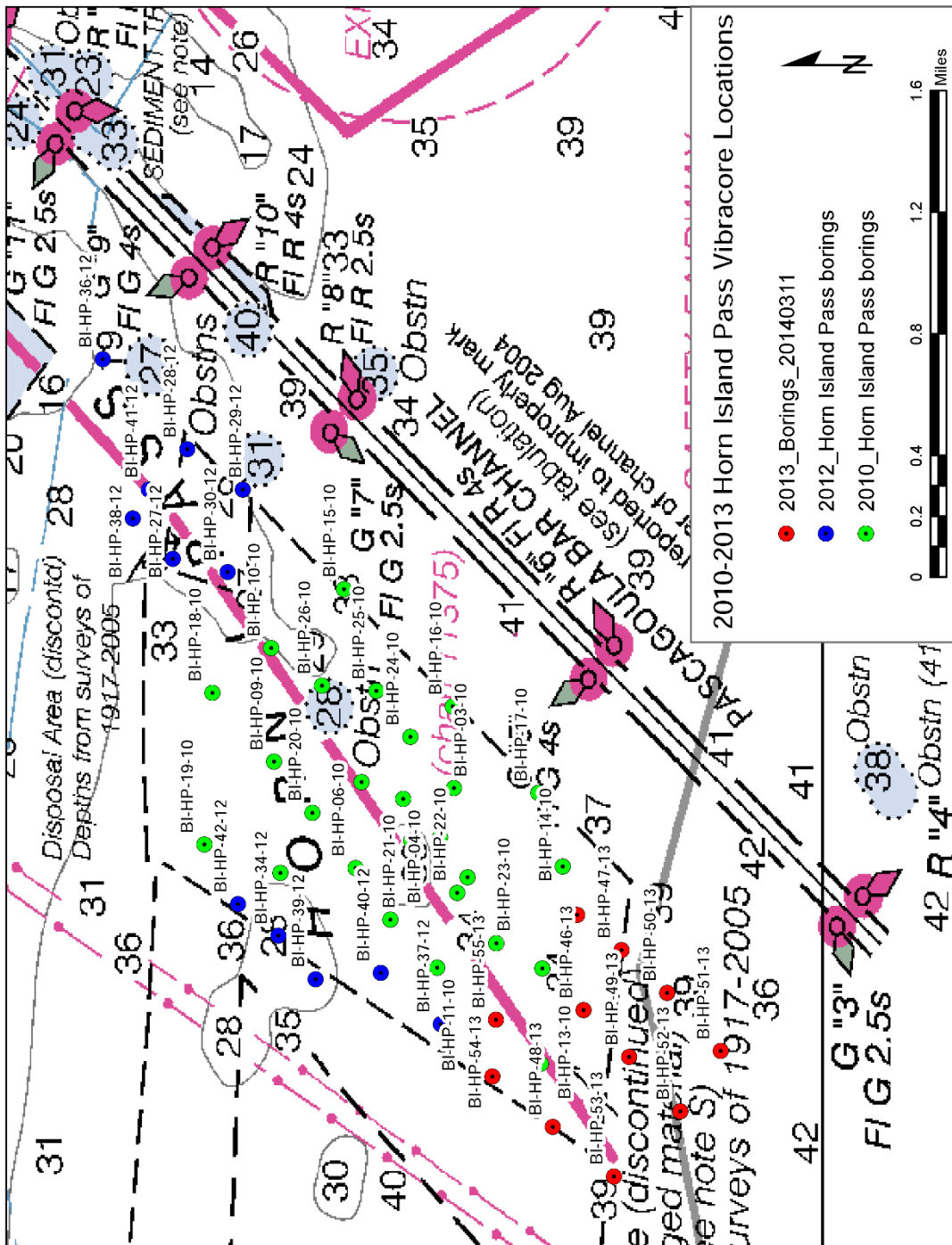


Figure C-1. 2010–2013 Horn Island Pass vibracore locations.

Only the cores and samples collected within and immediately adjacent to the HIP1 borrow site (the northeastern corner of the dashed box) are presented in this appendix.

Boring Designation BI-HP-09-10

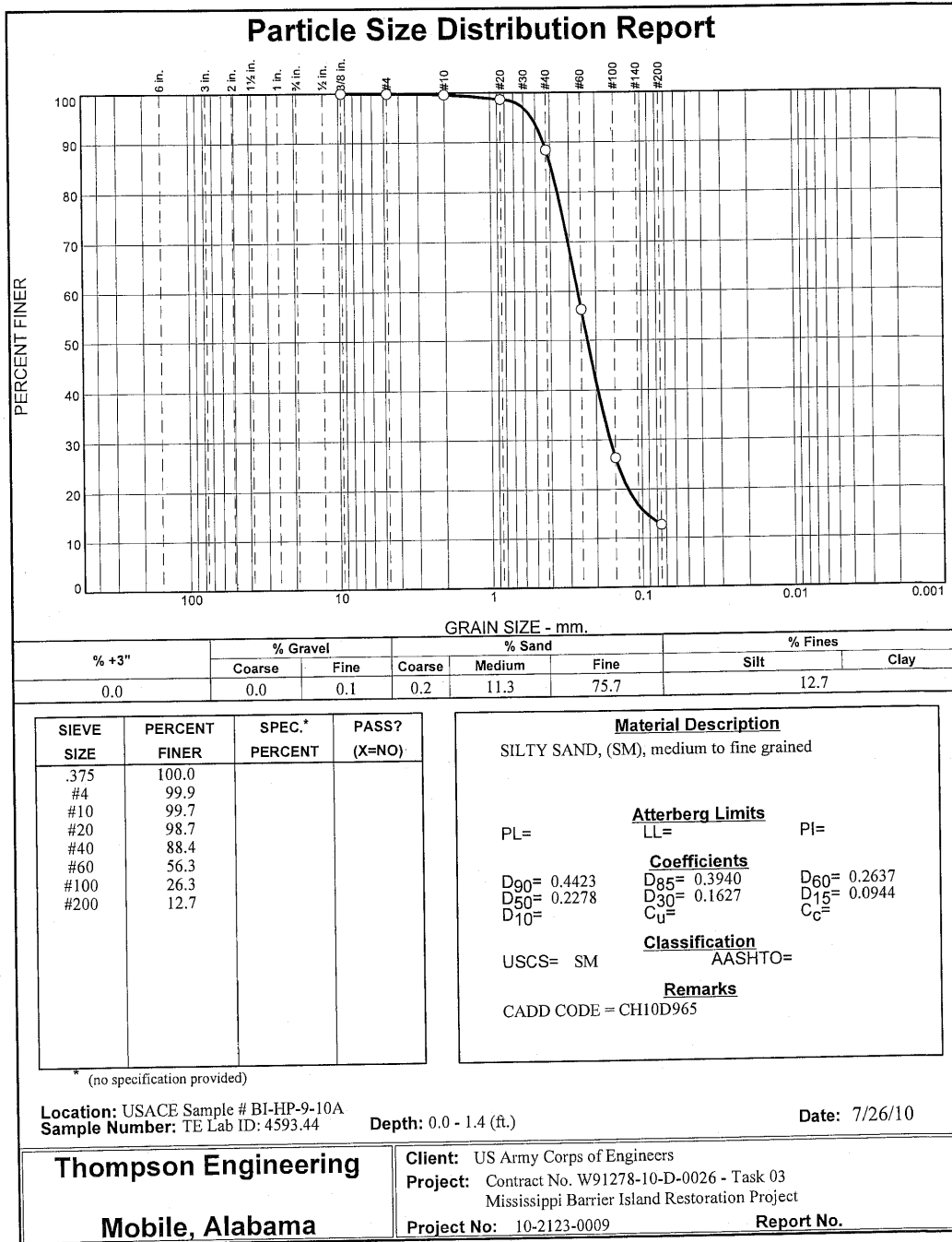
DRILLING LOG		DIVISION South Atlantic	INSTALLATION Mobile District	SHEET 1 OF 1 SHEETS
1. PROJECT MsCIP Barrier Island Restoration Horn Island Pass		9. SIZE AND TYPE OF BIT N/A		10. COORDINATE SYSTEM/DATUM State Plane, MSE (U.S. Ft.)
2. BORING DESIGNATION BI-HP-09-10		LOCATION COORDINATES E = 1,074,811 N = 252,037		HORIZONTAL NAD83
3. DRILLING AGENCY Corps of Engineers - CESAM		CONTRACTOR FILE NO.		VERTICAL NAVD88
4. NAME OF DRILLER Construction Solutions International, Inc.		11. MANUFACTURER'S DESIGNATION OF DRILL Vibracore		<input type="checkbox"/> AUTO HAMMER <input type="checkbox"/> MANUAL HAMMER
5. DIRECTION OF BORING <input checked="" type="checkbox"/> VERTICAL <input type="checkbox"/> INCLINED		DEG. FROM VERTICAL	BEARING	12. TOTAL SAMPLES DISTURBED: 1 UNDISTURBED (UD): 0
6. THICKNESS OF OVERBURDEN N/A		13. TOTAL NUMBER CORE BOXES		14. WATER DEPTH 36 Ft.
7. DEPTH DRILLED INTO ROCK N/A		15. DATE BORING STARTED: 07-14-10 COMPLETED: 07-14-10		16. ELEVATION TOP OF BORING -36.1 Ft.
8. TOTAL DEPTH OF BORING 18.7 Ft.		17. TOTAL RECOVERY FOR BORING 100%		18. SIGNATURE AND TITLE OF INSPECTOR John Baehr, Geologist

ELEV.	DEPTH	LEGEND	CLASSIFICATION OF MATERIALS	SAMPLE	LABORATORY RESULTS
-36.1	0.0				
-36.6	0.5				
-37.5	1.4		SAND, poorly-graded, mostly fine-grained sand-sized quartz, trace shell fragments, lt. gray (SP)	A	Classification: SM Color: 2.5Y 7/1-light gray D50: 0.2278 mm % Fines: 12.7
			SAND, silty, mostly fine-grained sand-sized quartz, some silt, lt. gray (SM)		
			SAND, clayey, mostly fine-grained sand-sized quartz, some clay, gray (SC)		
				NS	
-54.8	18.7				
NOTES:					
1. Soils are field visually classified in accordance with the Unified Soils Classification System.					
2. NS = Sample not submitted for laboratory analysis from this interval.					
3. Seafloor elevation determined from USACE hydrographic survey completed June 2014.					

SAM FORM 1836 - MsCIP
MAY 2010

Lat = 30.19274° Long = -88.54668°

Figure C-2. Drilling log for boring site BI-HP-09-10.



Tested By: G.Fancher Checked By: R.Byrd

Figure C-3. Particle size distribution report for sample # BI-HP-9-10A.

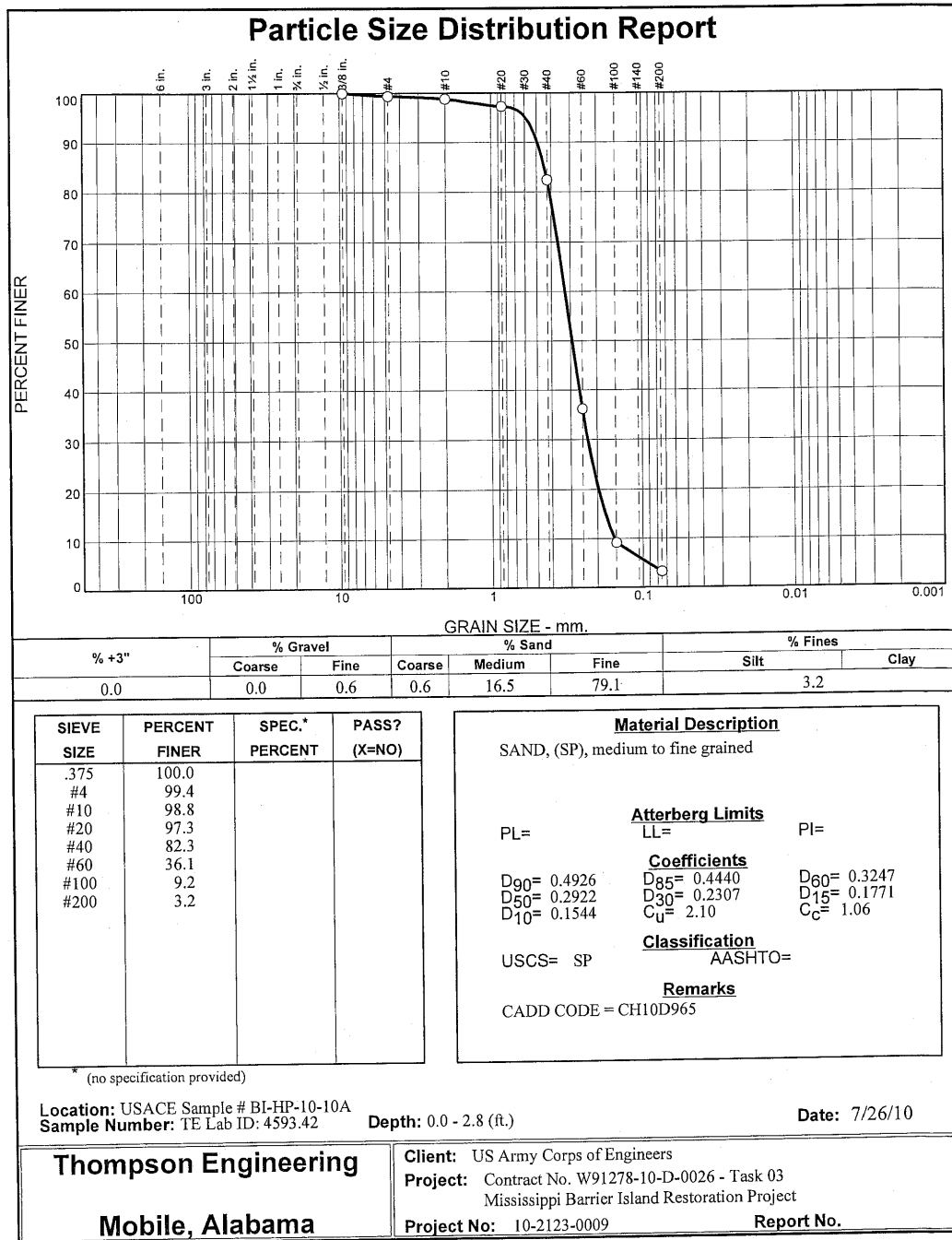
Boring Designation BI-HP-10-10

DRILLING LOG		DIVISION		INSTALLATION		SHEET 1	
		South Atlantic		Mobile District		OF 1 SHEETS	
1. PROJECT				9. SIZE AND TYPE OF BIT			
MsCIP Barrier Island Restoration Horn Island Pass				N/A			
2. BORING DESIGNATION		LOCATION COORDINATES		10. COORDINATE SYSTEM/DATUM		HORIZONTAL	
BI-HP-10-10		E = 1,076,520 N = 252,092		State Plane, MSE (U.S. Ft.)		NAD83	
3. DRILLING AGENCY		CONTRACTOR FILE NO.		11. MANUFACTURER'S DESIGNATION OF DRILL		<input type="checkbox"/> AUTO HAMMER <input type="checkbox"/> MANUAL HAMMER	
Corps of Engineers - CESAM				Vibracore			
4. NAME OF DRILLER				12. TOTAL SAMPLES		DISTURBED	
Construction Solutions International, Inc.				2		0	
5. DIRECTION OF BORING				13. TOTAL NUMBER CORE BOXES		14. WATER DEPTH	
<input checked="" type="checkbox"/> VERTICAL <input type="checkbox"/> INCLINED						31 Ft.	
6. THICKNESS OF OVERBURDEN				15. DATE BORING		STARTED	
N/A				07-14-10		COMPLETED	
7. DEPTH DRILLED INTO ROCK				16. ELEVATION TOP OF BORING		07-14-10	
N/A				-31.8 Ft.			
8. TOTAL DEPTH OF BORING				17. TOTAL RECOVERY FOR BORING		18. SIGNATURE AND TITLE OF INSPECTOR	
18.8 Ft.				100%		John Baehr, Geologist	

ELEV.	DEPTH	LEGEND	CLASSIFICATION OF MATERIALS	SAMPLE	LABORATORY RESULTS
-31.8	0.0				
			SAND, poorly-graded, mostly fine-grained sand-sized quartz, trace shell fragments (SP)	A	Classification: SP Color: 2.5Y 7/1-light gray D50: 0.2922 mm % Fines: 3.2
				B	Classification: SP Color: 2.5Y 7/1-light gray D50: 0.2576 mm % Fines: 3.5
-37.4	5.6				
			SAND, clayey, mostly fine-grained sand-sized quartz, some clay, gray (SC)	NS	
-50.6	18.8				
			NOTES:		
			1. Soils are field visually classified in accordance with the Unified Soils Classification System.		
			2. NS = Sample not submitted for laboratory analysis from this interval.		
			3. Seafloor elevation determined from USACE hydrographic survey completed June 2014.		

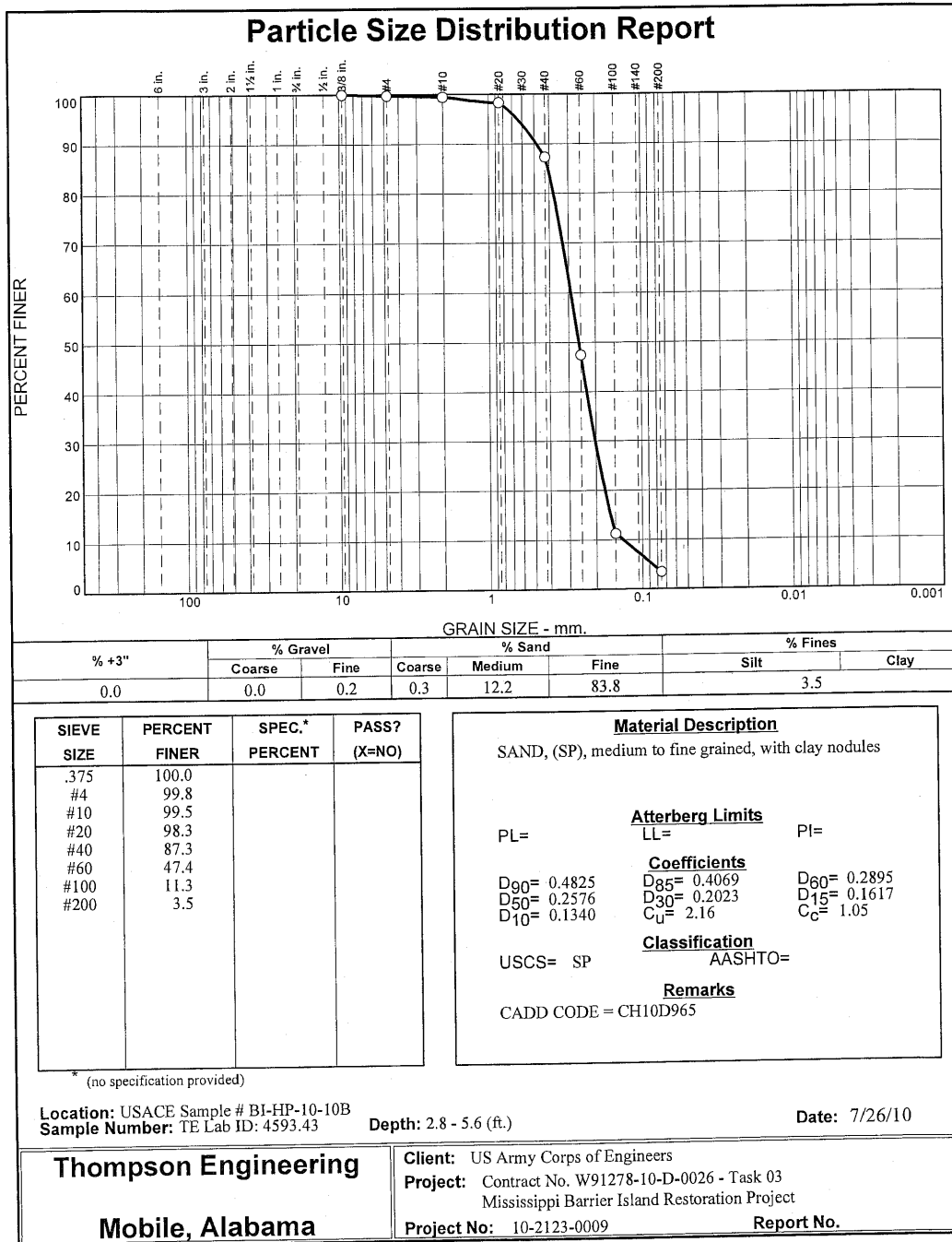
SAM FORM 1836 - MsCIP MAY 2010 Lat = 30.19288° Long = -88.54127°

Figure C-4. Drilling log for boring site BI-HP-10-10.



Tested By: G.Fancher Checked By: R.Byrd

Figure C-5. Particle size distribution report for sample # BI-HP-10-10A.



Tested By: G.Fancher Checked By: R.Byrd

Figure C-6. Particle size distribution report for sample # BI-HP-10-10B.

Boring Designation BI-HP-15-10

DRILLING LOG		DIVISION South Atlantic		INSTALLATION Mobile District		SHEET 1 OF 1 SHEETS	
1. PROJECT MsCIP Barrier Island Restoration Horn Island Pass				9. SIZE AND TYPE OF BIT N/A			
2. BORING DESIGNATION BI-HP-15-10		LOCATION COORDINATES E = 1,077,412 N = 250,836		10. COORDINATE SYSTEM/DATUM Slate Plane, MSE (U.S. Ft.)		HORIZONTAL NAD83	VERTICAL NAVD88
3. DRILLING AGENCY Corps of Engineers - CESAM		CONTRACTOR FILE NO.		11. MANUFACTURER'S DESIGNATION OF DRILL Vibracore		<input type="checkbox"/> AUTO HAMMER	<input type="checkbox"/> MANUAL HAMMER
4. NAME OF DRILLER Construction Solutions International, Inc.				12. TOTAL SAMPLES		DISTURBED 0	UNDISTURBED (UD) 0
5. DIRECTION OF BORING <input checked="" type="checkbox"/> VERTICAL <input type="checkbox"/> INCLINED				DEG. FROM VERTICAL	BEARING		13. TOTAL NUMBER CORE BOXES
6. THICKNESS OF OVERBURDEN N/A				14. WATER DEPTH 36 Ft.			
7. DEPTH DRILLED INTO ROCK N/A				15. DATE BORING		STARTED 07-14-10	COMPLETED 07-14-10
8. TOTAL DEPTH OF BORING 18.5 Ft.				16. ELEVATION TOP OF BORING -36.0 Ft.			
				17. TOTAL RECOVERY FOR BORING 100%			
				18. SIGNATURE AND TITLE OF INSPECTOR John Baehr, Geologist			
ELEV.	DEPTH	LEGEND	CLASSIFICATION OF MATERIALS	SAMPLE	LABORATORY RESULTS		
-36.0	0.0		SAND, clayey, mostly fine-grained sand-sized quartz, some clay, gray (SC)				
				NS			
-54.5	18.5		NOTES: 1. Soils are field visually classified in accordance with the Unified Soils Classification System. 2. NS = Sample not submitted for laboratory analysis from this interval. 3. Seafloor elevation determined from USACE hydrographic survey completed June 2014.				

SAM FORM 1836 - MsCIP
MAY 2010

Lat = 30.18942° Long = -88.53846°

Figure C-7. Drilling log for boring site BI-HP-15-10.

Boring Designation BI-HP-18-10

DRILLING LOG		DIVISION		INSTALLATION		SHEET 1	
		South Atlantic		Mobile District		OF 1 SHEETS	
1. PROJECT				9. SIZE AND TYPE OF BIT			
MsCIP Barrier Island Restoration Horn Island Pass				N/A			
2. BORING DESIGNATION		LOCATION COORDINATES		10. COORDINATE SYSTEM/DATUM		HORIZONTAL	
BI-HP-18-10		E = 1,075,845 N = 253,105		State Plane, MSE (U.S. Ft.)		NAD83	
3. DRILLING AGENCY		CONTRACTOR FILE NO.		11. MANUFACTURER'S DESIGNATION OF DRILL		<input type="checkbox"/> AUTO HAMMER <input type="checkbox"/> MANUAL HAMMER	
Corps of Engineers - CESAM				Vibracore		DISTURBED UNDISTURBED (UD) 0 0	
4. NAME OF DRILLER				13. TOTAL NUMBER CORE BOXES			
Construction Solutions International, Inc.							
5. DIRECTION OF BORING		DEG. FROM VERTICAL		14. WATER DEPTH		34 Ft.	
<input checked="" type="checkbox"/> VERTICAL <input type="checkbox"/> INCLINED				15. DATE BORING		STARTED COMPLETED 07-15-10 07-15-10	
6. THICKNESS OF OVERBURDEN		N/A		16. ELEVATION TOP OF BORING		-34.9 Ft.	
7. DEPTH DRILLED INTO ROCK		N/A		17. TOTAL RECOVERY FOR BORING		100%	
8. TOTAL DEPTH OF BORING		16.5 Ft.		18. SIGNATURE AND TITLE OF INSPECTOR			
				John Baehr, Geologist			
ELEV.	DEPTH	LEGEND	CLASSIFICATION OF MATERIALS	SAMPLE	LABORATORY RESULTS		
-34.9	0.0						
			SAND, clayey, mostly fine-grained sand-sized quartz, trace, gray (SC)				
				NS			
-50.0	15.1						
-51.4	16.5		CLAY, lean, yellow brown (CL)				
			NOTES:				
			1. Soils are field visually classified in accordance with the Unified Soils Classification System.				
			2. NS = Sample not submitted for laboratory analysis from this interval.				
			3. Seafloor elevation determined from USACE hydrographic survey completed June 2014.				



SAM FORM 1836 - MsCIP
MAY 2010

Lat = 30.19567° Long = -88.5434°

Figure C-8. Drilling log for boring site BI-HP-18-10.

Boring Designation BI-HP-25-10

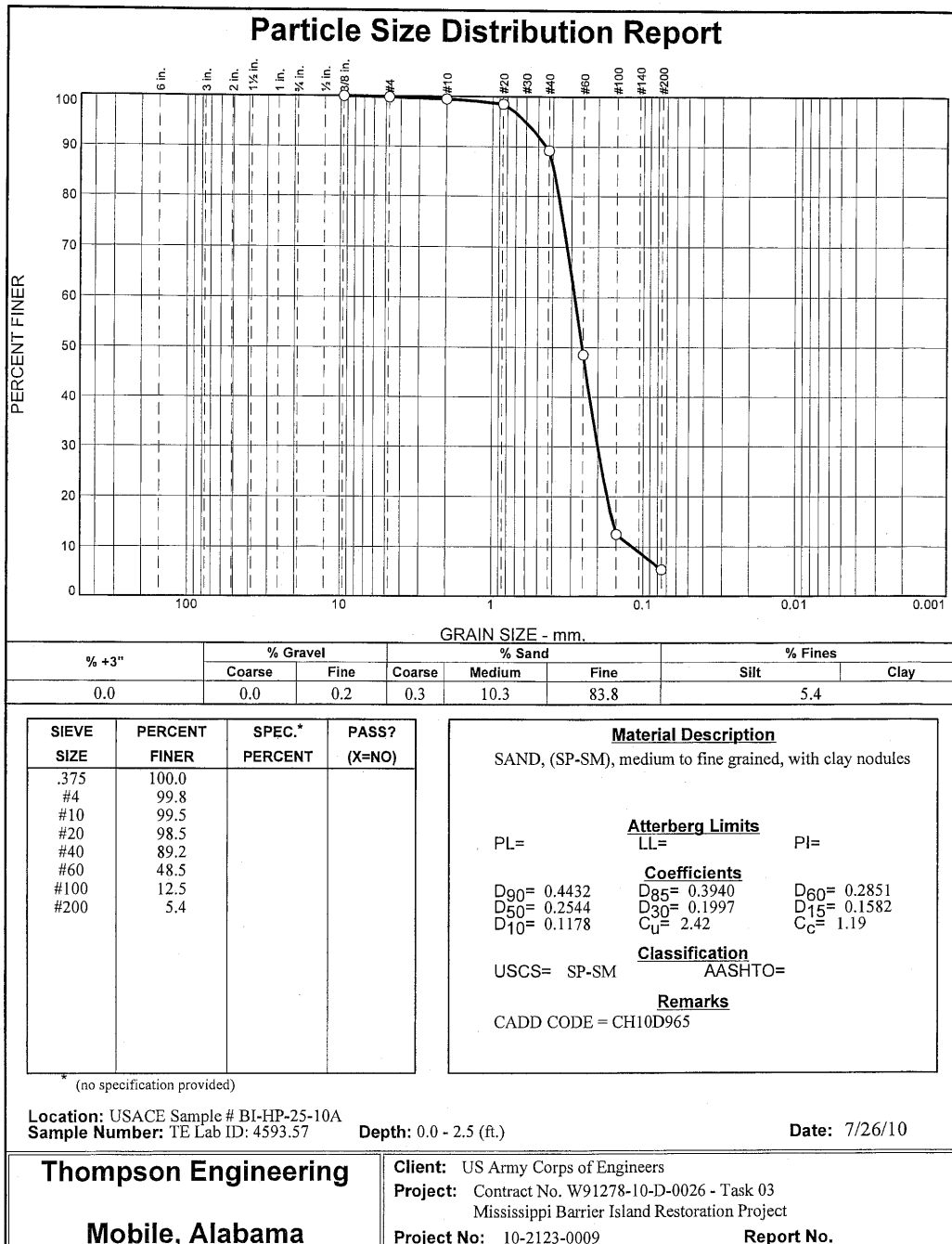
DRILLING LOG		DIVISION		INSTALLATION		SHEET 1	
		South Atlantic		Mobile District		OF 1 SHEETS	
1. PROJECT				9. SIZE AND TYPE OF BIT			
MsCIP Barrier Island Restoration Horn Island Pass				N/A			
2. BORING DESIGNATION		LOCATION COORDINATES		10. COORDINATE SYSTEM/DATUM		HORIZONTAL	
BI-HP-25-10		E = 1,075,884 N = 250,272		State Plane, MSE (U.S. Ft.)		NAD83	
3. DRILLING AGENCY		CONTRACTOR FILE NO.		11. MANUFACTURER'S DESIGNATION OF DRILL		<input type="checkbox"/> AUTO HAMMER	
Corps of Engineers - CESAM				Vibracore		<input type="checkbox"/> MANUAL HAMMER	
4. NAME OF DRILLER				12. TOTAL SAMPLES		DISTURBED	
Construction Solutions International, Inc.				1		UNDISTURBED (UD)	
5. DIRECTION OF BORING				13. TOTAL NUMBER CORE BOXES		14. WATER DEPTH	
<input checked="" type="checkbox"/> VERTICAL				DEG. FROM VERTICAL		35 Ft.	
<input type="checkbox"/> INCLINED				BEARING		15. DATE BORING	
						STARTED	
6. THICKNESS OF OVERBURDEN				16. ELEVATION TOP OF BORING		COMPLETED	
N/A				-34.9 Ft.		07-15-10	
7. DEPTH DRILLED INTO ROCK				17. TOTAL RECOVERY FOR BORING		07-15-10	
N/A				100%			
8. TOTAL DEPTH OF BORING				18. SIGNATURE AND TITLE OF INSPECTOR			
17.4 Ft.				John Baehr, Geologist			

ELEV.	DEPTH	LEGEND	CLASSIFICATION OF MATERIALS	SAMPLE	LABORATORY RESULTS
-34.9	0.0				
-37.4	2.5		SAND, poorly-graded, mostly fine-grained sand-sized quartz, trace shell fragments, occ. clay balls, lt. gray (SP)	A	Classification: SP-SM Color: 2.5Y 7/1-light gray D50: 0.2544 mm % Fines: 5.4
			SAND, clayey, mostly fine-grained sand-sized quartz, gray (SC)	NS	
-52.3	17.4				
			NOTES:		
			1. Soils are field visually classified in accordance with the Unified Soils Classification System.		
			2. NS = Sample not submitted for laboratory analysis from this interval.		
			3. Seafloor elevation determined from USACE hydrographic survey completed June 2014.		

SAM FORM 1836 - MsCIP
MAY 2010

Lat = 30.18788° Long = -88.5433°

Figure C-9. Drilling log for boring site BI-HP-25-10.



Tested By: G.Fancher Checked By: R.Byrd

Figure C-10. Particle size distribution report for sample # BI-HP-25-10A.

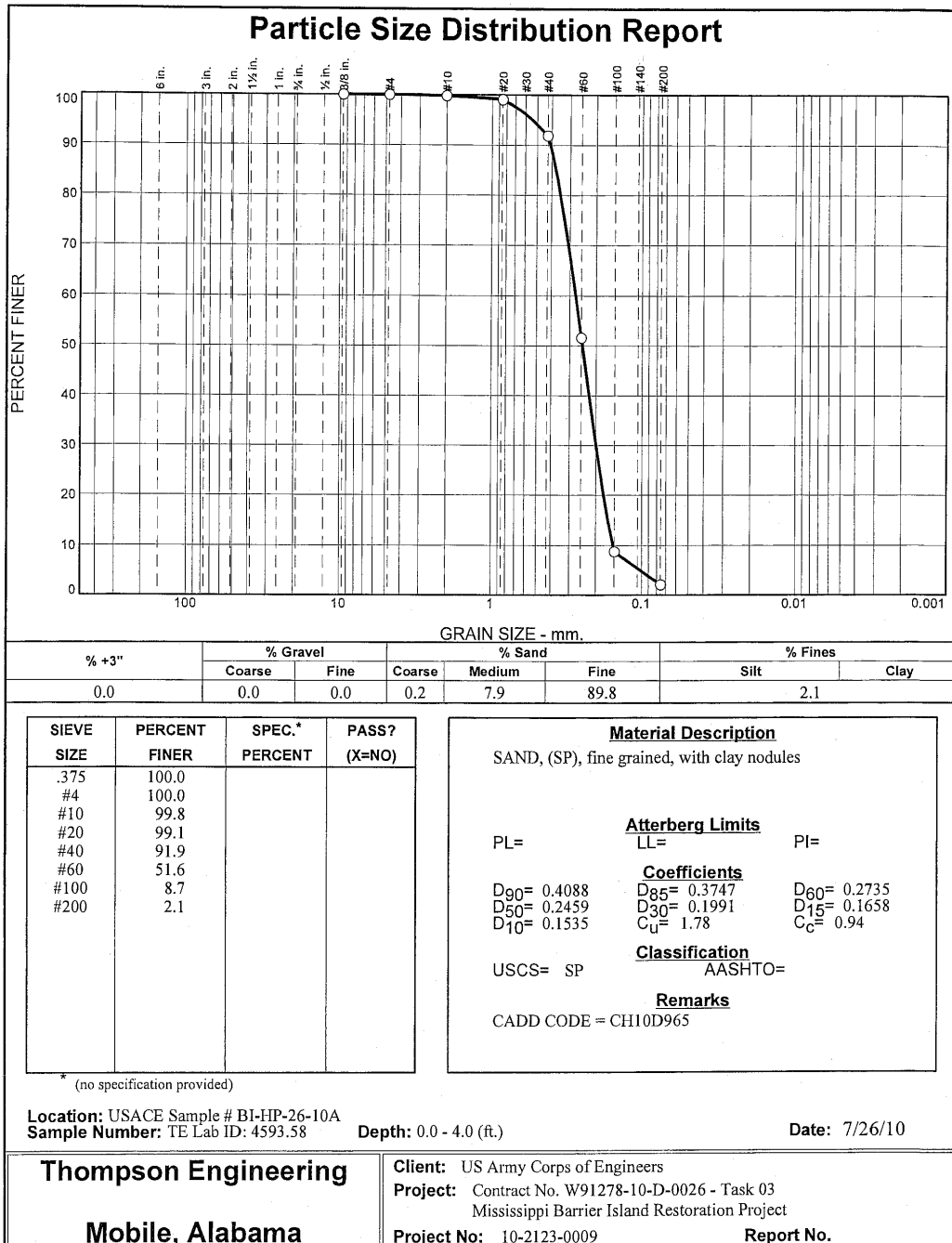
Boring Designation BI-HP-26-10

DRILLING LOG		DIVISION		INSTALLATION		SHEET 1	
		South Atlantic		Mobile District		OF 1 SHEETS	
1. PROJECT				9. SIZE AND TYPE OF BIT			
MsCIP Barrier Island Restoration Horn Island Pass				N/A			
2. BORING DESIGNATION		LOCATION COORDINATES		10. COORDINATE SYSTEM/DATUM		HORIZONTAL	
BI-HP-26-10		E = 1,075,957 N = 251,218		State Plane, MSE (U.S. Ft.)		NAD83	
3. DRILLING AGENCY		CONTRACTOR FILE NO.		11. MANUFACTURER'S DESIGNATION OF DRILL		<input type="checkbox"/> AUTO HAMMER <input type="checkbox"/> MANUAL HAMMER	
Corps of Engineers - CESAM				Vibracore		DISTURBED 1 0	
4. NAME OF DRILLER				12. TOTAL SAMPLES			
Construction Solutions International, Inc.				13. TOTAL NUMBER CORE BOXES			
5. DIRECTION OF BORING		DEG. FROM VERTICAL		14. WATER DEPTH		34 Ft.	
<input checked="" type="checkbox"/> VERTICAL <input type="checkbox"/> INCLINED				15. DATE BORING		STARTED COMPLETED 07-15-10 07-15-10	
6. THICKNESS OF OVERBURDEN				16. ELEVATION TOP OF BORING			
N/A				-33.3 Ft.			
7. DEPTH DRILLED INTO ROCK				17. TOTAL RECOVERY FOR BORING			
N/A				100%			
8. TOTAL DEPTH OF BORING				18. SIGNATURE AND TITLE OF INSPECTOR			
17.9 Ft.				John Baehr, Geologist			

ELEV.	DEPTH	LEGEND	CLASSIFICATION OF MATERIALS	SAMPLE	LABORATORY RESULTS
-33.3	0.0				
			SAND, poorly-graded, mostly fine-grained sand-sized quartz, trace shell fragments, lt. gray (SP)	A	Classification: SP Color: 2.5Y 7/1-light gray D50: 0.2459 mm % Fines: 2.1
-37.3	4.0		SAND, clayey, mostly fine-grained sand-sized quartz, trace shell fragments, gray (SC)	NS	
-51.2	17.9				
			NOTES:		
			1. Soils are field visually classified in accordance with the Unified Soils Classification System.		
			2. NS = Sample not submitted for laboratory analysis from this interval.		
			3. Seafloor elevation determined from USACE hydrographic survey completed June 2014.		

SAM FORM 1836 - MsCIP MAY 2010 Lat = 30.19048° Long = -88.54306°

Figure C-11. Drilling log for boring site BI-HP-26-10.



Tested By: G.Fancher Checked By: R.Byrd

Figure C-12. Particle size distribution report for sample # BI-HP-26-10A.

Boring Designation BI-HP-27-12

DRILLING LOG		DIVISION		INSTALLATION		SHEET 1	
		South Atlantic		Mobile District		OF 1 SHEETS	
1. PROJECT				9. SIZE AND TYPE OF BIT			
MsCIP Barrier Island Restoration Horn Island Pass				N/A			
2. BORING DESIGNATION		LOCATION COORDINATES		10. COORDINATE SYSTEM/DATUM		HORIZONTAL	
BI-HP-27-12		E = 1,077,859 N = 253,801		State Plane, MSE (U.S. Ft.)		NAD83	
3. DRILLING AGENCY		CONTRACTOR FILE NO.		11. MANUFACTURER'S DESIGNATION OF DRILL		<input type="checkbox"/> AUTO HAMMER <input type="checkbox"/> MANUAL HAMMER	
Corps of Engineers - CESAM				Vibracore		DISTURBED UNDISTURBED (UD)	
4. NAME OF DRILLER				12. TOTAL SAMPLES			
American Vibracore Systems, Inc.				0			
5. DIRECTION OF BORING				13. TOTAL NUMBER CORE BOXES			
<input checked="" type="checkbox"/> VERTICAL <input type="checkbox"/> INCLINED				29.6 Ft.			
6. THICKNESS OF OVERBURDEN				14. WATER DEPTH			
N/A				29.6 Ft.			
7. DEPTH DRILLED INTO ROCK				15. DATE BORING			
N/A				STARTED COMPLETED			
8. TOTAL DEPTH OF BORING				16. ELEVATION TOP OF BORING			
15.7 Ft.				-29.0 Ft.			
				17. TOTAL RECOVERY FOR BORING			
				100%			
				18. SIGNATURE AND TITLE OF INSPECTOR			
				Mike FitzHarris, Geologist			

ELEV.	DEPTH	LEGEND	CLASSIFICATION OF MATERIALS	SAMPLE	LABORATORY RESULTS
-29.0	0.0				
			SAND, poorly-graded, mostly fine to medium-grained sand-sized quartz, trace silt, trace shell fragments, trace clay nodules, lt. gray (SP)	A	Classification: SP Color: 2.5Y 7.5/2- D50: 0.3309 mm % Fines: 1.6
			SAND, poorly-graded with silt, mostly fine-grained sand-sized quartz, little silt, trace shell fragments, little clay stringers, lt gray with gray bands (SP-SM)	B	Classification: SP-SM Color: 2.5Y 7/2-light gray D50: 0.2966 mm % Fines: 7.4
			CLAY, lean, mostly clay, trace shell fragments, gray (CL)	NS	
			NOTES: 1. Soils are field visually classified in accordance with the Unified Soils Classification System. 2. NS = Sample not submitted for laboratory analysis from this interval. 3. Seafloor elevation determined from USACE hydrographic survey completed June 2014.		

SAM FORM 1836 - MsCIP
MAY 2010

Lat = 30.19757° Long = -88.53702°

Figure C-13. Drilling log for boring site BI-HP-27-12.

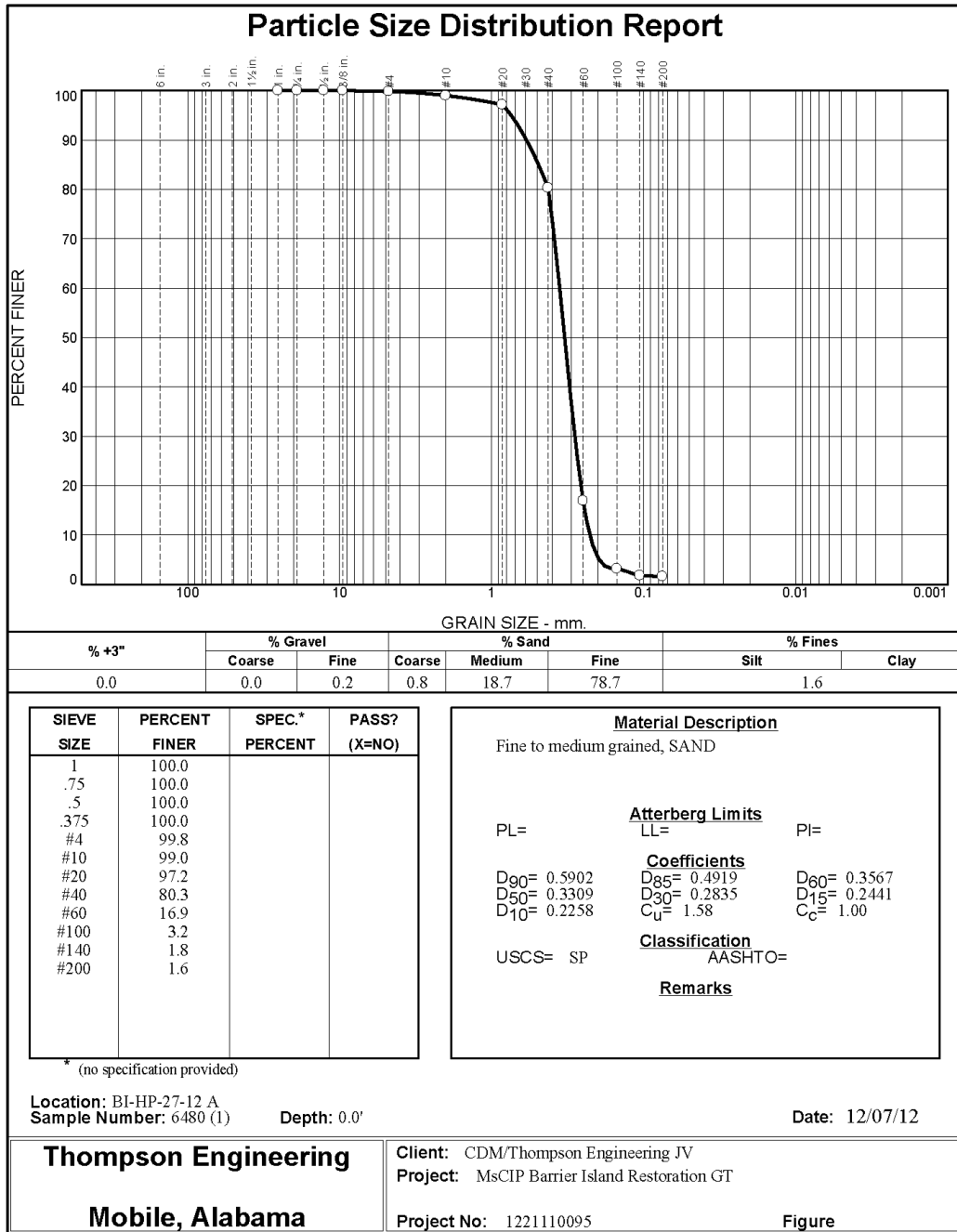


Figure C-14. Particle size distribution report for sample # BI-HP-27-12A.

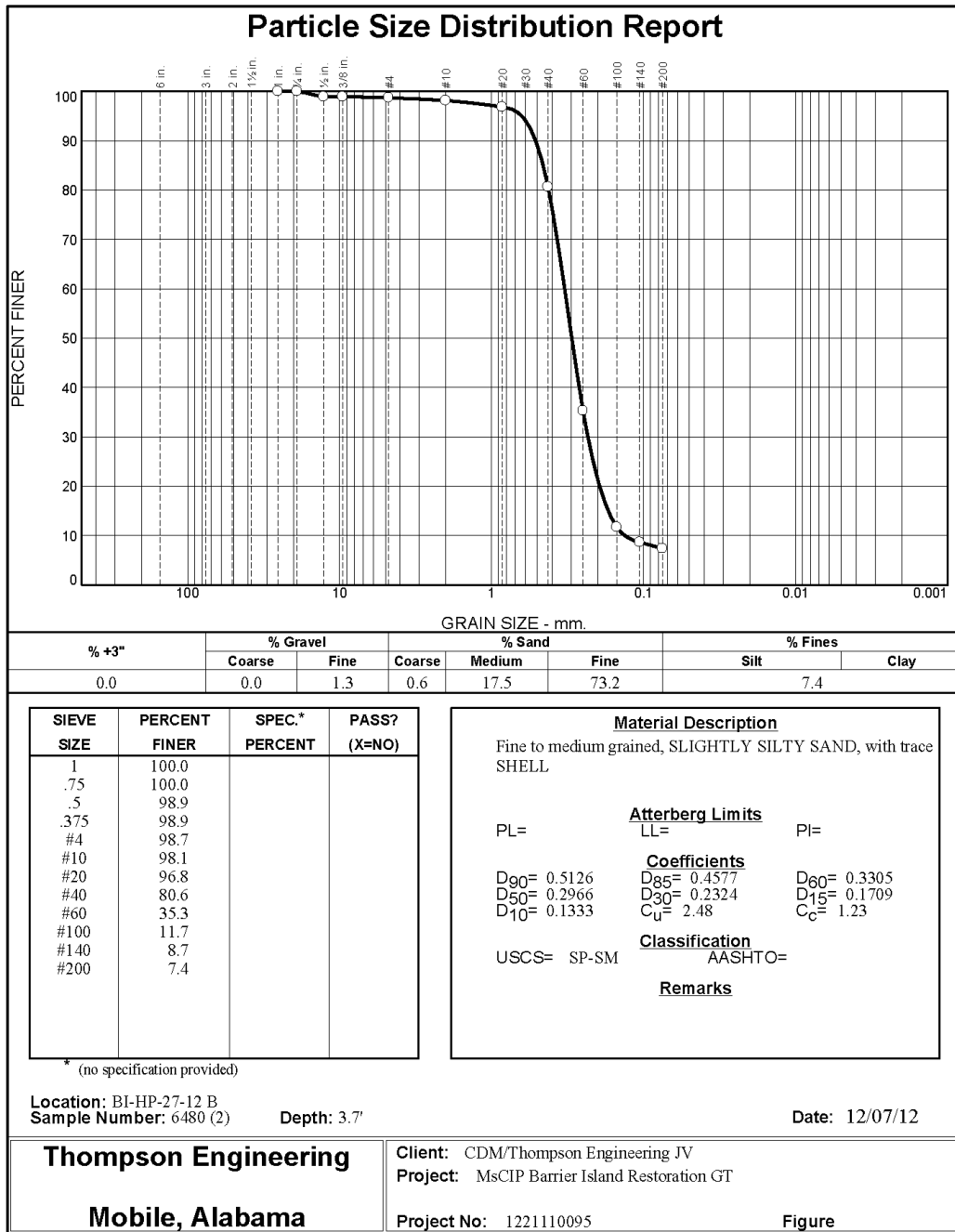


Figure C-15. Particle size distribution report for sample # BI-HP-27-12B.

Boring Designation BI-HP-28-12

DRILLING LOG		DIVISION		INSTALLATION		SHEET 1	
		South Atlantic		Mobile District		OF 2 SHEETS	
1. PROJECT				9. SIZE AND TYPE OF BIT			
MsCIP Barrier Island Restoration Horn Island Pass				N/A			
2. BORING DESIGNATION		LOCATION COORDINATES		10. COORDINATE SYSTEM/DATUM		HORIZONTAL	
BI-HP-28-12		E = 1,079,508 N = 253,551		State Plane, MSE (U.S. Ft.)		NAD83	
3. DRILLING AGENCY		CONTRACTOR FILE NO.		11. MANUFACTURER'S DESIGNATION OF DRILL		<input type="checkbox"/> AUTO HAMMER <input type="checkbox"/> MANUAL HAMMER	
Corps of Engineers - CESAM				Vibracore		<input type="checkbox"/> DISTURBED <input type="checkbox"/> UNDISTURBED (UD)	
4. NAME OF DRILLER				12. TOTAL SAMPLES			
American Vibracore Systems, Inc.				0			
5. DIRECTION OF BORING				13. TOTAL NUMBER CORE BOXES			
<input checked="" type="checkbox"/> VERTICAL <input type="checkbox"/> INCLINED				28.9 Ft.			
DEG. FROM VERTICAL				14. WATER DEPTH			
BEARING				28.9 Ft.			
6. THICKNESS OF OVERBURDEN				15. DATE BORING			
N/A				12-04-12			
7. DEPTH DRILLED INTO ROCK				16. ELEVATION TOP OF BORING			
N/A				-30.3 Ft.			
8. TOTAL DEPTH OF BORING				17. TOTAL RECOVERY FOR BORING			
20.0 Ft.				100%			
				18. SIGNATURE AND TITLE OF INSPECTOR			
				Mike FitzHarris, Geologist			

ELEV.	DEPTH	LEGEND	CLASSIFICATION OF MATERIALS	SAMPLE	LABORATORY RESULTS
-30.3	0.0				
			SAND, poorly-graded, mostly fine to medium-grained sand-sized quartz, trace shell fragments, trace silt, lt. gray to white (SP)	A	Classification: SP Color: 5Y 8/1-white D50: 0.3355 mm % Fines: 1.2
-35.8	5.5			NS	
-36.6	6.3		SAND, poorly-graded with silt, mostly fine-grained sand-sized quartz, few silt, trace clay nodules, clay lens at 6.2 ft., gray (SP-SM)	B	Classification: SP Color: 2.5Y 7/2-light gray D50: 0.2128 mm % Fines: 4.7
			CLAY, lean, mostly clay, some silt, trace shell fragments, gray (CL)	NS	
-50.3	20.0				
NOTES:					
1. Soils are field visually classified in accordance with the Unified Soils Classification System.					
2. NS = Sample not submitted for laboratory analysis from this interval.					
3. Seafloor elevation determined from USACE					

SAM FORM 1836 - MsCIP
MAY 2010

Lat = 30.19687° Long = -88.53180°

Figure C-16. Drilling log for boring site BI-HP-28-12.

DRILLING LOG (Cont. Sheet)			INSTALLATION Mobile District		SHEET 2 OF 2 SHEETS	
PROJECT MsCIP Barrier Island Restoration			COORDINATE SYSTEM/DATUM State Plane, MSE (U.S. Ft.)		HORIZONTAL NAD83	VERTICAL NAVD88
LOCATION COORDINATES X = 1,079,508 Y = 253,551			ELEVATION TOP OF BORING -30.3 Ft.			
ELEV.	DEPTH	LEGEND	CLASSIFICATION OF MATERIALS	SAMPLE	LABORATORY RESULTS	
			hydrographic survey completed June 2014.			



SAM FORM 1836 - MsCIP
MAY 2010

Lat = 30.19687° Long = -88.53180°

Figure C-17. Drilling log continued for boring site BI-HP-28-12.

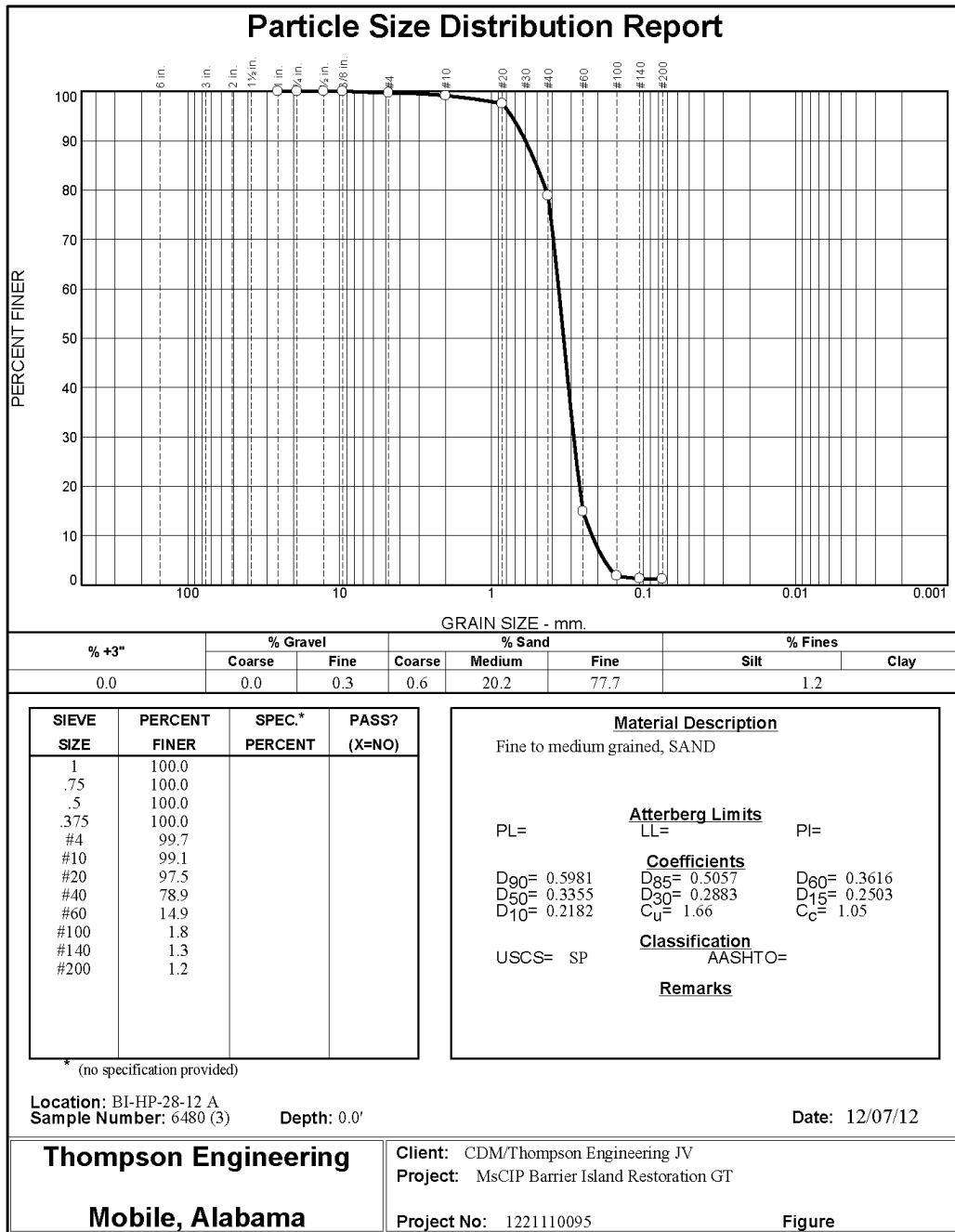


Figure C-18. Particle size distribution report for sample # BI-HP-28-12A.

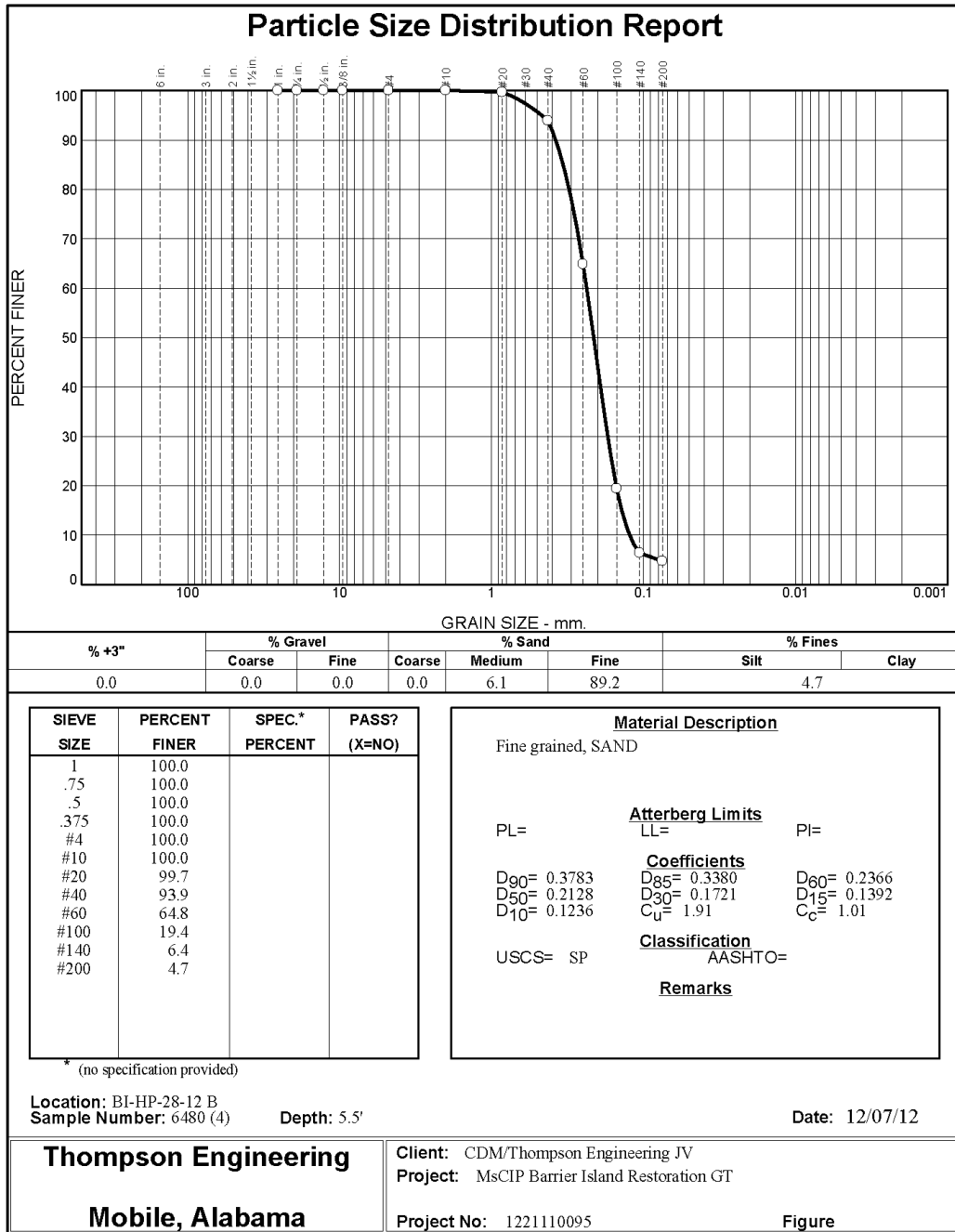


Figure C-19. Particle size distribution report for sample # BI-HP-28-12B.

Boring Designation BI-HP-29-12

DRILLING LOG		DIVISION		INSTALLATION		SHEET 1	
		South Atlantic		Mobile District		OF 1 SHEETS	
1. PROJECT				9. SIZE AND TYPE OF BIT			
MsCIP Barrier Island Restoration Horn Island Pass				N/A			
2. BORING DESIGNATION		LOCATION COORDINATES		10. COORDINATE SYSTEM/DATUM		HORIZONTAL	
BI-HP-29-12		E = 1,078,904 N = 252,586		State Plane, MSE (U.S. Ft.)		NAD83	
3. DRILLING AGENCY		CONTRACTOR FILE NO.		11. MANUFACTURER'S DESIGNATION OF DRILL		<input type="checkbox"/> AUTO HAMMER <input type="checkbox"/> MANUAL HAMMER	
Corps of Engineers - CESAM				Vibracore		<input type="checkbox"/> DISTURBED <input type="checkbox"/> UNDISTURBED (UD)	
4. NAME OF DRILLER				12. TOTAL SAMPLES			
American Vibracore Systems, Inc.				0			
5. DIRECTION OF BORING				13. TOTAL NUMBER CORE BOXES			
<input checked="" type="checkbox"/> VERTICAL <input type="checkbox"/> INCLINED				32.7 Ft.			
6. THICKNESS OF OVERBURDEN		DEG. FROM VERTICAL		14. WATER DEPTH		32.7 Ft.	
N/A				15. DATE BORING		STARTED 12-04-12 COMPLETED 12-04-12	
7. DEPTH DRILLED INTO ROCK		BEARING		16. ELEVATION TOP OF BORING			
N/A				-32.2 Ft.			
8. TOTAL DEPTH OF BORING				17. TOTAL RECOVERY FOR BORING			
18.5 Ft.				100%			
				18. SIGNATURE AND TITLE OF INSPECTOR			
				Mike FitzHarris, Geologist			
ELEV.	DEPTH	LEGEND	CLASSIFICATION OF MATERIALS	SAMPLE	LABORATORY RESULTS		
-32.2	0.0		SAND, poorly-graded, mostly fine to medium-grained sand-sized quartz, trace silt, trace shell fragments, trace wood debris, gray (SP) SAND, poorly-graded, mostly fine to medium-grained sand-sized quartz, trace silt, trace shell fragments, lt. gray (SP) SAND, poorly-graded, mostly fine to medium-grained sand-sized quartz, trace silt, trace shell fragments, lt. gray to pale brown (SP)	A	Classification: SP-SM Color: 2.5Y 7/2-light gray D50: 0.3244 mm % Fines: 6.7		
-33.1	0.9			B	Classification: SP Color: 5Y 7/2-light gray D50: 0.2781 mm % Fines: 1.3		
-35.7	3.5			C	Classification: SP Color: 2.5Y 7.5/2- D50: 0.2868 mm % Fines: 1.9		
-37.3	5.1			CLAY, lean, mostly fine-grained sand-sized clay, some silt, trace shells, trace shell fragments, alternating sandy clay and clayey sands, gray to brownish gray (CL)	NS		
-50.7	18.5						
NOTES: 1. Soils are field visually classified in accordance with the Unified Soils Classification System. 2. NS = Sample not submitted for laboratory analysis from this interval. 3. Seafloor elevation determined from USACE hydrographic survey completed June 2014.							

SAM FORM 1836 - MsCIP
MAY 2010

Lat = 30.19422° Long = -88.53372°

Figure C-20. Drilling log for boring site BI-HP-29-12.

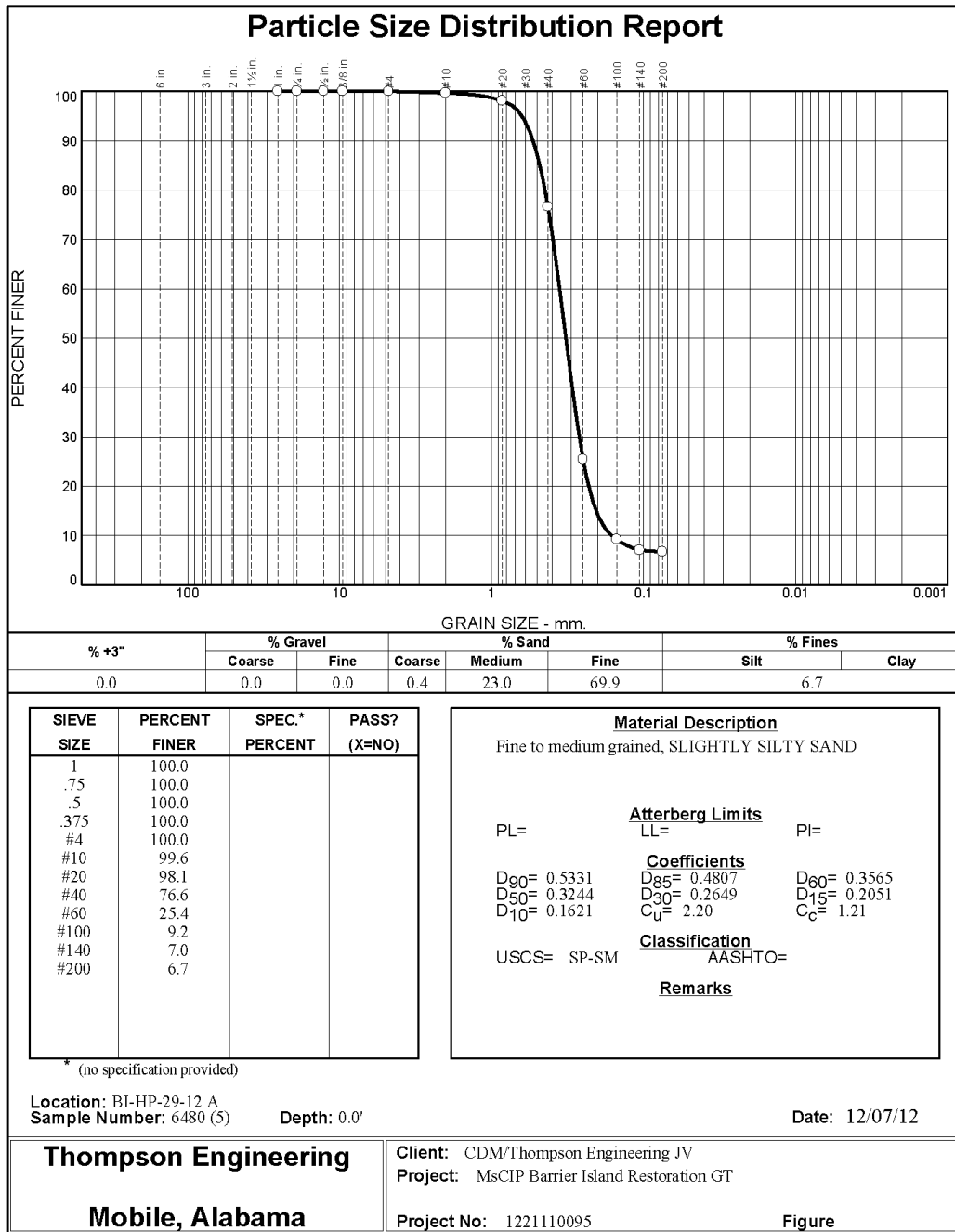


Figure C-21. Particle size distribution report for sample # BI-HP-29-12A.

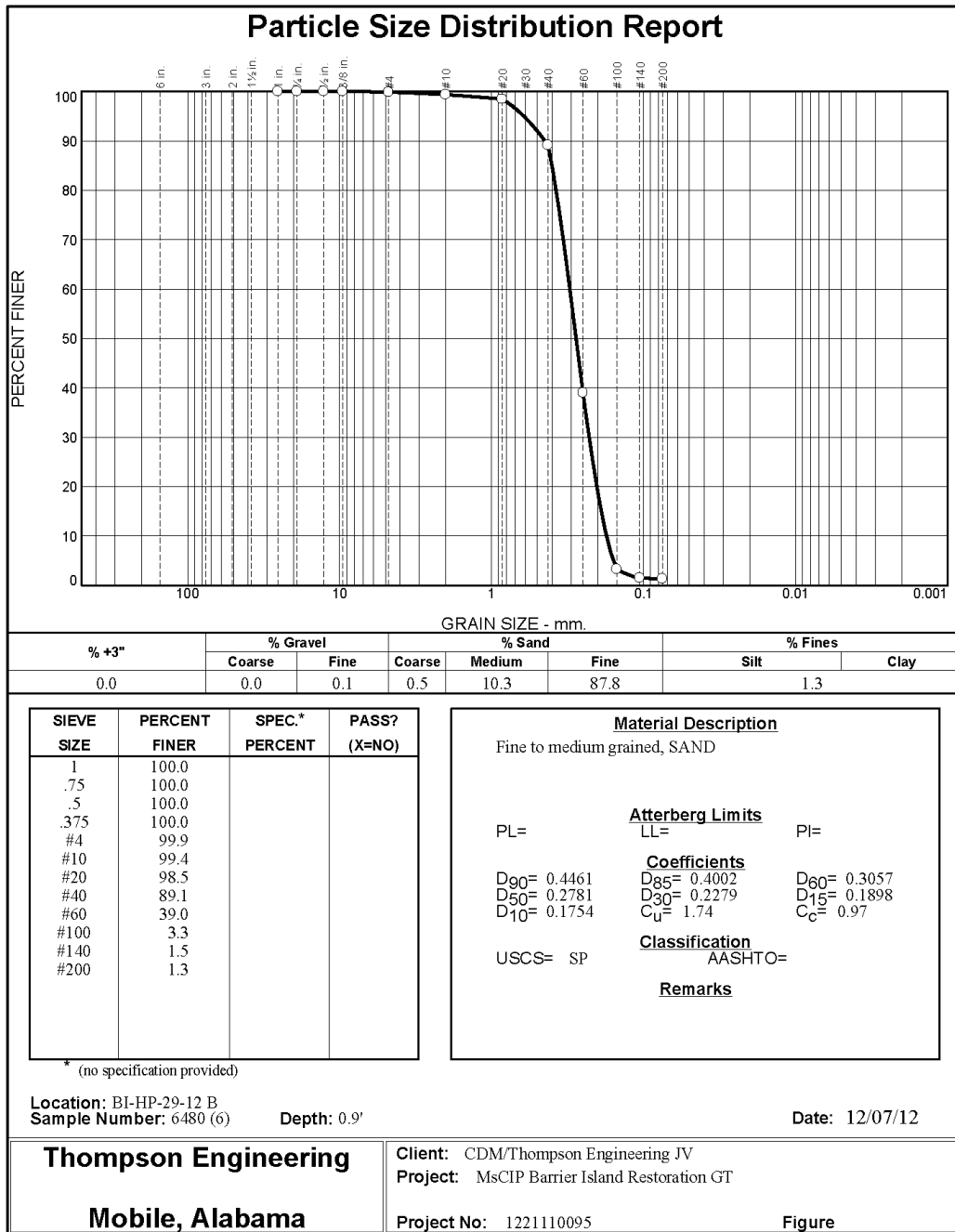


Figure C-22. Particle size distribution report for sample # BI-HP-29-12B.

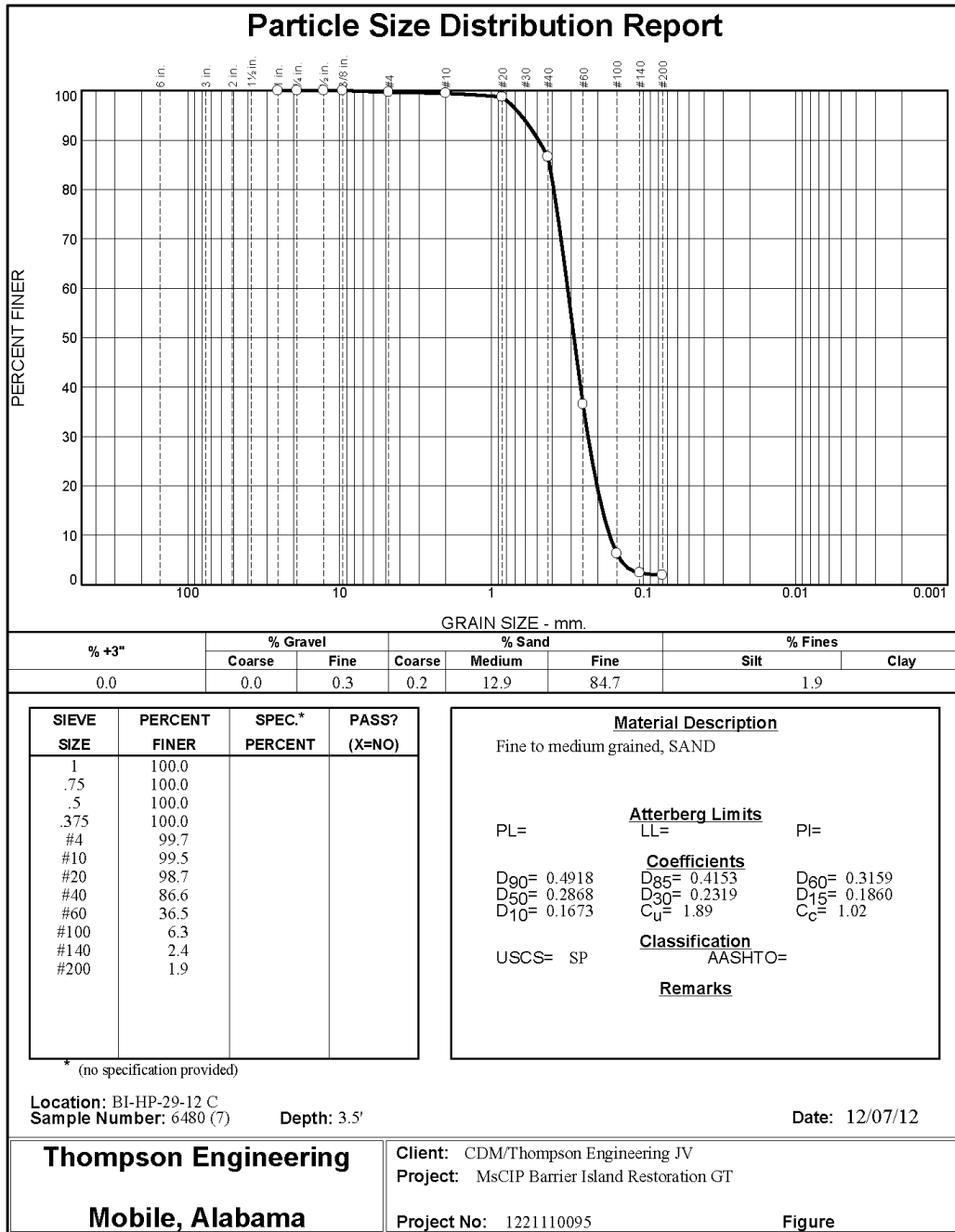


Figure C-23. Particle size distribution report for sample # BI-HP-29-12C.

Boring Designation BI-HP-30-12

DRILLING LOG		DIVISION		INSTALLATION		SHEET 1	
		South Atlantic		Mobile District		OF 1 SHEETS	
1. PROJECT				9. SIZE AND TYPE OF BIT			
MsCIP Barrier Island Restoration Horn Island Pass				N/A			
2. BORING DESIGNATION		LOCATION COORDINATES		10. COORDINATE SYSTEM/DATUM		HORIZONTAL	
BI-HP-30-12		E = 1,077,662 N = 252,848		State Plane, MSE (U.S. Ft.)		NAD83	
3. DRILLING AGENCY		CONTRACTOR FILE NO.		11. MANUFACTURER'S DESIGNATION OF DRILL		<input type="checkbox"/> AUTO HAMMER <input type="checkbox"/> MANUAL HAMMER	
Corps of Engineers - CESAM				Vibracore		<input type="checkbox"/> DISTURBED <input type="checkbox"/> UNDISTURBED (UD)	
4. NAME OF DRILLER				12. TOTAL SAMPLES			
American Vibracore Systems, Inc.				0			
5. DIRECTION OF BORING				13. TOTAL NUMBER CORE BOXES			
<input checked="" type="checkbox"/> VERTICAL <input type="checkbox"/> INCLINED				29.8 Ft.			
		DEG. FROM VERTICAL		14. WATER DEPTH		29.8 Ft.	
		BEARING		15. DATE BORING		STARTED 12-04-12 COMPLETED 12-04-12	
6. THICKNESS OF OVERBURDEN				16. ELEVATION TOP OF BORING			
N/A				-29.2 Ft.			
7. DEPTH DRILLED INTO ROCK				17. TOTAL RECOVERY FOR BORING			
N/A				100%			
8. TOTAL DEPTH OF BORING				18. SIGNATURE AND TITLE OF INSPECTOR			
19.0 Ft.				Mike FitzHarris, Geologist			
ELEV.	DEPTH	LEGEND	CLASSIFICATION OF MATERIALS	SAMPLE	LABORATORY RESULTS		
-29.2	0.0						
-31.6	2.4		SAND, poorly-graded, mostly fine to medium-grained sand-sized quartz, trace silt, trace shell fragments, trace wood debris, lt gray with pale brown at 0.7 thru 1.0 ft (SP)	A	Classification: SP Color: 2.5Y 8/1-white D50: 0.3133 mm % Fines: 4.5		
-34.6	5.4		SAND, poorly-graded with silt, mostly fine to medium-grained sand-sized quartz, little silt, trace shell fragments, few clay stringers throughout and a clay band at 4.2 ft., gray (SP-SM)	B	Classification: SP Color: 2.5Y 7/2-light gray D50: 0.2705 mm % Fines: 3.4		
-37.1	7.9		SAND, poorly-graded, mostly fine-grained sand-sized quartz, trace silt, trace shell fragments, gray to lt. gray (SP)	C	Classification: SP Color: 2.5Y 7/2-light gray D50: 0.3164 mm % Fines: 1.7		
			CLAY, lean, mostly clay, trace shells, alternating clay and sandy clay layers, gray (CL)	NS			
-48.2	19.0						
			NOTES:				
			1. Soils are field visually classified in accordance with the Unified Soils Classification System.				
			2. NS = Sample not submitted for laboratory analysis from this interval.				
			3. Seafloor elevation determined from USACE hydrographic survey completed June 2014.				

SAM FORM 1836 - MsCIP
MAY 2010

Lat = 30.19495° Long = -88.53765°

Figure C-24. Drilling log for boring site BI-HP-30-12.

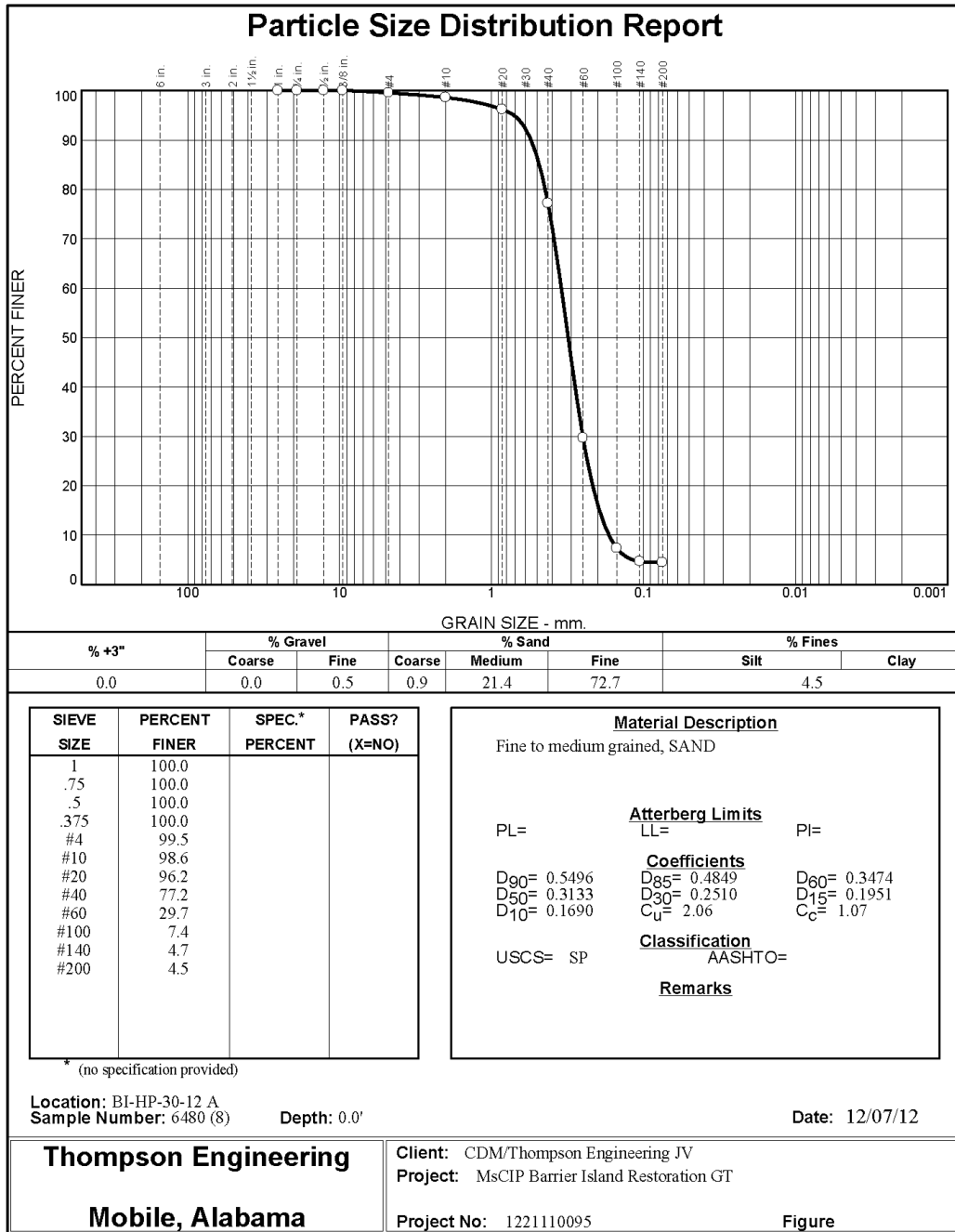


Figure C-25. Particle size distribution report for sample # BI-HP-30-12A.

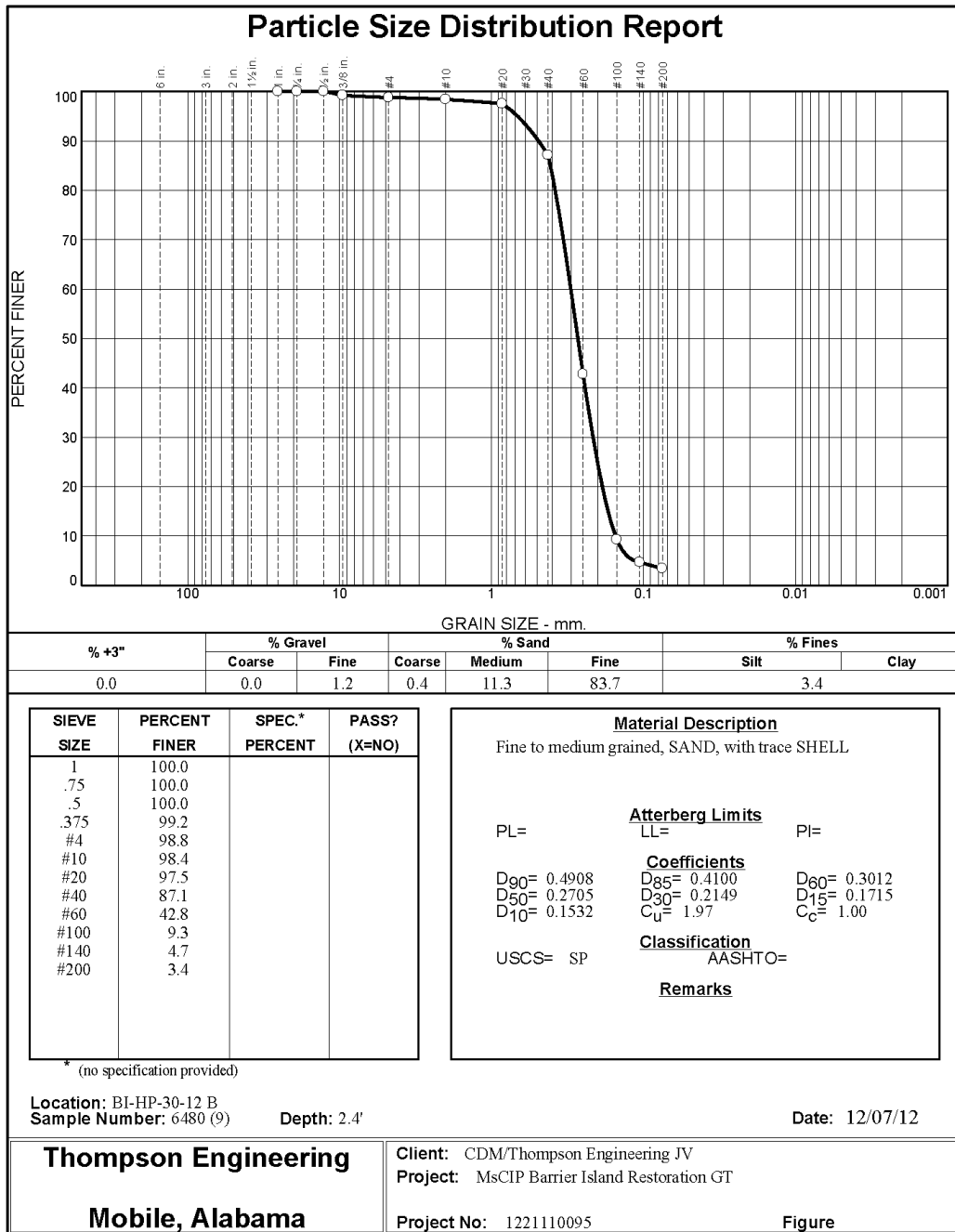


Figure C-26. Particle size distribution report for sample # BI-HP-30-12B.

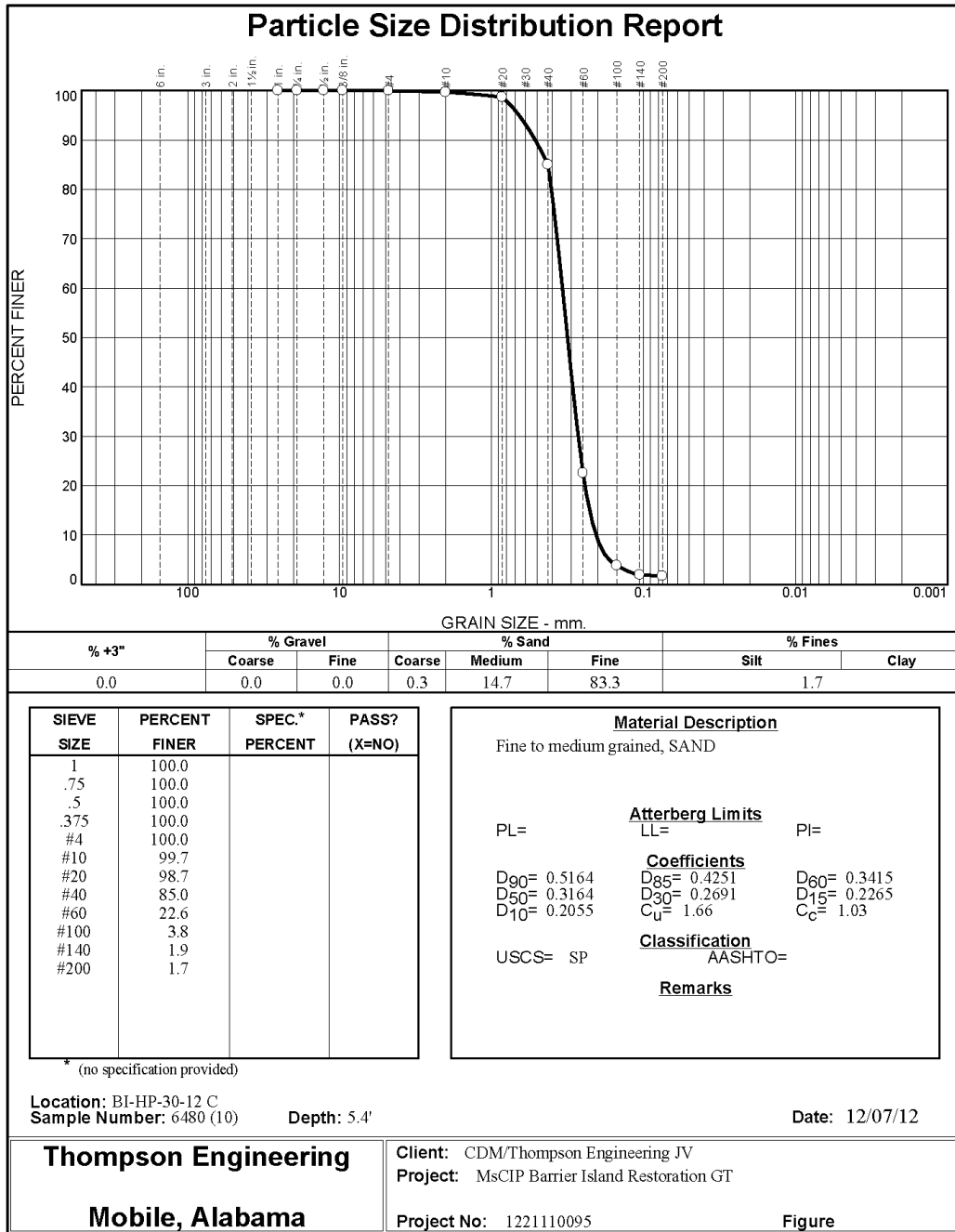


Figure C-27. Particle size distribution report for sample # BI-HP-30-12C.

Boring Designation BI-HP-38-12

DRILLING LOG		DIVISION		INSTALLATION		SHEET 1	
		South Atlantic		Mobile District		OF 1 SHEETS	
1. PROJECT				9. SIZE AND TYPE OF BIT			
MsCIP Barrier Island Restoration Horn Island Pass				N/A			
2. BORING DESIGNATION		LOCATION COORDINATES		10. COORDINATE SYSTEM/DATUM		HORIZONTAL	
BI-HP-38-12		E = 1,078,463 N = 254,494		Slate Plane, MSE (U.S. Ft.)		NAD83	
3. DRILLING AGENCY		CONTRACTOR FILE NO.		11. MANUFACTURER'S DESIGNATION OF DRILL		<input type="checkbox"/> AUTO HAMMER <input type="checkbox"/> MANUAL HAMMER	
Corps of Engineers - CESAM				Vibracore		<input type="checkbox"/> DISTURBED <input type="checkbox"/> UNDISTURBED (UD)	
4. NAME OF DRILLER				12. TOTAL SAMPLES			
American Vibracore Systems, Inc.				0			
5. DIRECTION OF BORING				13. TOTAL NUMBER CORE BOXES			
<input checked="" type="checkbox"/> VERTICAL <input type="checkbox"/> INCLINED				14. WATER DEPTH			
DEG. FROM VERTICAL				29.2 Ft.			
BEARING				15. DATE BORING			
				<input type="checkbox"/> STARTED <input type="checkbox"/> COMPLETED			
6. THICKNESS OF OVERBURDEN				16. ELEVATION TOP OF BORING			
N/A				-29.8 Ft.			
7. DEPTH DRILLED INTO ROCK				17. TOTAL RECOVERY FOR BORING			
N/A				100%			
8. TOTAL DEPTH OF BORING				18. SIGNATURE AND TITLE OF INSPECTOR			
16.1 Ft.				Mike FitzHarris, Geologist			

ELEV.	DEPTH	LEGEND	CLASSIFICATION OF MATERIALS	SAMPLE	LABORATORY RESULTS
-29.8	0.0				
			SAND, poorly-graded, mostly fine to medium-grained sand-sized quartz, trace shell fragments, trace clayey bands, pale lt. brown (SP)	A	Classification: SP-SM Color: 5Y 7/2-light gray D50: 0.3044 mm % Fines: 5.3
-33.4	3.6		SILT, inorganic-L, mostly silt, some clay, trace fine-grained sand-sized quartz, trace shell fragments, dark gray (ML)		
-37.8	8.0				
-39.5	9.7		SAND, silty, mostly fine-grained sand-sized quartz, some silt, few shell fragments, trace clay, dark gray (SM)	NS	
			SILT, inorganic-L, mostly silt, some clay, some fine-grained sand-sized quartz, little shell fragments, dark gray (ML)		
-45.9	16.1				
			NOTES: 1. Soils are field visually classified in accordance with the Unified Soils Classification System. 2. NS = Sample not submitted for laboratory analysis from this interval. 3. Seafloor elevation determined from USACE hydrographic survey completed June 2014.		

SAM FORM 1836 - MsCIP
MAY 2010

Lat = 30.19947° Long = -88.53510°

Figure C-28. Drilling log for boring site BI-HP-38-12.

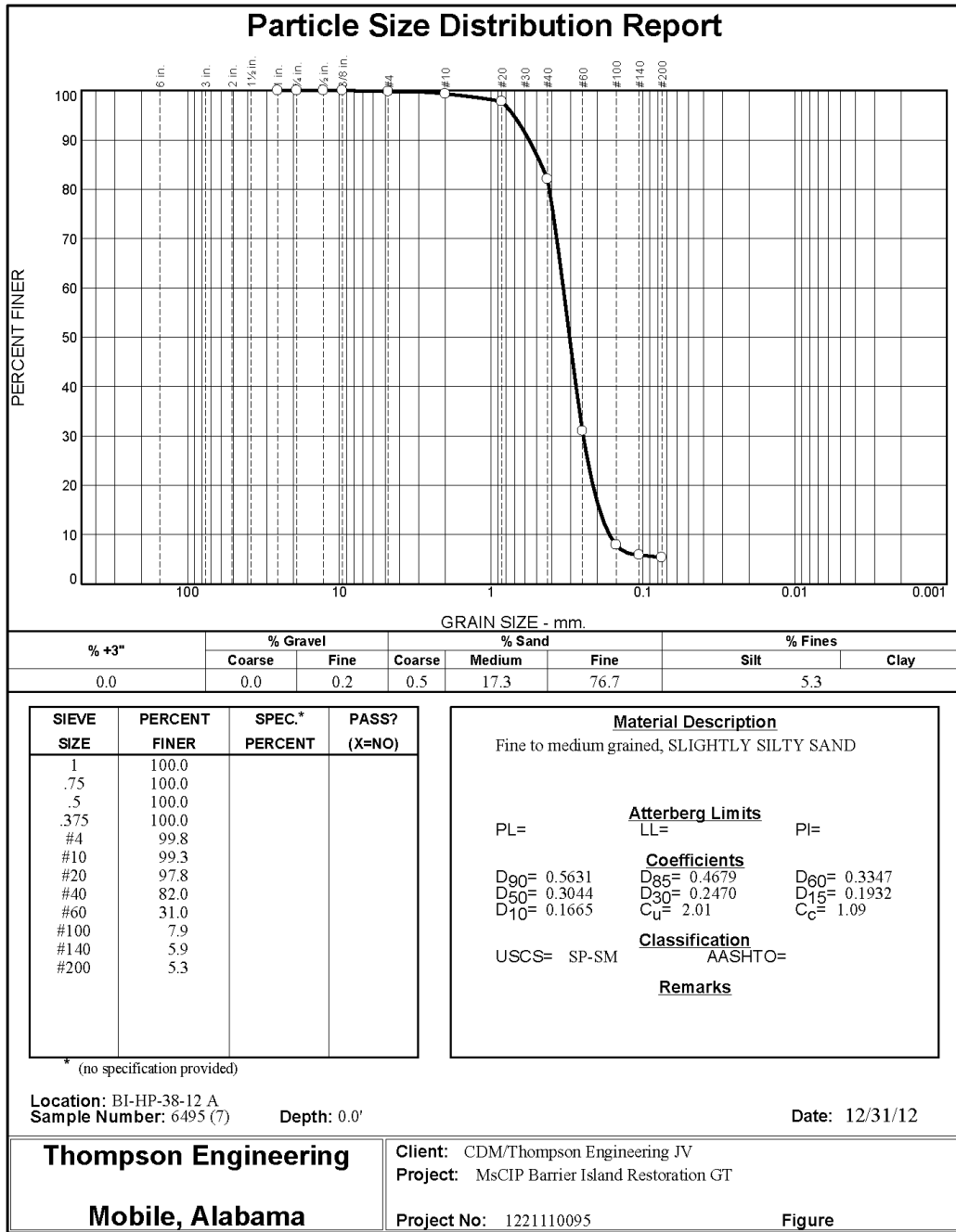


Figure C-29. Particle size distribution report for sample # BI-HP-38-12A.

Boring Designation BI-HP-39-12

DRILLING LOG		DIVISION South Atlantic	INSTALLATION Mobile District	SHEET 1 OF 1 SHEETS
1. PROJECT MsCIP Barrier Island Restoration Horn Island Pass		9. SIZE AND TYPE OF BIT N/A		10. COORDINATE SYSTEM/DATUM State Plane, MSE (U.S. Ft.)
2. BORING DESIGNATION BI-HP-39-12		LOCATION COORDINATES E = 1,071,547 N = 251,312		HORIZONTAL NAD83 VERTICAL NAVD88
3. DRILLING AGENCY Corps of Engineers - CESAM		CONTRACTOR FILE NO.		11. MANUFACTURER'S DESIGNATION OF DRILL Vibracore
4. NAME OF DRILLER American Vibracore Systems, Inc.		12. TOTAL SAMPLES		<input type="checkbox"/> AUTO HAMMER <input type="checkbox"/> MANUAL HAMMER
5. DIRECTION OF BORING <input checked="" type="checkbox"/> VERTICAL <input type="checkbox"/> INCLINED		DEG. FROM VERTICAL	BEARING	12. TOTAL SAMPLES DISTURBED UNDISTURBED (UD) 0
6. THICKNESS OF OVERBURDEN N/A		13. TOTAL NUMBER CORE BOXES		14. WATER DEPTH 32 Ft.
7. DEPTH DRILLED INTO ROCK N/A		15. DATE BORING		STARTED 12-21-12 COMPLETED 12-21-12
8. TOTAL DEPTH OF BORING 17.4 Ft.		16. ELEVATION TOP OF BORING -31.9 Ft.		17. TOTAL RECOVERY FOR BORING 100%
		18. SIGNATURE AND TITLE OF INSPECTOR Mike FitzHarris, Geologist		

ELEV.	DEPTH	LEGEND	CLASSIFICATION OF MATERIALS	SAMPLE	LABORATORY RESULTS
-31.9	0.0	[Dotted pattern]	SAND, poorly-graded, mostly fine to medium-grained sand-sized quartz, trace fines, trace shell fragments, trace clayey bands and silty zones, lt. pale brown to lt. gray (SP)	A	Classification: SP Color: 5Y 7/2-light gray D50: 0.2983 mm % Fines: 1.2
				B	Classification: SP Color: 5Y 7/2-light gray D50: 0.2688 mm % Fines: 1.8
-41.4	9.5			C	Classification: SP Color: 5Y 6/2-light olive gray D50: 0.2974 mm % Fines: 2.1
		[Vertical lines pattern]	SILT, inorganic-L, mostly silt, some clay, some fine-grained sand-sized quartz, little shell fragments, soft, dark gray (ML)	NS	
-49.3	17.4				
			NOTES: 1. Soils are field visually classified in accordance with the Unified Soils Classification System. 2. NS = Sample not submitted for laboratory analysis from this interval. 3. Seafloor elevation determined from USACE hydrographic survey completed June 2014.		

SAM FORM 1836 - MsCIP MAY 2010 Lat = 30.19077° Long = -88.55702°

Figure C-30. Drilling log for boring site BI-HP-39-12.

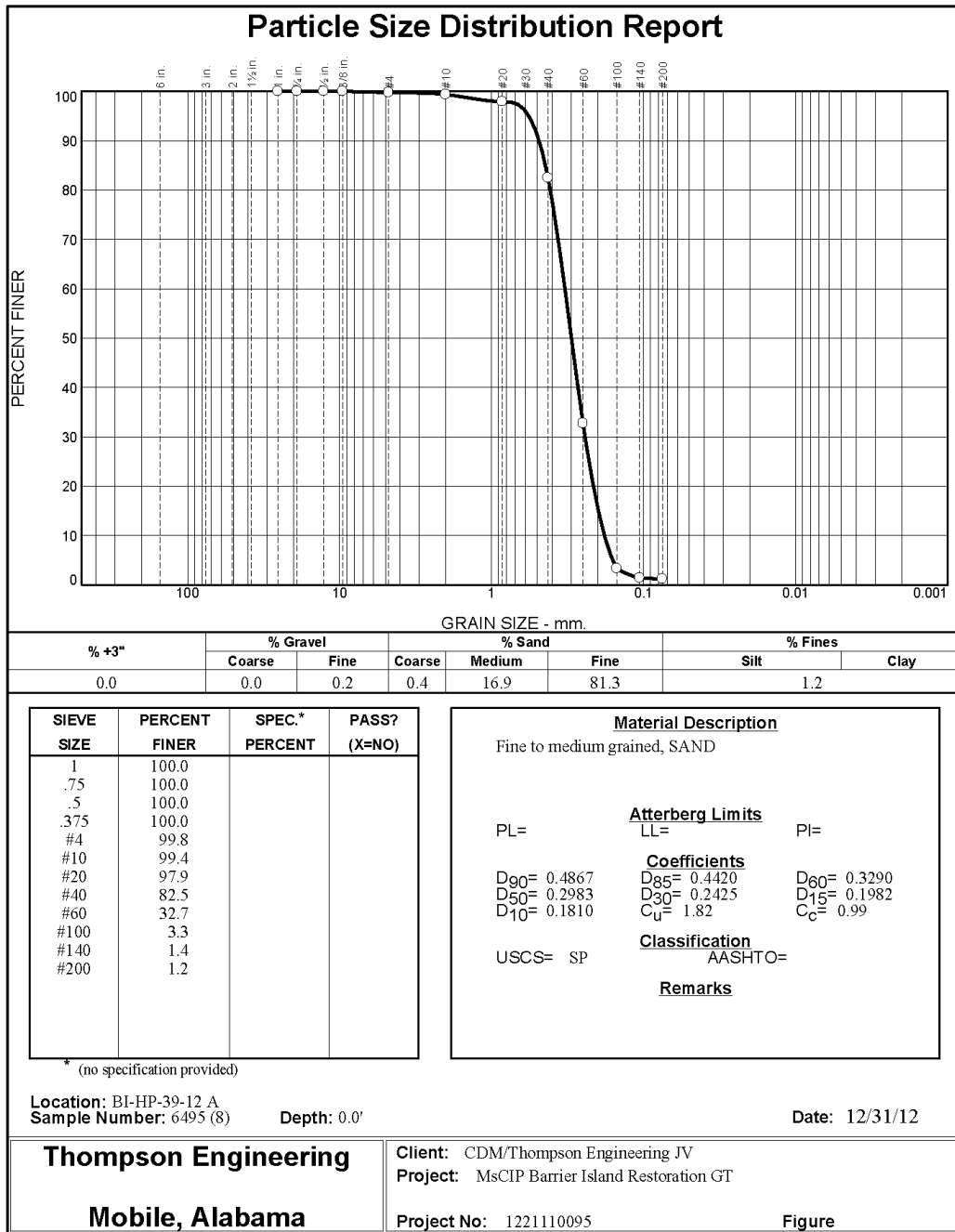


Figure C-31. Particle size distribution report for sample # BI-HP-39-12A.

Boring Designation BI-HP-41-12

DRILLING LOG		DIVISION		INSTALLATION		SHEET 1 OF 1 SHEETS	
1. PROJECT MsCIP Barrier Island Restoration Horn Island Pass		South Atlantic		Mobile District			
2. BORING DESIGNATION BI-HP-41-12		LOCATION COORDINATES E = 1,078,900 N = 254,215		9. SIZE AND TYPE OF BIT N/A		10. COORDINATE SYSTEM/DATUM Slate Plane, MSE (U.S. Ft.)	
3. DRILLING AGENCY Corps of Engineers - CESAM		CONTRACTOR FILE NO.		11. MANUFACTURER'S DESIGNATION OF DRILL Vibracore		HORIZONTAL NAD83	
4. NAME OF DRILLER American Vibracore Systems, Inc.				12. TOTAL SAMPLES		VERTICAL NAVD88	
5. DIRECTION OF BORING <input checked="" type="checkbox"/> VERTICAL <input type="checkbox"/> INCLINED		DEG. FROM VERTICAL		13. TOTAL NUMBER CORE BOXES		<input type="checkbox"/> AUTO HAMMER <input type="checkbox"/> MANUAL HAMMER	
6. THICKNESS OF OVERBURDEN N/A		BEARING		14. WATER DEPTH 28.5 Ft.		DISTURBED UNDISTURBED (UD)	
7. DEPTH DRILLED INTO ROCK N/A				15. DATE BORING 01-05-13		0	
8. TOTAL DEPTH OF BORING 14.8 Ft.				16. ELEVATION TOP OF BORING -28.2 Ft.		17. TOTAL RECOVERY FOR BORING 100%	
				18. SIGNATURE AND TITLE OF INSPECTOR Mike FitzHarris, Geologist			
ELEV.	DEPTH	LEGEND	CLASSIFICATION OF MATERIALS	SAMPLE	LABORATORY RESULTS		
-28.2	0.0						
-29.7	1.5		SAND, poorly-graded, mostly fine to medium-grained sand-sized quartz, trace fines, trace shell fragments, lt. pale brown (SP)	A	Classification: SP Color: 2.5Y 8/1-white D50: 0.3021 mm % Fines: 1.9		
-32.4	4.2		SAND, poorly-graded, mostly fine to medium-grained sand-sized quartz, trace fines, trace shell fragments, few clay lenses, lt. gray (SP)	B	Classification: SP-SM Color: 2.5Y 6/2-light brownish gray D50: 0.286 mm % Fines: 6.4		
-35.3	7.1		SAND, poorly-graded, mostly fine to medium-grained sand-sized quartz, trace clay, trace shell fragments, trace clay lenses, lt. gray (SP)	C	Classification: SP Color: 2.5Y 7/2-light gray D50: 0.2785 mm % Fines: 4.1		
-38.2	10.0		SILT, inorganic-L, mostly silt, some fine-grained sand-sized quartz, trace clay, trace shell fragments, soft, gray (ML)				
-39.3	11.1		SAND, silty, mostly fine-grained sand-sized quartz, some silt, few shell fragments, gray (SM)	NS			
-43.0	14.8		SILT, inorganic-L, mostly silt, some fine-grained sand-sized quartz, few shell fragments, trace clay, soft, gray (ML)				
			NOTES: 1. Soils are field visually classified in accordance with the Unified Soils Classification System. 2. NS = Sample not submitted for laboratory analysis from this interval. 3. Seafloor elevation determined from USACE hydrographic survey completed June 2014.				

SAM FORM 1836 - MsCIP
MAY 2010

Lat = 30.19870° Long = -88.53372°

Figure C-32. Drilling log for boring site BI-HP-41-12.

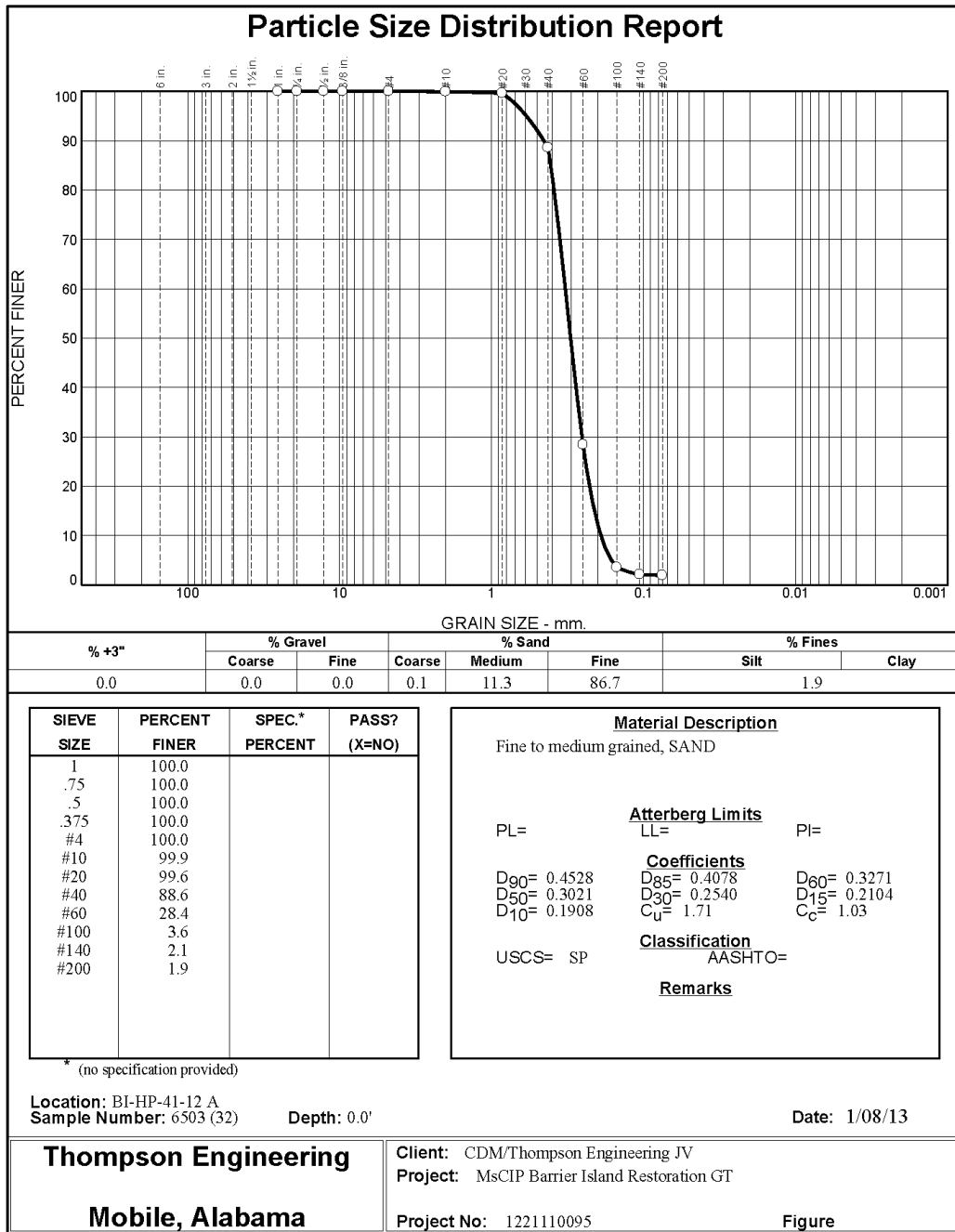


Figure C-33. Particle size distribution report for sample # BI-HP-41-12A.

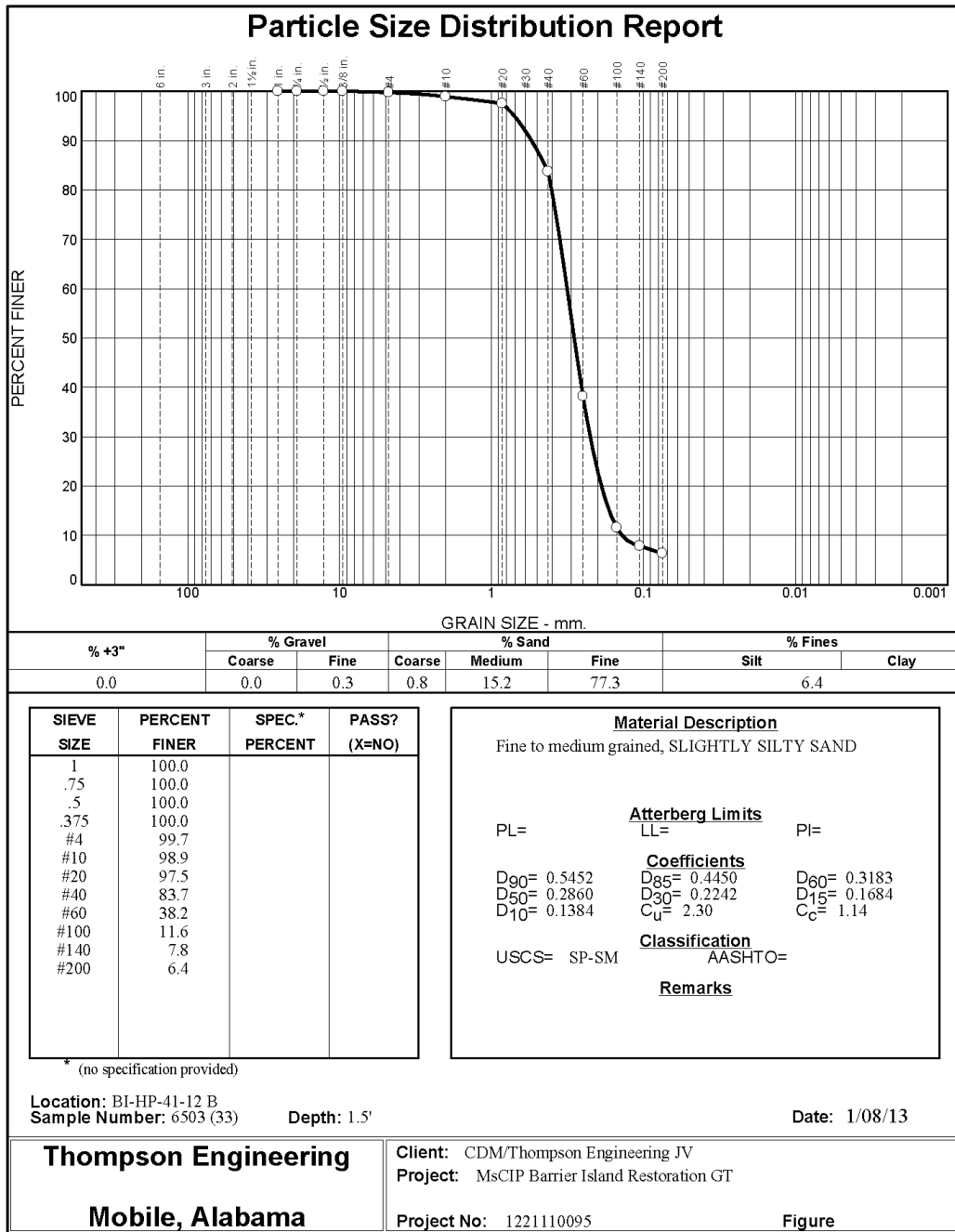


Figure C-34. Particle size distribution report for sample # BI-HP-41-12B.

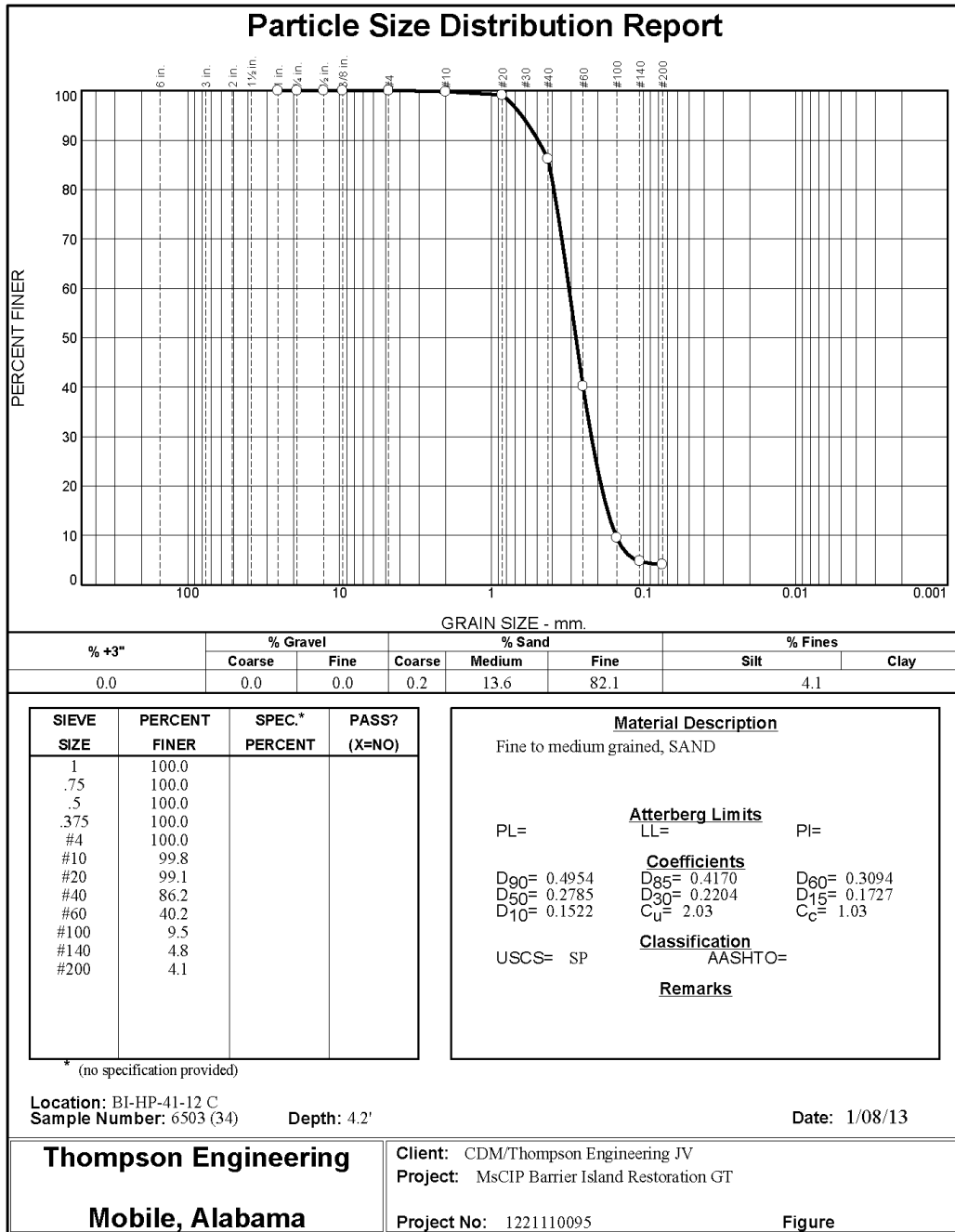


Figure C-35. Particle size distribution report for sample # BI-HP-41-12C.



Department of the Interior (DOI)

The Department of the Interior protects and manages the Nation's natural resources and cultural heritage; provides scientific and other information about those resources; and honors the Nation's trust responsibilities or special commitments to American Indians, Alaska Natives, and affiliated island communities.



Bureau of Ocean Energy Management (BOEM)

The mission of the Bureau of Ocean Energy Management is to manage development of U.S. Outer Continental Shelf energy and mineral resources in an environmentally and economically responsible way.

BOEM Environmental Studies Program

The mission of the Environmental Studies Program is to provide the information needed to predict, assess, and manage impacts from offshore energy and marine mineral exploration, development, and production activities on human, marine, and coastal environments. The proposal, selection, research, review, collaboration, production, and dissemination of each of BOEM's Environmental Studies follows the DOI Code of Scientific and Scholarly Conduct, in support of a culture of scientific and professional integrity, as set out in the DOI Departmental Manual (305 DM 3).